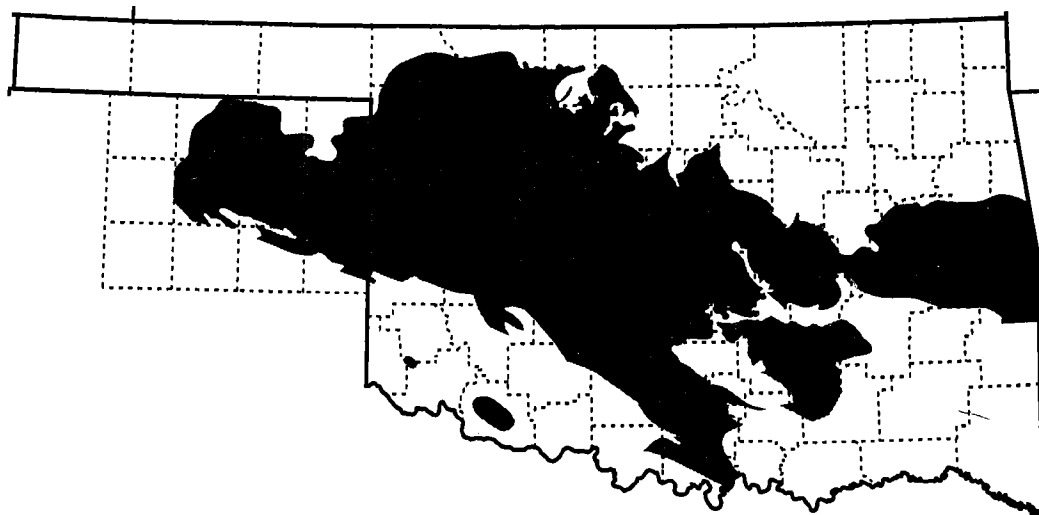




Oklahoma
Geological
Survey
2000

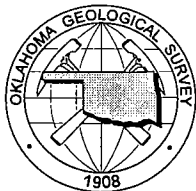
Special Publication 2000-2

Hunton Play in Oklahoma (Including Northeast Texas Panhandle)



Workshop co-sponsored by:
Oklahoma Geological Survey
and
Petroleum Technology Transfer Council





Oklahoma Geological Survey
Charles J. Mankin, *Director*

Special Publication 2000-2
ISSN 0275-0929

Hunton Play in Oklahoma (Including Northeast Texas Panhandle)

PART I.—Overview and Goals of the Workshop
Kurt Rottmann

PART II.—Carbonate-Reservoir Basics
Edward A. Beaumont

PART III.—History of Hunton Oil and Gas Exploration and Development in Oklahoma
Robert A. Northcutt

PART IV.—Hunton Stratigraphy
Kurt Rottmann

**PART V.—The Hunton Group: Sequence Stratigraphy,
Facies, Dolomitization, and Karstification**
Zuhair Al-Shaieb, Jim Puckette, and Paul Blubaugh

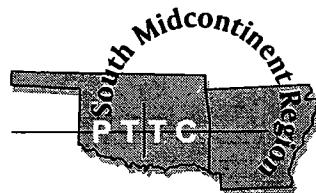
PART VI.—Leedey Field Hunton Reservoir Study
Kurt Rottmann

PART VII.—East Arnett Field Hunton Reservoir Study
Kurt Rottmann

PART VIII.—Prairie Gem Field Hunton Reservoir Study
Kurt Rottmann

Prepared for a one-day workshop, this volume is part of a continuing series that provides information and technical assistance to Oklahoma's oil and gas operators.

Co-sponsored by:
Oklahoma Geological Survey
and
Petroleum Technology Transfer Council



The University of Oklahoma
Norman, Oklahoma

2000

SPECIAL PUBLICATION SERIES

The Oklahoma Geological Survey's Special Publication series is designed to bring timely geologic information to the public quickly and economically. Review and editing of this material has been minimized in order to expedite publication.

Front Cover

Oklahoma is home to some of the largest oil and gas producing provinces in the continental United States. The Hunton Group is one of the more important producing horizons in Oklahoma. As the shading on the map shows, the Hunton Group is present in the Anadarko basin and its associated shelf and in the Arkoma basin and its associated Cherokee shelf. The Hunton has supplied significant production to our nation, and its abundant reserve potential will contribute to our future economic stability.

This publication, printed by the Oklahoma Geological Survey, is issued by the Oklahoma Geological Survey as authorized by Title 70, Oklahoma Statutes, 1981, Section 3310, and Title 74, Oklahoma Statutes, 1981, Sections 231–238. 1,000 copies have been prepared at a cost of \$13,015 to the taxpayers of the State of Oklahoma. Copies have been deposited with the Publications Clearinghouse of the Oklahoma Department of Libraries.



*Thomas W. Amsden
(1915–2000)*

Dedication

This publication is dedicated to Dr. Thomas W. Amsden in recognition of his devoted study of the Late Ordovician–Devonian Hunton Group in Oklahoma. He worked almost exclusively on the Hunton Group from 1955, when he joined the Oklahoma Geological Survey, to his retirement in 1985. Dr. Amsden has long been recognized as a leading authority on Silurian–Devonian brachiopods and on all aspects of geology of the Hunton Group. His detailed study of the biostratigraphy of the Hunton, based on outcrop and subsurface work, has established a wealth of data and understanding upon which other workers continue to build.

When Dr. Amsden died in February 2000, I wanted to be at his memorial service, even though we had never met. For years, I have poured over his writings, absorbed his knowledge, and marveled at how thorough he was in his studies. In his writings, he could make complex subjects easy to understand.

As I studied his many published works and read between the lines, I came to appreciate his eagerness for, and openness to, new ideas. He was devoted to understanding the entire truth in his field of study, not just parts of it, and the maturation of his knowledge over time is reflected in his writings. He continually sought and incorporated new information into his work and always recognized the contributions of colleagues with the highest regard, whether or not he agreed with them. His writings also reveal a man dedicated to sharing his knowledge with those who would come after him—with you, with me, and with the young student just discovering this field.

There are many planes of friendship. Although I didn't know Dr. Amsden personally, he has long been my friend intellectually. It is with deep gratitude that this publication is dedicated to him.

Kurt Rottmann

CONTENTS

PART I – Overview and Goals of the Workshop

Introduction	1
Prior Investigations	1
Area of Study	1
Goals	2
Acknowledgments	3

PART II – Carbonate-Reservoir Basics

Introduction	4
Carbonate-Mineral Types	4
Carbonate-Rock Types	5
Grains	5
Matrix	5
Cement	5
Carbonate Depositional Settings	6
Preservation or Destruction of Pore Space	7

PART III – History of Hunton Oil and Gas Exploration and Development in Oklahoma

Introduction	9
Hunton Exploration and Development	9
Beebe–Southwest Konawa Field, Pontotoc County	10
Fitts Field, Pontotoc County	11
West Edmond Field, Oklahoma, Canadian, and Kingfisher Counties	12
North Custer City Field, Custer County	14
Aledo Field, Custer and Dewey Counties	15
West Mayfield Field, Beckham County	15
Golden Trend, Garvin, Grady, and McClain Counties	17
Depth Range of Hunton Reservoirs in Oklahoma	19
Summary	19
Acknowledgments	19

PART IV – Hunton Stratigraphy

Building the Stratigraphic Column	21
Type Log	21
Ordovician	26
Sylvan Shale	26
Ordovician–Silurian	27
Chimneyhill Subgroup	27
Silurian	30
Henryhouse Formation	30
Devonian	34
Haragan/Bois d’Arc Formations	34
Frisco Formation	35
Unnamed Carbonate Unit	36
Sallisaw Formation	37
Misener and Sylamore Sandstones	37
Devonian–Mississippian	38
Woodford/Chattanooga Shale	38

PART V – The Hunton Group: Sequence Stratigraphy, Facies, Dolomitization, and Karstification

Abstract	39
Introduction	39
Depositional Facies and Environments	40

Henryhouse–Haragan/Bois d’Arc Formations	40
Facies I	42
Facies II	42
Facies III	43
Dolomitization	43
Porosity	44
Karstic Features	46
Type 1 Reservoirs	46
Type 2 Reservoirs	47
Paleotopography and Production	47
Implications	50
PART VI – Leedey Field Hunton Reservoir Study	
Introduction	51
Stratigraphy	53
Isopach Mapping	54
Isopaching the Hunton Near Pre-Woodford Erosional Channels	59
Structural Implications of the Silurian–Devonian Isopachs	61
Pre-Woodford-Channel Hydrocarbon Seals	63
Cores	67
Reservoir Parameters and Productions	67
PART VII – East Arnett Field Hunton Reservoir Study	
Introduction	71
Stratigraphy	73
Isopach Mapping	75
Structure	77
Pratt Anticline Extension	80
Woodward Anticline	80
Ellis Anticline	80
Canadian Flexure	81
Structural Highs versus Topographic Highs	83
Cores	86
Production and Reservoir Parameters	86
PART VIII – Prairie Gem Field Hunton Reservoir Study	
Introduction	88
Stratigraphy	89
Basinward Distribution of Prairie Gem Producing Facies	99
Dolomitization of Hunton Strata	101
Possible Model for Silurian Dolomitization	105
Isopach Mapping	108
Structure	108
Production	109
Reservoir Observations for the Carney Hunton Play	111
Observations on Production for the Carney Hunton Play	112
Possible Explanation for “Retrograde Oil” Production	114
References Cited	121
Appendix 1: Application of Submersible Pumps to Hunton Reservoirs	126
Appendix 2: Glossary of Terms	127
Appendix 3: Abbreviations and Symbols Used in This Volume	131

LIST OF ILLUSTRATIONS

Figures

Part I—Workshop Overview

1. Generalized location map of Oklahoma and adjacent areas, illustrating areas of study 2

Part II—Carbonate-Reservoir Basics

2. Typical carbonate facies that develop within the three main zones of carbonate deposition 7
3. A platform's seaward edge steepens with time because subsidence cannot keep pace with carbonate sedimentation 7
4. Carbonate-rock fabric and nonfabric pore geometries and the processes that create them 8
5. Paths of diagenesis of carbonate rocks 8

Part III—History of Hunton Oil and Gas

6. Oklahoma geologic provinces and selected oil and gas fields that produce from Hunton Group rocks 9
7. Seminole area oil fields, in Pottawatomie, Seminole, and Pontotoc Counties 11
8. Structure map depicting the top of the Ordovician (Viola) in the Seminole area 11
9. Structure map depicting the top of the Hunton Group in Fitts field 12
10. Structural cross section A–A' across Fitts field 13
11. Structure-contour map of West Edmond field, depicting the top of the Haragan Formation 14
12. Structural cross section A–B, West Edmond field.. 14
13. Structure map depicting the top of the Hunton Group in the Anadarko basin 15
14. Cross section and structure map of North Custer City field 16
15. Structure map of Aledo field, depicting the top of the Hunton Group 17
16. Structure map and cross section of West Mayfield field 18
17. Structure map of Golden Trend, depicting the top of the Hunton Group 19
18. Structure map of part of Antioch area in the Golden Trend at the top of the Hunton Group 20
19. Distribution of wells producing oil and/or gas from Hunton reservoirs 20

Part IV—Hunton Stratigraphy

20. Correlation charts showing stratigraphic relationships of Ordovician through Mississippian strata 22–23
21. Type log showing Hunton Group formations, members, and other subdivisions 24
22. Schematic Ordovician paleogeologic maps 25
23. Northwest–southeast stratigraphic cross section, showing gradation of Sylvan Shale 26
24. Isopach map of the Sylvan Shale in Seminole County 27
25. Cross section A–A', illustrating Hunton strata deposited on a Sylvan erosional surface 28

26. Lithofacies–biofacies pattern in strata of Chimneyhill Subgroup 29
27. Distribution of Henryhouse marlstone facies in the southern Midcontinent region 31
28. Distribution of major lithofacies in Henryhouse Formation and correlative *Kirkidium* biofacies 32
29. Schematic cross sections illustrating proposed northward shifting of the Silurian depocenter in the Anadarko basin 33
30. Northwest–southeast stratigraphic section showing Henryhouse–Haragan/Bois d'Arc stratigraphic relationships 35
31. Frequency diagrams showing distribution of $MgCO_3$ in Frisco Formation 36

Part V—Facies, Dolomitization, and Karstification

32. General stratigraphic nomenclature of the Hunton Group in Oklahoma 40
33. Cross section showing the Henryhouse–Haragan/Bois d'Arc type 1 carbonate sequence, bounding unconformities, and correlation of outcrop and subsurface facies 41
34. Distribution of subtidal, intertidal, and supratidal facies in the Henryhouse Formation 41
35. Generalized model of depositional environments and facies of the Henryhouse Formation 42
36. Typical vertical facies sequence, showing sedimentological, faunal, and mineralogical features 42
37. Photomicrographs of oolitic subfacies 43
38. Pre-Woodford subcrop map of the Hunton Group showing lagoonal and shoal subfacies 43
39. Dolomite types in the Hunton Group 44
40. Movement of hypersaline brines and their role in dolomitizing Hunton carbonate during regression.. 45
41. Porosity types in the Hunton Group 45
42. Examples of breccia types from the Hunton Group 46
43. Enlarged moldic porosity in dolo-wackestone with vugs greater than twice the average grain size 47
44. Hunton oil and gas fields in the Anadarko basin, and the dolomite porosity fairway 48
45. Woodford Shale thickness in the Anadarko basin, major paleodrainage patterns, and Hunton penetrations 48
46. Hunton dolomite porosity fairway in the Anadarko basin, with DST permeability indexes 49
47. Hunton Group thickness in the Anadarko basin, showing relationship between thinning or truncation of the Hunton and productive trends 49

Part VI—Leedey Field

48. Leedey field Hunton study area, Dewey County ... 51
49. Producing reservoirs for wells in Leedey field Hunton study area 52
50. Type log for Leedey field showing Hunton units .. 54
51. Stratigraphic cross section C–C' and index map of Leedey field in envelope

52. Gross-isopach map of Hunton Group in Leedey field study area	55	80. Isopach map of net porosity in East Arnett field study area	77
53. Hypothetical stratigraphic sections, showing rock-stratigraphic units and time-stratigraphic units ...	56	81. Structure-contour map of top of Hunton Group in East Arnett field study area	78
54. Two hypotheses for Woodford Shale deposition ..	56	82. Type log indicating section isopached in Figure 83 .	79
55. Isopach map of Woodford Shale in Leedey field study area	57	83. Isopach map of interval from top of Chester "B" zone to top of Woodford Shale	79
56. Schematic cross sections showing two stages of post-Hunton erosion and subsequent deposition of Woodford Shale	58	84. Paleozoic structural features identified from Hunton, Mississippian, and Pennsylvanian isopach and structure maps	80
57. Isopach map of Woodford channel-fill facies	59	85. Structure-contour map of top of Sylvan Shale in Canadian County	81
58. Isopach map of Woodford channel-fill facies in Leedey field study area	60	86. Isopach map of Chimneyhill Subgroup in Canadian County	82
59. Isopach map of restored Hunton thickness	61	87. Northwest-southeast stratigraphic cross section H-H'	in envelope
60. Composite map of restored Hunton isopachs and restored Woodford channel-fill facies	62	88. Relation of Viola and Simpson production to faults as determined by Chimneyhill isopach map and Sylvan structure map	83
61. Isopach map of Hunton Group in Leedey field study area	63	89. Isopach map of Woodford Shale	84
62. Isopach map of restored Hunton sequence	64	90. Isopach map of lower member of Woodford Shale	85
63. Isopach map of Hunton thickness plus uncompacted thickness of Woodford Shale and Kinderhook shale	65	91. Modified cross section B-B' showing restored Woodford and Hunton thicknesses	85
64. Structure-contour map depicting top of Hunton Group in Leedy field study area	66	92. Gas-production curve for East Arnett Hunton field study area	87
65. Isopach map of Hunton thickness plus uncompacted thickness of Woodford Shale and Kinderhook shale	67		
66. Cross section D-D', constructed by using compacted present-day Woodford Shale thicknesses..	68	<i>Part VIII—Prairie Gem Field</i>	
67. Schematic cross sections interpreting Woodford Shale compaction	68	93. Prairie Gem field Hunton study area, Lincoln County	88
68. Revised cross section D-D', constructed by using restored Woodford Shale thicknesses	69	94. South-north stratigraphic section P-P' across Prairie Gem field	in envelope
69. Isopach map of Kinderhook shale	69	95. Operators, lease names, well numbers, and producing reservoirs for wells in Prairie Gem field	89
70. Schematic cross sections, illustrating incorrect method of using present-day Woodford Shale thicknesses, and correct method of using restored Woodford Shale thicknesses, when exploring for Hunton Group porosity seals from Woodford Shale channel deposits	70	96. Type log for Prairie Gem Hunton field showing Hunton formations	89
71. Gas-production curve for Leedey field Hunton study area	70	97. Comparison of sigma shape of SP curves	90
		98. Stratigraphic cross section I-I'	91
<i>Part VII—East Arnett Field</i>		99. Location map for cross sections I-I', J-J', K-K', L-L', and M-M'	91
72. East Arnett field Hunton study area, Ellis County..	71	100. Cross sections J-J', K-K', and L-L'	92
73. Stratigraphic cross section E-E' showing inferred relationships of Viola-Sylvan-Hunton-Woodford strata	72	101. Revised cross section I-I'	92
74. South-north stratigraphic cross section F-F'	in envelope	102. Gross-isopach map of Hunton Group	93
75. West-east cross section G-G'	in envelope	103. Isopach map of zone C of Hunton Group	93
76. Producing reservoir(s) for wells in East Arnett Hunton field study area	72	104. Isopach map of zone B of Hunton Group	94
77. Type log for East Arnett field showing Hunton section	74	105. Isopach map of zone A of Hunton Group	94
78. Gross-isopach map of Hunton Group in East Arnett field study area	75	106. Depositional model showing details of progradation and aggradation	95
79. Isopach map of Woodford Shale in East Arnett field study area	76	107. Schematic cross sections	96
		108. (A) Schematic environmental model of a submarine fan; (B-F) Hypothetical submarine-fan stratigraphic sequence produced by fan progradation	97
		109. Submarine fan at Shark Bay, Australia	98
		110. Hydrologic model for Ste. Genevieve Limestone in Bridgeport field area, Illinois	99
		111. West-east stratigraphic cross section N-N'	in envelope

(continued on next page)

112. Geologic map of North American craton showing Silurian deposits	100
113. Schematic section of two wells in eastern Oklahoma showing relationship of Frisco Formation to dolomites of Quarry Mountain and Sallisaw Formations	101
114. Frequency diagram based on analyses of surface samples and core samples	102
115. Relationship of porosity to $MgCO_3$	103
116. Geologic sketch map showing dolomite and limestone relationships	104
117. Southwest–northeast cross section O–O'	in envelope
118. Southwest–northeast cross section O–O', revised	in envelope
119. Mixing of meteoric fresh water with seawater may cause dolomitization	105
120. Percentage of dolomite in relation to channel deposits for Ste. Genevieve Limestone in Bridgeport field area, Illinois	106
121. Gross-isopach map of Hunton Group in Prairie Gem field study area	107
122. Isopach map of net Hunton zone B porosity in Prairie Gem field study area	108
123. Structure-contour map of top of Hunton Group in Prairie Gem field study area	109
124. Oil-production curve for Prairie Gem field	110
125. Oil, gas, and gas/oil-ratio curves for two Hunton wells	110
126. Isopach map of Mississippian strata in northwestern Lincoln County	111
127. South–north cross section Q–Q'	113
128. Typical curves for GOR and FVF for a reservoir producing above the bubble point	113
129. General GOR curves for three primary drive mechanisms	114
130. Schematic diagram of Hunton reservoir in contact with drillstem-test tool	116
131. Schematic diagram of Hunton reservoir in contact with completion string and producing with low-volume rod pump	116
132. Schematic diagram of Hunton reservoir in contact with completion string and producing with high-volume pump at virgin conditions....	117
133. Schematic diagram of Hunton reservoir in contact with completion string and producing with high-volume pump at mature conditions	117
134. Typical waterflood performance in water-wet and oil-wet sandstone cores at moderate oil/water viscosity ratios	119
135. Water–oil relative-permeability curves for strongly oil-wet rock	119

Plates

1. Isopach map of Hunton Group in envelope
2. Isopach map of Woodford Shale in envelope
3. Structure map of Hunton Group in envelope
4. Stratigraphic cross sections A–A' and B–B' in envelope
5. Isopach map of Chimneyhill Subgroup .. in envelope
6. Pre-Woodford subcrop map, Oklahoma and Texas Panhandle, showing wells studied in envelope

TABLES

1. Goals of the Hunton workshop	3
2. Classification of carbonate rocks according to depositional texture	6
3. Helpful steps in determining rock type in accord with Dunham's 1962 classification	6
4. Selected fields with Hunton oil and gas production in Oklahoma	10
5. Well tabulation keyed to Figure 49 showing data for Leedey field	53
6. Geological/engineering data for Hunton Limestone, Leedey field study area	68
7. Well tabulation keyed to Figure 76 showing data for East Arnett field	73
8. Geological/engineering data for Hunton Limestone, East Arnett field study area	86
9. Characteristics of Hunton strata in the Prairie Gem field study area	95
10. Geological/engineering data for Hunton Limestone, Prairie Gem oil field and Carney Hunton play	112
11. Reservoir parameters for the Carney Hunton play	114
12. Oil and gas initial production, initial GORs, and GFRs for parts of the Carney Hunton reservoir area	115

PART I

Overview and Goals of the Workshop

Kurt Rottmann

Consulting Geologist
Oklahoma City, Oklahoma

INTRODUCTION

Oklahoma is home to some of the largest oil- and gas-producing provinces in the continental United States. The Anadarko basin and Arkoma basin, with their associated Anadarko shelf and Cherokee platform provinces, respectively, have supplied significant production to our nation and will contribute abundant reserve potential for our future economic stability. The Hunton Group is one of the more important producing sequences of Oklahoma and is the principal subject of this workshop.

This study is regional in scope and will emphasize the lithostratigraphic–lithofacies relationships of the Hunton Group's individual formations and their relationships to the underlying Sylvan Shale and overlying Woodford Shale. Understanding and incorporating these relationships into any exploration or development program is vital to the success of that program. The shallower parts of the provinces previously mentioned have been drilled intensively, providing considerable geological information for defining such issues as environment of deposition, stratigraphic relationships, and economic potential. But large parts of these oil- and gas-producing provinces remain either essentially unexplored, as in the deep part of the Anadarko basin, or underdeveloped, as in the Carney Hunton high-water-cut production play currently in progress on the Cherokee platform in Lincoln County, Oklahoma.

This workshop will assimilate much of the existing geological information and use it as a basis for projecting profitable ventures into these underdeveloped areas.

PRIOR INVESTIGATIONS

In 1902, Taff studied Silurian–Lower Devonian strata that crop out in the Arbuckle Mountains–Criner Hills of south-central Oklahoma. This carbonate sequence lies between the Ordovician Sylvan Shale and the Late Devonian–Early Mississippian Woodford Shale. Taff named this carbonate sequence the Hunton Formation after the old Hunton townsite near the type section. This section is easily recognizable both in the surface and subsurface, owing to the overall shale–carbonate–shale sequence.

The Hunton has been the subject of many stratigraphic and paleontological studies. The following are some of the more important of these studies: Reeds (1911), Maxwell (1931), Christian (1953), Amsden (1958a,b, 1960, 1961, 1963a,b, 1968, 1974, 1975, 1980, 1993), Amsden and Rowland (1965), Amsden and Ventress (1963), Barrick and Klapper (1976), Campbell (1967, 1977), Lundin (1965, 1968), Sutherland (1965), and Amsden and Barrick (1988). Information from these studies and from my own studies was used as the framework for this workshop.

The Hunton was later elevated to group status to include all the Late Ordovician (Keel Formation) through Early Devonian (Sallisaw Formation) carbonate strata (Amsden, 1980). For the deep Anadarko basin, Amsden suggested that this sequence probably represents continuous deposition and may include some late Early and Middle Devonian carbonate strata (Amsden, 1980, p. 8).

AREA OF STUDY

In the early days of exploration, much of what was known about the Hunton was derived from the analysis of surface exposures in the Arbuckle Mountains–Criner Hills area of south-central Oklahoma and outcrops in the vicinity of Marble City, northeastern Oklahoma. Little biostratigraphic information was known concerning the age and lithologic relationships of the Hunton in the deeper parts of the Anadarko and Arkoma basins. Correlations by geophysical logs from the outcrop areas into the basins obviously confirmed the shale–carbonate–shale relationships of the Sylvan, Hunton, and Woodford, but detailed biostratigraphic information was lacking for determining or confirming age relationships of the various formations of the Hunton mapped in the subsurface. As a result, much of the older literature concerning formation identification is not precise or is erroneous—not so much from the lack of well control but from the complex internal changes that occur laterally in carbonate stratigraphy that often are not recognizable on geophysical logs alone.

In 1975, 1980, and again in 1993, Thomas W. Amsden published, through the Oklahoma Geological Sur-

vey, two bulletins and an appendix to a map set that were of monumental importance in contributing to our understanding of the biostratigraphy and lithostratigraphy of the Hunton Group in the Anadarko and Arkoma basins. These publications include biostratigraphic information from more than 140 cores that play a large part in understanding the distribution, stratigraphic relationships, and ages of the various formations of the Hunton Group in the deeper parts of the basins.

The cores were examined for fossil content, especially for megafossils. Other researchers, including P. K. Sutherland, J. E. Barrick, and Gilbert Klapper, collaborated with Amsden in identifying and determining age relationships of the faunal content of these cores. The lithostratigraphic character of the cores was studied from hand samples, thin sections, and chemical analysis. Approximately 400–500 thin sections were studied for calcium carbonate (CaCO_3) and magnesium carbonate (MgCO_3) content, terrigenous detritus or HCl-insoluble residues, fossils, character and kind of cement, porosity and permeability, and other textural features. However, because most of the cores were obtained from the shallower parts of the Anadarko and Arkoma basins, Amsden also incorporated well samples, or cuttings, from more than 145 wells to supplement this information in those areas where core information was lacking or sparse. Many of these samples came from the Arkoma basin and from those wells generally deeper than 15,000 ft in the Anadarko basin, and from the shallow fault blocks adjacent to the Wichita uplift. These samples were studied megascopically and were supplemented by more than 1,000 thin sections, most of which were treated with alizarin Red-S to distinguish dolomite from calcite. The thin sections also were used to analyze terrigenous material, cement, and other textural features. Thin sections from samples provided little biostratigraphic information, but, coupled with information from the cores and surface exposures, they should enable a reasonable interpretation of Hunton strata where core information is lacking.

Figure 1 illustrates the area of investigation for Amsden's 1975 and 1980 publications. A third source of information used for those studies was open-hole logs. Amsden points out in the 1975 report that open-hole logs were used mainly to check the Woodford–Hunton and Hunton–Sylvan contacts. However, correlation of the various lithostratigraphic divisions from the core and sample logs was also possible, owing to common characteristic features on gamma-ray and spontaneous-potential (SP) logs. In Amsden's 1980 publication, open-hole logs were heavily incorporated with the subsurface mapping in the Arkoma basin. This was true in areas of sparse control. In areas of dense drilling (ap-

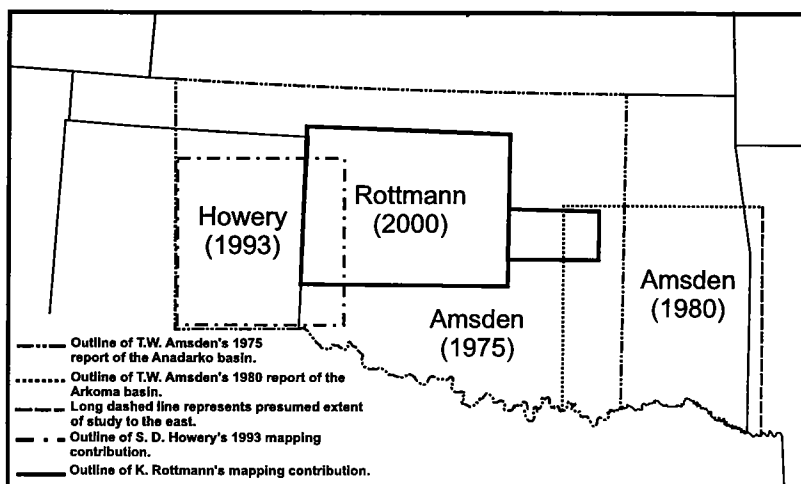


Figure 1. Generalized location map of Oklahoma and adjacent areas, illustrating areas of study. Patterned lines indicate Amsden's 1975 report of the Anadarko basin, his 1980 report of the Arkoma basin, Howery's contribution, and Rottmann's current contribution.

proximately R. 4 E. to R. 9 E.), about one well per section was incorporated.

Figure 1 shows the area of my research. I incorporated Amsden's biostratigraphic control in a study of the Hunton Group involving more than 2,000 geophysical logs, mainly gamma-ray logs. Because of the distribution of the wells from which Amsden studied cores and samples, I was able to correlate most of the wells within the study area. The mapping on Plates 1, 2, 3, 5, and 6 (in envelope) represents a merging of Amsden's 1975 and 1980 mapping with my 2000 version, with the intent of supplying the operator or explorationist with as thorough and complete regional mapping as possible for the Hunton Group. Figure 1 also shows an area of contribution from Sherrill Howery. His structure mapping of the Texas Panhandle and deep Anadarko basin was incorporated in Plate 3. Plate 4 (in envelope) represents two regional cross sections, one from eastern to western Oklahoma, and the other from southern to northern Oklahoma. These cross sections show various regional facies relationships for the Hunton.

GOALS

In light of the thoroughness of previous investigations of the Hunton Group and the density of well control, it would seem that any further Hunton studies would simply be rephrasing or rehashing old information. This could not be further from the truth, for two reasons. First, approximately one-half of the Anadarko basin is relatively unexplored. The overpressured Atoka, Morrow, and Springer reservoirs serve to mark a boundary between relatively inexpensive Hunton penetrations and expensive and complicated ones. *Complicated* and *expensive*, by definition, mean that an operator must set an intermediate string of casing to protect lower pressured formations (e.g., Upper Pennsylvanian, Mississippian, Hunton) from the overpres-

TABLE 1. — Goals of the Hunton Workshop

1. Attempt to project trends and depositional environments into the deep Anadarko basin based upon increased well control from the shelf.
2. Tie Dr. Amsden's paleontological and lithologic descriptions into the subsurface.
3. Discuss the importance of karstification on the Hunton paleotopographic surface, with implications for reservoir development.
4. Address the Hunton–Woodford stratigraphic relationships and their effect on reservoir geometry.
5. Discuss the effects of structure on Hunton reservoirs and address the concept of persistent structural movement during the Paleozoic.
6. Discuss possible origins and depositional environments of the dolomites of the Chimneyhill Subgroup and Henryhouse Formation.
7. Offer suggestions for completion techniques of high-water-cut Hunton oil reservoirs.

sured reservoirs of the Morrow and Springer. Because of the high cost of drilling Hunton tests in the overpressured areas, it is necessary that a knowledge of potential pay zones—such as reservoir characteristics, depositional environment, and lateral lithofacies—be extrapolated from the shallow part of the Anadarko basin to the deep part.

A second reason for the need of further research on the Hunton Group has become obvious by the recent “retrograde oil cut” (ROC; term applied by the University of Tulsa) play presently in progress on the Cherokee platform. New production techniques have turned virtually uneconomic Hunton stripper wells into highly profitable Hunton producers. With respect to this production technique, it has become obvious that only an intimate knowledge of a reservoir's depositional environment and parameters will separate a potentially productive well from an unproductive one.

A list of goals for this workshop and publication is given in Table 1. It is the mutual feeling of the authors that these subjects will provide a thorough understanding of important exploratory issues regarding the Hunton Group necessary for its successful exploration.

ACKNOWLEDGMENTS

Sincere appreciation is extended to those individuals and companies who have contributed to the success of this workshop and publication.

First, I would like to thank the Petroleum Technology Transfer Council and the Oklahoma Geological Survey, University of Oklahoma, for making this workshop possible. Their dedication and encouragement as a group are largely responsible for the quality and pro-

fessionalism of these workshops. I thank Wayne Furr, manager of cartography, and Jim Anderson, OGS cartographic drafting technician, for their work on the plates and figures. I wish to thank Christie Cooper, OGS editor, and William D. Rose, geologist/contract editor, for their input and effort toward completing this publication. Sincere appreciation is extended to Jock Campbell, OGS geologist, for his review and encouragement toward improving the text and illustrations of this publication, and to Tom Stanley, OGS geologist, for his insight and contributions to the Hunton field trip. I would like to thank David Brown, Geo Information Systems, University of Oklahoma, for his time and contributions. I especially thank Walt Esry, Larry Austin, and Ivy Graham, OGS Core and Sample Library, for their efforts and support. I am grateful to Michelle Summers, OGS technical project coordinator, for her organization and support of the workshop. I am deeply grateful to Charles J. Mankin, OGS director, whose support and dedication to this workshop has been a key contribution toward its success.

I wish to thank the many individuals and companies who have contributed time, information, data, and advice for this publication. I thank Andrew Abarr (petroleum engineer, Oklahoma City), Louis Boyce (Statco Engineering, Oklahoma City), and David Crutchfield (reservoir engineer, Oklahoma City) for their insights and advice on reservoir and production issues. I thank T. L. Rowland (consulting geologist, Oklahoma City) for his memorial to Thomas W. Amsden. I thank Sherrill D. Howery (consulting geologist, Oklahoma City) for his contribution to this publication. I thank Edward A. Beaumont (consulting geologist, Tulsa) for his contribution to the publication and as a guest lecturer. I thank Zuhair Al-Shaieb, Jim Puckette, and Paul Blubaugh (Oklahoma State University) for their contribution to this publication, providing core for review, and for contributing a guest lecturer. I thank Paul Bryden (geologist, New Dominion LLC, Tulsa) for his review of parts of the manuscript and his insight into Hunton concepts. I thank David Chernicky (president, New Dominion LLC, Tulsa) and John Special (president, Special Energy, Stillwater) for support of this publication. I especially want to thank Bob Northcutt (independent geologist, Oklahoma City) for his support, insight, and review of the manuscript and for serving as a guest lecturer. Special thanks are extended to Pat Brown (production engineer, New Dominion LLC, Stillwater) for his insight, advice, and contribution to this publication and for serving as a guest lecturer. I express sincere gratitude and deep respect for the memory of Dr. Thomas W. Amsden; his tireless dedication to the understanding of the Silurian–Devonian Hunton sequence was instrumental in making this publication possible.

And I would like to thank my wife, Karen, for the many hours she dedicated to typing, transferring data, map making, critiquing, and assisting me. Her effort has been appreciated more than she will ever know.

PART II

Carbonate-Reservoir Basics

Edward A. Beaumont

Consulting Geologist
Tulsa, Oklahoma

INTRODUCTION

Carbonate reservoirs range from pure limestone (CaCO_3) to pure dolomite ($(\text{Ca}_{1-x}\text{Mg}_x)\text{CO}_3$), where x , in the dolomite formula, is in the range of 0.4. Carbonates whose x values range from 0.01 to 0.25 are termed *dolomitic limestones* to *calcitic dolomites*, respectively. There are many ways in which carbonates are formed, the most common being an interplay of hydrologic and biologic factors. This contrasts sharply with the ways in which clastic sediments like sandstones and shales are formed, which are deposited as the result of an interplay of hydrologic and erosional factors. Sands are carried into a basin by wind or water.

The most common way carbonates are formed involves the life and death of carbonate-producing organisms. These carbonate particles are commonly the hard parts of invertebrates. These organisms have secreted their calcareous hard parts either as the mineral aragonite or as low-magnesium or high-magnesium calcite. The reason why certain faunas secrete certain minerals is not fully known.

Some of the more important carbonate-secreting organisms include mollusks, brachiopods, corals, foraminifers, echinoderms, and calcareous benthic and planktonic algae. These organisms form a biotic community, resulting in a typically characteristic death assemblage of calcareous debris. The carbonate secretions are usually modified by postmortem physical, chemical, and biological destruction and redistribution. Deposition of these biogenic carbonate sediments is usually limited to water that is warm, shallow, clear, sunlit, and free of suspended clay, because most faunas require these conditions. When these conditions prevail, carbonates can accumulate rapidly. Some oceanic carbonates may form from the settling of carbonate material from carbonate-secreting pelagic organisms. These deposits usually occur as calcareous oozes, which accumulate slowly in maximum water depths of 3.5–5 km (Leeder, 1983). Water depths exceeding these ranges become understaturated with respect to carbonates, with the material being subject to re-solution.

A second method of carbonate deposition is that of carbonate precipitation. Shallow seawater is supersaturated with respect to aragonite, calcite, and dolo-

mite, and of the three, only aragonite seems to precipitate directly from seawater, with calcite and dolomite generally forming diagenetically from a pore-water environment. One possible explanation for this comes from the experimental and theoretical studies that indicate that Mg^{2+} ions inhibit the growth of calcite and not aragonite (Leeder, 1983). Oolites are a specific type of carbonate that is partially formed by precipitation of carbonate material about a nucleus usually composed of detrital material. Oolites are spherical to slightly ovoid, well-rounded particles that are composed of concentrically laminated layers of fine-grained aragonite or high-magnesium calcite. They usually occur in areas of strong tidal currents such as sand-wave or dune complexes (Leeder, 1983).

Sandstone reservoirs have simple pore networks in comparison to carbonates. Besides pore space between grains (intergranular), pore space in carbonates can be the result of solution of the rock or recrystallization of the rock from limestone to dolomite. Complex pore systems make the evaluation of carbonate reservoirs more difficult, and therefore riskier, than the evaluation of sandstone reservoirs. Learning about carbonate deposition and the processes that create or destroy porosity (diagenesis) can lead to better exploration and development decisions regarding carbonate reservoirs.

CARBONATE-MINERAL TYPES

The principal carbonate minerals found in rocks today are calcite and dolomite; the latter is commonly referred to as $\text{CaMg}(\text{CO}_3)_2$. Calcium carbonate (CaCO_3) in limestone occurs as the mineral polymorphs calcite and aragonite. Ancient limestones are generally composed of low-magnesium calcite, whereas modern limestones are generally composed of aragonite and high-magnesium calcite. Aragonite is formed by many invertebrate faunas, including algae, pelecypods, and bryozoans. Calcite and high-magnesium calcite are secreted by echinoids, crinoids, foraminifers, and by some algae, pelecypods, and gastropods (Selley, 1988). Dolomite is commonly found in ancient carbonates and is usually formed as a secondary replacement mineral in crystalline form or by primary precipitation or pene-

contemporaneous replacement of other carbonates in cryptocrystalline form. Dolomite does not form as a biogenic skeletal mineral.

Siderite, which is an iron carbonate (FeCO_3), is a rarer form of carbonate. Its occurrence is primarily as a precipitate in oolites. It can also occur as thin bands or concretions in shaly deposits, especially in deltaic facies. These bands usually become contorted or fractured by soft-sediment deformation (Selley, 1988).

Carbonate diagenesis has important implications for the hydrocarbon potential of carbonate reservoirs. The lack of aragonite in ancient sediments is caused by the instability of aragonite near the Earth's surface, although aragonite is stable under high-pressure conditions such as those for blueschist metamorphic facies. Increases in temperature brought about by burial may cause aragonite crystals to convert to calcite crystals. This conversion results in a general loss of pore space (Bathurst, 1975). A second alteration that may occur is the conversion of calcite or magnesium-rich calcite to dolomite, either by the additional presence of magnesium made available in mobile pore water or by the increased saturation of dolomite as a result of mixing of formation water and meteoric water (Badiozamani, 1973). The alteration of low- or high-magnesium calcites to dolomites results in an increase of pore volume. A third alteration that may occur is a magnesium-rich calcite recrystallizing as a low-magnesium calcite.

CARBONATE-ROCK TYPES

Carbonate classification depends upon recognition of the physical components of carbonate rocks. These primary components include grain type, matrix, and cement. Pore space represents a secondary aspect of carbonate classification. The following is a brief description of the three primary components.

Grains

Grains are the particles that constitute the framework of the carbonate. There are many types of grains, which are usually sand size or larger.

The first type of grain is detrital, which consists of (1) lithoclasts, rock fragments that originated outside the depositional area, and (2) intraclasts, which are re-worked rock fragments.

A second major grain type, perhaps the most important, is that composed of skeletal debris or bioclastic material. The size of skeletal material may vary sharply, ranging from the largest shell to individual crystals of aragonite or calcite secreted by organisms. These grains are commonly modified by abrasion from wave or current action and by biological processes that modify or destroy the original fabric.

A third type of grain is peloids, which are composed predominantly of pellets. Pellets are formed by marine invertebrates as excrement of fecal material that crystallizes into carbonate material. The origin of peloids is important, because this grain type may constitute most

of the carbonate in some Paleozoic limestones. The peloids represent a sheltered, shallow inner-shelf environment characteristic of lagoons. Where several peloids are held together by micrite, these aggregations are termed *lumps* or *grapestones*.

The last of the major grain types is coated grains, which show a concentric or radial arrangement of crystals about a nucleus, as mentioned and described previously. The most common of these are the oolites contained in a sedimentary rock called an *oolite*. Oolites commonly contain a nucleus composed of a quartz grain or a shell fragment. Oolites tend to occur in environments of high energy such as sand banks or tidal deltas. They are generally well sorted, matrix free, and cross-bedded. They are thought to be formed by the bonding of aragonite crystals around the nuclei in environments where cool, dilute seawater mixes with warm, concentrated waters of lagoons and restricted shelves (Selley, 1988). Blue-green algae may contribute to oolite formation by facilitating aragonite precipitation.

Matrix

Matrix, by definition, is the finer grained material that encloses, or fills the interstices between, the larger grains or particles of a sediment or sedimentary rock. In carbonate sedimentary rocks, the matrix usually consists of clay minerals or micritic components surrounding coarser material (Jackson, 1997). Carbonate mud is termed *micrite*. It may be present in small quantities as a matrix within a grain-supported carbonate sand, or it may compose the majority of the rock, forming a mudstone or micrite. Modern lime muds are composed of aragonite, and ancient lime sedimentary rocks are composed of calcite. Several processes are thought to be responsible for lime-mud formation. The abrasive action of wind, waves, tides, and currents may grind up bioclastic material almost to its individual constituent crystals. Biological action, such as burrowing or ingestion of carbonate fragments by organisms, serves to break up the carbonate fragments into minuscule particles. The pitting of blue-green algae on skeletal fragments leads to micritization of the grain surfaces.

Micrite may form as an inorganic precipitation of aragonite muds. *Whittings*, in the Bahamas and the Persian Gulf, are waters in which carbonate material is suspended, producing a white color and containing needlelike aragonite crystals that have been precipitated from supersaturated seawater. Micrite can also form as a secondary cryptocrystalline cement.

Cement

The third component of carbonate rocks is cement, which is the crystalline material that grows within the sediment fabric during diagenesis (Selley, 1988). The most common cement in limestones is calcite and is termed *spar* or *sparite*. Other types of cement include dolomite, anhydrite, and silica.

TABLE 2. – Classification of Carbonate Rocks According to Depositional Texture^a

Depositional Texture Recognizable					Depositional Texture Not Recognizable
Original components not bound together during deposition			Lacks mud and is grain-supported	Original components were bound together during deposition . . . as shown by inter-grown skeletal matter, lamination contrary to gravity, or sediment-floored cavities that are roofed over by organic or questionably organic matter and are too large to be interstices	
Contains mud (particles of clay and fine silt size)		Grain-supported			
Mud-supported					
Less than 10% grains	More than 10% grains				
Mudstone	Wackestone	Packstone	Grainstone	Boundstone	
					<i>Crystalline carbonate</i>
					(Subdivide according to classifications designed to bear on physical texture or diagenesis)

^aModified from Dunham (1962, table I).

The classification of a rock type may be accomplished by two useful but different classification methods. The first, proposed by Folk in 1962, divides limestones into two major clans—either micrites or sparites, depending upon the amount or predominance of each sort of matrix in the rock. Each of these major divisions is subdivided according to the major components or allochems present. Perhaps a disadvantage of this classification method is that it ignores rather recent or partially lithified limestones with abundant pore spaces.

A second method of carbonate classification was proposed by R. J. Durham in 1962. This method represents a classification of carbonate rocks according to depositional texture (Table 2). The advantage of Dunham's classification is that it is not dependent upon cement content, and thus unlithified carbonate sediments may be classified. Thus, the classification is based upon depositional characteristics. Table 3 is a simple chart with several steps for using Dunham's method for classifying carbonate rocks. Three aspects of carbonate texture are taken into account: (1) the presence or absence of carbonate mud, (2) the abundance of grains, and (3) the amount of binding by organisms growing together. The amount of grains present in the rock tells something about how the rock was deposited. In high-energy environments, little or no mud is present. There are five basic rock types in this classification: grainstone, packstone, wackestone, mudstone, and boundstone.

CARBONATE DEPOSITIONAL SETTINGS

In general, carbonate facies are formed within limited depositional environments. For carbonate sedimentation to occur, this environment usually must be

TABLE 3. – Helpful Steps in Determining Rock Type in Accord with Dunham's 1962 Classification

Step	Rock texture
1	Can you recognize any original texture in the rock? If yes, go to step 2. If no, then the rock is a crystalline carbonate (usually a dolomitic crystalline carbonate).
2	Were the original constituents bound together during deposition? If yes, the rock is a boundstone. If no, go to step 3.
3	Is carbonate mud present in the rock? If no, then the rock is a grainstone. If yes, then go to step 4.
4	Do the grains touch one another? If yes, then the rock is a packstone. If no, then go to step 5.
5	Does 10% of the rock consist of grains? If yes, then the rock is a wackestone. If no, then the rock is a mudstone.

that of a warm, generally shallow, clear marine water. These conditions are favorable for marine life, which accounts for the majority of carbonate biogenic material. Carbonate formation is generally thought of as being autochthonous, which implies that it was formed or produced in place. This is opposed to allochthonous material, which was formed elsewhere and introduced to its present depositional position. In carbonate environments, it is not uncommon for wave, tidal, or current action to displace organic material, thereby modifying the texture or the material in the process.

The factors that commonly control carbonate-facies distribution are depositional slope, geologic age, water energy, and climate. Light control is also important, which limits biological production to the photic zone, or that portion where there is sufficient light penetration to support photosynthesis.

Carbonate facies develop on gently sloping shelves that can be divided into three main zones. The first is a basinward zone below normal wave base, extending into deep water. The facies patterns associated with this environment are the basin, slope, and slope-mound patterns illustrated in Figure 2. The carbonate facies associated with a deep-water (basinal) environment are lime mudstones and pelagic oozes. Near the shelf margin, biogenic muds may occur as well as debris flows and turbidites.

A second zone is where wave energy interacts with the sediment between low and high tide. This is a high-energy environment marked by the transport and winnowing of sediments and by organic buildups of mounds and reefs. The facies patterns of Figure 2 associated with this environment are the slope mound and shelf crest and may contain talus deposits, mounds, reefs, islands, dunes, barrier bars, passes, and tidal flats and channels. Lagoonal facies are low-energy areas within this pattern.

A third zone is that of a landward low-energy zone. This is usually the area above high tide. It is generally dominated by increased sediment pore-water salinity, which leads to evaporite precipitation and dolomitization. The environments of deposition for this zone include sabkhas and supratidal marshes.

Figure 3 illustrates a stratigraphic model showing the creation of a shelf-to-basin topography caused by differential rates of carbonate sedimentation. The zone of clastic influx is that area where fluvial processes interact with marine processes. Carbonate production is limited or hindered by the influx of clastic material. The zone of optimum carbonate production is generally the warm, shallow photic zone of the subtidal environment. The high organic productivity leads to the production of carbonate platforms that project basinward. The basinward limit of these platforms is a sudden break in slope, commonly at the maximum depth of the photic zone and marking the zone of diminished carbonate production (Leeder, 1983).

There is a balance between subsidence and rate of sedimentation. Carbonate deposits may accumulate rapidly under favorable conditions. The result can be a regressive pattern or a basinward projec-

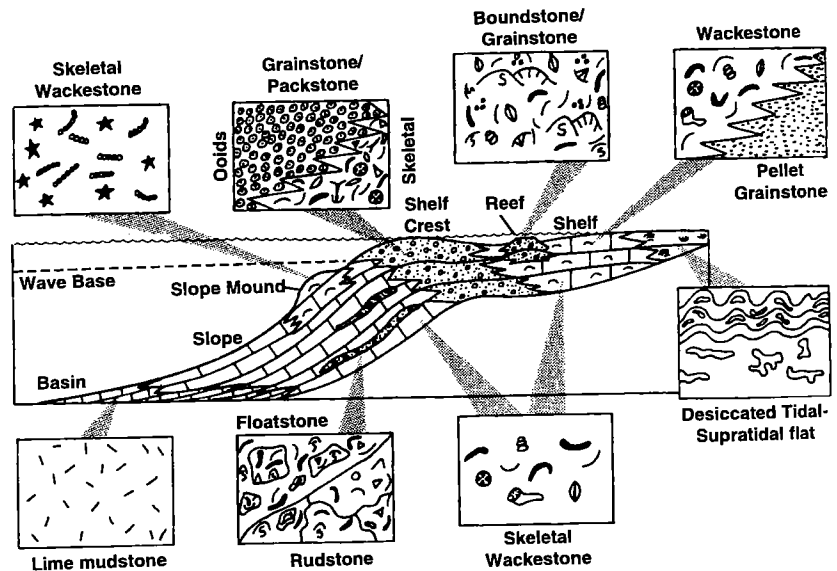


Figure 2. Diagram showing typical carbonate facies that develop within the three main zones of carbonate deposition. Modified from Sarg (1988); reprinted by permission of Society for Sedimentary Geology (SEPM).

tion of the shelf margin with either steplike or steady outbuilding of carbonate platforms.

PRESERVATION OR DESTRUCTION OF PORE SPACE

How much influence do the original constituents of a carbonate rock (grains, mud, and pore space) have to do with the porosity and permeability preserved in the rock after millions of years of burial? Which processes have more impact on reservoir quality of carbonates—the ones that occur soon after deposition, or the ones that occur later after deep burial? The interaction of *early* rock-forming processes determines, in most cases, the ultimate reservoir quality of carbonate rocks. A rock that begins with good porosity and permeability has a better chance of retaining those qualities than does a poor-quality rock for becoming a good-quality rock later. One should be aware of the possibility that porosity can be created late in a rock's life; however, concentrating on the early history of a carbonate rock generally will be more rewarding when searching for reservoir-quality rocks.

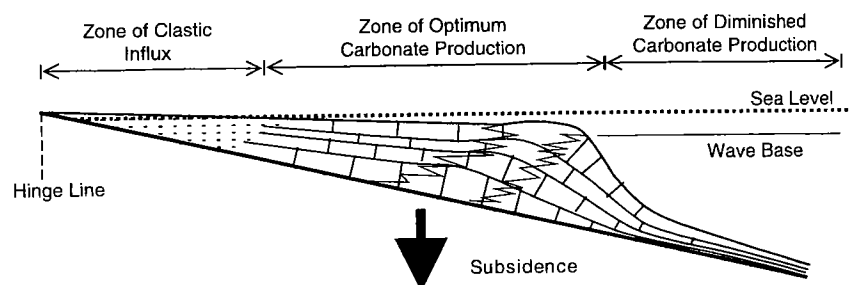


Figure 3. As shown in Figure 2, a platform's seaward edge steepens with time because subsidence cannot keep pace with carbonate sedimentation.






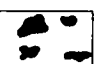
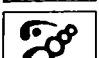

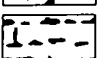
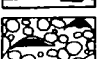

Fabric Selective Porosity		Nonfabric Selective Porosity	
Geometry	Genesis	Geometry	Genesis
 Interparticle	Diagenetic	 Fracture	Deformation
 Intraparticle	Depositional	 Channel	Dissolution
 Intercrystalline	Diagenetic	 Vug	Dissolution
 Moldic	Diagenetic	 Cavern	Dissolution
 Fenestral	Depositional		
 Shelter	Depositional		
 Growth or Framework	Depositional		

Figure 4. Diagram showing carbonate-rock fabric and nonfabric pore geometries and the processes that create them. Modified from Choquette and Pray (1970); reprinted by permission of American Association of Petroleum Geologists.

The initial solid constituents of a carbonate rock normally determine its initial pore type and geometry, and strongly influence diagenesis. Early pore space in carbonate rocks generally has fabric-selective characteristics, but late pore space does not (Choquette and Pray, 1970). Surface and shallow diagenesis mainly occurs in fabric-selective pore geometries that allow the greatest fluid flow (mostly interparticle or intercrystalline). Late-stage shallow diagenesis occurs mainly in nonfabric-selective pore geometries that allow the greatest fluid flow (mostly fracture related). Deep diagenetic processes can be both fabric selective (fluid flow through interparticle or intercrystalline pores) and nonfabric selective (compaction).

Figure 4 shows fabric and nonfabric pore geometries and the processes that create them. Three major geologic stages determine the porosity of carbonate rocks (Choquette and Pray, 1970):

1. Pre-depositional.—This stage is the time when sedimentary material first forms to the time when it is finally deposited. Porosity created during the pre-depositional stage is mainly chambers or cell structures of skeletal grains or within non-skeletal grains such as pellets or ooids.

2. Depositional.—This stage is the relatively short time involved in final deposition at the site of ultimate burial of a carbonate sediment. Most porosity formed is intergranular, although some can be framework.

3. Post-depositional.—This stage is all the time that elapses after final deposition. All the porosity that forms during this stage is diagenetic or secondary in origin. Diagenetic processes are related to changes in water chemistry, water movement, and changes in temperature and pressure. This time period obviously can be quite long and can be divided into early, middle, and late.

The parts of the path of diagenesis a carbonate sediment follows determine the evolution of its porosity. Figure 5, modified from Harris (1985), summarizes the diagenesis that occurs along this path. Some pore systems gain

quality as a result of diagenesis; however, the general trend of pore-system quality with time and burial is toward destruction. Certain processes can temporarily interrupt this trend, which are “preserved” pore systems. Some of the processes that preserve pore systems (Feazel and Schatzinger, 1985) are (1) reduced burial stress from overpressuring, (2) increased rigidity of framework grains, (3) oil entry into pore space, and (4) permeability barriers that isolate the reservoir.

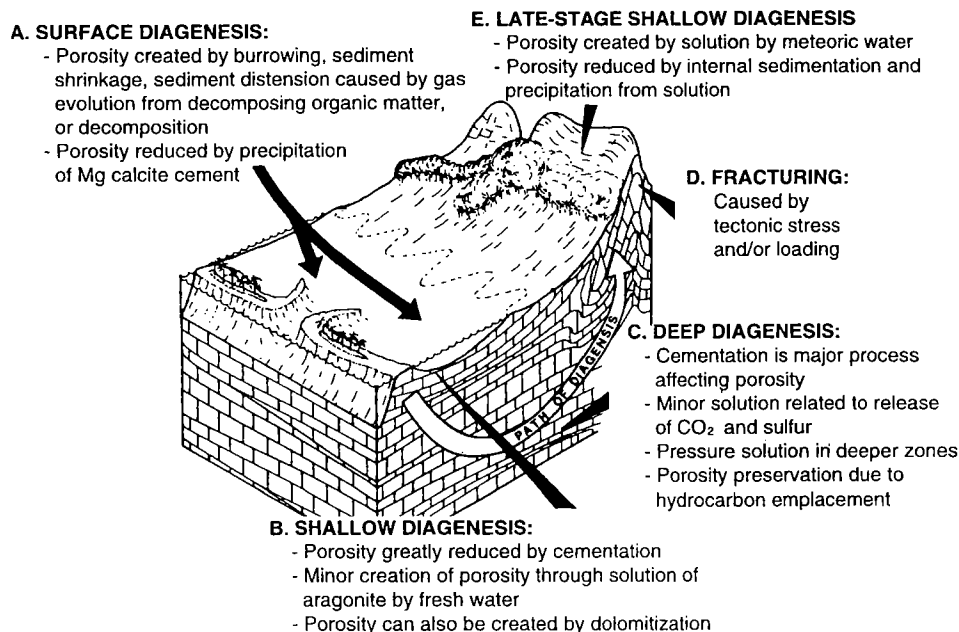


Figure 5. Diagram summarizing the paths of diagenesis of carbonate rocks. Modified from Harris (1985); reprinted by permission of Society for Sedimentary Geology (SEPM).

PART III

History of Hunton Oil and Gas Exploration and Development in Oklahoma

Robert A. Northcutt

Independent Petroleum Geologist
Oklahoma City, Oklahoma

INTRODUCTION

The Hunton play in Oklahoma includes most of the Anadarko, Ardmore, Marietta, and Arkoma basins, and the southwestern part of the Cherokee platform. Shallow-marine carbonate rocks of the Hunton Group (Silurian–Devonian) are present in the subsurface throughout much of Oklahoma (Fig. 6). Hunton rocks are absent by erosion on the regional Wichita and Arbuckle uplifts and are truncated to the north as the result of regional tilting in Pennsylvanian time. In local areas, such as on the Oklahoma City anticline, these rocks are eroded owing to structural uplift.

Both structural and stratigraphic traps are present in the Hunton play. The structural traps are primarily in the southwestern part of the Cherokee platform, the

Arkoma basin, the deep Anadarko basin, and the Ardmore basin. Stratigraphic traps are mainly on the central Cherokee platform and the Anadarko shelf, approaching the erosional limit of the Hunton. Many of the structural traps are characterized by elements of stratigraphic trapping, in which facies changes and diagenesis play an important role in reservoir enhancement.

HUNTON EXPLORATION AND DEVELOPMENT

Oil and gas exploration and development began in Oklahoma as early as 1897, with the discovery of Bartlesville field in Washington County. Following this discovery, exploration and development in Oklahoma spread from northeastern Oklahoma to the south and

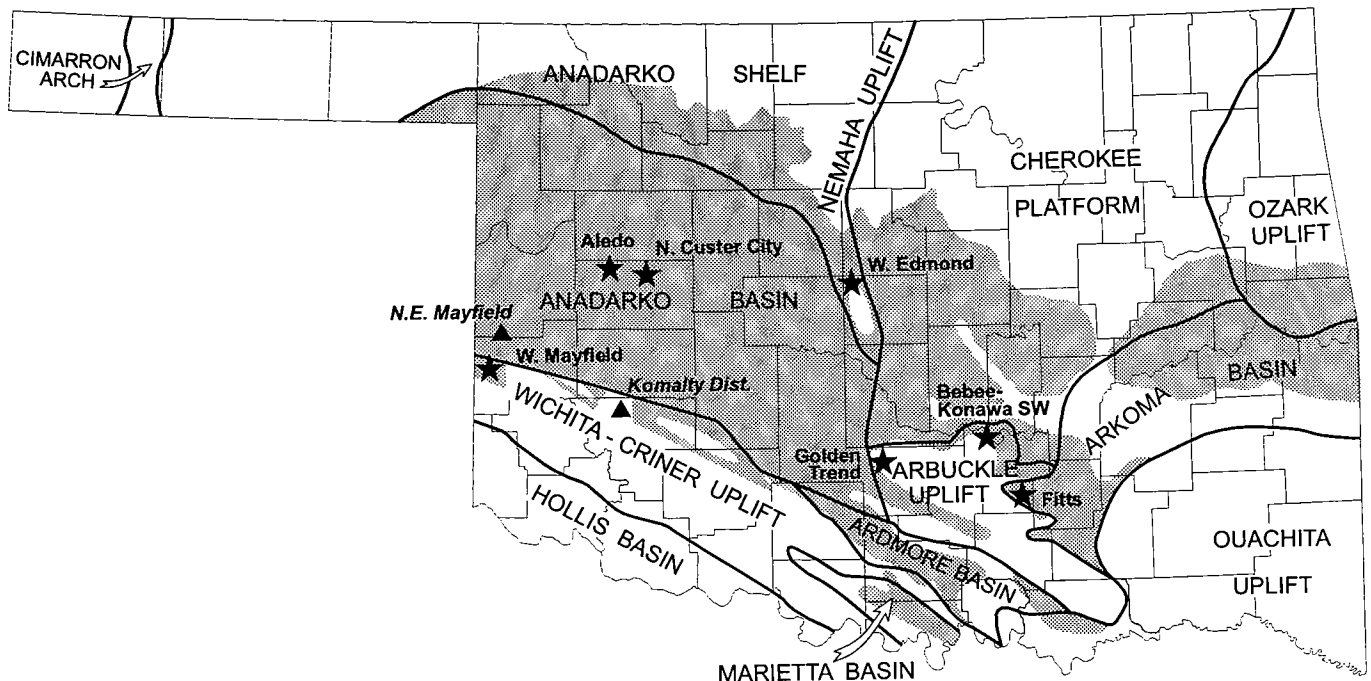


Figure 6. Map of Oklahoma showing geologic provinces and selected oil and gas fields that produce from rocks of the Hunton Group. Seven Hunton fields are indicated by stars; shallowest and deepest Hunton fields are indicated by triangles. Pre-Woodford subcrop of Hunton shown in light stipple pattern. Modified from Northcutt and Campbell (1996) and Jordan (1964).

TABLE 4. – Selected Fields with Hunton Oil and Gas Production in Oklahoma

Field name	Discovery year	County	Hunton discovery date	Discovery method	Trapping mechanism	Field significance
Bebee–SW Konawa	1921	Pontotoc	Aug. 1921	Unknown	Structural: anticline	First Hunton oil production in State
Fitts	1933	Pontotoc	July 1933	Surface geology	Structural: faulted anticline	First Hunton oil production in Arkoma basin
West Edmond	1943	Oklahoma	April 1943	None (“doodle bug”)	Stratigraphic: unconformity	First Hunton oil production in Anadarko shelf
North Custer City	1959	Custer	April 1959	Seismograph	Structural: faulted anticline	First Hunton gas production in deep Anadarko basin
Aledo	1967	Custer	1967	Seismograph	Structural: faulted anticline	High gas recovery per well
West Mayfield	1972	Beckham	Nov. 1976	Subsurface geology and seismograph	Structural: faulted anticline	First deep Hunton gas in Wichita frontal fault zone
Golden Trend	1946	Garvin	1981 (Antioch area)	Subsurface geology and log analysis	Combination: faulted and unconformity	Recent oil development in mature area

west. Most of the earliest discoveries were from shallow Pennsylvanian and Permian sandstones drilled on not much more than a hunch or by “creekology” or “closeology.” With the advent and acceptance of geological principles, and the use of surface geologic mapping in defining structural features during the 1910s, the search for oil and gas in deeper structures began in earnest. The result of this search ushered in what I called the “Black Gold Era” of oil and gas development in Oklahoma from 1908 to 1928 (Northcutt, 1985). During this period, the discovery and development of Hunton and other deeper oil and gas reservoirs spread across central Oklahoma but remained east of the Nemaha fault zone.

Seven oil and gas fields were selected that are significant to the exploration and development of Hunton oil and gas reservoirs in Oklahoma. These fields are listed in Table 4 and follow the progress of the Hunton play from 1921 to 1987.

Oil and gas were discovered in shallow Pennsylvanian sandstones in the Allen district of the Seminole area in 1913 (Fig. 7). Although deeper tests were drilled to the Hunton, Viola, and “Wilcox” in this district, no deeper producible hydrocarbons were found (Conkling, 1930). The presence of these potential reservoirs provided the incentive for additional exploration in the area, leading to the discovery of the first Hunton oil production in Oklahoma at Bebee–Southwest Konawa field (Kunsman, 1967).

Bebee–Southwest Konawa Field, Pontotoc County

In August 1921, the Nance Syndicate No. 1 Haggard, a wildcat well in the NW¼ sec. 4, T. 4 N., R. 5 E., near the town of Bebee, Pontotoc County, found producible Hunton oil at a depth of 2,412 ft. The well encountered the top of the Hunton at 2,305 ft, and after penetrating 105 ft of Hunton with a small show of oil, the well was shot with 200 quarts of nitroglycerin and completed for an initial flowing potential of 125 barrels of oil per day (BOPD). Limestone fragments thrown out of the drill hole by the explosion of the nitroglycerin were examined and identified as being of Silurian age (Morgan, 1922).

According to a Viola structure map (Fig. 8), the No. 1 Haggard well was drilled on a small closure in a graben between the Hunton uplift on the south and the Seminole arch to the north. This location in the graben accounts for the relatively thick Hunton section, 107+ ft, compared to other wells in the area, which encountered about 50 ft of Hunton (Morgan, 1922).

The total production for Bebee–Southwest Konawa field to October 1999 was 41,027,786 BO and 398,677 thousand cubic ft of gas (MCFG) (Petroleum Information/Dwight’s LLC—PI/Dwight’s). Accurate data are not available on cumulative production for the Hunton reservoir. However, Kunsman (1967) reported Hunton oil production from the fields now included in Bebee–Southwest Konawa field at 4,911,000 BO as of January

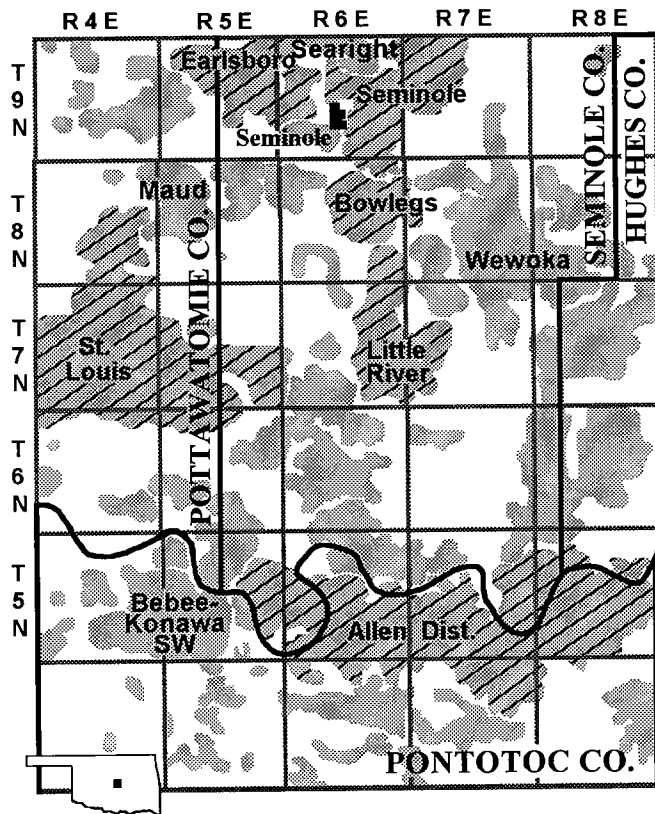


Figure 7. Seminole area oil fields, in Pottawatomie, Seminole, and Pontotoc Counties. Fields that have produced >100 MMBO from all reservoirs are indicated by hatching. Field data were plotted by Natural Resources Information System (NRIS), University of Oklahoma. Modified from Northcutt and Johnson (1997).

1, 1967. Records of many old wells in the field do not identify the producing formation, so that allocation of production to a specific formation is difficult.

Following the 1921 Hunton discovery at Bebee, Hunton production was established in the nearby Allen district (Conkling, 1930). Exploration for Hunton reservoirs in the Seminole area during the 1920s discovered many new fields (Fig. 7). Among these fields are Wewoka in 1924; St. Louis, Seminole City (now Seminole), and Searight in 1926; Pearson Switch (now part of St. Louis) in 1927; and Maud in 1928. Owing to rapid depletion of the Hunton reservoirs, many of these wells were drilled deeper to the Ordovician Viola and "Wilcox." Hunton development continued in the Seminole area, although mostly as salvage operations after unsuccessful tests of the deeper Viola and "Wilcox" (Kunsman, 1967).

Fitts Field, Pontotoc County

A. I. Levorsen, a consulting geologist, recommended that a well be drilled on the basis of a surface nose in the Franks graben of the western Arkoma basin. This well was the discovery of Fitts field (Fig. 6), a significant Hunton producer that later became a major oil field

with reservoirs in the Fernvale-Viola Limestone, Bromide sandstones, and McLish sandstones (Mann, 1958).

The discovery well was the E. H. Moore No. 1 Wirick, in the SE $\frac{1}{4}$ SE $\frac{1}{4}$ SW $\frac{1}{4}$ sec. 29, T. 2 N., R. 7 E., Pontotoc County (see Fig. 9). The well was completed in July 1933 with an initial flowing potential of 75 BOPD from the lower Hunton (Chimneyhill) limestone (Mann, 1958). The top of the Hunton limestone in Fitts field varies in depth from 3,045 to 3,820 ft and is 163–408 ft thick (Kunsman, 1967).

A structure map depicting the top of the Hunton (Fig. 9) shows Fitts field on a large faulted anticline within the Franks graben. The Hunton was exposed to erosion by the pre-Atokan (Wichita) orogeny on the upthrown sides of both the north and south faults of the Franks graben (Mann, 1958). A structural cross section (Fig. 10) shows the relationship of the Fitts field area to the Fitts fault and to the graben-bounding Stonewall fault to the north. The Fitts fault has as much as 800 ft of vertical displacement, whereas the Stonewall fault has as much as 3,250 ft of vertical displacement.

At least 452 producing wells were drilled in Fitts field. Cumulative production as of October 1999 was

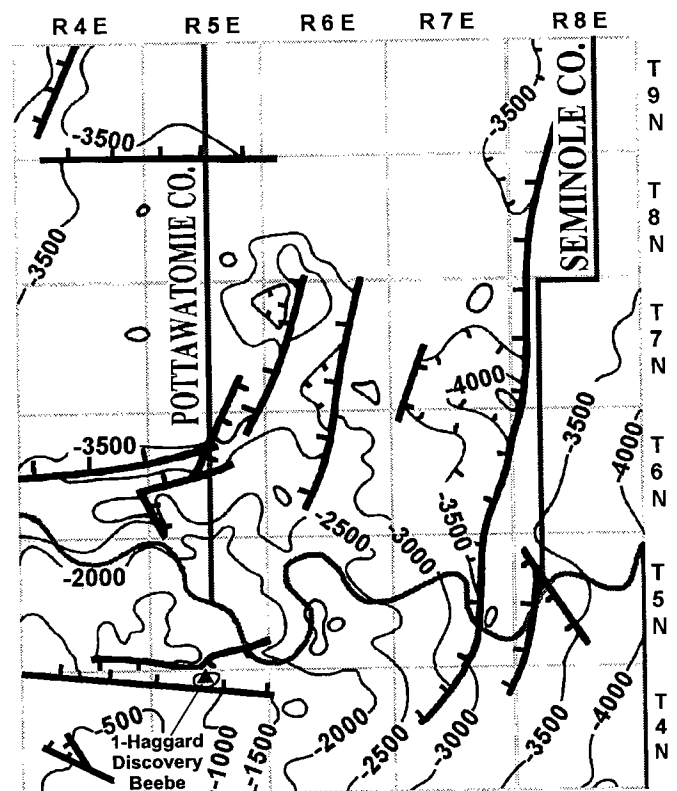


Figure 8. Structure map depicting the top of the Ordovician (Viola) in the Seminole area. Contour interval is 500 ft. Modified from Northcutt and Johnson (1997). Hachures on faults indicate downthrown sides; hachures on contours indicate structural lows. Location of discovery well for Bebee-Southwest Konawa field (No. 1 Haggard) shown by triangle.

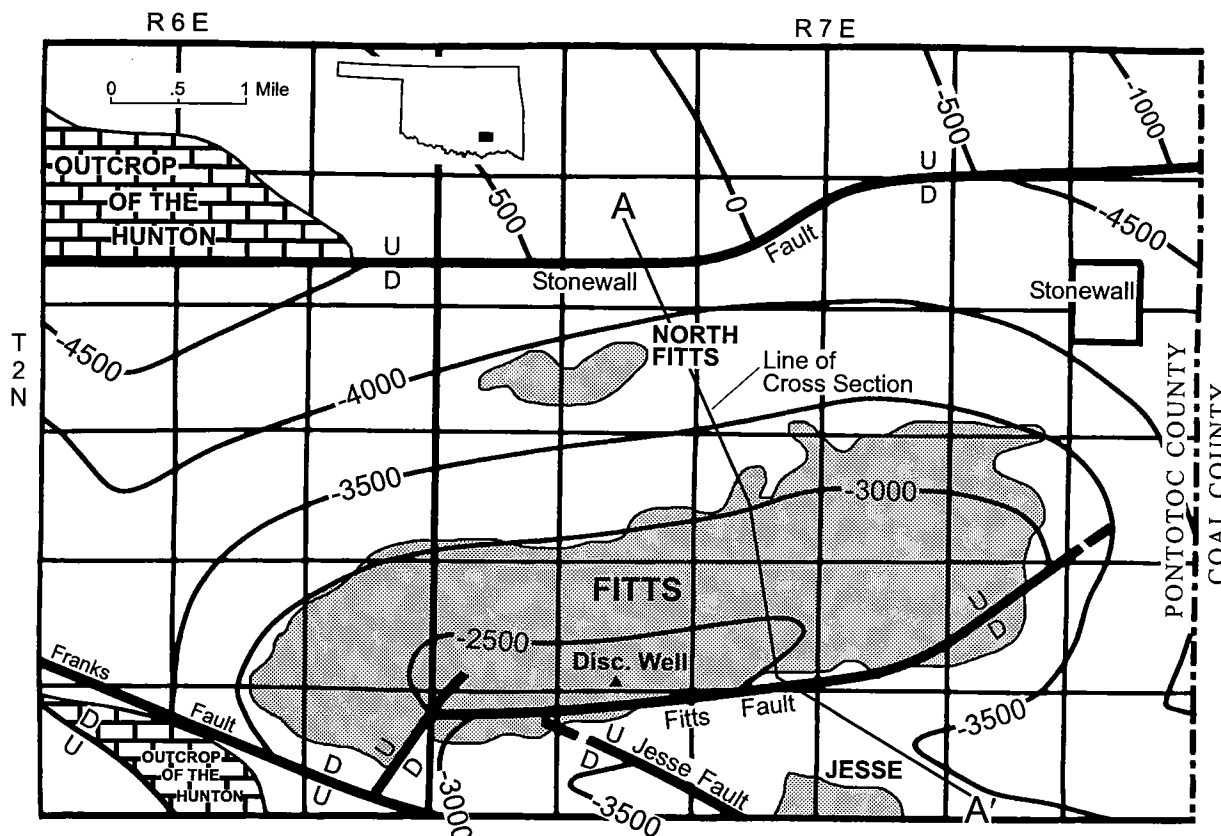


Figure 9. Structure map depicting the top of the Hunton Group in Fitts field, Pontotoc County. Contour interval is 500 ft. Field producing area shown in stippled pattern. Cross section A–A' shown in Figure 10. Modified from Mann (1958).

222,681,617 BO and 53,485,479 MCFG (PI/Dwight's). As of January 1, 1967, Kunsman (1967) reported that the Hunton had produced 12,390,000 BO from 331 wells. Production data by formation is incomplete for the older fields because operators generally did not release those data.

In 1935, producible Hunton oil was discovered in Jesse field, south of Fitts field. Jesse field was the last significant Hunton discovery in the Oklahoma part of the Arkoma basin until the discovery of gas in Haskell County in 1977 at West Stigler field (Campbell, 1993).

The Hunton play expanded northward and eastward on the Cherokee platform with the discovery of Hunton reservoirs in Dill field in Okfuskee County in 1934 and Ramsey field in Payne County in 1938. Most of the exploration for Hunton reservoirs for the next several years was directed toward the search along the pinch-out line on the Cherokee platform in northeastern Oklahoma (Fig. 6). The discovery of West Edmond field on the Anadarko shelf initiated the search for Hunton reservoirs in the deeper areas west of the Nemaha fault zone (Kunsman, 1967).

West Edmond Field, Oklahoma, Canadian, and Kingfisher Counties

The drill bit discovered West Edmond field (Fig. 1). No geological or acceptable geophysical methods were

used—just the “doodlebug.” After many attempts to promote a well on this large acreage block, Ace Gutowsky finally succeeded in getting enough financing, and with other investors the well was drilled and resulted in the discovery of the first major Hunton reservoir west of the Nemaha fault zone. The Gutowsky No. 1 Wagner, a “Wilcox” wildcat, was drilled in the NW¼NW¼SW¼ sec. 32, T. 14 N., R. 4 W., in Oklahoma County. After reaching a total depth of 7,690 ft in the “Wilcox,” the well was plugged back to test the Hunton, which was encountered at 6,866 ft. The No. 1 Wagner was completed April 28, 1943, from perforations at 6,951–6,956 ft in the Hunton, flowing 522 BOPD (McGee and Jenkins, 1946).

A generalized structure map depicting the top of the Haragan Formation of the Hunton Group (Fig. 11) shows a gently sloping west dip, with the erosional updip limit of the Bois d'Arc Formation forming an ideal stratigraphic trap. A cross section (Fig. 12) illustrates the pinch-out that is sealed by the overlying Woodford Shale over much of the potentially productive area. Farther northeastward, beyond the erosional limit of the Woodford Shale, the trap is sealed by Lower Pennsylvanian shale.

Originally, the producing zone was considered to be the Bois d'Arc Formation of the Hunton Group. However, later work by Swesnik (1948) and Amsden (1975)

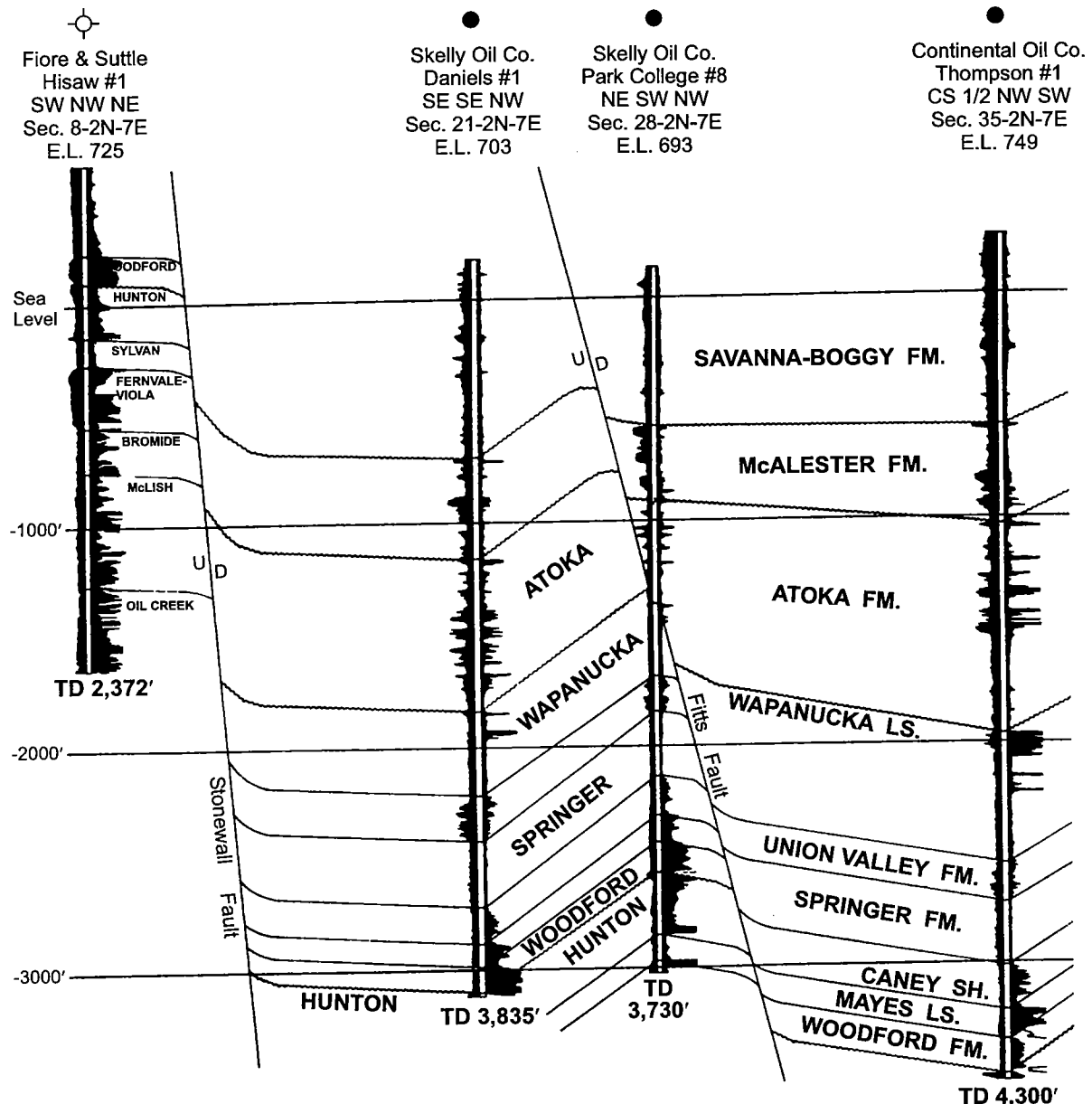


Figure 10. Structural cross section A-A' across Fitts field. See Figure 9 for line of cross section. Vertical exaggeration is 6.6:1. Modified from Mann (1958).

determined that the production was mostly from the younger Frisco Formation of the Hunton, a coarsely crystalline limestone unconformably overlying the Bois d'Arc. There is also production from the Bois d'Arc and all other units of the Hunton Group where porosity has been developed either by dissolution or dolomitization.

By June 1947, approximately 750 wells had been drilled in West Edmond field. Only the north and south ends of the field were not yet defined, and at that time it was geographically the largest field in Oklahoma (Swesnik, 1948). Kunsman (1967) reported that the field had produced 106,033,000 BO by January 1967 from 754 Hunton wells. The total production from all reservoirs in West Edmond field by October 1, 1999,

was 165,420,411 BO and 375,335,943 MCFG (PI/Dwight's).

On July 29, 1947, the Oklahoma Corporation Commission unitized the West Edmond Hunton Lime Unit as a repressurization project by Phillips Petroleum Co. The result of this effort was less successful than expected. Still, West Edmond field represented a major milestone in the development of Hunton reservoirs in Oklahoma.

After initial development of the Hunton reservoir at West Edmond field in 1947, exploration for Hunton fields continued on the Cherokee platform and spread into Kingfisher County to the northwest and southward to Cleveland and McClain Counties in the late 1940s and 1950s. Farther south, in the Ardmore basin, pro-

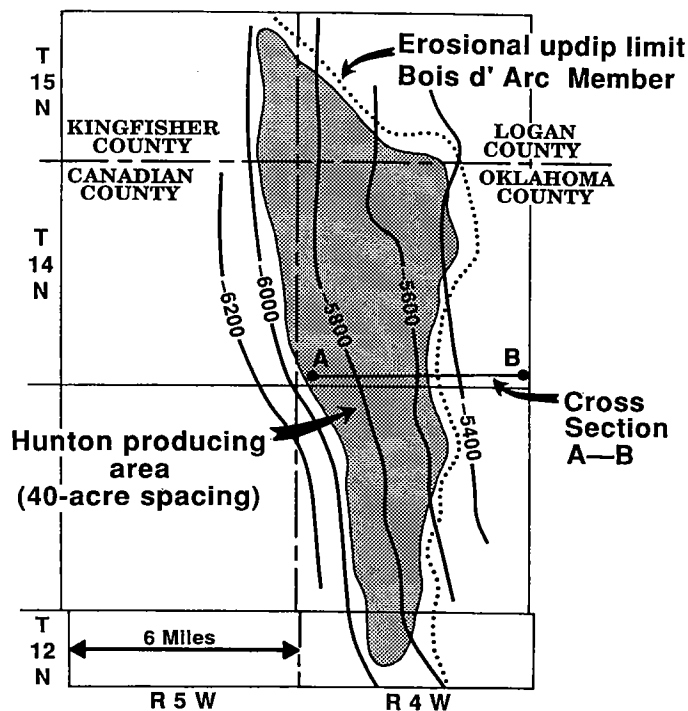


Figure 11. Structure-contour map of West Edmond field, depicting the top of the Haragan Formation (Hunton Group), Oklahoma County and parts of adjacent counties. Contour interval is 200 ft. Producing area shown in stippled pattern. Cross section A-B shown in Figure 12. Modified from McGee and Jenkins (1946). (AAPG ©1946. Reprinted by permission of the AAPG, whose permission is required for further use.)

ducible Hunton oil was found in Caddo field in 1952 and Joiner City field in 1953. Exploration for Hunton reservoirs spread across the Anadarko shelf and into the deeper part of the Anadarko basin, encouraged by the development of better drilling techniques and equipment that provided improved penetration rates in the thick Mississippian limestone section (Kunsman, 1967).

A structure map depicting the top of the Hunton (Fig. 13) shows the oil and gas fields developed on the Anadarko shelf and in the Anadarko basin. The trend of fields at the northern Hunton truncation limit are all stratigraphic traps. Stratigraphic traps are dominant in the shelf area and the shallower part of the Anadarko basin, where large reserves in fields such as West Campbell (1959), East Campbell (1960), Star (1962), and Lacy (1962) were discovered in Kingfisher and Major Counties (Logsdon and Brown, 1967). Along the eastern limit of the Anadarko basin, a large area of Canadian County produces gas from stratigraphic traps in fractured Hunton limestone; this area was developed in the 1970s (Kirk, 1974; Morrison, 1980).

Exploration for deep Hunton gas reservoirs in the Anadarko basin of Oklahoma began with discovery of North Custer City field in

Custer County along an east-west trend of up-to-the-basin faulting near the Custer-Dewey county line.

North Custer City Field, Custer County

The discovery well for North Custer City field was the Mobil Oil Co. No. 1 Boyd-Miller in the SE $\frac{1}{4}$ NW $\frac{1}{4}$ sec. 22, T. 15 N., R. 16 W. The well was drilled on the basis of a seismic survey conducted by Mobil Oil Co. (Coleman, 1963). The Boyd-Miller well was drilled to a total depth of 17,000 ft to the Arbuckle and completed in April 1959. Perforations in the Haragan (dolomitized limestone) from 14,383 to 14,472 ft and the Chimney-hill (fractured limestone) from 14,773 to 14,793 ft resulted in an initial calculated open-flow rate of 95,000 MCFGPD (Coleman, 1963).

A structure map of North Custer City field (Fig. 14) depicting the top of the Hunton Group shows a north-bounding up-to-the-basin fault with approximately 250 ft of vertical displacement and a north-south-trending fault on the east side with as much as 500 ft of vertical displacement. A schematic diagram above the map shows a cross section through the field.

The total production from all reservoirs in North Custer City field by October 1, 1999, was 353,958 BO and 247,627,628 MCFG. Production from the 21 listed Hunton producing wells was 47,333 BO and 178,341,454 MCFG by October 1, 1999 (PI/Dwight's). The average production for the Hunton wells is 8.5 billion cubic feet of gas (BCFG) per well. Seven wells produced more than 10 BCFG, and one well produced more than 48 BCFG.

The Mobil Oil Co. No. 1 Boyd-Miller was the first commercial producer in Custer County (Jordan, 1959). The development of North Custer City field provided the incentive for more exploration for Hunton gas reservoirs in the Anadarko basin. No significant Hunton reservoirs were found by additional exploration in the deep part of the Anadarko basin until discovery of Aledo

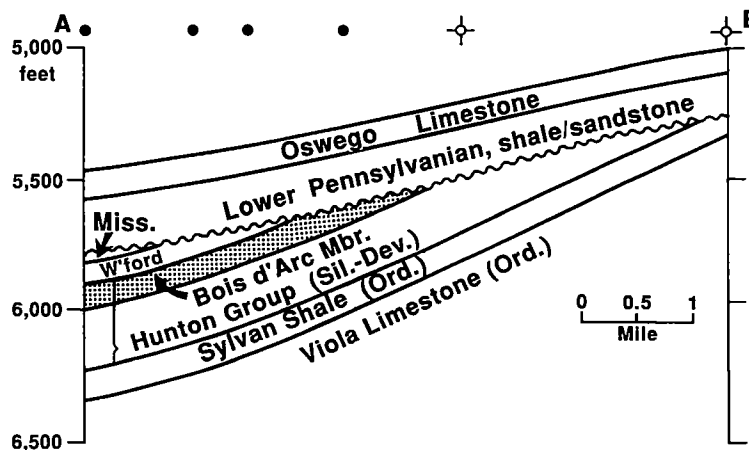


Figure 12. Structural cross section A-B, West Edmond field, Oklahoma County. Line of section shown in Figure 11. Modified from McGee and Jenkins (1946). (AAPG ©1946. Reprinted by permission of the AAPG, whose permission is required for further use.)

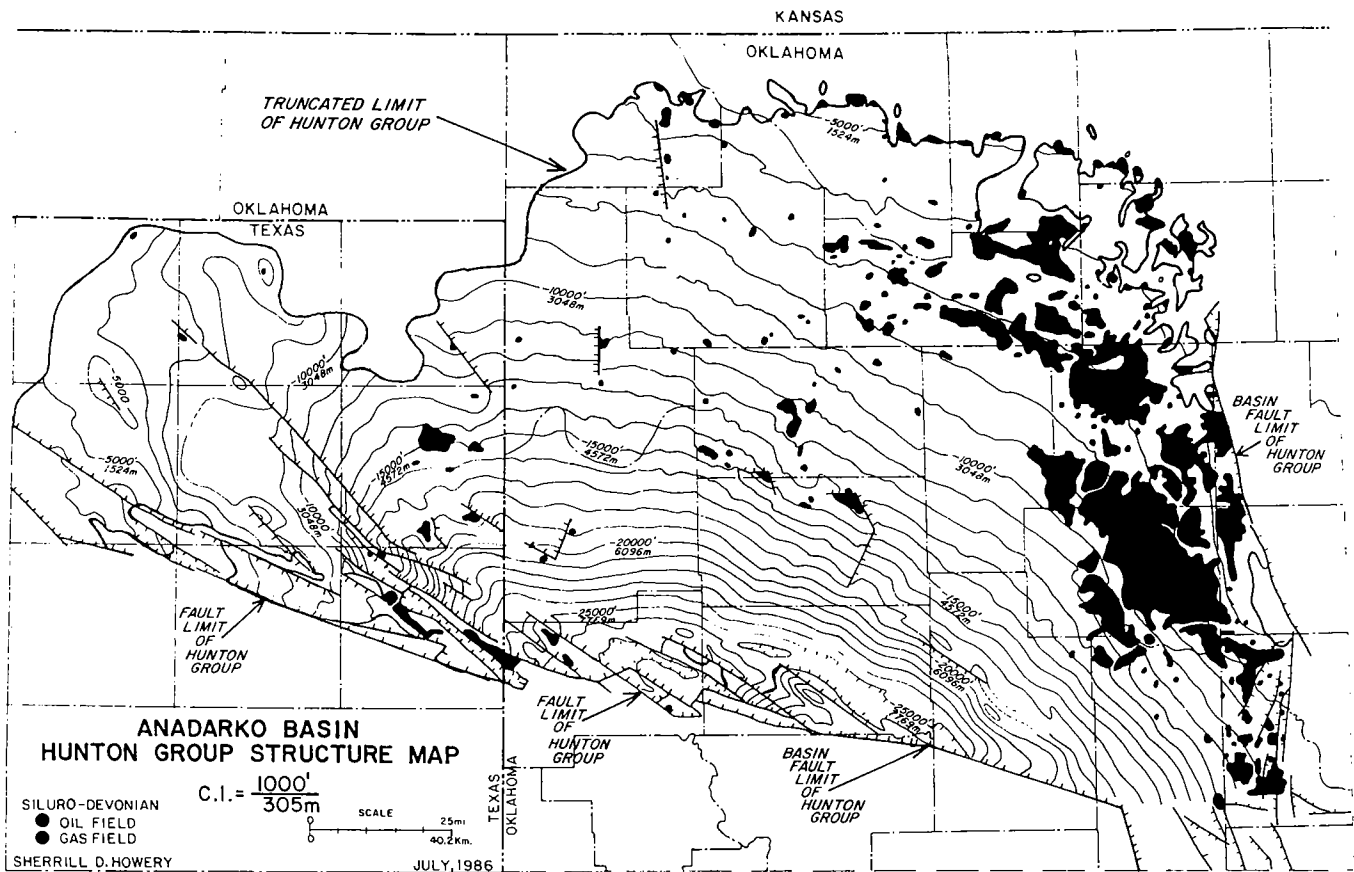


Figure 13. Structure map depicting the top of the Hunton Group in the Anadarko basin of Oklahoma and Texas Panhandle, showing Hunton oil and gas fields in black. Contour interval is 1,000 ft. Modified from Howery (1993).

field in 1967, 8 years after North Custer City field was discovered.

Aledo Field, Custer and Dewey Counties

The discovery well for Aledo field was the J. C. Barnes Oil Co. No. 1 E. H. Walker, in the SE $\frac{1}{4}$ NW $\frac{1}{4}$ sec. 5, T. 15 N., R. 18 W., Custer County. The well was completed in 1967 from perforations at 15,385–15,420 ft. A calculated open-flow potential of 106,000 MCFGPD was reported for that well (Kennedy, 1982). The field is characterized by a faulted anticline (Fig. 15) bounded on the north and east by an up-to-the-basin fault with about 700 ft of vertical displacement. The producing zone is a fractured dolomite with 93 ft of pay.

Aledo field produces from several formations that had a cumulative production of 1,066,123 BO and 299,664,144 MCFG as of October 1, 1999. The Hunton reservoir is productive from seven wells and has produced 17,340 BO and 254,760,385 MCFG. The average production per well is 36,394,341 MCFG, and the best well had produced 83,587,105 MCFG by October 1, 1999 (PI/Dwight's).

A shallow Pawhuska limestone (Pennsylvanian, Virgilian) gas well was completed in 1954 after drilling to a total depth of 10,294 ft. This was the discovery well of Southwest Mayfield field, sec. 25, T. 10 N., R. 26 W.,

Beckham County, 1 mi east of West Mayfield field. This was the first well to be completed as a producer in the western Oklahoma frontal fault zone of the Wichita uplift.

West Mayfield Field, Beckham County

The area was dormant until 1971, when Continental Oil Co. drilled the No. 1 Gordon in the SE $\frac{1}{4}$ sec. 20, T. 10 N., R. 26 W. This well was drilled to a total depth of 19,969 ft in rocks of the Arbuckle Group and tested zones in the Arbuckle and Hunton without finding commercial production. The well was plugged back and completed in arkosic sandstone ("granite wash") in September 1972 and was designated the discovery well for West Mayfield field.

The Helmerich and Payne, Inc., No. 1 Cupp well was drilled in the SE $\frac{1}{4}$ NW $\frac{1}{4}$ sec. 27, T. 10 N., R. 26 W., and was completed in July 1974 as the discovery of the Arbuckle reservoir in the field.

The Apexco, Inc., No. 1-19 Mills in the SW $\frac{1}{4}$ sec. 19, T. 10 N., R. 27 W., was drilled to the Sylvan Shale at a total depth of 19,060 ft. This well was completed in the Hunton from perforations at 18,240–18,996 ft in November 1976. The well had a calculated open flow of 103,000 MCFGPD and was the discovery well for the

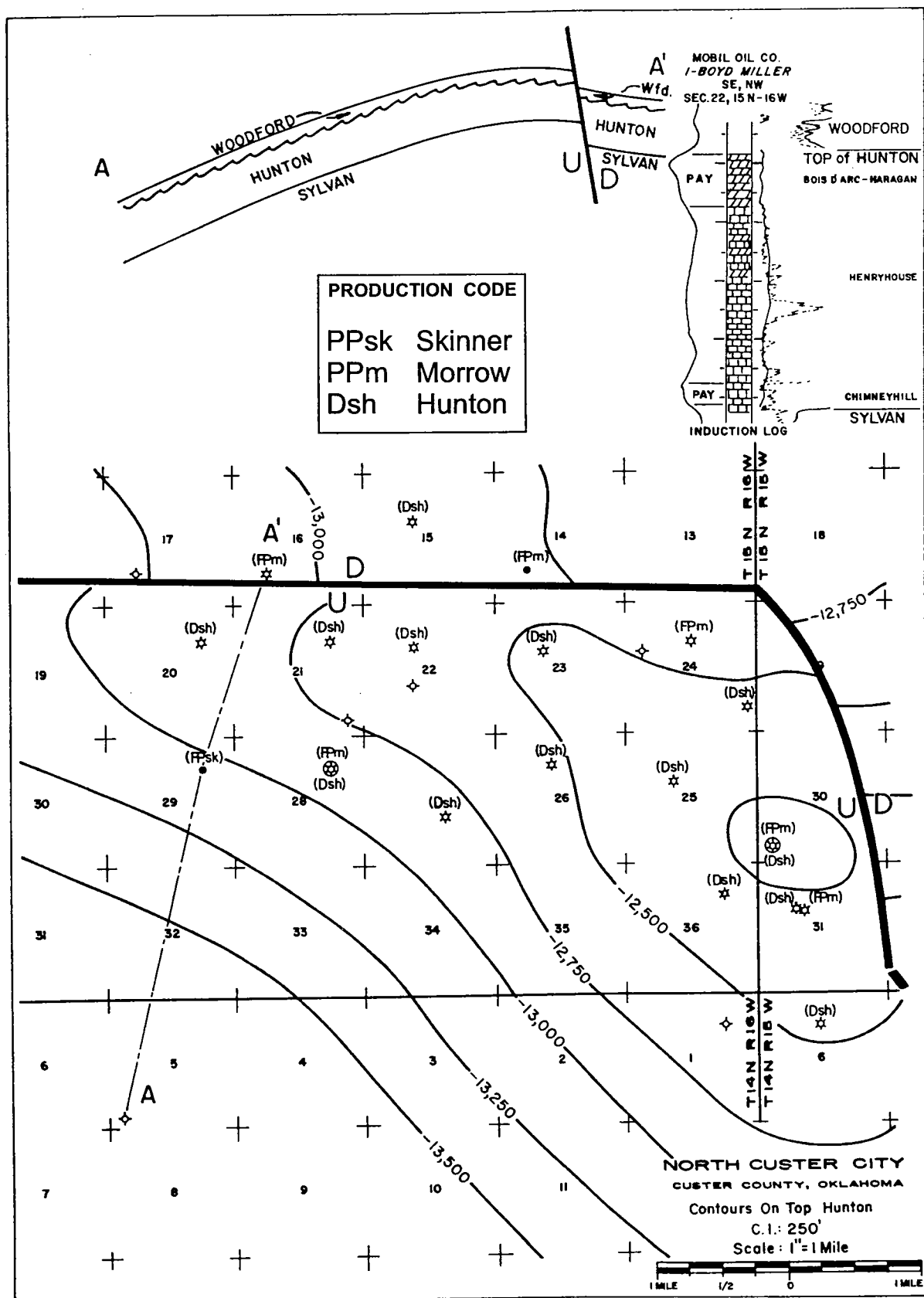


Figure 14. Cross section and structure map of North Custer City field, Custer County. (Top) Cross section A-A', showing the north-bounding up-to-the-basin fault and the characteristic electric log of the Mobil Oil Co. No. 1 Boyd Miller well. (Bottom) Structure map depicting the top of the Hunton Group. Wells producing gas from the Hunton are indicated by the symbol *Dsh*. From Berg (1974).

Hunton reservoir in West Mayfield field (Kennedy, 1982).

The West Mayfield structure is a complexly faulted anticline in the frontal fault zone of the Wichita uplift (Fig. 16). The field was discovered through a combination of subsurface geology and seismic-reflection data. The upper Hunton zone (Haragan) is a highly fractured dolomitized limestone, and the lower Hunton zone (Chimneyhill) is a highly dolomitized limestone. Rapid development in the field resulted in the drilling of 90 producing wells, of which 22 produce from the Hunton.

The total cumulative production from West Mayfield field was 1,365,780 BO and 388,408,334 MCFG as of October 1, 1999. The 22 Hunton wells have produced a total of 421,616 BO and 213,115,693 MCFG (PI/Dwight's). The average gas production for a Hunton well is 9,607,077 MCFG, and the best producer has a cumulative production of 29 BCFG. These deep Hunton gas wells in West Mayfield field have been some of the most prolific gas producers in Oklahoma.

Golden Trend, Garvin, Grady, and McClain Counties

The Golden Trend was formed in 1954 by the Nomenclature Committee of the Kansas-Oklahoma Division of the Mid-Continent Oil and Gas Association, the designated body that names and determines field boundaries in the State of Oklahoma. The Golden Trend includes 29 previously named fields with oil and gas production from reservoirs ranging in age from the Simpson Group (Ordovician) to the Permian. Hunton production was established in the area as early as 1947 in what was then called the Northeast Lindsay field (Swesnik, 1950).

In 1981, deeper development drilling in the Antioch area in Ts. 2 and 3 N., Rs. 2 and 3 W., discovered Hunton production in the Anadarko Petroleum Corp. No. 1 Bradshaw well in the NE¼ sec. 26, T. 3 N., R. 3 W., Garvin County (Figs. 17, 18). The No. 1 Bradshaw was completed as an oil well flowing 50 BO and 230 MCFG per day from a fractured limestone interval in the Bois d'Arc section of the Hunton. The first offset well was a

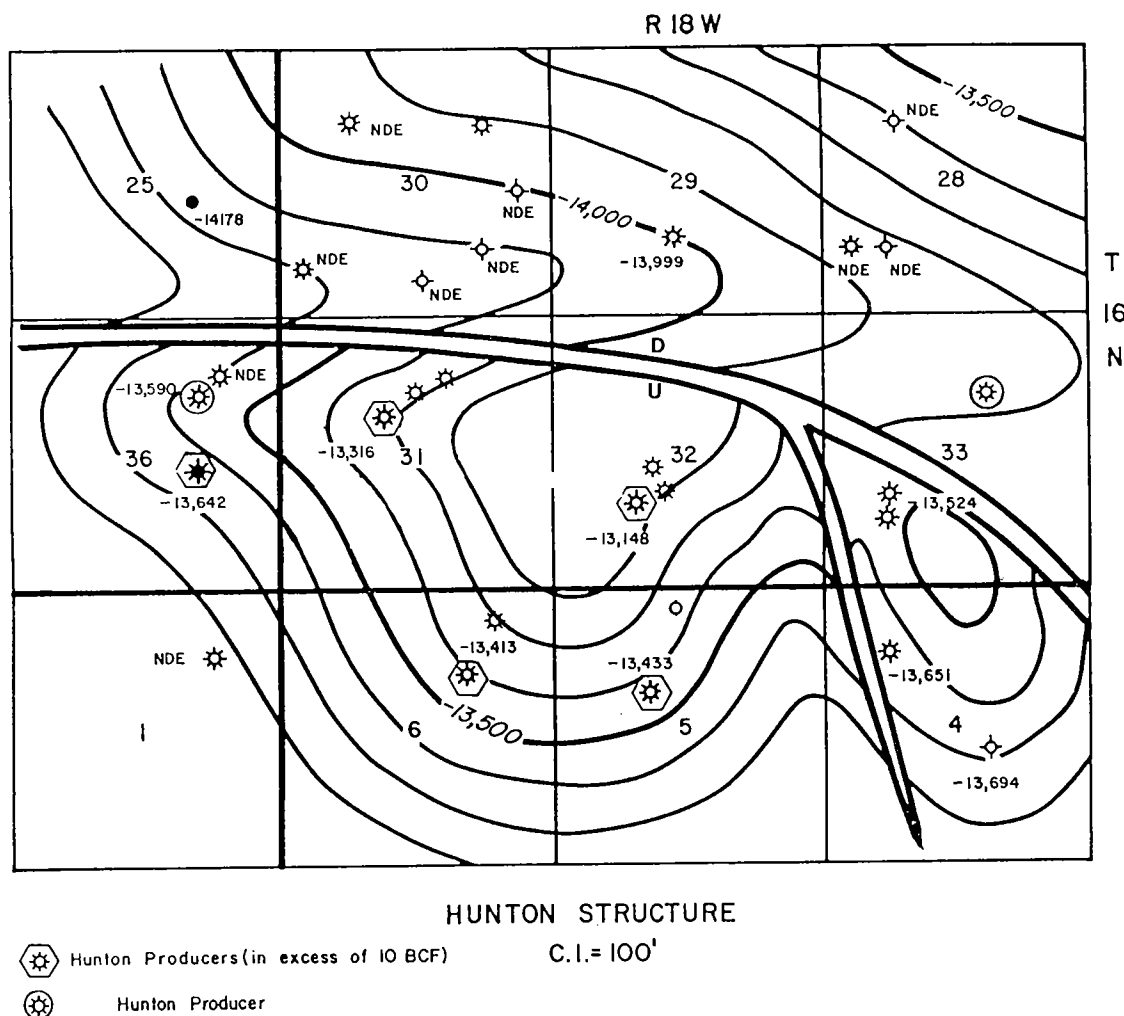


Figure 15. Structure map of Aledo field, depicting the top of the Hunton Group, Custer and Dewey Counties. NDE = not deep enough. From Bruce (1989).

dual completion in the Hunton and the Sycamore (Mississippian) for a daily initial flowing potential of 650 BO and 1,100,000 MCFG. Subsequent drilling confirmed the existence of a large Hunton productive area that led to a development-drilling program for the Hunton and Sycamore. More than 160 wells were completed during the program (R. P. Sorenson, F. W. White, and C. N. Clark, personal communication, 1987). Accurate production data for these newly developed wells are not readily available.

This most recent oil produced from the Hunton is stratigraphically trapped along a wedge-edge to the

east on the west flank of the Pauls Valley uplift. The Woodford Shale overlies the Hunton to the point at which it is truncated to the east, where the Hunton is overlain by Desmoinesian (Pennsylvanian) shale to form the top seal for this trap. The reservoir is highly fractured and occurs in the Bois d'Arc and Chimneyhill Formations of the Hunton. The area is complexly faulted (Fig. 17) by a series of north-south-trending normal faults that are downthrown to the west. This large Hunton reservoir area was found through subsurface geological work, the application of well-log analysis, and new completion techniques.

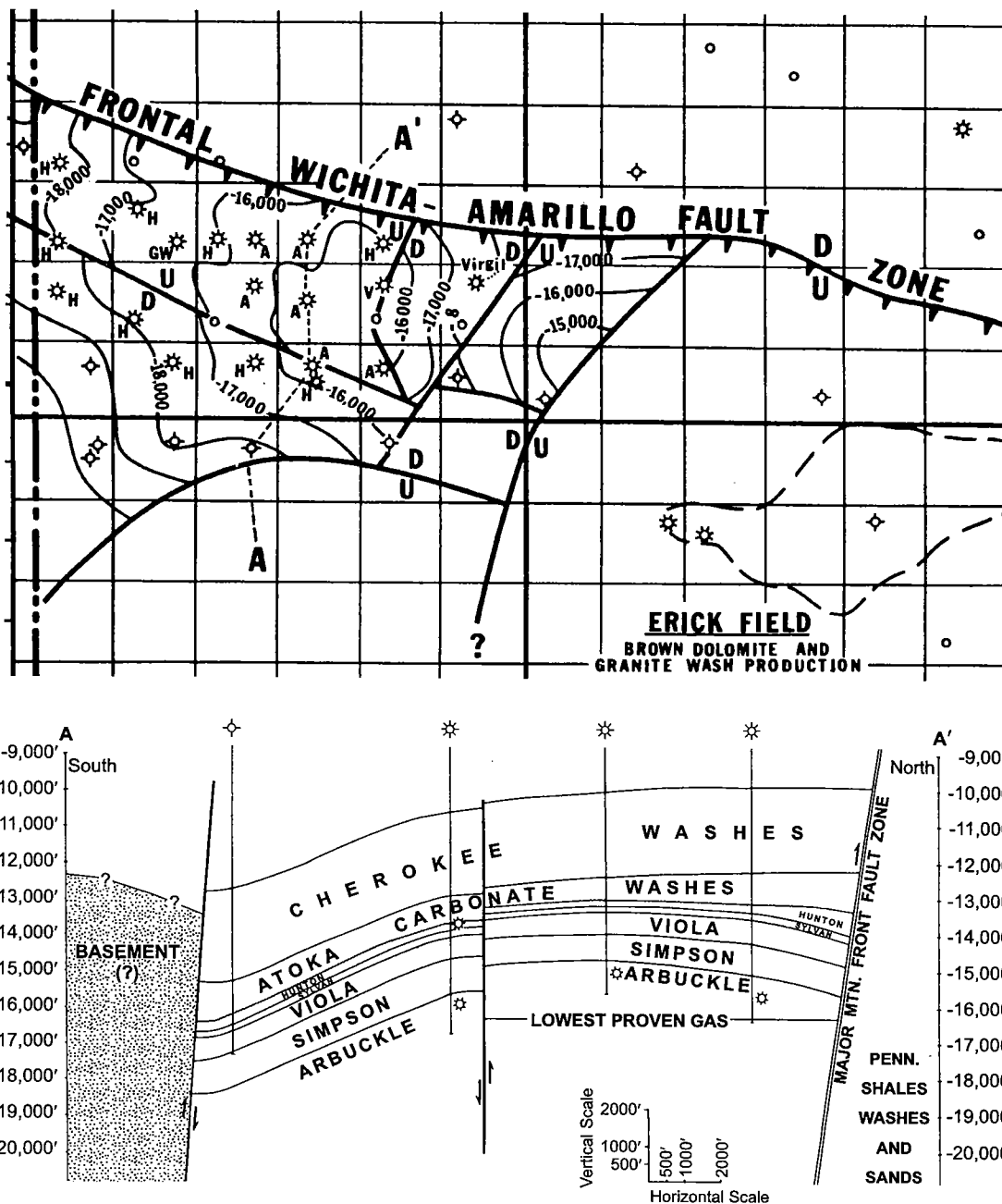


Figure 16. Structure map and cross section of West Mayfield field, Beckham County. (Top) Structure map depicting the top of the Arbuckle dolomite. Contour interval is 1,000 ft. Complex faulting in field has been simplified. Wells producing gas from the Hunton are indicated by the symbol H. (Bottom) Cross section A-A', showing the large, north-bounding thrust fault of the frontal Wichita fault zone. Line of section shown on structure map. Vertical and horizontal scales are equal. From Solter (1980).

DEPTH RANGE OF HUNTON RESERVOIRS IN OKLAHOMA

The depths to Hunton oil and gas reservoirs range from 465 ft in Kiowa County to 24,928 ft in Beckham County (Fig. 6). Hunton reservoirs on the Cherokee platform range from depths of 2,100 to 9,900 ft; in the Arkoma basin they range from 3,050 to 6,140 ft, and on the Arbuckle uplift, from 1,990 to 8,600 ft. In the Ardmore–Marietta basin the depths of Hunton reservoirs range from 3,700 to 9,050 ft. Hunton reservoirs on the Anadarko shelf range from 6,100 to 8,400 ft deep, and in the Anadarko basin they range from 7,060 to 25,000 ft deep. In the frontal fault zone of the Wichita–Criner uplift, Hunton reservoirs range in depth from 465 to 19,000 ft.

The shallowest Hunton production is in Komalty field in Kiowa County (Fig. 6), where oil was discovered in 1945 in the Hunton at a depth of 465 ft. This field was combined with the Komalty district in 1946, which now includes parts of Ts. 6 and 7 N., Rs. 16 and 17 W., and produces oil from Permian arkosic sandstone (“granite wash”), Pennsylvanian sandstone, and Arbuckle dolomite in addition to the limestones of the Hunton Group. The Komalty district is in the frontal fault zone of the Wichita uplift geologic province, where lower Paleozoic sedimentary rocks are preserved and covered by Permian and Lower Pennsylvanian shale and sandstone.

The deepest Hunton reservoir is in Northeast Mayfield field, discovered by Carter Oil Co. in June 1951, which originally produced oil from the Hoxbar Group (Pennsylvanian, Missourian). This reservoir is in Beckham County, in the deep Anadarko basin (Fig. 6). It was not until March 1972 that the Union Oil Co. of California et al. No. 1-33 Bruner well in sec. 33, T. 11 N., R. 25 W., was completed as a Hunton gas discovery, flowing 2,800 MCFGPD per day from 24,065 to 24,584 ft. At the time of its completion, the No. 1-33 Bruner was the deepest producing well in the world (Oklahoma Geological Survey, 1972). Subsequent drilling along the trend found deeper production in Texas in 1977. In August 1982, Mesa Petroleum Co. completed their No. 2-29 Tipton well in Northeast Mayfield field in sec. 29, T. 11 N., R. 25 W. The well produced gas from the Hunton at the rate of 14,600 MCFGPD from perforations at 24,928–24,969 ft, making it the deepest producing well in Oklahoma (Kennedy, 1982).

SUMMARY

The Hunton play in Oklahoma has found significant reserves of oil and gas in both structural and stratigraphic traps throughout the State at depths ranging from 465 to 24,928 ft. A map of Oklahoma (Fig. 19) shows

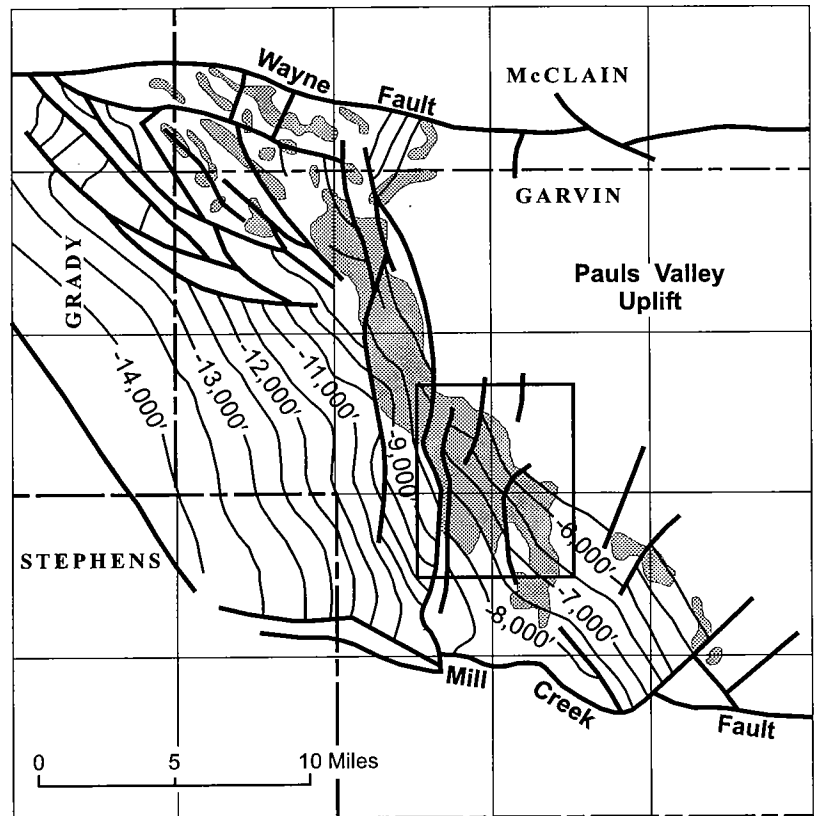


Figure 17. Structure map of Golden Trend, depicting the top of the Hunton Group, Garvin County and parts of adjacent counties. Contour interval is 500 ft. Sycamore (Mississippian) and Hunton producing areas are stippled. Outline is area of detailed structure map shown in Figure 18. From R. P. Sorenson, F. W. White, and C. N. Clark (personal communication, 1987).

a plot of all wells that are identified as Hunton producers in the well-history file of the Natural Resources Information System (NRIS) at the University of Oklahoma. Hunton oil and gas reservoirs are present in 48 of Oklahoma's 77 counties. Cumulative production from Hunton reservoirs for the period from January 1979 through September 1999 was 157,118,000 BO and 46,759,666 MCFG (NRIS).

ACKNOWLEDGMENTS

I greatly appreciate the efforts of Jock A. Campbell, senior petroleum geologist, Oklahoma Geological Survey, for his critical review of this manuscript. His comments and suggestions were most helpful to me in making this a better study. I thank Wayne Furr, OGS manager of cartography, and Jim Anderson, OGS cartographic technician, for their help and expertise in preparing the illustrations and visual aids for this presentation. I also thank David Brown, Geo Information Systems, who provided NRIS well data and production data for this study. Petroleum Information/Dwight's LLC (PI/Dwight's), a member of IHS Energy Group, supplied the production information for the selected fields from their Oklahoma Production Reports.

Figure 18. Structure map of part of Antioch area in the Golden Trend at the top of the Hunton Group, showing Hunton development wells (large well symbols) and earlier, shallower development wells (small well symbols). Contour interval is 500 ft. From R. P. Sorenson, F. W. White, and C. N. Clark (personal communication, 1987).

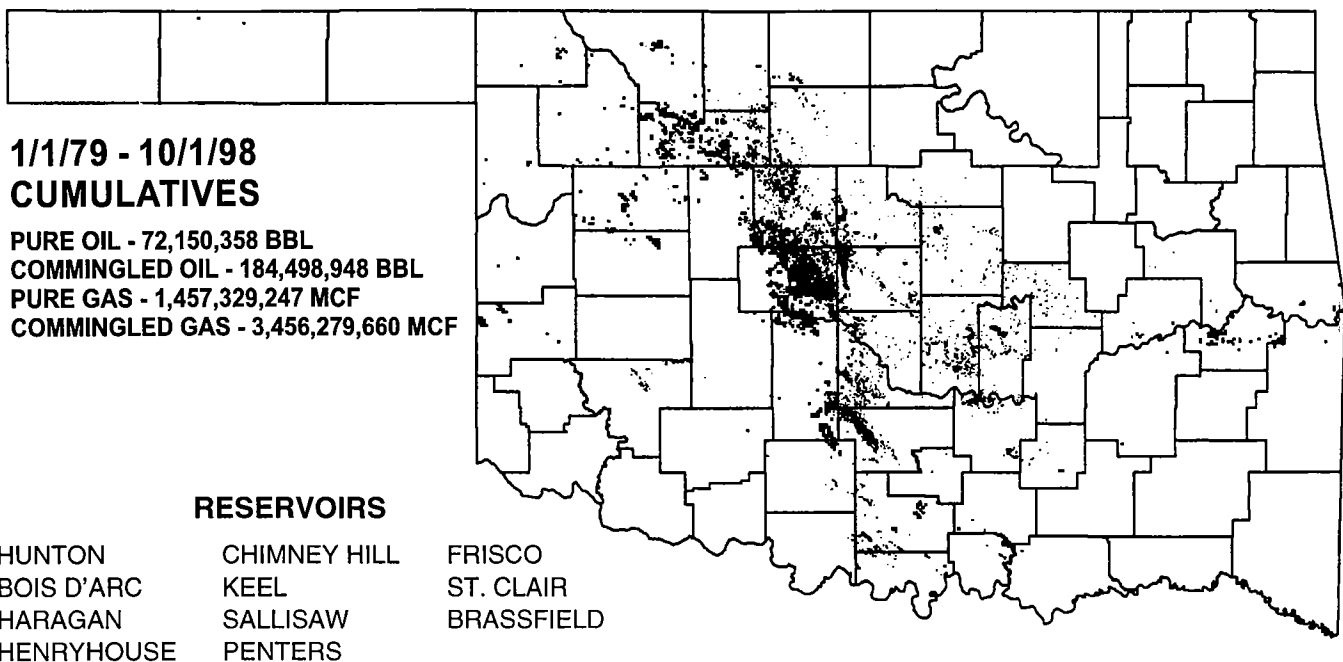
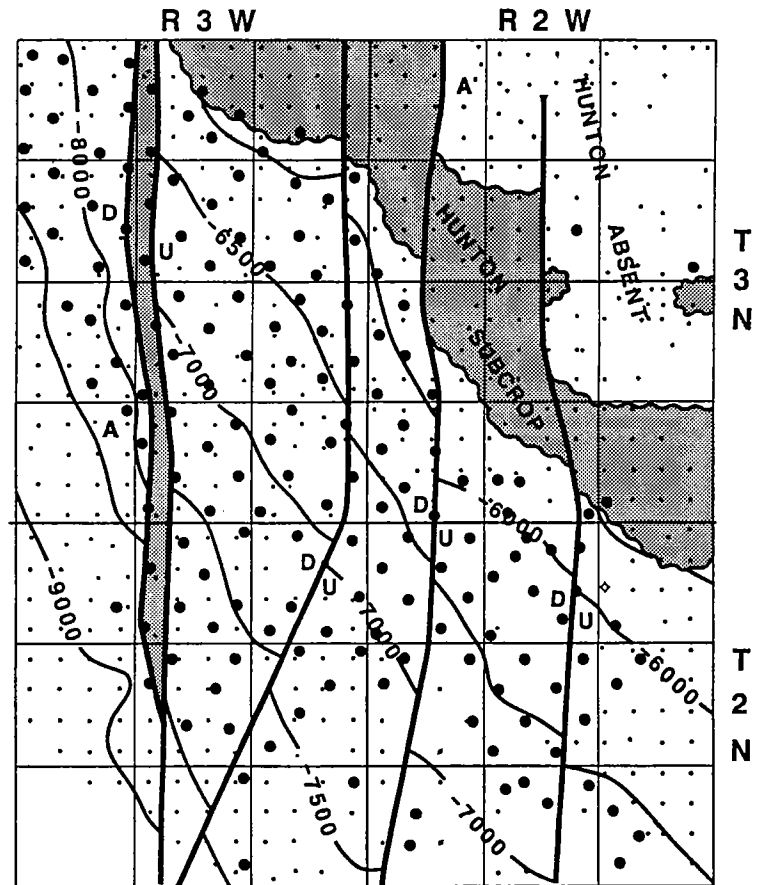


Figure 19. Map of Oklahoma showing distribution of wells producing oil and/or gas from Silurian-Devonian (Hunton) reservoirs. Data are from the well-history file, Natural Resources Information System (NRIS), University of Oklahoma.

PART IV

Hunton Stratigraphy

Kurt Rottmann

BUILDING THE STRATIGRAPHIC COLUMN

Figure 20A,B shows modified stratigraphic columns taken from Amsden (1988) to represent the sequence of strata for the present area of study (Fig. 1, this report). The stratigraphic column illustrates the age and correlation of various groups, formations, and members. Each column of the chart depicts a geographic area noted for similarity of rock type. Amsden developed the correlation chart using primarily his own brachiopod studies, although he mentions trying to incorporate brachiopod data as well as age-relationship data from other faunal groups, including trilobites, corals, ostracodes, conodonts, chitinozoans, palynomorphs, and graptolites, into the stratigraphic column. Although many zones and biozones are listed, Amsden stated that most of the divisions are based primarily on lithostratigraphy.

I feel at this point that a comment on the use of biostratigraphic elements in studying the Hunton should be mentioned. Amsden and other researchers have meticulously worked out biostratigraphic relations of the Late Ordovician Sylvan Shale through the Late Devonian Woodford Shale. Consequently, a tremendous amount of such information is available, but except for specific examples, this information will not be incorporated into the workshop. This by no means is intended to diminish the importance of their work. On the contrary, many of the subjects addressed in this workshop would not be possible if it were not for the detailed paleontological work of these researchers. The biostratigraphy of the Hunton encompasses a massive amount of material and should be treated in a separate workshop.

TYPE LOG

Figure 21 is the type log chosen to represent the Hunton Group in Oklahoma. This log is the Universal Resources Corp. No. 3-17 Heupel, drilled in the NE $\frac{1}{4}$ SE $\frac{1}{4}$ sec. 17, T. 13 N., R. 6 W., Canadian County, Oklahoma. This was a difficult choice, as no one locality includes all the formations of the Hunton Group. This log was chosen because many of the subjects that will be discussed in this workshop are manifested in this log. The lithologic section represented is actually fairly complete, lacking only representation from the Haragan/Bois d'Arc Formations and the Sallisaw Formation.

One point that is addressed later in this section is the possible extrapolation of the various formations and members of the Chimneyhill Subgroup, described by Amsden from surface exposures of the Arbuckle Mountains-Criner Hills, to the subsurface of central and western Oklahoma. Thus, the Keel and Cochrane Formations and the Prices Falls and Fitzhugh Members of the Clarita Formation are shown as dashed lines, suggesting that their presence is only probable, based on their lithology and stratigraphic positions. The probability that these formations and members are present is not without merit.

One of the greatest tools available for understanding the lithostratigraphy of the Hunton is Amsden's detailed descriptions of the cores and samples studied. The wells from which these cores and samples came are plotted and tabulated on Plate 6. Of even greater importance to me is the knowledge that the individual formations, members, and beds can be associated with the geophysical-log responses for unique lithologic zones given in the core and sample descriptions (Amsden, 1975, p. 5). It is my opinion that many of these formations, members, and/or beds can be correlated, from log to log confidently on a regional basis with the integrity of those correlations being maintained and verified by Amsden's descriptions of associated cores and/or samples. Because of this ability to correlate these zones from geophysical logs, it is an aim of this workshop at least to suggest the probable presence of some of these zones in the subsurface of central and western Oklahoma.

The type log of Figure 21 illustrates the formations and members that are described in some detail in the next section. Included are those units from the Upper Ordovician Sylvan Shale through the Upper Devonian-Lower Mississippian Woodford Shale. It also must be mentioned that many correlatable units have various formation names, depending on locality. The correlation chart addresses this matter, but it should be noted that the description of the stratigraphic column and the usage of terms within this workshop will concentrate on central and western Oklahoma terminology.

In order to describe the geologic column of Oklahoma accurately, it is necessary first to describe the general geologic setting prior to deposition of the Sylvan Shale. Figure 22 is a schematic depiction of Ordovi-

				WESTERN OKLAHOMA			
		TEXAS PANHANDLE		HOLLIS BASIN		WESTERN ANADARKO BASIN	
		ANADARKO BASIN					
EUROPE	SERIES	STAGE	EASTERN NORTH AMERICA		①	②	③
			SERIES	STAGE			
MISSISSIPPIAN					OCHELTREE AND ROBERTS COUNTIES Phillips 1C Lint - Shickel 1 Lips (subsurface)	WHEELER COUNTY Phillips 1C Lee (subsurface)	JACKSON COUNTY (subsurface)
					WOODFORD SHALE	WOODFORD SHALE	PENNSYLVANIAN?
					WOODFORD SHALE	WOODFORD SHALE	PENNSYLVANIAN?
					WOODFORD SHALE	WOODFORD SHALE	WOODFORD SHALE
DEVONIAN					WOODFORD SHALE	WOODFORD SHALE	WOODFORD SHALE
					WOODFORD SHALE	WOODFORD SHALE	WOODFORD SHALE
					WOODFORD SHALE	WOODFORD SHALE	WOODFORD SHALE
					WOODFORD SHALE	WOODFORD SHALE	WOODFORD SHALE
LOWER					WOODFORD SHALE	WOODFORD SHALE	WOODFORD SHALE
					WOODFORD SHALE	WOODFORD SHALE	WOODFORD SHALE
					WOODFORD SHALE	WOODFORD SHALE	WOODFORD SHALE
					WOODFORD SHALE	WOODFORD SHALE	WOODFORD SHALE
UPPER					WOODFORD SHALE	WOODFORD SHALE	WOODFORD SHALE
					WOODFORD SHALE	WOODFORD SHALE	WOODFORD SHALE
					WOODFORD SHALE	WOODFORD SHALE	WOODFORD SHALE
					WOODFORD SHALE	WOODFORD SHALE	WOODFORD SHALE
SILURIAN					WOODFORD SHALE	WOODFORD SHALE	WOODFORD SHALE
					WOODFORD SHALE	WOODFORD SHALE	WOODFORD SHALE
					WOODFORD SHALE	WOODFORD SHALE	WOODFORD SHALE
					WOODFORD SHALE	WOODFORD SHALE	WOODFORD SHALE
LOWER					WOODFORD SHALE	WOODFORD SHALE	WOODFORD SHALE
					WOODFORD SHALE	WOODFORD SHALE	WOODFORD SHALE
					WOODFORD SHALE	WOODFORD SHALE	WOODFORD SHALE
					WOODFORD SHALE	WOODFORD SHALE	WOODFORD SHALE
UPPER					WOODFORD SHALE	WOODFORD SHALE	WOODFORD SHALE
					WOODFORD SHALE	WOODFORD SHALE	WOODFORD SHALE
					WOODFORD SHALE	WOODFORD SHALE	WOODFORD SHALE
					WOODFORD SHALE	WOODFORD SHALE	WOODFORD SHALE
OROVICIAN					WOODFORD SHALE	WOODFORD SHALE	WOODFORD SHALE
					WOODFORD SHALE	WOODFORD SHALE	WOODFORD SHALE
					WOODFORD SHALE	WOODFORD SHALE	WOODFORD SHALE
					WOODFORD SHALE	WOODFORD SHALE	WOODFORD SHALE

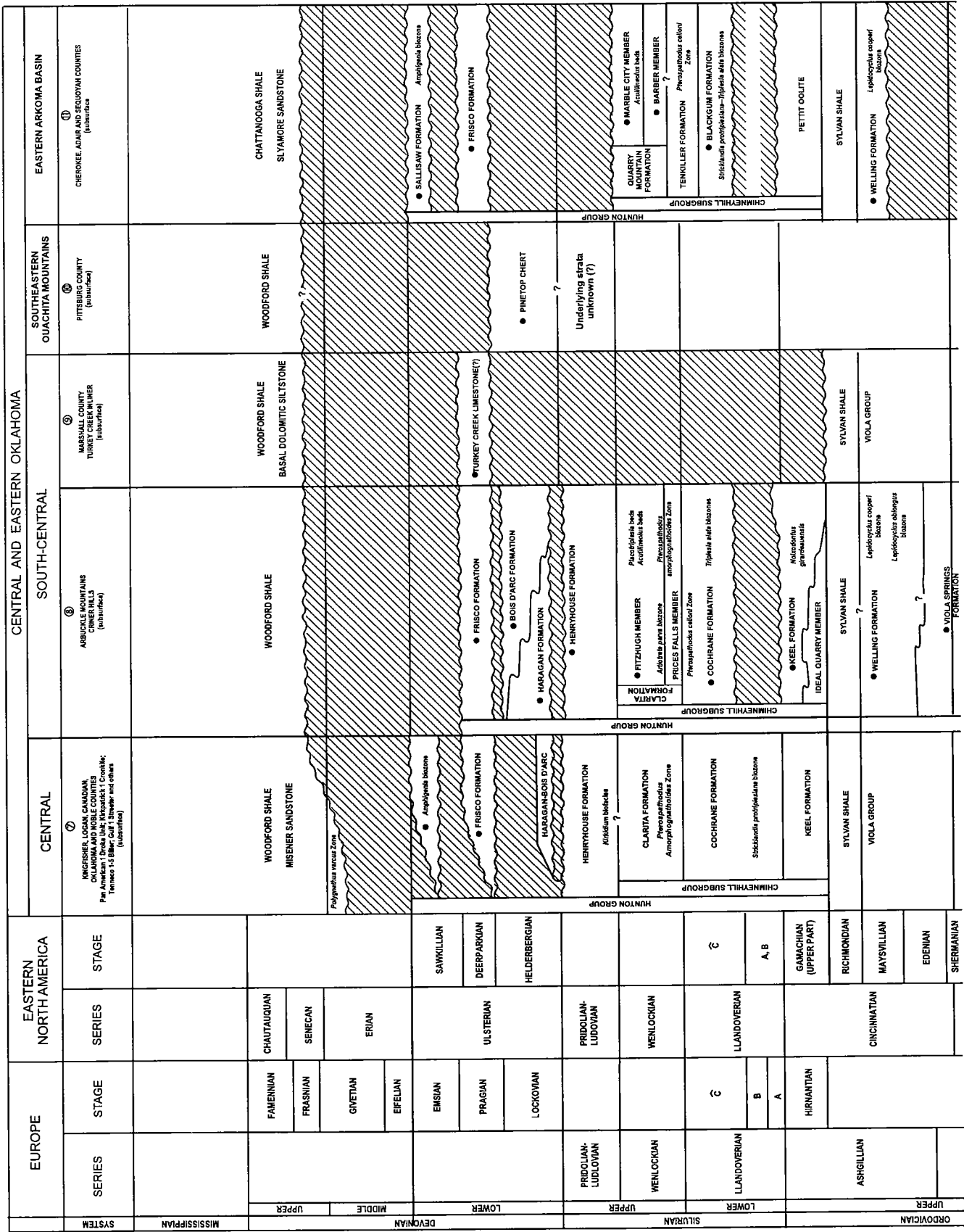


Figure 20. (A) Correlation chart showing stratigraphic relationships of Upper Ordovician through Lower Mississippian strata in western Oklahoma and Texas Panhandle. (B) Correlation chart showing stratigraphic relationships of equivalent strata in central and eastern Oklahoma.

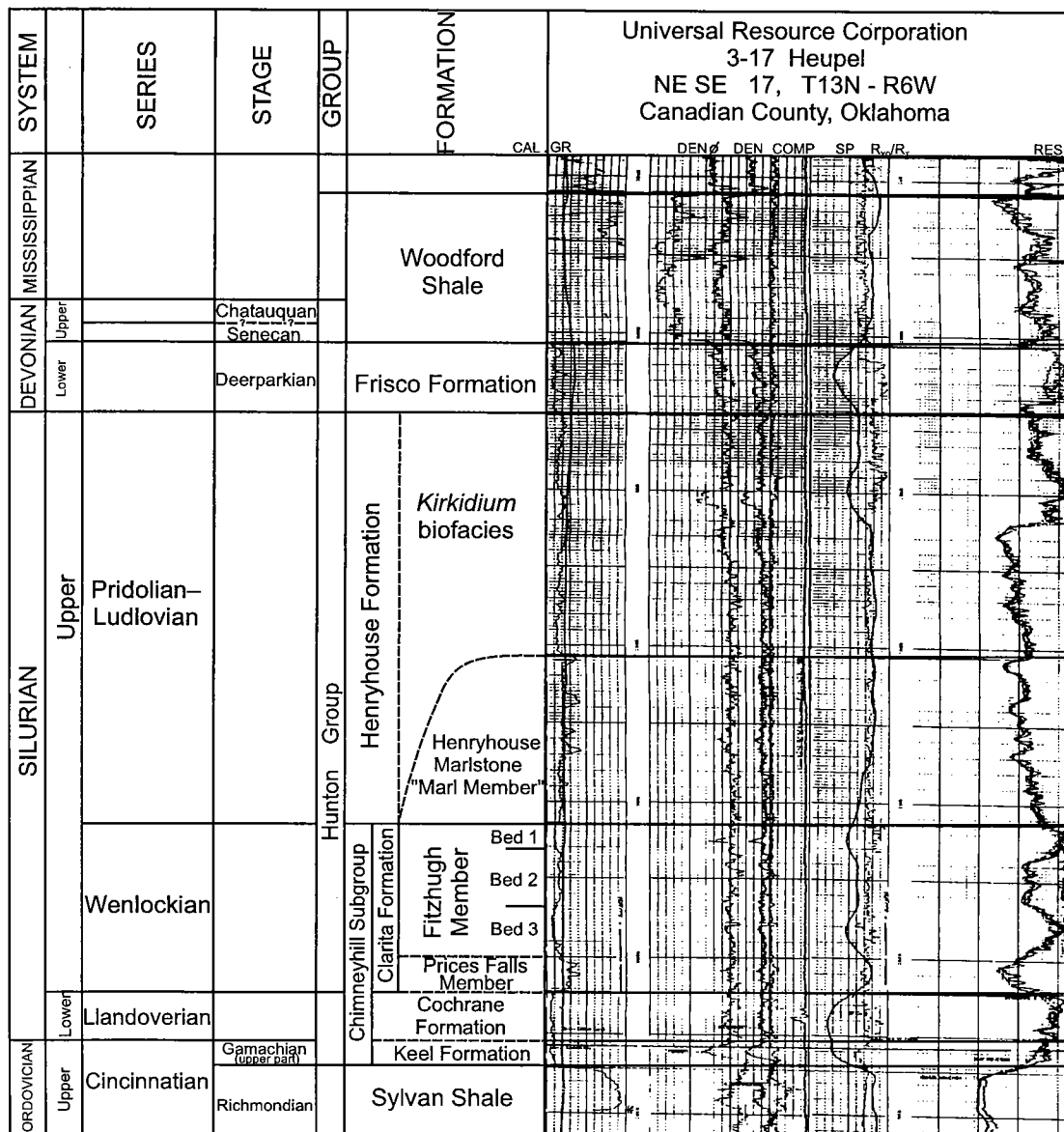


Figure 21. Type log showing Hunton Group formations, members, and other subdivisions. Characteristic geophysical-log signatures are shown. Dashed lines indicate uncertain but probable stratigraphic identification. CAL = caliper; GR = gamma ray; DEN ϕ = density porosity; DEN COMP = density compensated; SP = spontaneous potential; R_{xo}/R_t = ratio of resistivity of flushed zone to resistivity of uninvaded zone, or true resistivity; RES = resistivity.

cian paleogeologic maps of the craton prior to deposition of the Sylvan Shale. In Early Ordovician time the craton was bordered by two belts, the Cordilleran belt on the west and the Appalachian belt on the east (Fig. 22A). These belts supplied clastic deposits, but the deposits were localized only in those areas adjacent to the belts. The craton itself was inundated by a shallow-marine sea where invertebrate faunas thrived. This environment resulted in thick deposits of dolomite and limestone. During the Middle Ordovician, sea level dropped (Fig. 22B), resulting in widespread exposure of the craton and subsequent erosion of the carbonate deposits. In many areas, erosion was complete, exposing Precambrian granites and large areas of Cambrian

sandstones. Transgression of the Middle Ordovician seas resulted in onlap deposits of sandstones over much of the craton (Fig. 22C). The Bromide sandstones of the Simpson Group were part of this event. With complete inundation of the craton, carbonate deposition resumed, resulting in thick fossiliferous deposits. In Oklahoma, the Welling Formation of the Viola Group was deposited.

However, in the east, the Appalachian belt became active, and a mountain-building event, the Taconic Orogeny, occurred. Figure 22D illustrates the distribution of deposits during the Late Ordovician (Cincinnatian). In the Appalachian region, many of the deposits during this period resulted in mudstones, gray-

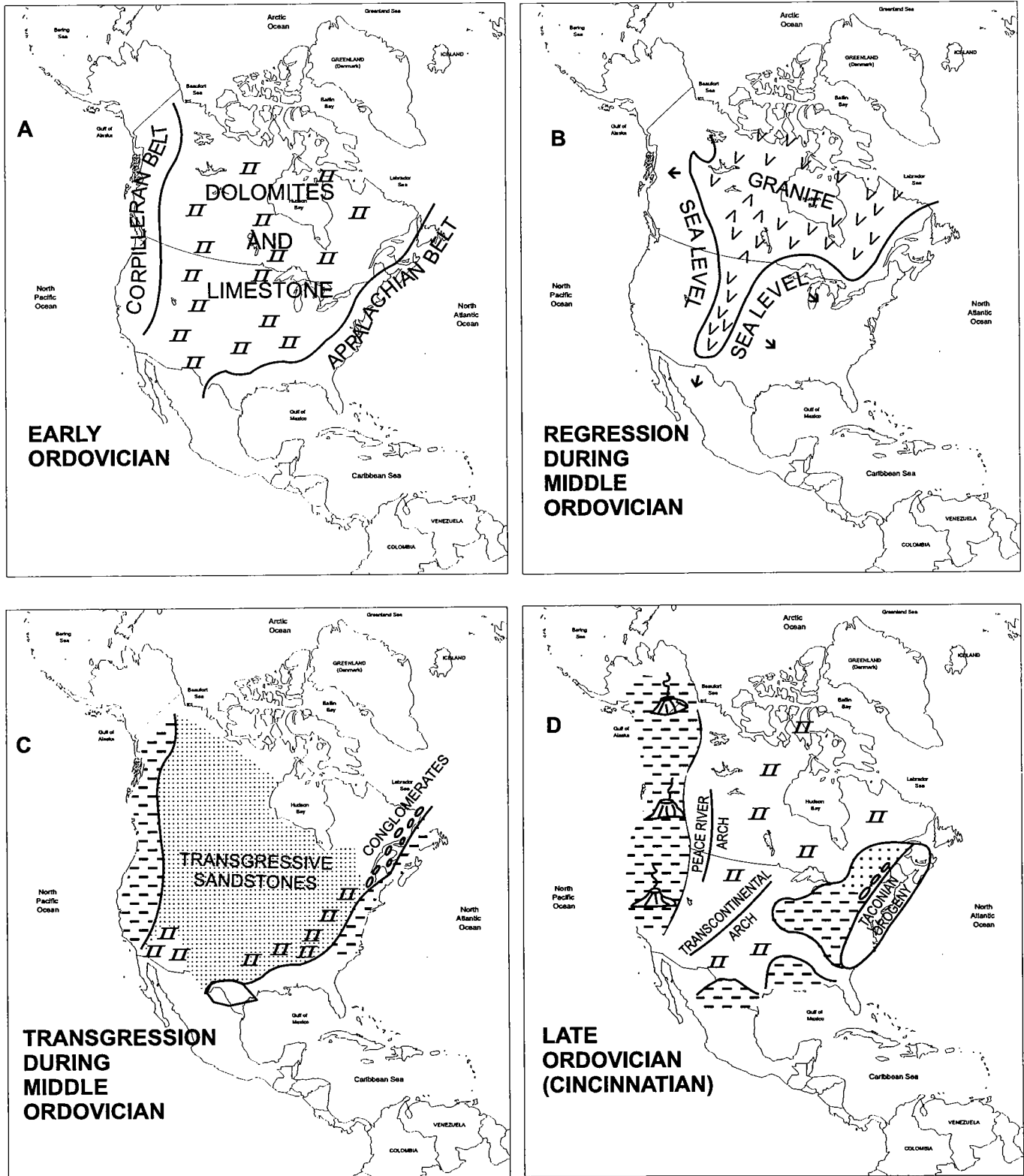


Figure 22. Schematic Ordovician paleogeologic maps. (A) Major carbonate deposition during the Early Ordovician on the craton, flanked by the Cordilleran belt and the Appalachian belt. (B) Major regression and erosion of carbonates, exposing and eroding major areas of the craton during the Middle Ordovician. (C) Transgression, depositing sandstones of Middle Ordovician age. (D) Renewal of carbonate deposition and terrigenous deposits during the Late Ordovician. See text for detailed explanation. From Dott and Batten (1971).

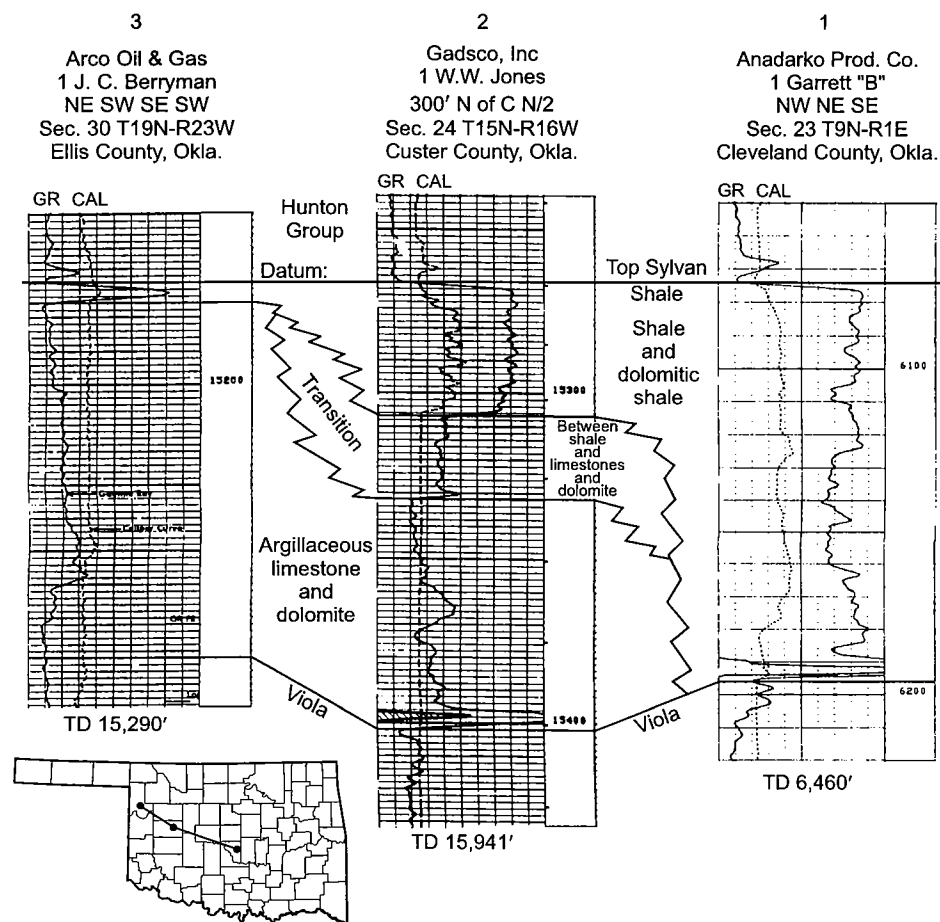


Figure 23. Northwest-southeast stratigraphic cross section, showing gradation of Sylvan Shale from a calcareous or dolomitic shale (well 1) to an argillaceous limestone or dolomite (well 3).

wackes, and cherts. Volcanic activity was also prevalent, both in the Appalachian and Cordilleran belts. As terrigenous material increased, deposition spread from east to west over the craton. It is at this point that the Sylvan Shale was deposited.

ORDOVICIAN Sylvan Shale

The type locality of the Sylvan Shale is near the town of Sylvan, Johnston County, Oklahoma (Taff, 1902). In the area of this report, the Sylvan is underlain by carbonates of the Viola Group and overlain by carbonates of the Hunton Group. This makes identification of the Sylvan readily apparent, except in western Oklahoma, as will be discussed.

Amsden describes the Sylvan as consisting essentially of an upper part of greenish-gray dolomitic shale that locally grades into argillaceous dolomite, and a lower part of dark-gray noncalcareous shale. In western Oklahoma, the Sylvan grades into strongly calcareous shale and argillaceous limestone. Correlation can be exceedingly difficult. Figure 23 is a northwest-southeast stratigraphic cross section from Ellis County

to Cleveland County, Oklahoma, that illustrates the change from essentially a shale to an argillaceous limestone and dolomite. Few regional correlatable features remain, and determining the Sylvan in this carbonate (Viola)-argillaceous carbonate (Sylvan)-carbonate (Hunton) sequence can be taxing.

Decker (1935) assigned the Sylvan Shale to the Late Ordovician on the basis of his studies of graptolites from the lower part of the formation. In 1970, Jenkins (1970, p. 284-285) recovered chitinozoans of Late Ordovician age from the entire Sylvan Formation. The Sylvan had a muddy substrate, and vagrant or sessile shelly fauna are almost entirely lacking.

Ham and Wilson (1967, p. 352) and Jenkins (1970, p. 264) cite physical evidence of an unconformity between the Viola and Sylvan. Amsden (1975, p. 12) states that the Keel-Sylvan contact is only rarely exposed and that the relationship between the Keel and Sylvan is only conjectural. As Amsden points out (see Fig. 20B, south-central Oklahoma), an unconformity of some significance is present between the Late Ordovician Keel Formation and the Early Silurian Cochrane Formation.

The Keel is a thin, oolitic carbonate that commonly is truncated, with post-Keel deposits lying unconformably above the Sylvan Shale. Locally in central and east-central Oklahoma, this unconformity is associated with minor uplift and erosion of the upper part of the Sylvan Shale. Explorationists have often used a "Sylvan thin" as an indicator for structural uplift and closure for the sandstones of the Simpson Group. However, this is not always the case. Figure 24 is an isopach map of the Sylvan Shale in east-central Oklahoma. The isopach thin centered about the center of the NW¼SW¼ sec. 29 is just such a feature, with the abandoned wells in the proximity of this thin having produced from the "Wilcox" sand. However, this isopach map also shows a pronounced thin oriented east-west-southwest from the S½ sec. 20 through sec. 30 into the W½ sec. 31. This thinning is clearly due to a post-Sylvan unconformity that created an erosional drainage system incised into the Sylvan Shale. Cross section A-A' (Fig. 25) is a stratigraphic section illustrating the Sylvan erosion. Carbonates of the Hunton Group were later deposited on this erosional surface.

Keel Formation/Pettit Oolite

The type locality of the Keel Formation is at the Laurence Quarry, Ideal Cement Co., near the northern end of the Arbuckle Mountains, Pontotoc County, Oklahoma (Amsden, 1960, p. 35–44). Amsden assigned this formation to the Late Ordovician Hirnantian Stage on the basis of his brachiopod studies. However, Ams-

The Keel is correlative with the Pettit Oolite, which was assigned formation status by Amsden in 1993. The type locality of the Pettit is approximately 3 mi southwest of the town of Pettit in Cherokee County, Oklahoma (Amsden and Rowland, 1965, p. 22–27). The Pettit Oolite is separated from the overlying Blackgum Formation by an erosional unconformity (see Fig. 20B, eastern Oklahoma).

The Keel Formation is generally less than 15 ft thick and usually is irregular in occurrence owing to the erosional unconformity that followed its deposition. Amsden describes the Keel as a low-magnesium oolite; the ooliths that make up the rock are spherical, and most have a radial or concentric internal structure (Amsden,

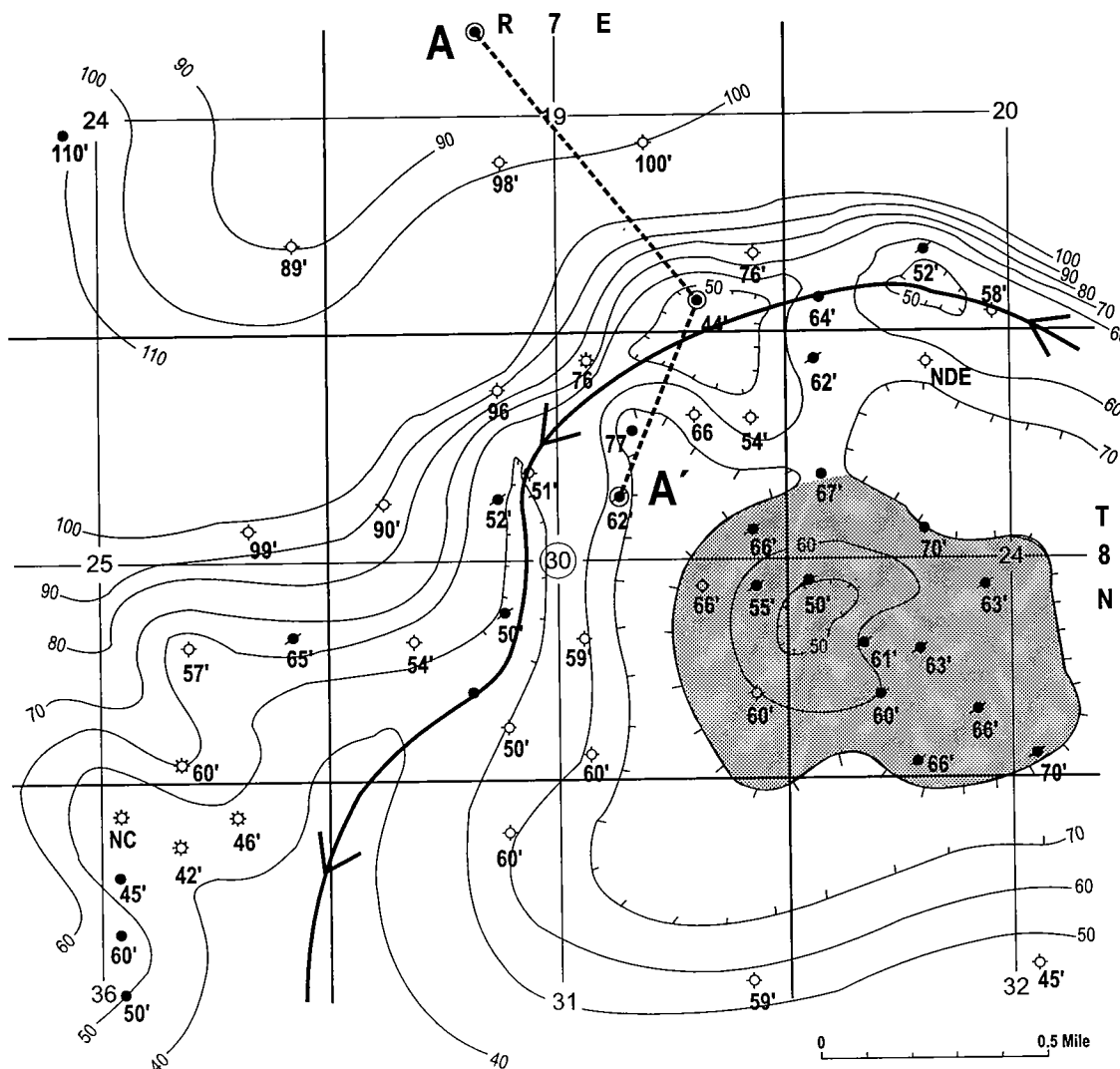


Figure 24. Isopach map of the Sylvan Shale in Seminole County, east-central Oklahoma, illustrating thinning of the Sylvan from fluvial (arrowed line) and structural (shaded area) influences. Contour interval is 10 ft. Hachures indicate areas of thinning. Cross section A–A' is shown in Figure 25.

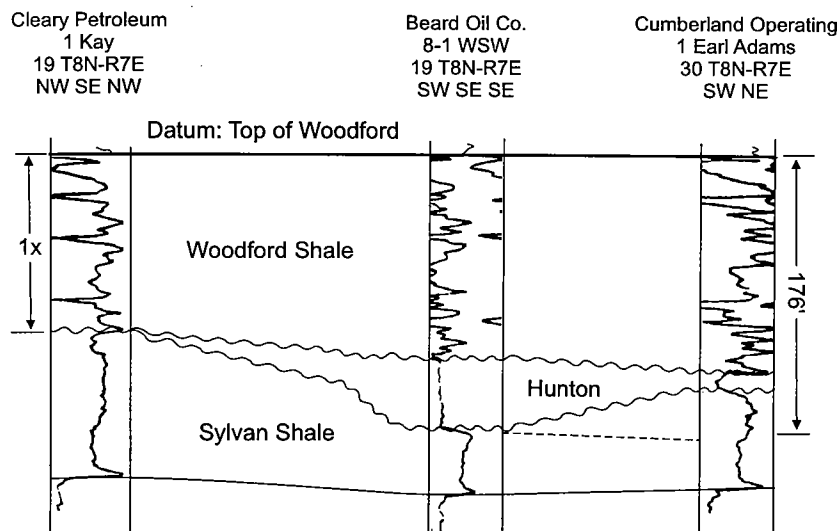


Figure 25. Cross section A-A', illustrating Hunton strata deposited on a Sylvan erosional surface. Line of section on Figure 24. From Rottmann (2000, fig. 14).

1960, pl. 10, figs. 4–6). Most of the oolites have an organic nucleus, and locally the Keel grades into an organo-detrital limestone in which the fossils are lightly coated with precipitated carbonate material (Amsden, 1980, p. 16).

Amsden points out that the presence of oolites is not unique to the Keel or the Pettit Formation. Oolite beds occur in the *Kirkidium* biofacies of the Henryhouse Formation in central Oklahoma (Amsden, 1975, p. 29–30, panel 11) and in the Early Devonian Frisco Formation (Amsden, 1975, p. 69–70, pl. 2, fig. 6). However, the oolites are usually distinctive for the Keel and Pettit Formations. It has been my experience that the oolites of the Keel Formation can be seen readily in drill-cutting samples. However, care must be given to the gathering of those samples, because many wells that reach total depth in the Sylvan do not completely circulate samples to the surface. Figure 21 illustrates the position of the Keel with respect to the underlying Sylvan Shale. The Keel is almost impossible to determine from geophysical logs; well samples or cores are the primary method for determining its presence.

Cochrane Formation/Blackgum Formation/Tenkiller Formation

The type locality of the Cochrane Formation is near the South Fork of Jackfork Creek (formerly Chimneyhill Creek), at the northern end of the Arbuckle Mountains, Pontotoc County, Oklahoma (Amsden, 1960, p. 44–50; 1967). The Cochrane is correlative with the Blackgum Formation of eastern Oklahoma. The type locality of the Blackgum is Blackgum Landing on the south shore of Lake Tenkiller, Cherokee County, Oklahoma (Amsden and Rowland, 1965, p. 20–22).

Amsden describes the Cochrane as a low-magnesium skeletal limestone with abundant benthic fauna, including brachiopods, trilobites, bryozoans, corals, and mollusks (Amsden, 1971; see also Reeds, 1911;

Maxwell, 1936). The Blackgum Formation is similar in fossil content, but it is more dolomitic in chemical makeup than its western Oklahoma counterpart. Amsden notes that chert beds are common in the lower part of the Blackgum and that dolomite is also common, particularly in the lower 5 ft, where it is informally called the tan dolomite member (Amsden, 1980, p. 24). A common constituent of the Cochrane is glauconite. In fact, as stated previously, this formation was referred to as the glauconitic member of the Chimneyhill Formation. Glauconite is not found in all areas and is actually not a good indicator of the presence of this formation. Amsden points out that glauconite can be found in the Clarita, Bois d'Arc, and Frisco Formations (Amsden, 1960, p. 58, 108, 117, 126, 128, 131). He also notes that the Cochrane loses its glauconitic component

in some areas and grades into a pink crinoidal limestone that could be hard to distinguish from the overlying Clarita Formation (Amsden, 1957, p. 21–22; Amsden, 1960, p. 214–218). Perhaps the most distinguishing characteristic of the Cochrane and the correlative Blackgum Formation is the presence of chert and the presence of irregular bedding in outcrop. These two features clearly separate the Cochrane from the overlying Clarita Formation, where present (Amsden, 1980, p. 17).

Amsden states that the Cochrane Formation ranges up to 60 ft in thickness but generally averages about 20 ft. Plate 5 is an isopach map of the Chimneyhill Subgroup. The isopach mostly comprises the Clarita Formation, but I have reason to believe that the Cochrane may be more than 200 ft thick in southwestern Oklahoma on the basis of correlation and sample descriptions from wells drilled through the Cochrane and described by Amsden (1975).

It should be noted at this point that most areas of the ancestral Anadarko basin, Anadarko shelf, Cherokee platform, and Arkoma basin are characterized by factors that suggest a very shallow water depth for deposition of the Sylvan through Cochrane sequence. These indicators include a fairly uniformly thin Sylvan thickness (in comparison to Cambrian and Ordovician deposits in Oklahoma such as the Arbuckle, Simpson, and Viola Groups), oolites of the Keel and Pettit Formations, and a strongly diverse sessile and benthic fauna that required shallow water for Cochrane deposition. The author builds on the importance of this in the section on the Henryhouse Formation.

Figure 20B illustrates stratigraphic relationships in eastern Oklahoma. One formation unique to eastern Oklahoma is the Tenkiller Formation, whose type locality is at Blackgum Landing on the south shore of Lake Tenkiller, Cherokee County, eastern Oklahoma (Amsden and Rowland, 1965, p. 43–41). Lithologically,

this unit is a gray to pinkish-gray, low-magnesium, organo-detrital limestone with well-defined, even beds. The pink color is derived from the disarticulated "pinkish" pelmatozoan plates that constitute the primary part of the faunal debris. The pink crinoids are not unique to this formation and are commonly found in other formations of the Hunton Group, specifically the Clarita and Frisco Formations. Chert is sparse, but quartz crystals are the predominant detritus (Amsden, 1980, p. 25).

On the basis of conodont studies by Klapper (personal letter to Amsden, May 14, 1976), the Tenkiller Formation is assigned a late Llandoveryan age and is correlative with the Cochrane Formation farther to the west.

Clarita Formation/Quarry Mountain Formation

The type locality of the Clarita Formation is near old Hunton townsite in Coal County, Oklahoma (Amsden, 1960, p. 52, 182–188). The Clarita is divided into two members (see correlation chart, Fig. 20A,B), a lower Prices Falls Member and an upper Fitzhugh Member.

The Prices Falls Member consists of a thin but persistent low-calcium shale whose type locality is at Prices Falls in the central part of the Arbuckles (Amsden, 1980). The lithostratigraphic division between this member and the overlying Fitzhugh Member is distinct and, according to Amsden, can be recognized throughout the Arbuckle Mountains and Criner Hills. I have researched the literature and have not been able to locate a source identifying the presence of the Prices Falls Member in the subsurface. However, an interesting relationship occurs in the Clarita Formation in the subsurface of southern, central, and western Oklahoma. A thin, persistent shale or calcareous shale occurs in the same approximate stratigraphic position that the Prices Falls would occupy. To my knowledge, Amsden never alluded to this regional shale as the Prices Falls. Well 3 of cross section A-A' (Pl. 4) is perhaps the easternmost well illustrated in this workshop where this shale is likely to be present. This shale member was identified in wells 4, 5, 7, 8, 9, and 10. In western Oklahoma, this shale member becomes thicker, approaching 40 ft in thickness. Generally, this zone in western Oklahoma is a marlstone and locally grades into a shale laterally, but the zone is correlatable and recognizable in virtually every well.

Cross section B-B' (Pl. 4) also illustrates the probable presence of the Prices Falls Member. The shale lithology is readily apparent in wells 2 and 4. Wells 1 and 3 show the zone, but the facies has changed to a marlstone. Wells 5 through 10 illustrate the marly presence of the member, but in this part of the basin the zone has thickened consider-

ably to almost 40 ft. Other cross sections from this workshop also illustrate the probable presence of this member—for example, wells 1 through 5 of cross section H-H' (Fig. 87); wells 3 through 6 of cross section N-N' (Fig. 111); and wells 1, 3, 4, 5, 6, and 7 of cross section O-O' (Fig. 117).

The type locality of the upper member of the Clarita Formation, the Fitzhugh Member, is along the South Fork of Jackfork Creek at the northeastern end of the Arbuckle Mountains (Amsden, 1960, p. 27–30; Amsden, 1967). The Fitzhugh is a low-magnesium, organo-detrital limestone that is noted for its thin, even-bedded character (Amsden, 1960, pl. 3, figs. 1, 2). Amsden describes the thin, evenly bedded strata as sheets of organic debris spread out on the sea floor. Articulated brachiopod shells are common, which indicates that transport has been minimal and that the fauna present probably represents faunal assemblages. A large part of the faunal debris consists of disarticulated pelmatozoans, probably crinoids, which have a pinkish color, and which led early investigators to call this member "pink crinoidal limestone."

Amsden (1980, p. 19) points out that the Fitzhugh Member can be divided into three lithofacies–biofacies (Fig. 26): (1) crinoidal sparite, (2) arthropod micrite, and (3) ostracode silty marlstone. Each of these has distinctive features, and they probably grade into one another locally. Amsden states that these biofacies are characterized by distinctive environments. The cri-

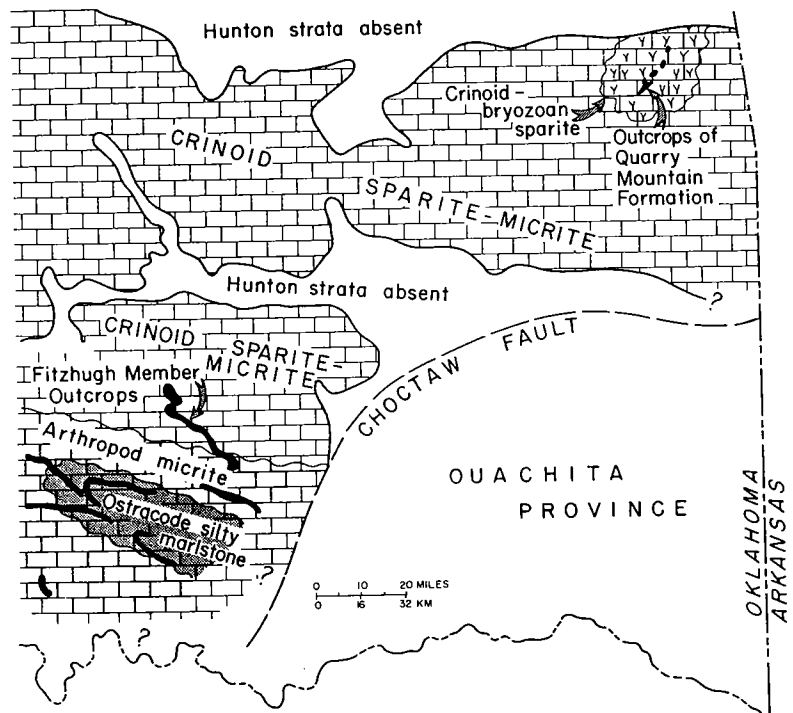


Figure 26. Map showing lithofacies–biofacies pattern in strata of Chimneyhill Subgroup, eastern Oklahoma. Includes strata of Fitzhugh Member of Clarita Formation and Marble City Member of Quarry Mountain Formation. Dolomitization not shown. From Amsden (1980, fig. 6).

noidal sparites represent a broad carbonate platform with a firm substrate and probably clear, shallow water. The floor, or substrate, was probably composed of organic debris. To the south, the sparites were replaced by micrites, representing lime mud. Terrigenous material increased, and the associated fauna responded by changing from a crinoid and brachiopod fauna to mollusk and arthropod faunal assemblages. The ostracode silty marlstone facies is an indication of a muddy substrate and an increase in terrigenous material. This terrigenous material probably originated from the southeast, possibly from the same source that provided the clastic sediments for the Ouachita province, shown in Figure 26. Owing to the muddy substrate, the benthos was almost eliminated, with ostracodes and conodonts representing the predominant faunal elements (Amsden, 1975).

In the subsurface, information necessary to interpret biofacies and lithofacies can realistically be derived only from the evaluation of core data. Amsden suggests, on the basis of his correlation of unique lithologic sequences to corresponding gamma-ray or SP log characteristics, that a reasonable corollary exists between lithology and geophysical logs and that these characteristics can be traced from well to well in the subsurface. I have come to a similar conclusion. Dealing with correlations regionally, it has become obvious that certain geophysical-log patterns in the Clarita Formation are distinctive and maintain a uniformity in character over considerable distances. This predictable sequence of strata in the Clarita is prevalent in southern, central, and west-central Oklahoma. In far western Oklahoma, the correlation of similar beds becomes increasingly difficult, if not impossible.

The type log of Figure 21 illustrates the Clarita Formation. This formation was correlated to this well from several cored wells from which the Clarita Formation was identified. To my knowledge, Amsden never divided the Clarita Formation into its component members in the subsurface. On the basis of lithology and stratigraphic position, the Prices Falls Member is suggested as occupying the lower 20 ft of the Clarita Formation on the type log. It is also suggested, again on the basis of lithology and stratigraphic position, that the upper part of the Clarita is probably the Fitzhugh Member. The zone in the type log is an organic-rich, pinkish limestone, with pelmatozoan plates (mostly crinoids) being responsible for the pinkish color. The general shape of the gamma-ray curve suggests three beds of unique lithology, labeled *bed 1*, *bed 2*, and *bed 3*. Beds 1 and 3 are organo-detrital limestones with abundant pink crinoids. Bed 2 is a marlstone or marly limestone with scattered thin shale streaks. Of interest is Amsden's allusion to the Fitzhugh Member as an organo-detrital limestone grading into a marlstone, resembling the Henryhouse marlstone (ostracode silty marlstone; Amsden, 1980, p. 18). Because of the regional extent of these beds, it is probable that bed 2 is correlative with the argillaceous marlstone of the upper

Clarita Formation that Amsden describes in the outcrop. It also stands to reason that the basin may have a more complete stratigraphic section of the Fitzhugh Member. Bed 1 may be a continuation of deposition that may or may not have been present in the Arbuckle Mountains area because of the unconformity between the Chimneyhill and the Henryhouse. I believe that a subtle erosional unconformity is present between the Wenlockian Clarita and the Ludlovian Henryhouse in the subsurface of south, central, and west-central Oklahoma.

The gamma-ray characters of beds 1, 2, and 3 of the Clarita Formation are remarkably persistent in their regional distribution and geophysical-log character. The importance of this fact is discussed in greater detail in the East Arnett field reservoir study and the Prairie Gem field reservoir study. The regional distribution of beds 1, 2, and 3 can be identified on a number of the wells making up the cross sections of this report. For example, beds 1, 2, and 3 of the Clarita Formation are identified on cross section A-A' (Pl. 4), B-B' (Pl. 4), H-H' (Fig. 87), N-N' (Fig. 111), and O-O' (Fig. 117).

In eastern Oklahoma, the upper Chimneyhill Subgroup is composed of the Quarry Mountain Formation. This formation's type section is on Quarry Mountain, approximately 1 mi north of Marble City, Sequoyah County, Oklahoma (Amsden and Rowland, 1965, p. 42–43). The formation is divided into two members, a lower Barber Member and an upper Marble City Member. The distinction between the two is based on magnesium carbonate ($MgCO_3$) content, with the lower Barber Member composed predominantly of dolomite and the upper Marble City Member predominantly of limestone. Amsden states that the contact is gradational and may be difficult to discern away from the outcrop area (Amsden, 1980, p. 28). The lower magnesian beds of the Barber Member are composed of organo-detrital pelmatozoan–bryozoan limestone similar to that of the overlying Marble City Member. As dolomitization increased, the dolomite crystals replaced the matrix and gradually impinged on the fossil clasts until eventually, as the rock approached crystalline dolomite, the fossils were completely replaced (Amsden, 1980, p. 26). The Marble City Member is a light-gray to pinkish-gray organo-detrital limestone. The insoluble residues are exceedingly low, and in places the Marble City Member is a high-calcium limestone, which is mined as a source of lime.

Amsden described the brachiopods from the Marble City Member and the upper part of the Barber Member and assigned the Quarry Mountain Formation a Wenlockian age and correlated it with the Clarita Formation of the Arbuckle Mountains (Amsden, 1980).

SILURIAN

Henryhouse Formation

The type locality of the Henryhouse Formation is on Henryhouse Creek in the western part of the Arbuckle Mountains, Carter County, Oklahoma (Amsden, 1960,

p. 66–84). On the basis of graptolite studies (Decker, 1935; Jaeger, 1967, p. 282; Amsden, 1975, p. 24), articulate brachiopods (Amsden, 1951), crinoids (Strimple, 1963), ostracodes (Lundin, 1965), rugose corals (Sutherland, 1965), and trilobites (Campbell, 1967), the Henryhouse is assigned to the Late Silurian. On the basis of conodont studies by Barrick (1980), the lower part of the Henryhouse is assigned to the Ludlovian Stage, and the upper part to the Pridolian.

The Henryhouse is largely a marlstone with a mud-supported texture. Terrigenous materials generally comprise variable amounts of silt and clay detritus, and in places this facies grades into calcareous shale. Amsden points out that the terrigenous detritus approaches 20% and that the concentration of this detritus forms a broad belt bordering the Marathon–Ouachita province. Figure 27 is a modified regional map illustrating this province and the Henryhouse marlstone facies. The map suggests that the source of the terrigenous material may have been to the south or southeast (Amsden, 1975, p. 23–24).

Figure 28 illustrates in greater detail the facies relationships of the Henryhouse Formation. Marlstones and calcareous shales are concentrated in the southeastern part of the Anadarko basin. As terrigenous material decreased, the strata changed from calcareous shale to marlstone. Farther to the north and northwest,

the strata changed to a skeletal grain-supported limestone. The fauna associated with this facies is termed the *Kirkidium* biofacies of the Henryhouse Formation (Amsden, 1969; 1975, p. 29–56, panel 11; 1980, p. 22; 1981). The name of this biofacies was derived from the large pentamerid brachiopods that dominate the shelly fauna. The predominant species are *Kirkidium pingue pingue* and *K. pingue latum*. Generally, this biofacies is found in the upper part of the Henryhouse, but thicknesses within the Henryhouse are variable. The type log of Figure 21 suggests that this biofacies may occupy the entire Henryhouse interval. This interpretation is based on Amsden's description of the Gulf No. 1 Streeter core (Amsden, 1975, p. 101). Specimens of *Kirkidium* are found in a fossiliferous marlstone directly above the Chimneyhill Subgroup.

The position of the *Kirkidium* biofacies lies within that area subjected to Hunton-age dolomitization. Figure 27 illustrates a dolomite–limestone boundary, which is part of a much broader geometry involving the entire craton during the Silurian Period. This topic is discussed in more detail in the Prairie Gem field study. Amsden points out that the strata within the dolomite front vary from weakly to strongly dolomitized beds with excellent porosity. The skeletal material within the dolomitized beds commonly has been obliterated by the alteration.

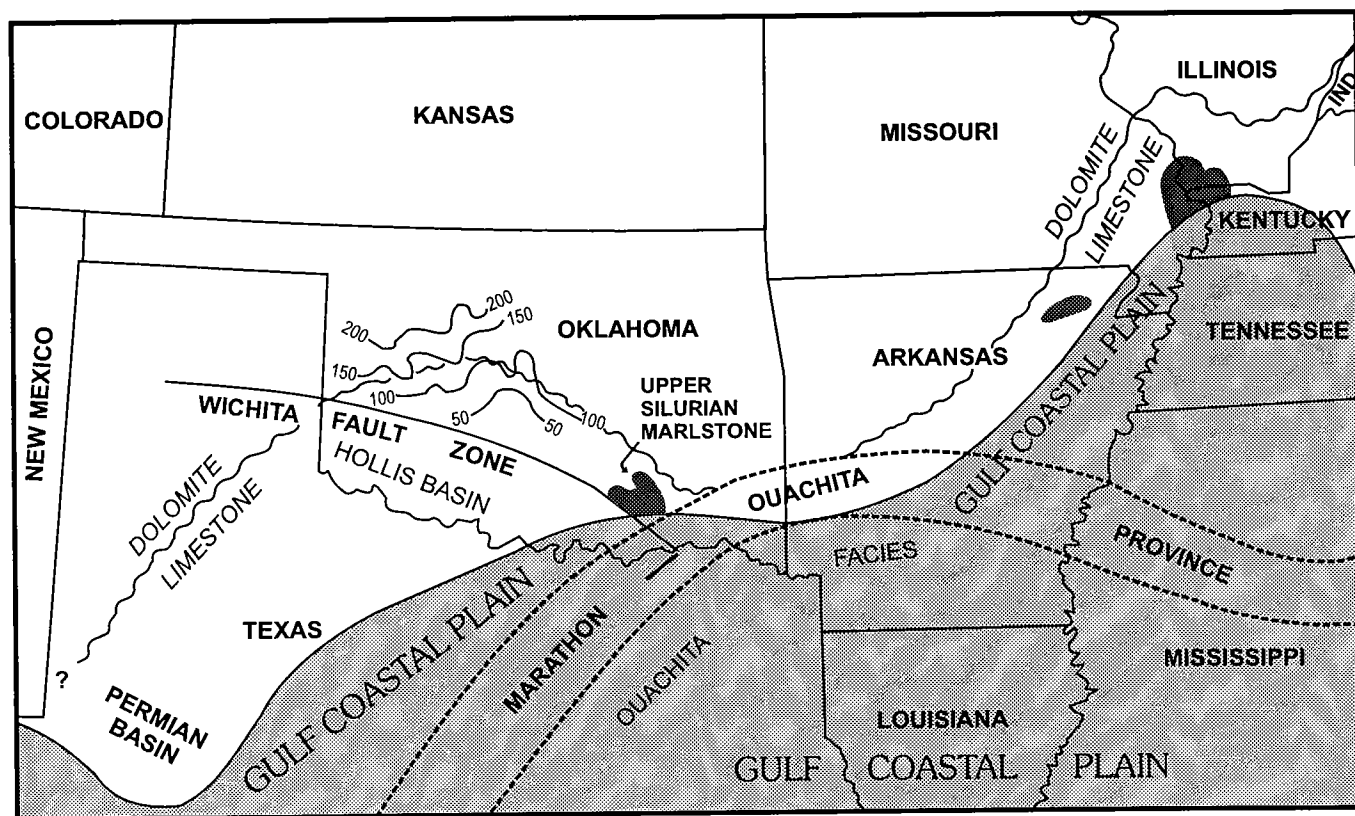


Figure 27. Map showing distribution of Henryhouse marlstone facies (areas in black) in the southern Midcontinent region. Isochachs are of an uneroded marlstone sequence ("Marl member" in Fig. 21); contour interval is 50 ft. Dolomite and limestone facies are separated by a wavy line. Modified from Amsden (1988, fig. 8).

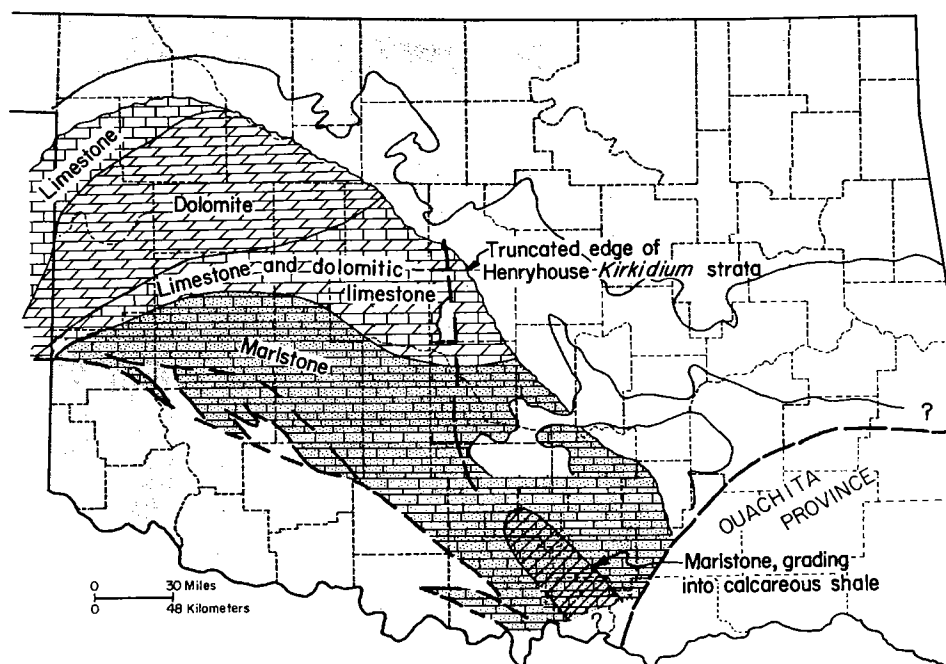


Figure 28. Map showing distribution of major lithofacies in Henryhouse Formation and correlative *Kirkidium* biofacies. From Amsden (1980, fig. 7).

The type log of Figure 21 shows a section within the Henryhouse Formation that I call informally the Henryhouse “marlstone.” This zone is a sequence of strata that has maintained its overall gamma-ray pattern and configuration in almost every well of east-central, central, west-central, and south-central Oklahoma. The zone is composed of marlstone and several prominent beds of calcareous shale. Cross section A–A’ (Pl. 4) illustrates the regional nature and high degree of correlation of this zone. The cross section shows that the zone increases in thickness from east to west. Cross section B–B’ (Pl. 4) also illustrates the uniformity of this zone. Individual beds seem to be in an identical, yet vertically proportional, position within this zone, depending on its overall thickness. The zone thickens to the north and west, as illustrated on cross section B–B’ (Pl. 4) with one of the thickest intervals in well 10. Figure 27 includes an isopach map of this marlstone interval. Adjacent to the Wichita fault zone, this zone is approximately 50 ft thick. The isopach thickens to the north, where the interval exceeds 225 ft in thickness. The isopach does not thin again, because this isopach represents the total thickness of the zone, which is unaffected by uplift, tilting, or regional erosion. Farther north, this interval thins as a result of regional tilting and subsequent erosion of Hunton strata and so has not been isopached.

Of interest to me is the uncanny duplication, or identical geometry, of this section from well to well over the entire region of deposition. This implies that when an impulse of fine clay detritus was introduced into the basin from its source, it must have been uniformly distributed over a wide area. Even the “cleaner” gamma-ray signatures indicate that less shaly beds are correlatable from well to well. This implies that almost

the entire eastern and central parts of the Anadarko basin reflected a bed-to-bed uniform depositional environment. The upper part of the Henryhouse (*Kirkidium* biofacies) also reflects similar log characteristics, although they are not as obvious. Some marker beds are easily correlatable from well to well over virtually the entire eastern and central parts of the basin, becoming obscure only in highly dolomitized areas. Proponents of sequence stratigraphy who imply a stratigraphic model comprising individual sequences of strata in the Henryhouse will need to address and incorporate these regional uniform depositional characteristics of the Henryhouse. This uniformity of deposition over large areas was also recognized for the Clarita Formation. The question of sequence stratigraphy and regionally identical sequences of strata is addressed again in the Prairie Gem field study.

The Henryhouse–Chimneyhill contact is one of the most easily recognizable contacts within the Hunton Group. Typically, the Henryhouse, being a marlstone, lies on top of an organo-detrital limestone of the Clarita, whose gamma-ray signature is characteristically much “cleaner.” This contact is usually associated with a significant drop in resistivity from the Clarita to the Henryhouse (assuming that water has not caused the deflection). The type log (Fig. 21) shows a typical such contact. Amsden suggested an unconformity between the Clarita and the Henryhouse in the Arbuckle Mountains–Criner Hills surface exposures (see Fig. 20B). However, he felt that the nature of this boundary in the subsurface of central and western Oklahoma is not known. The underlying Fitzhugh Member of the Clarita exhibits this regional uniformity of log character and strata sequence; beds 1, 2, and 3 can be recognized almost basinwide. Wells 1 and 2 of cross section B–B’ (Pl.

4) illustrate the marlstones of the Henryhouse overlying the marly limestones of bed 2 of the Clarita. Where this sequence of strata occurs, identification of the Chimneyhill–Henryhouse boundary can be difficult. Both wells 1 and 2 are surrounded by wells in which bed 1 is present. I interpret the absence of bed 1 in these two wells as due to erosion rather than nondeposition.

The Henryhouse Formation represents the last of the Silurian deposits in Oklahoma. It would be prudent at this point to consider a few observations concerning the geometry and history of the Anadarko basin during the Late Ordovician and Silurian. This time period was marked by a complex history of marine sedimentation, uplift, and erosion. The Anadarko basin was a structural–sedimentary basin that was actively subsiding

during the Cambrian and Early and Middle Ordovician. The Wichita fault zone was probably developing (Ham and others, 1964, p. 33–37, 149–154; Amsden, 1980, p. 59), with the north side being downthrown, producing a sedimentary basin, and the south side possibly occurring as an intermittent high. Evidence of this subsidence on the north side of the Wichita fault zone is seen in Figure 29A. Near the depocenter of the basin, strata of the Simpson and Viola Groups were deposited as thick sequences that thinned dramatically to the north, toward the intrabasinal shelf.

I believe that at this time (post-Viola–pre-Sylvan) subsidence in the Anadarko basin changed with respect to rate and to location of the depocenter. An examination of Amsden's Sylvan Shale isopach map is the first indicator of this change (Amsden, 1975, panel

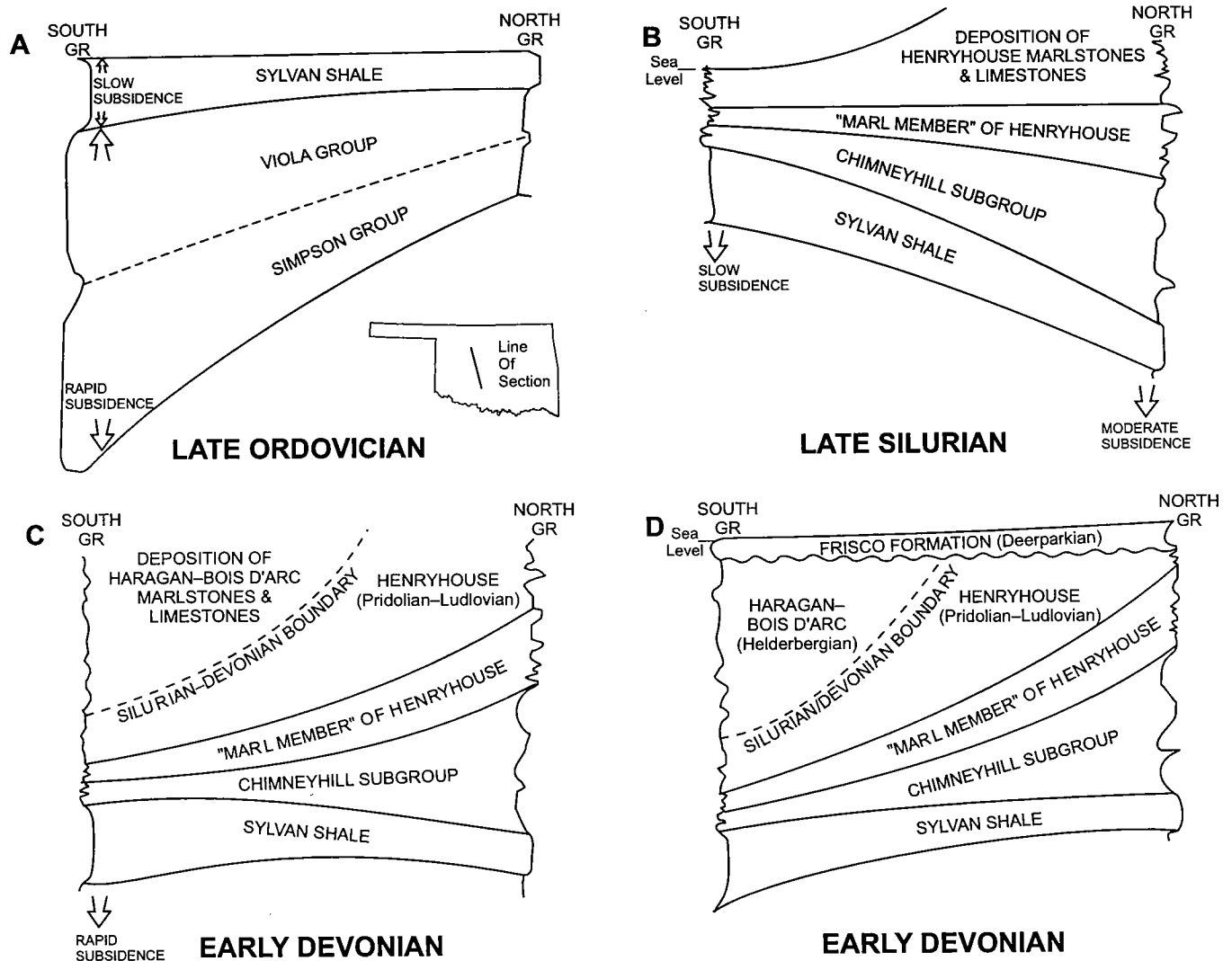


Figure 29. Schematic cross sections illustrating proposed northward shifting of the Silurian depocenter in the Anadarko basin. (A) Thickening in the structurally deep Anadarko basin, with thinning northward. (B) Series of thin deposits in southern Oklahoma, with all sequences thickening northward, suggesting subsidence rates greater in northern Oklahoma. (C) Renewed subsidence in southern Oklahoma, resulting in deposition of the Haragan/Bois d'Arc carbonate sequence. (D) Uplift and erosion of Helderbergian strata, with subsequent deposition of Deerparkian strata (Frisco Formation).

8). The Sylvan isopach suggests that the Sylvan ranges from 50–100 ft to approximately 200 ft in thickness near what is considered to be the structurally deep part of the basin. Adjacent to the Wichita fault zone, the Sylvan isopach abruptly thickens, reaching thicknesses exceeding 400 ft. These areas are probably grabens that filled rapidly with Sylvan strata. The fact that the Sylvan does not vary in thickness even as much as 100 ft from the depocenter of the basin to its outer margins suggests that subsidence had slowed considerably and that the grabens represent isolated structural events rather than interbasinal events.

Amsden points out that the Sylvan is composed of evenly bedded deposits whose source area probably was a considerable distance away. The lack of a vagrant or sessile benthic fauna in the Sylvan suggests three possible environments of deposition: (1) relatively deep water (Ham, 1969, p. 11), (2) cold water, or (3) a basin with restricted bottom circulation (Amsden, 1980, p. 60). Amsden felt that the lateral gradation of shale facies to carbonate facies suggests the latter. If the basin had a restricted circulation, it could have been that at this time (post-Sylvan) circulation increased, providing calcium-rich waters for the formation of oolites that occur from the Texas Panhandle eastward through Oklahoma. The presence of these oolites also suggests that the water depth must have been exceedingly shallow, again with subsidence in all areas at a minimum. The organically rich Cochrane Formation also suggests that shallow warm water was present throughout the Anadarko basin at that time.

Amsden states that deposition in the southern, structurally deep part of the Anadarko basin may have been essentially continuous from Late Ordovician time into Mississippian time (Amsden 1980, p. 60). His conclusion was based on the following data: (1) all stratigraphic units thicken from north to south, with their thickest accumulations in the structurally deepest part of the basin; and (2) his Hunton isopachs display irregularities in the northern, shallower part of the basin and become more uniform, paralleling structure contours in the deeper part of the basin (Amsden, 1980, p. 60).

As mentioned previously, I interpret that subsidence, both in the structurally deep part of the Anadarko basin and in the shallow parts, was minimal during deposition of the Ordovician Sylvan Shale, the Hiranian Keel Formation, and the Llandoveryan Cochrane Formation. I believe that deposition of the Wenlockian Clarita Formation and the Pridolian–Ludlovian Henryhouse Formation deviated from the accepted loci of subsidence and the rate and pattern of deposition in the basin. The isopach map of the Chimneyhill Subgroup clearly shows a thickening from south to north, as opposed to Amsden's conclusion that thickening occurred in all zones from north to south. It could be argued that thinning in the Clarita, in the vicinity of the structurally deep part of the basin, could have been due to uplift and erosion. However, cross sections A–A' (Pl. 4), B–B' (Pl. 4), and N–N' (Fig. 111)

were specifically designed to illustrate that the Clarita thickens not only to the north and northwest, but also that regionally correlatable beds 1, 2, and 3 of the Clarita thicken individually to the north and northwest. Furthermore, the isopach in Figure 27 is of the zone identified as the marlstone member of the Henryhouse Formation shown on the type log (Fig. 21). As described previously, this zone is the interval whose overall lithostratigraphic pattern, as identified on geophysical logs, is uniform in character and can be correlated regionally. The isopach illustrates that this zone also increases in thickness from south to north. Examination of the individual beds constituting this zone also indicates a thickening from south to north.

The *Kirkidium* biofacies is thick in the northern part of Oklahoma and tends to thicken to the south as the underlying marlstone member thins. However, the boundary between the marlstones of the upper Henryhouse and those of the Devonian Haragan Formation is obscure and indistinct, as biostratigraphic control is sparse. Thus, the apparent thickening of the upper Henryhouse to the south may, in fact, actually be a result of renewed subsidence in the south in Early Devonian time, which initiated deposition of the Haragan Formation, as illustrated in Figure 29C.

In conclusion, then, for this topic, I believe that the depocenter of the Anadarko basin shifted northward during the Silurian. The thicker sequences of strata in the Clarita and Henryhouse Formations support this view. This shifting of the depocenter is interpreted as a temporary cessation of basement subsidence in the southern part of the basin and is associated with a gradual and continuous subsidence in the northern part of the basin. Renewal of subsidence in the structurally deep part of the basin resumed during latest Silurian or Early Devonian time and continued essentially unabated at least through Early Mississippian time, as illustrated in Figure 29C,D.

DEVONIAN

Haragan/Bois d'Arc Formations

The type locality of the Haragan Formation is along Haragan Creek near White Mound, in the central part of the Arbuckle Mountains, Murray County, Oklahoma (Amsden, 1960, p. 86–99). The Haragan is composed of marlstones similar in lithology to the underlying Henryhouse. A notable exception to the continuation of this depositional environment of the Henryhouse is that the Haragan contains a prolific invertebrate fauna of distinctly Helderbergian age (Amsden 1958a, p. 11–17; Lundin, 1968, p. 10–17; Campbell, 1977). This faunal age difference is the only available criterion for distinguishing the Henryhouse from the Haragan, as they are almost lithologically identical.

The type locality of the Bois d'Arc Formation is along Bois d'Arc Creek in the northern part of the Arbuckle Mountains, Pontotoc County, Oklahoma (Amsden, 1960, p. 99–104). Amsden considers the Bois d'Arc to be

a lateral facies of the Haragan Formation. Figure 30 illustrates the lateral facies relationship between the Haragan and the Bois d'Arc. The Bois d'Arc Formation is composed of two members, the cherty marlstones of the Cravatt Member and the organo-detrital sparites of the overlying Fittstown Member. Amsden (1975) noted both a lateral and vertical gradation between the Cravatt and Fittstown Members.

The Haragan Formation is characterized by a generally mud-supported fabric with fossils scattered in varying degrees of intensity (Amsden, 1980, p. 44). Amsden points out that the insoluble residues vary widely but generally average about 16%. The lateral gradation from the Haragan to the Cravatt Member of the Bois d'Arc is discerned by an increase in chert content. As detritus decreases in content, the strata become more of an organo-detrital limestone or grain-supported calcarenite, with chert accompanying this lateral facies change; this facies is the Fittstown Member of the Bois d'Arc. The facies of the Fittstown Member can easily be confused with the similar facies of the overlying Frisco Formation on the basis of geophysical-log or well-sample correlations. Only faunal control can differentiate the Bois d'Arc from the Frisco.

The Haragan and Bois d'Arc Formations are confined to the southeastern part of the Anadarko basin. This distribution may in large part be due to the pre-Frisco erosional unconformity, which modified the thicknesses of the underlying strata. Another factor conducive to Helderbergian deposition in the south-

eastern part of the Anadarko basin was renewed subsidence of the basin in its structurally deep part, as illustrated in Figure 29C. This is a plausible explanation for the lateral gradation from north to south of Silurian Henryhouse marlstones to Devonian Haragan marlstones. Examination of Figure 30 shows an erosional unconformity between the Henryhouse and Haragan Formations. Clearly, Devonian strata rest unconformably upon Henryhouse, Clarita, or Cochrane strata. Amsden makes an interesting observation concerning this unconformity; he noted only one locality that exhibited any physical evidence of an unconformity (Amsden, 1980, p. 9).

Hydrocarbon production is often attributed to the Bois d'Arc. While this may be the case, Amsden and I agree that most production is either from the Frisco Formation or from Silurian zones, specifically from local dolomitic beds in the Clarita or the *Kirkidium* biofacies.

Frisco Formation

The type locality of the Frisco Formation is along Bois d'Arc Creek near the northeastern end of the Arbuckle Mountains, Pontotoc County, Oklahoma (Amsden, 1960, p. 125–135; 1961, p. 23–45). On the basis of articulate-brachiopod studies by Amsden and Ventress (1963, p. 41–59), the Frisco is assigned a middle Early Devonian (Deerparkian) age (Fig. 20A,B).

The Frisco is a light-gray to pinkish-gray organo-detrital grain-supported limestone whose pinkish hue comes from disarticulated pelamatozoan plates, most-

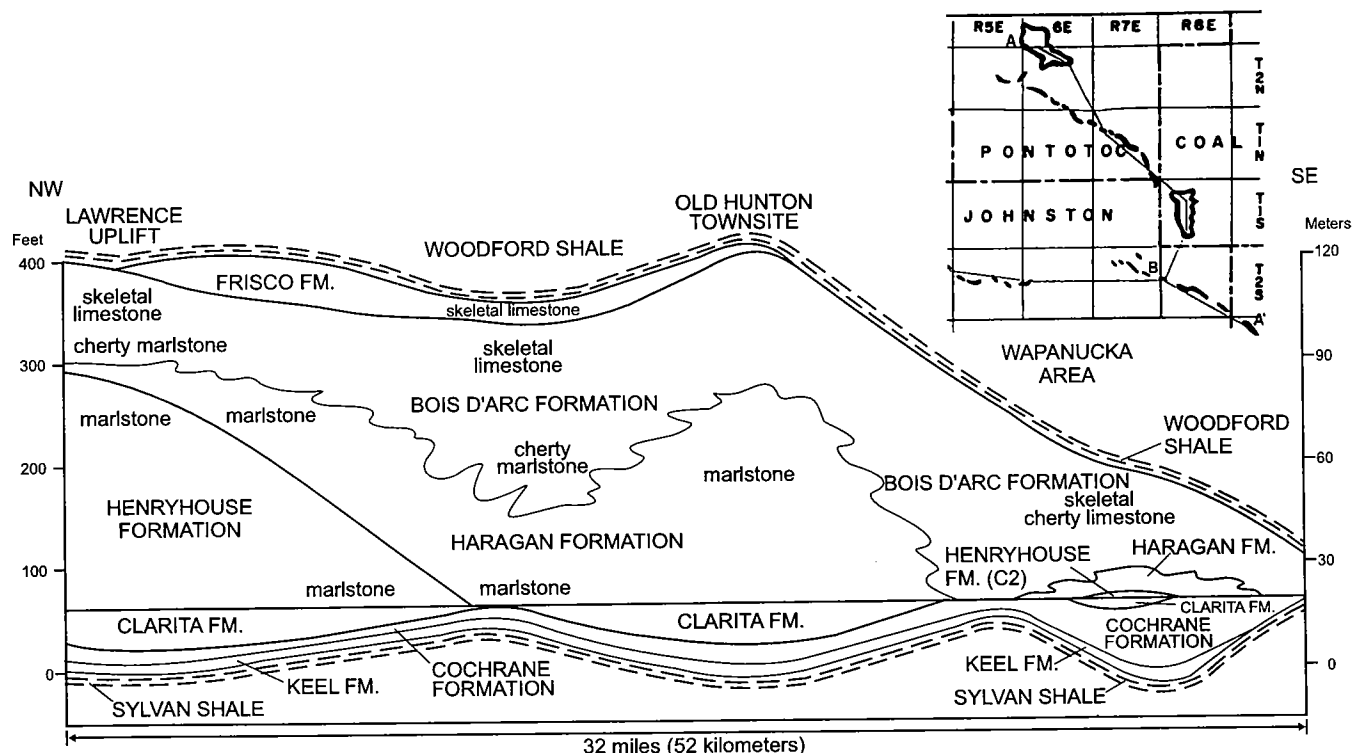


Figure 30. Northwest-southeast stratigraphic section showing Henryhouse-Haragan/Bois d'Arc stratigraphic relationships along the northeastern margin of the Arbuckle Mountains from the Lawrence uplift in Pontotoc County to the Wapanucka area in Johnston County, Oklahoma. Modified from Amsden and Barrick (1988, p. 8).

ly crinoids. The Frisco is highly organic, and Amsden states that most of the debris is highly fragmented. Figure 31 are two graphs showing that the magnesium carbonate content of the Frisco is exceedingly low in eastern, central, and western Oklahoma. This is important, because dolomite occurs in strata both above and below this limestone, and this dolomitization did not affect the Frisco. Insoluble residues are also very low, rarely exceeding 2–3% (Amsden, 1980, p. 46).

An unconformity of considerable magnitude lies between the Helderbergian Haragan/Bois d'Arc and the Deerparkian Frisco Formations, seen on the correlation chart of Figure 20A,B and on the pre-Woodford subcrop map of Plate 6. Depositional relationships also suggest the magnitude of this unconformity. The Frisco Formation was deposited on various older strata. At the north end of the Arbuckle Mountains, the Frisco was deposited on the Bois d'Arc Formation. Where the underlying unit is the Fittstown Member of the Bois d'Arc, the contact can be difficult to determine. Generally, the Frisco contains substantially less detrital material and displays abundant evidence of solution and recrystallization (Amsden, 1975, p. 73). In the Anadarko basin, biostratigraphic control from a number of cores indicates that the Frisco was deposited on the fossiliferous *Kirkidium* biofacies of the Henryhouse Formation (Ams-

den, 1980, p. 47). In eastern Oklahoma, the Frisco was deposited on the Silurian Quarry Mountain Formation of the Chimneyhill Subgroup. And finally, in the Hollis basin of southwestern Oklahoma, the Frisco was deposited on the Ordovician Viola Limestone (Amsden, 1975).

Amsden suggests that the pre-Frisco unconformity is erosional in nature. In outcrops, considerable dissolution is evidenced in the underlying strata. Commonly, these strata were eroded by dissolution channels, which were filled with tongues of Frisco sediment (Amsden, 1980, p. 47). Some of these solution cavities approach 2–3 ft in depth. In western Oklahoma, some of the solution channels are filled with detritus, perhaps of Misener Sandstone, a basal deposit of the Woodford Shale. The underlying surface was lithified prior to the pre-Frisco erosional period, as shells are commonly cut off at the unconformity (Amsden, 1980, p. 48). The dissolution of the underlying surface probably increased porosity and permeability dramatically.

Unnamed Carbonate Unit

There appears to be a facies in the upper Hunton Group in western Oklahoma that is unique in its log character and stratigraphic position. Lithostratigraphic and biostratigraphic control are sparse for this facies, which is identified on the pre-Woodford subcrop map of Plate 6. From my experience, the log character is distinct and easily recognizable. Well 9 of cross section A–A' (Pl. 4) shows an excellent example of this facies. A mud log of the well indicated that the facies is predominantly finely crystalline dolomite and dolomitic limestone and is present from 15,576 to 15,876 ft.

Two additional occurrences of this facies are incorporated into cross section B–B' (Pl. 4). Well 8 was drilled within a Hunton-age graben (Rottmann, 2000); the graben is oriented northwest–southeast (see Hunton structure map, Pl. 3). Well 7 was drilled on the south flank of the graben on the up-thrown block. The lower section of the Hunton in both wells 7 and 8 is correlative. However, the upper 210 ft of well 8 has no equivalent section in any offset well. The Woodford Shale in wells 7 and 8 are almost identical in thickness, indicating that prior to deposition of the Woodford, the Hunton paleosurface must have been flat and featureless (see Leedey field study for information on Woodford–Hunton stratigraphic relationships). The flat surface of the Hunton suggests that the 210 ft of upper Hunton in well 8 was a preserved section in the Hunton-age graben, and it may represent a fill deposit prior to Woodford deposition.

A second occurrence of this facies can be observed in wells 9 and 10 on cross section B–B' (Pl. 4). Well 9 has almost 280 ft of

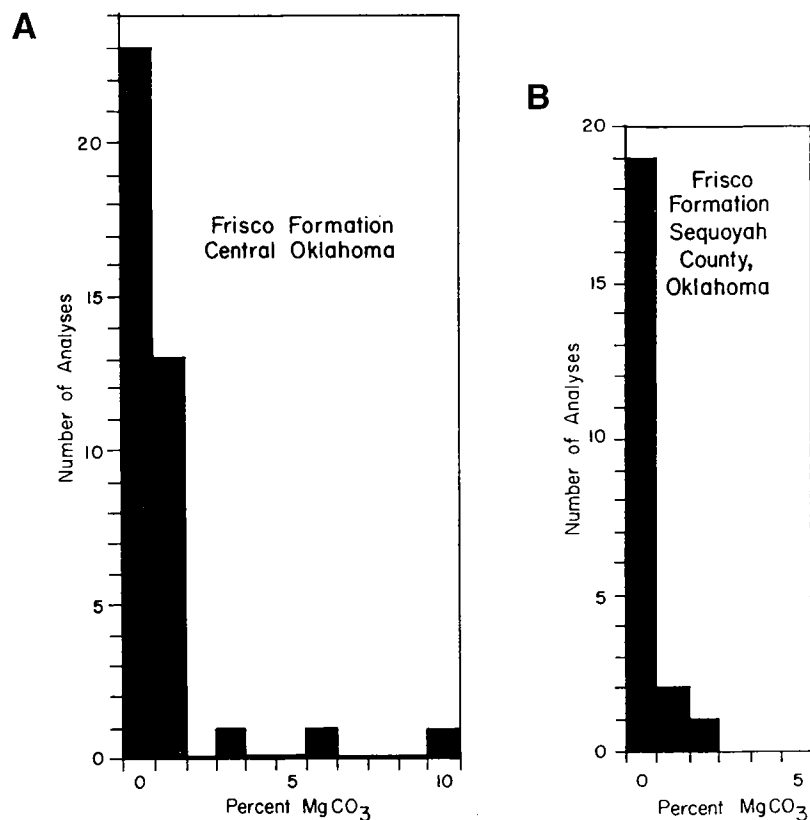


Figure 31. Frequency diagrams showing distribution of MgCO₃ in Frisco Formation. (A) From Arbuckle Mountains and from well cores, central and western Oklahoma. (B) From outcrop area, Sequoyah County, eastern Oklahoma. From Amsden (1975, figs. 37, 39).

this facies in the upper Hunton. Well 10 has 70 ft of this facies, also in the upper Hunton. The “clean,” almost blocky nature of the facies is characteristic, as is the abrupt basal contact with underlying strata. I have noticed that this facies is invariably overlain by the Woodford Shale. By this, I mean that I have never recognized this facies lying between sections of known strata.

The age of this facies is unknown. Without biostratigraphic control, it is almost impossible to differentiate the facies from those of the Devonian or uppermost Silurian. Based on its stratigraphic position in wells in which the Silurian Henryhouse Formation is recognizable, the facies is at least Silurian in age, and more likely Devonian.

I can also only speculate as to the origin of this facies. After discussing its presence with other researchers, two possible explanations for its origin seem to prevail. The first is that the facies may represent a zone of alteration of original Hunton strata. It is possible that typical Hunton strata were deposited, with the uppermost section having been subjected to fracturing, weathering, or dissolution, and having undergone subsequent dolomitization. Well 9 of cross section A-A' (Pl. 4) is adjacent to a north-south-trending fault. This fault complex continues northward from this well and may be represented locally in a fault or fracture complex to the north (see pre-Woodford subcrop map, Pl. 6). It is possible that these faults or fractures were a conduit for the waters that could have been responsible for the alteration of this zone in this area.

A second explanation for the origin of this facies is that it was a fill deposit from an erosional period some time after deposition of the Henryhouse Formation. In my opinion, this explanation seems to be the more likely, because some of the characteristics of a cut-and-fill environment seem to be consistently evident. These characteristics include a sharp basal contact between this facies and underlying Hunton strata that are commonly correlative with known Hunton strata. The facies almost always has a uniformly “clean” gamma-ray profile almost like that of a “clean,” blocky channel sand. Well 9 of cross section A-A' (Pl. 4) lies between two wells that have a normal Hunton section. And finally, as mentioned previously, the zone varies in thickness but is always found directly underneath the Woodford Shale.

The age of this facies is unknown, but I do not believe it to be post-Sallisaw. It is possible, on the basis of Amsden's observations of the Bois d'Arc-Frisco contact, that this unit may represent deposition on a similar pre-Frisco erosional surface, but on a much larger scale.

Sallisaw Formation

The type locality of the Sallisaw Formation is along Sallisaw Creek in Sequoyah County, Oklahoma (Amsden, 1961, p. 45-49). Amsden describes the Sallisaw as an arenaceous, dolomitic limestone containing an average of 9.5% quartz detritus and commonly traces of

glauconite. The dolomite content is variable and may range from <1% to 25% MgCO_3 (Amsden, 1980, p. 49). Nodules and lenses of chert commonly are present in the Sallisaw, and locally the arenaceous, dolomitic limestone may grade into a bedded arenaceous chert (Amsden, 1980, p. 49).

Amsden described 11 species of articulate brachiopods from the Sallisaw, which he assigned to the Sawkillian Stage of the Early Devonian. There is an unconformity between the Sallisaw of Sawkillian age and the Frisco Formation of Deerparkian age. In eastern Oklahoma, the Sallisaw rests on the Frisco Formation, or on strata of the Chimneyhill Subgroup where the Frisco has been eroded. Of notable interest is the presence of Sawkillian strata in central Oklahoma and the Texas Panhandle (Pl. 6). Amsden identified fauna of Sawkillian age in cores from central Oklahoma in the Kirkpatrick No. 1 Cronkite well (Amsden, 1975, p. 83) and from the Texas Panhandle in the Phillips No. 1-C Lina and Mobil No. 1 Walker wells (Amsden, 1975, p. 94, 102).

Misener and Sylamore Sandstones

The Misener Sandstone of western and central Oklahoma, and the correlative Sylamore Sandstone of eastern Oklahoma, represent an end to the carbonate depositional sequence from Late Ordovician through Early Devonian time. These sandstones are actually a basal deposit of the Woodford/Chattanooga Shale. Prior to deposition of these sands, a significant erosional period existed from the end of the Early Devonian through the Middle Devonian. Amsden considers these sands to be residual debris left from this erosional period (Amsden 1988, p. 46). Examination of the Woodford isopach map of Plate 2 reveals two distinct drainage patterns in western Oklahoma. The southernmost system drains to the south. Cores from southwestern Oklahoma contain a dolomitic siltstone facies equivalent to the Misener. Amsden refers to the facies as being a residual detritus that accumulated from this south-flowing drainage system (Amsden, 1980).

In northern Oklahoma, a second drainage system is apparent. The basal Misener Sandstone is considered a second-generation sandstone by Amsden, owing to its maturity in roundness of grains. The source of the sand is thought to have been exposed sandstones of the Ordovician (Amsden, 1975, p. 11). These sands have a dolomitic matrix and range from a sandy dolomite to a dolomitic sandstone. Where porosity and permeability are present, these sandstones can be prolific hydrocarbon reservoirs.

An interesting observation that Amsden makes is the diachronous nature of the Misener Sandstone. Cores from the Misener yield a conodont fauna of late Middle to early Late Devonian age (Amsden and Klapper, 1972). The age of the Misener is essentially equal to the age of the post-Hunton erosional period.

The Misener was named after Fred D. Misener for a sandstone interval above the Hunton in the No. 1

McWilliams well in sec. 23, T. 15 N., R. 10 W., Creek County, Oklahoma. The type locality of the Sylamore Sandstone is along Sylamore Creek, Stone County, north-central Arkansas (Amsden, 1988, p. 46, 51).

DEVONIAN–MISSISSIPPIAN

Woodford/Chattanooga Shale

The type locality of the Woodford Shale is exposures near Woodford, Carter County, Oklahoma. The term *Woodford* essentially describes the dark, silty shale that overlies the Hunton Group in the Anadarko basin and Cherokee platform. In eastern Oklahoma, and especially in Arkansas, this shale is also termed *Chattanooga* from its type locality near Chattanooga, Tennessee (Amsden, 1988, p. 37). This report deals mainly with the Woodford Shale, and additional information on its relationship with the underlying Hunton Group is discussed in the Leedey field study of this report.

Based upon conodont and spore studies, the Woodford Shale is Late Devonian to Early Mississippian in age (Amsden, 1980, p. 11). It is an organic-rich, silty black shale that commonly contains chert. At some localities the Woodford contains a basal dolomitic sandstone or siltstone lithofacies referred to as the Misener Sandstone in the Anadarko basin, and the Sylamore Sandstone in eastern Oklahoma (see previous section). The boundary between the Woodford Shale (including the Misener) and underlying strata is known to be diachronous (Freeman and Schumacher, 1969; Amsden and Klapper, p. 2330–2331). In the Arbuckle Mountains, the Woodford contains scattered beds of thin chert, as described by Taff in 1902. The presence of the chert perhaps reflects a gradual gradation from shale to chert deposits in the Ouachita Mountain province. These chert deposits are termed the Arkansas Novaculite (Amsden and others, 1967, p. 917, 926).

PART V

The Hunton Group: Sequence Stratigraphy, Facies, Dolomitization, and Karstification

Zuhair Al-Shaieb, Jim Puckette, and Paul Blubaugh

Oklahoma State University
Stillwater, Oklahoma

ABSTRACT.—The Hunton Group consists of shallow-water carbonates that were deposited on a gently inclined ramp. In this setting, facies belts developed subparallel to bathymetric contours. Sea-level changes caused extensive migration of facies and generated multiple disconformities that are used to define major stratigraphic divisions within the Hunton. The Henryhouse and Haragan/Bois d’Arc (HHB) section represents a type 1 carbonate sequence. The lower boundary is the unconformity that separates the Henryhouse from the underlying Chimneyhill Subgroup. The upper boundary is the pre-Woodford (or pre-Frisco) unconformity. The Henryhouse–Haragan/Bois d’Arc sequence is a major oil and gas reservoir in the Anadarko basin.

Henryhouse–Haragan/Bois d’Arc facies in the Arbuckle Mountain section are notably different from those examined in cores from the Anadarko basin. Outcrop parasequences consist only of subtidal facies, whereas time-equivalent rocks in the western Anadarko basin include intertidal and supratidal facies. The thickening of these additional facies indicates a northwestward shallowing of the basin during the Late Silurian–Early Devonian. Sedimentary structures, lithology, fossil content, and fabric relationships were used as criteria to recognize various depositional facies bands that parallel the paleoshoreline. Supratidal (I), intertidal (II), and subtidal (III) facies are readily recognized, and their spatial relationships consistently indicate shallowing-upward sequences.

Three stages of dolomitization are documented in the Henryhouse Formation: (1) penecontemporaneous hypersaline dolomite, (2) marine and freshwater mixed dolomite, and (3) deep-burial or thermal dolomite. Four types of porosity that developed are moldic, vuggy, intercrystalline, and fracture. Moldic and intercrystalline porosity are fabric selective, whereas vuggy and fracture porosity are nonfabric selective.

Cores from the Hunton exhibit a variety of paleokarstic and other diagenetic features. Vuggy porosity, solution-enlarged fractures, breccias, and infill sediments are common. Paleokarstic reservoirs were classified into two types. Type 1 are focused-flow reservoirs with solution-enlarged conduits, collapse breccias, and cavern-fill parabreccia. Type 2, which are diffuse-flow reservoirs with interparticle and vuggy porosity, are the major hydrocarbon-producing reservoirs.

INTRODUCTION

The general stratigraphic divisions of the Hunton are the Chimneyhill Subgroup (Keel, Cochrane, and Clarita Formations); the Henryhouse, Haragan, and Bois d’Arc Formations (HHB type 1 carbonate sequence); and the Frisco Formation (Amsden, 1980, 1989) (Fig. 32). The Frisco is genetically different from earlier Hunton rocks because it was deposited mainly as bryozoan–crinoid carbonate bioherms (Medlock, 1984) on a post-epeirogenic unconformity surface. Henryhouse–Haragan/Bois d’Arc depositional facies

are different from those of the underlying Clarita Formation and the overlying Woodford or Frisco Formation. The vertical juxtaposition of Chimneyhill, Frisco, or Woodford facies against distinctly different Henryhouse–Haragan/Bois d’Arc facies identifies depositional breaks or disconformities in the section. A significant disconformity separates the Chimneyhill Subgroup from the overlying Henryhouse–Haragan/Bois d’Arc sequence. Two major epeirogenies interrupted deposition during the Devonian (Amsden, 1975). The Early Devonian (pre-Frisco) and pre-Woodford uplifts

(declines in sea level) generated unconformities that affected the entire region. Erosion associated with this later episode truncated the Hunton and removed it from much of the northeastern Oklahoma platform.

As a result of its economic importance, the Hunton has been the focus of numerous studies. Many researchers have presented evidence regarding the subject of unconformities and their use in establishing stratigraphic divisions. Reeds (1911) refers to "times of no deposition as well as eroded sediments" before and after Chimneyhill deposition, as well as for the Henryhouse and Haragan/Bois d'Arc. Others who discussed possible unconformities include Maxwell (1936), Anderson (1939), Tarr (1955), Bowles (1959), Maxwell (1959), Amsden (1960, 1975, 1980), Withrow (1971), Manni (1985), and Morgan (1985). Fritz and Medlock (1995) showed the impact of regional unconformities on Hunton reservoirs. Matthews (1992) and Matthews and Al-Shaieb (1993) presented the first systematic classification of Hunton paleokarst and indicated its importance to oil and gas productivity.

Investigations conducted by Beardall (1983), Medlock (1984), Manni (1985), and Menke (1986) addressed specific Hunton stratigraphic units and established depositional models for reservoir facies. Morgan (1985)

showed the importance of oolitic facies and certain aspects of reservoir development. Al-Shaieb and Puckette (2000) showed the Henryhouse–Haragan/Bois d'Arc interval to be a type 1 carbonate sequence defined by bounding unconformities (Fig. 33).

Other important studies addressing various aspects of Hunton geology include Morgan (1922), Ballard (1930), Posey (1932), Decker (1935), Swesnick (1948), Tarr (1955), Oxley (1958), England (1965), Kunsman (1967), Harvey (1969), Isom (1973), Hollrah (1977), Borak (1978), and Throckmorton and Al-Shaieb (1986).

DEPOSITIONAL FACIES AND ENVIRONMENTS

Pre-Woodford erosion removed much of the Henryhouse–Haragan/Bois d'Arc sequence in Oklahoma. The absence of the Haragan/Bois d'Arc in the subsurface prevents the interpretation of its depositional facies. However, similar bathymetric conditions prevailed throughout deposition of the Henryhouse–Haragan/Bois d'Arc sequence, and the processes that affected the Henryhouse can be applied uniformly across the sequence. As a result, the Henryhouse is used to illustrate facies and reservoir characteristics that are analogous to all pre-Frisco units.

During the Silurian, the Midcontinent region remained a stable province (Adler, 1971; Feinstein, 1981). Under these tectonic conditions, the Henryhouse Formation was deposited over much of Oklahoma without any major unconformities (Shannon, 1962). The distribution of depositional facies for the Henryhouse is shown in Figure 34. These facies and reservoir characteristics are generally analogous to all pre-Frisco Hunton units.

HENRYHOUSE–HARAGAN/BOIS D'ARC FORMATIONS

The Henryhouse–Haragan/Bois d'Arc (HHB) Formations are genetically related strata. This is evident in outcrop where the HHB interval is bounded by unconformities; rock types above and below the unconformities are distinctly different. Erosion associated with the upper unconformity truncated the Hunton across northern Oklahoma, and the Woodford Shale is disconformable on the eroded surface. Erosion below the lower bounding unconformity thinned the Clarita Formation. Subaerial exposure and erosion are characteristic of type 1 carbonate-sequence boundaries (Sarg, 1988). These enclosing unconformities, as well as the genetically related strata, define the HHB carbonates as a type 1 sequence.

The HHB sequence contains shallowing-upward shale–carbonate cycles (para-

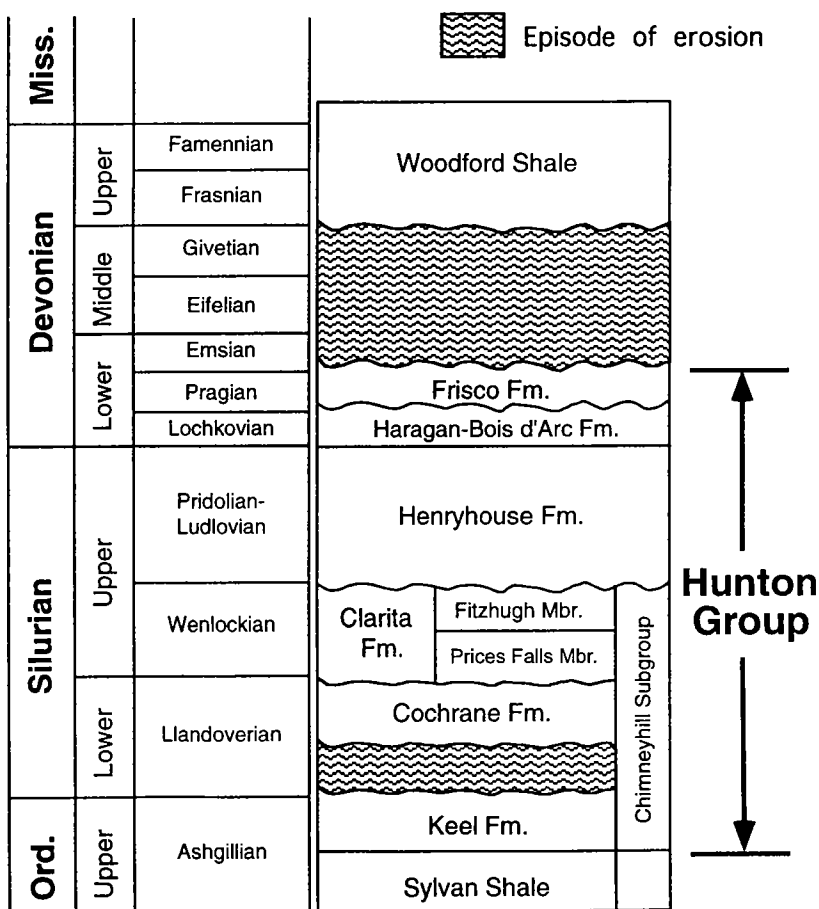


Figure 32. General stratigraphic nomenclature of the Hunton Group in Oklahoma. Modified from Barrick and others (1990) and Amsden (1989).

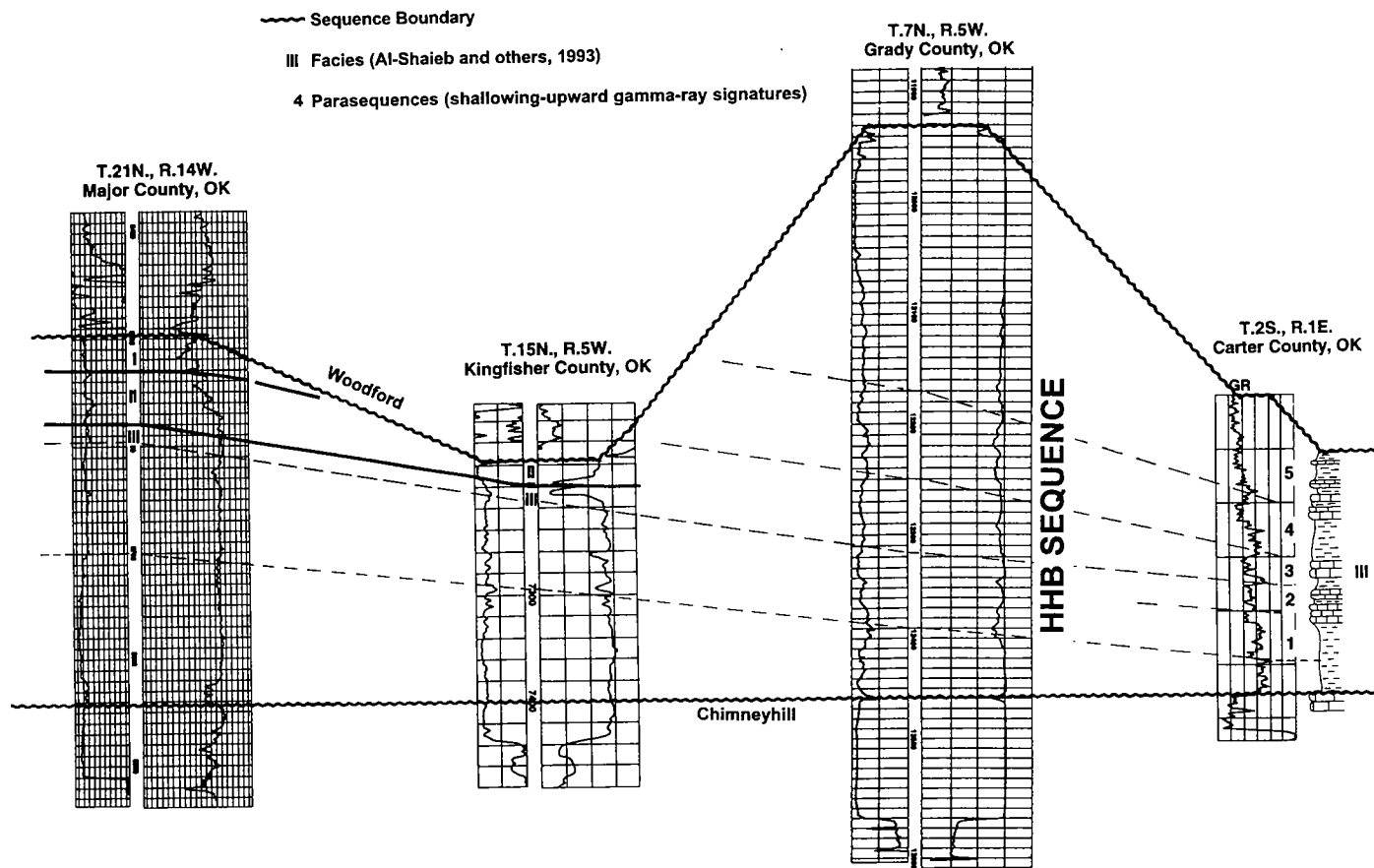


Figure 33. Cross section showing the Henryhouse–Haragan/Bois d'Arc (HHB) type 1 carbonate sequence, bounding unconformities, and correlation of outcrop and subsurface facies. North and west of the Arbuckle Mountains, parasequences are thicker and contain additional intertidal and supratidal facies. Line of section shown in Figure 34. Five parasequences (shallowing-upward gamma-ray signatures) are indicated by Arabic numerals; facies are indicated by Roman numerals. Modified from Al-Shaieb and Puckette (2000, fig. 8).

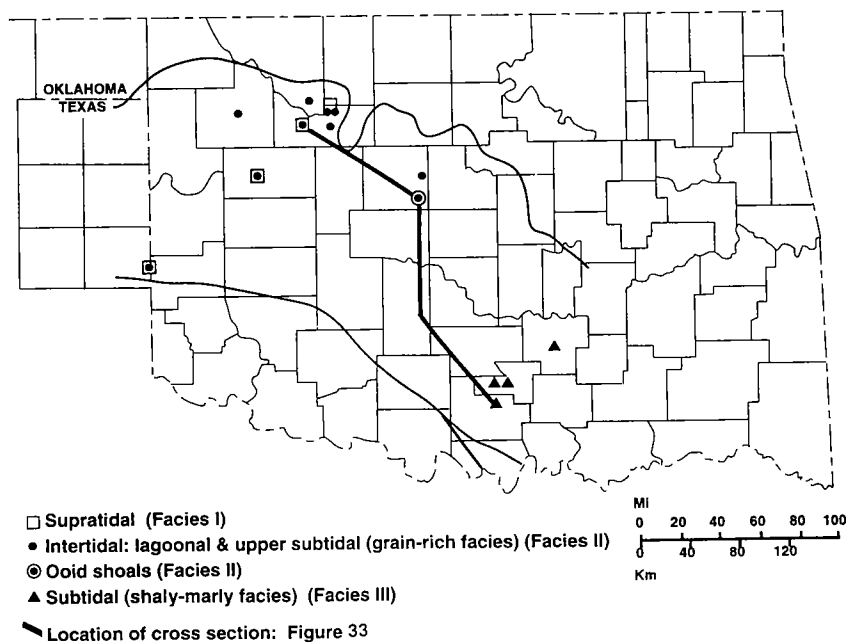
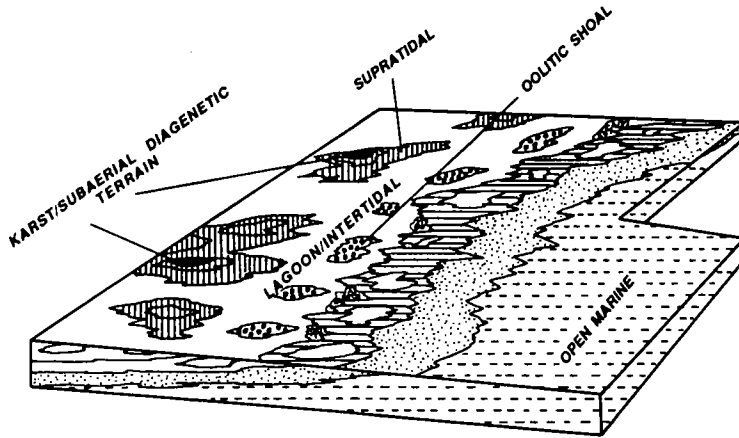


Figure 34. Distribution of subtidal, intertidal, and supratidal facies in the Henryhouse Formation. Cross section shown in Figure 33. Modified from Al-Shaieb and Puckette (2000, fig. 9).

sequences). Although subtidal facies is the only one present in the Arbuckle Mountains, equivalent rocks in the western and northern parts of the Anadarko basin contain additional intertidal and supratidal facies. Parasequences to the north and west of the Arbuckle Mountains are thicker and composed mainly of carbonate (Fig. 33). A general absence of shale and marly carbonates is evident in comparison to the outcrops. These additional facies and cycle thickening indicate a northwestward shallowing of the basin during the Late Silurian–Early Devonian. An interpretation of the HHB sequence lithofacies in the context of sequence stratigraphy is discussed in Al-Shaieb and Puckette (2000).

The shallow, low-energy sea developed facies belts (Fig. 35) subparallel to bathymetric contours (Al-Shaieb and others, 1993). Facies classification is based on vertical successions of facies or aggradational sequences. Transgression and regression apparently caused extensive migration of



FACIES I	KARST/SUBAERIAL DIAGENETIC TERRAIN		KARST	
	SUPRATIDAL		DOLOMUDSTONE	
FACIES II	INTERTIDAL	IIa. LAGOONAL	PELLET MUDSTONE/WACKESTONE	
		IIb. OOLITIC SHOAL	OOLITIC GRAINSTONE	
FACIES III	SUBTIDAL	UPPER SUBTIDAL	SKELETAL GRAINSTONE	
		LOWER SUBTIDAL	SKELETAL WACKESTONE	
		OPEN MARINE	MUDSTONE	

Figure 35. Schematic diagram showing generalized model of depositional environments and facies of the Henryhouse Formation. From Al-Shaieb and others (1993, fig. 5).

facies, thereby producing similarity of log signatures across large areas of the basin. Environmental interpretations of facies were determined by using the criteria established by Wilson (1975) and Al-Shaieb and others (1993).

Facies I

Facies I sediments were deposited on the supratidal tidal flat very near, or above, mean high tide. Cryptal algal fabrics, fenestral fabrics (Fig. 36), an absence of fossils, and a scarcity of burrowing are prominent features of this facies. Silica nodules, silt-sized quartz, intraclasts, and peloids may be present in the low-porosity dolo-mudstones that characterize this facies. A shallow, restricted environment (Fig. 35) is indicated for facies I.

Facies II

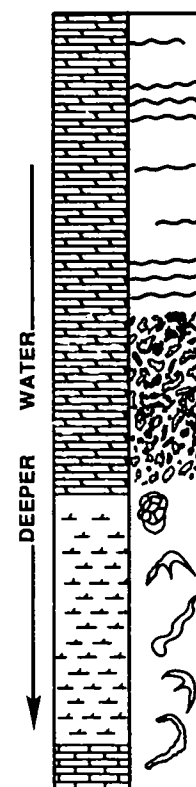
The sediments of this facies were deposited in a shallow, restricted subtidal to upper intertidal environment. Burrow-mottling features are a distinct characteristic. Rocks of the facies are dominantly dolo-wackestones. They are completely

dolomitized, with significant porosity. Fossil percentages and types are estimated as a result of the dissolution of original grains. Molds and scattered remaining grains indicate that crinoids were the most common bioclasts (Fig. 36). Vertical burrows and crinoid fragments suggest shallowing, with increasing energy (Fig. 35).

Oolitic grainstones and peloid-rich mudstone occur in this facies in central Oklahoma and are used to subdivide facies II into subfacies: intertidal lagoonal (IIa) and oolitic (IIb).

The lagoonal subfacies (IIa) likely represents restricted marine conditions, as fossils are rare but burrows are present. The rock is typically massive peloidal dolo-mudstone. The original texture in facies IIa is commonly masked by dolomitization. The facies represents deposition in quiet water, landward of oolitic shoals (Fig. 35).

The oolitic subfacies (IIb) contains abundant ooids (Fig. 37) and locally bioclastic debris and peloids. Cross-bedding and horizontal laminations are common. Dolomitization obliterates original textures in some of these grainstones. Facies IIb developed in the lower intertidal-upper subtidal environment (Fig. 35) (Al-Shaieb and others, 1993). Morgan (1985) mapped the distribution of the calcitic-oolite subfacies in Oklahoma County. He attributed the thinning and absence of the facies to removal by a tidal channel, post-Henryhouse erosion, or nondeposition.



FACIES I

CRYPTAL ALGAL FABRIC
FENESTRAL FABRIC
IRREGULAR LAMINATIONS
DOLOMUDSTONE
MASSIVE

FACIES II

BURROW MOTTLING
REPLACED SULFATES
DOLOWACKESTONE
ABUNDANT PELMATAZOANS

FACIES III

MASSIVE
WELL PRESERVED FOSSILS
DIVERSE FAUNA
NON-ORIENTED FOSSILS
DOLOMITIC MUD/WACKESTONE

Figure 36 (right). Typical vertical facies sequence, showing sedimentological, faunal, and mineralogical features from cores and thin sections of the Henryhouse Formation. From Al-Shaieb and others (1993, fig. 6).

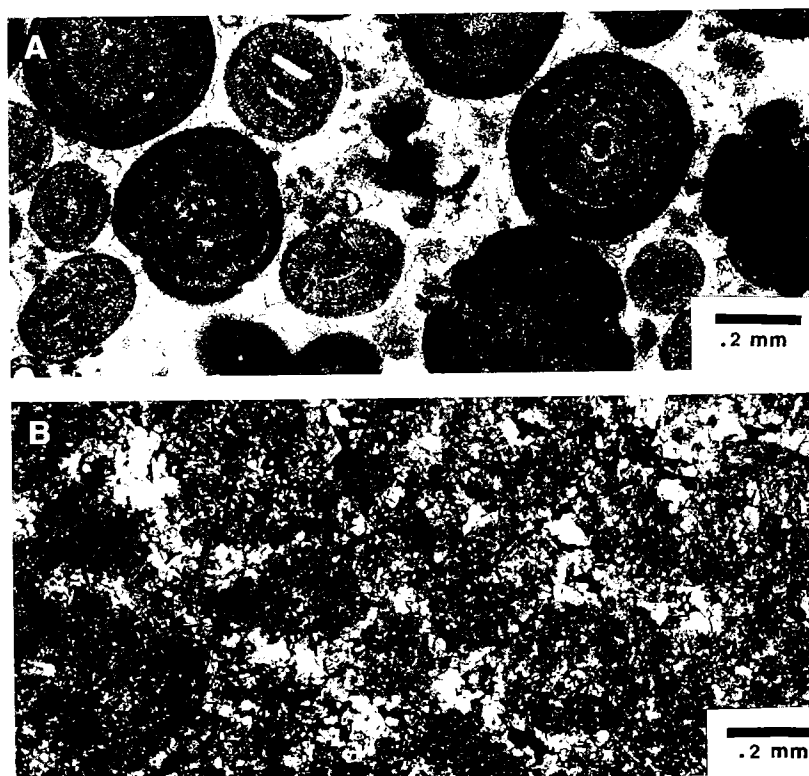


Figure 37. Photomicrographs of oolitic subfacies (IIb). (A) Ooids with isopachous calcite cement that fills interooidal space (Kirkpatrick Cronkite well, 7,119 ft). (B) Dolomitized ooid ghosts with clear rims (Duncan Garrett well, 8,751 ft; Medlock, 1984).

Facies III

This facies developed in a subtidal environment and is typically a medium-dark, silty, dolomitic mudstone (Fig. 36). Fossils include brachiopods, trilobites, ostracodes, bryozoans, and echinoderms. This facies may be featureless or contain burrows, nodular bedding, or storm-type deposits. The more diverse, better preserved fossils indicate a lower energy, shallow, open-water environment (Fig. 35) below normal wave base (Al-Shaieb and others, 1993).

DOLOMITIZATION

Reservoir rocks of the Hunton Group, specifically the Chimneyhill Subgroup and Henryhouse Formation, are mostly dolomitized. Howery (1993) tied the location of Hunton fields to a regional dolomite trend in the Anadarko basin that coincides with the Henryhouse and Chimneyhill subcrop (Fig. 38). Amsden (1975) interpreted dolomite in the Silurian Hunton rocks as being the penecontemporaneous-replacement type, formed seaward of the tidal zone. Beardall and Al-Shaieb (1984) recognized three distinct types of dolomite: hypersaline, mixed water, and deep burial (Fig. 39).

Hypersaline dolomite (Fig. 39) formed in the supratidal area of the restricted inner-ramp-shelf areas. Anhydrite in the Henryhouse suggests that evaporation of the supratidal area was of sufficient intensity and duration to form hypersaline brines. Seaward of the supratidal area, normal-marine conditions were hospitable to organisms that thoroughly burrowed sediments in the intertidal-shallow-subtidal area. A consequence of the precipitation of calcium sulfate (CaSO_4) is an increase in the $\text{Mg}^{2+}/\text{Ca}^{2+}$ ratio, which is of major importance to the formation of dolomite. Fluids with high $\text{Mg}^{2+}/\text{Ca}^{2+}$ ratios probably enhanced dolomitization of the intertidal-shallow-subtidal facies (Fig. 40).

Mixed-water dolomites (Fig. 39) formed where migrating meteoric water mixed with ocean-derived brines. A sea-level drop and the resulting basinward shift of the shoreline during deposition of the Hunton carbonates would have allowed meteoric water to migrate through the sediments. As

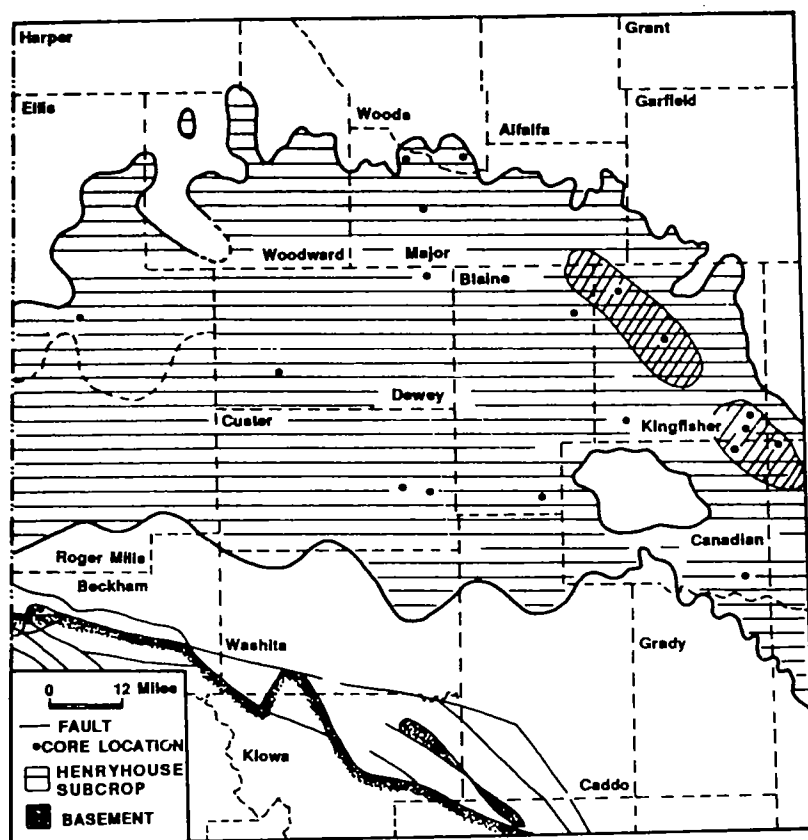
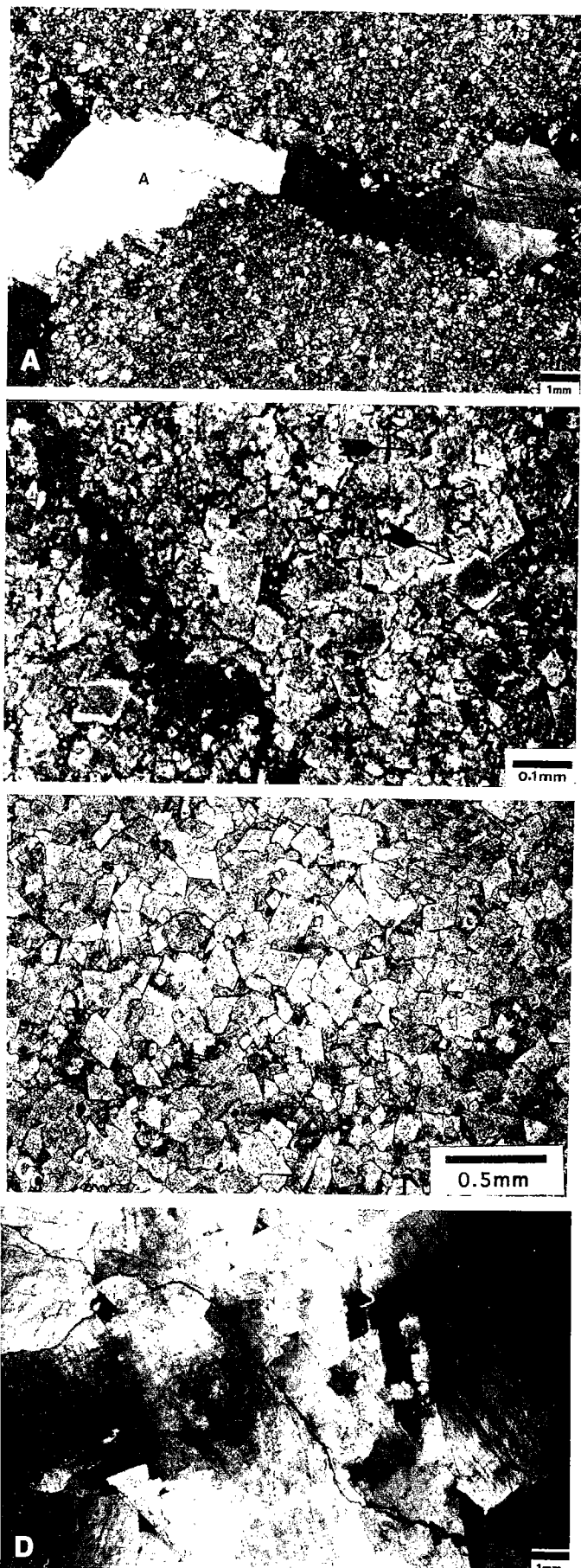


Figure 38 (left). Pre-Woodford subcrop map of the Hunton Group, Anadarko basin, showing lagoonal and shoal subfacies (crosshatched).



the shoreline advanced basinward across the newly deposited carbonate, a wide zone of dolomitization would have formed. A mixed-water mechanism is supported by exceedingly clean overgrowths of dolomite and their near-uniform distribution across facies. Cathodoluminescence of dolomite from the Henryhouse is regionally similar, which suggests a common diagenetic history (Choquette and Steinen, 1980).

During the hiatuses that occurred within and after Hunton deposition, a system of recharge and hydrodynamics may have developed that was sufficient to generate additional mixing dolomite in the Hunton. Lenses of fresh water, developed under exposed terrains of carbonate rock, could have migrated basinward and mixed with interstitial seawater that is richer in Mg^{2+} . The mixing of fresh water and connate seawater is considered the most likely mechanism for paleotopographic dolomitization of the Chimneyhill and Henryhouse.

Deep-burial dolomite or saddle dolomite (Fig. 39) is evident in voids or vugs in the Hunton. The distorted crystal lattice and curved crystal faces of saddle dolomite are found only in dolomitized zones. These crystals usually fill secondary vugs and fractures, and rarely molds of fossils. Fracture- and vug-filling saddle dolomite is a relatively deep-burial, late-diagenetic mineral. Radke and Mathis (1980) postulated that it forms at temperatures $>80^{\circ}C$, thus implying a deep-burial or hydrothermal origin at shallower depths (Al-Shaieb and others, 1993).

POROSITY

Four types of porosity are recognized in Hunton rocks (Fig. 41). These porosity types belong to both general porosity classes (fabric selective and nonfabric selective) described by Choquette and Pray (1971). Two fabric-selective porosity types are (1) moldic and (2) intercrystalline. These types are responsible for most high-porosity zones in cores.

Moldic porosity is generated by dissolution of fossil grains, predominantly crinoid and mollusk fragments. Occasionally, partially dissolved faunal remnants are found within the molds. Late saddle dolomite or calcite subsequently filled molds.

Intercrystalline pore space evolved primarily as a consequence of the dissolution of nondolomitized cryptocrystalline calcite matrix. Important solution enlargement of this porosity is common. Intercrystalline porosity is likely to have developed between larger

Figure 39 (left). Dolomite types in the Hunton Group. (A) Hypersaline dolomite characterized by poorly formed rhombohedra and cloudy appearance. Porosity is filled with anhydrite cement (A). (B) Mixed-water dolomite with euhedral rhombohedra formed around dark centers. (C) Mixed-water euhedral dolomite rhombohedra. (D) Thermal or saddle-type dolomite with large size and curved morphology.

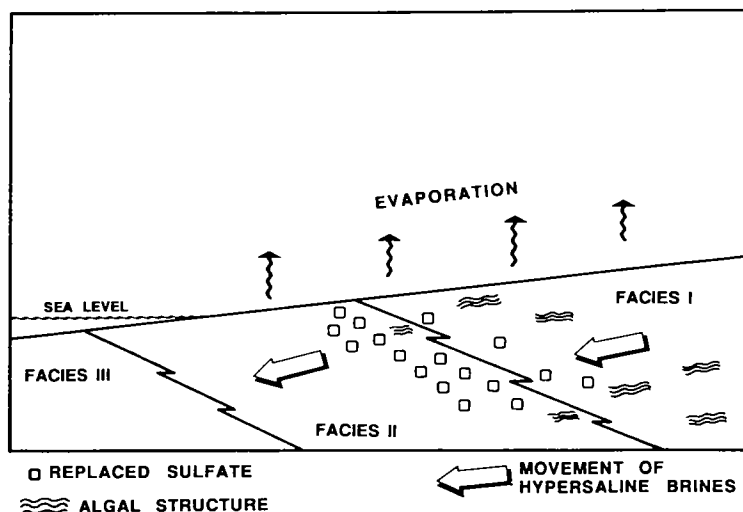


Figure 40. Schematic diagram illustrating movement of hypersaline brines and their role in dolomitizing Hunton carbonate during regression. From Al-Shaieb and others (1993, fig. 18).

rhombs in mixed-water dolomite (Fig. 41). Late calcite cement may occlude some intercrystalline porosity.

Porosity is better developed in intertidal facies (facies II), especially in the bioturbated and burrowed wackestone. A positive relationship between dolomitization and porosity is clearly evident (Al-Shaieb and others, 1993), but depositional facies has a strong influence. If both facies I and II are completely dolomitized, only facies II would have significant porosity.

The characteristics of facies II that cause it to be preferentially porous are burrowing and common pelmatozoan debris. Burrowing is important because it redistributes finer particles, allowing low-pH fluids to move through the rock and dissolve nondolomitized matrix. The resultant patchy, irregular porosity distribution is clearly evident in cores and thin sections (Al-Shaieb and others, 1993).

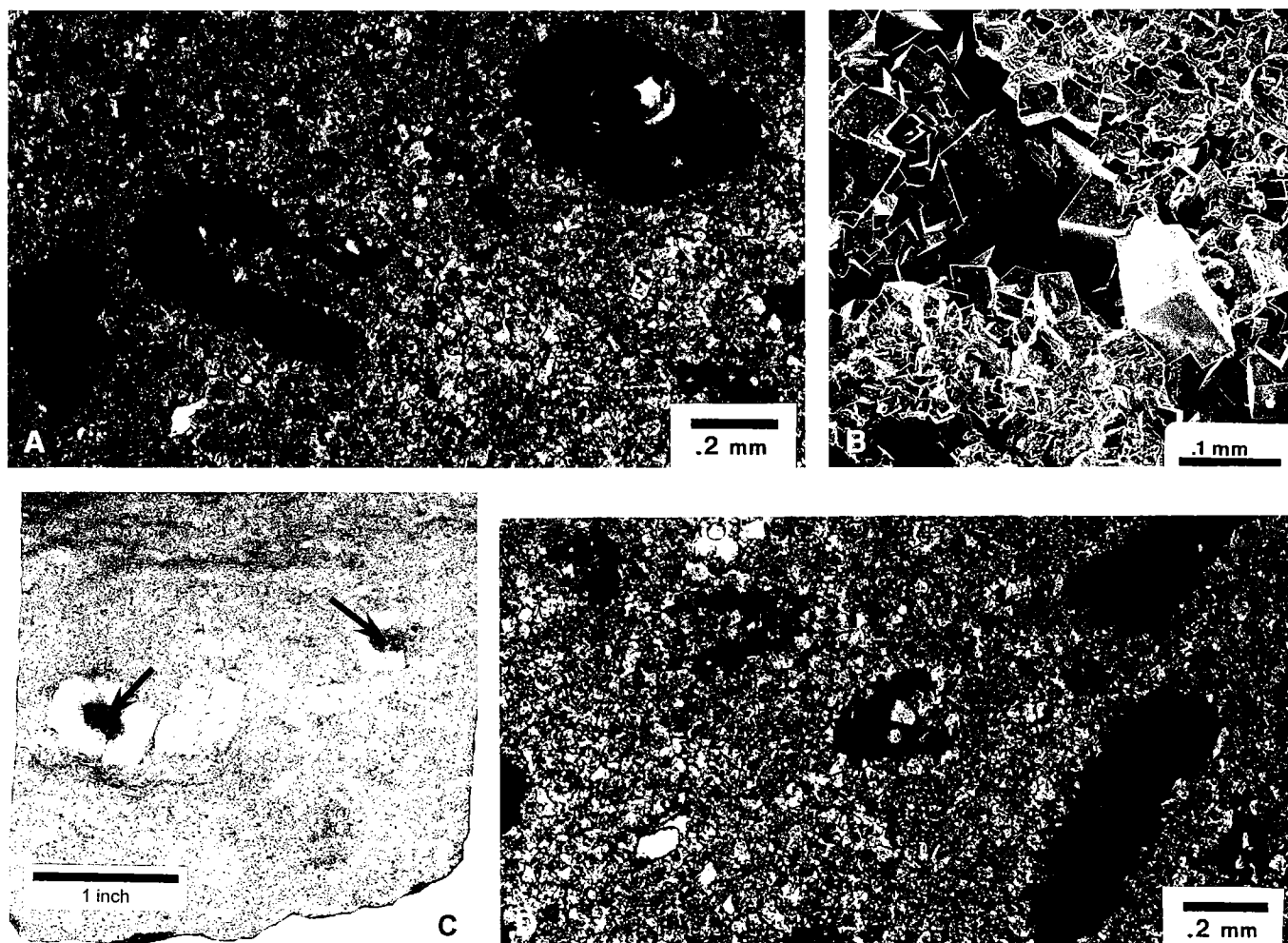


Figure 41. Porosity types in the Hunton Group. (A) Interooid porosity in oolitic subfacies, Henryhouse Formation. (B) Intercrystalline porosity, Chimneyhill Subgroup (Apexco Green well, 17,000 ft). (C) Intrabioclastic porosity (arrows), Frisco Formation (Mobil East Fitts Unit well, 3,450 ft). (D) Moldic porosity, Henryhouse Formation.

Moldic porosity is important in grain-rich rocks (Fig. 41). Both facies II and III are fossiliferous, but the highly dolomitized facies II develops much higher moldic porosity. Porosity in oolitic grainstones is predominantly interooid (Fig. 41). This type of porosity shows a strong correlation with the degree of dolomitization, and porosity in nondolomitized oolitic rocks is commonly poorly developed because of early cementation by sparry calcite.

The most important nonfabric-selective porosity is dissolution porosity. Commonly, vuggy pores are solution-enlarged molds (Fig. 41) in which the original fossil outlines have been destroyed. The coincidence of vuggy porosity with fossiliferous, moldic zones supports this interpretation. The dissolution of fragmented fossils within the less densely burrowed zones was the most important mechanism in development of moldic or vuggy karstic porosity.

KARSTIC FEATURES

Subaerial exposure during regression resulted in extensive meteoric diagenesis and the development of paleokarstic features. Many of these features are found below the pre-Woodford and pre-Henryhouse unconformities (Manni, 1985; Matthews, 1992). An extensive description of Hunton paleokarst genesis, features, and textures is provided by Matthews and Al-Shaieb (1993); furthermore, they classified Hunton Group reservoirs into two types: type 1 and type 2.

Type 1 Reservoirs

Type 1 paleokarstic reservoirs consist of massive limestone with low interparticle or matrix porosity. These tightly cemented rocks forced water to flow along bedding planes or fractures. As dissolution progressed, solution-widened joints and caves formed. Kerans (1989) called this type conduit-flow karst, and White (1969) used the term free-flow karst hydrologic regime to characterize fluid movement.

Breccia is the most distinctive feature of large-scale conduit-flow paleokarst. Collapse breccia, an aggregate of pieces derived from the conduit (cave) roof, is common in Hunton type 1 reservoirs (Fig. 42). Collapse breccia is a main indicator of subaerial exposure (Esteban and Klappa, 1983) and is a result of the structural collapse of a cave roof into a previously open cavern. A diversity of clasts, poor sorting, and angularity of grains characterizes collapse breccia (Matthews and Al-Shaieb, 1993). If the clasts are supported by matrix, it is called a cavern-fill parabreccia (Lynch, 1990).

Other breccias associated with cavern-roof foundering are crackle and mosaic (Fig. 42). They represent in-place brecciation of the cave roof (Kerans, 1989). Both are evident in the Hunton and tend to grade into one another (Matthews, 1992).

Pores in type 1 reservoirs are typically sparse. Porosity in collapse breccias can occur between the clasts. However, type 1 reservoirs are often low in porosity because the fractures, solution-widened joints, and

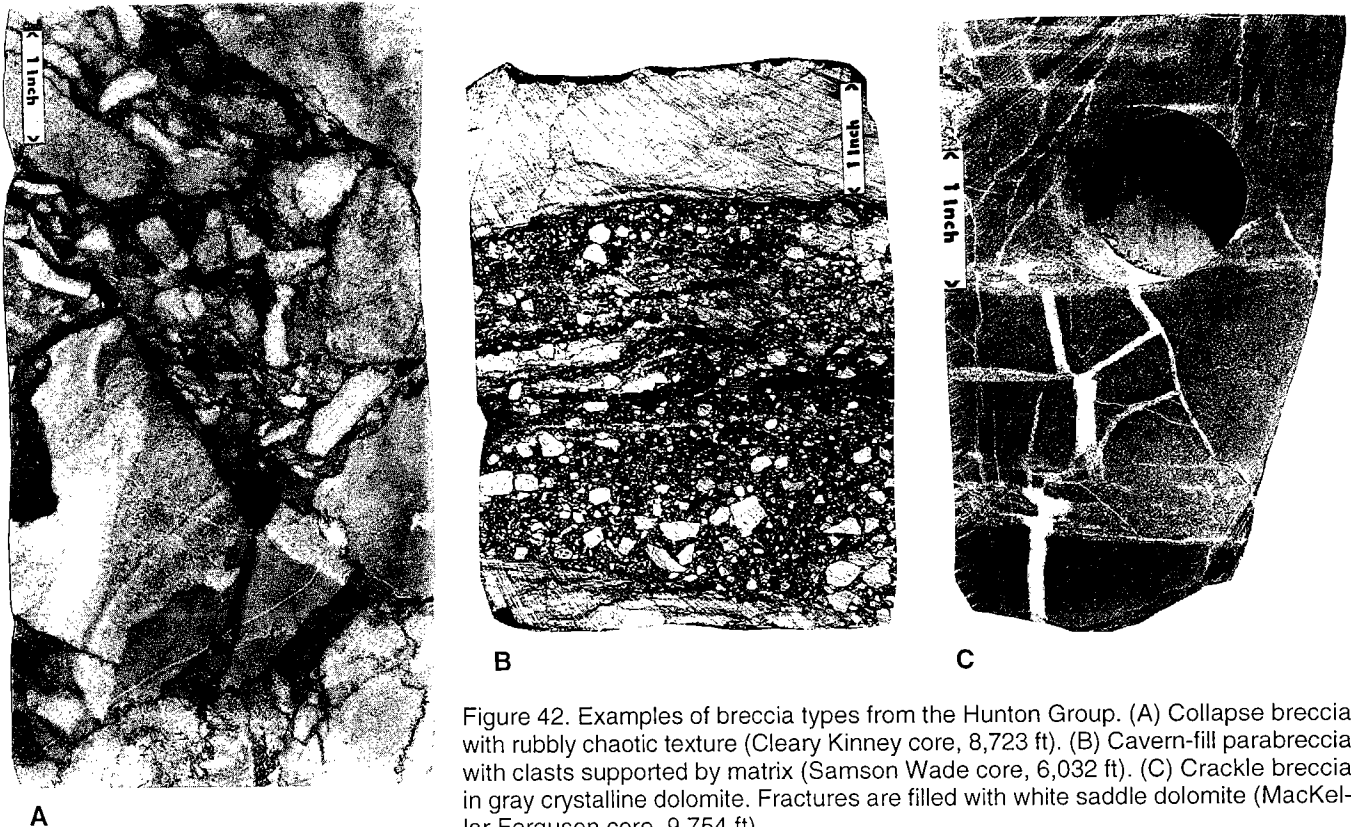


Figure 42. Examples of breccia types from the Hunton Group. (A) Collapse breccia with rubbly chaotic texture (Cleary Kinney core, 8,723 ft). (B) Cavern-fill parabreccia with clasts supported by matrix (Samson Wade core, 6,032 ft). (C) Crackle breccia in gray crystalline dolomite. Fractures are filled with white saddle dolomite (MacKellar Ferguson core, 9,754 ft).

vugs were filled with cave sediments and cements. Many type 1 Hunton paleokarstic reservoirs are not major producers of oil or gas (Matthews and Al-Shaieb, 1993). Some are characterized by high initial flow rates but exhibit a sharp decline in fluid production as solution-enlarged fractures are drained.

Type 2 Reservoirs

Type 2 reservoirs are porous grain-rich rocks that allow fluid to flow through the rock. This flow is called interparticle (Kerans, 1989) or diffuse (White, 1969). Rocks with diffuse-flow characteristics are believed to represent intertidal deposits (facies II) that underwent extensive burrowing and dolomitization. Karstic dissolution enhanced porosity and permeability in facies II rocks by enlarging existing pores (Fig. 43). Type 2 porosity is common in the Hunton and is characterized by high-volume fluid flow. Reservoirs not capable of producing oil or gas deliver high volumes of salt water to the wellbore. This reflects the interconnected pore network inherent in type 2 paleokarstic reservoirs.

The differences in composition and fabric of type 1 conduit-flow and type 2 diffuse-flow lithologies are

noticeably apparent in cores. In type 1 lithologies, meteoric fluids moved through the rock in solution-enlarged channels or along bedding planes and formed cavern-sized pores. In type 2 lithologies, water passed through the interparticle pores with little or no additional dissolution of carbonate. Consequently, collapse and cavern-filling parabreccias are rare in type 2 reservoirs. Cores with multiple karst episodes commonly contain both type 1 and type 2 lithologies. In some cores, type 1 features associated with the pre-Woodford unconformity are superposed on carbonate with type 2 reservoirs.

PALEOTOPOGRAPHY AND PRODUCTION

Hunton rocks are believed to have been subaerially exposed and weathered at various times in their history (Amsden, 1975, 1980; Fritz and Medlock, 1995). Amsden (1975) asserts that the Hunton represents an incomplete depositional sequence with significant time-stratigraphic gaps. Local unconformities probably existed during pre-Cochrane, pre-Clarita, pre-Henryhouse, pre-Haragan/Bois d'Arc, and pre-Frisco times (Amsden, 1980). The pre-Woodford unconformity in Oklahoma resulted in a fairly uniform regional beveling of the Hunton toward the north and its complete removal across the north-central and northeastern parts of the State. Within the Hunton outcrop area of the Arbuckle Mountains, pre-Woodford erosion locally truncates the Hunton, allowing the Woodford to rest unconformably on the Sylvan Shale (Amsden, 1975).

Drainage patterns developed during the pre-Woodford depositional hiatus are evident on the eroded Hunton topography. Subaerial exposure and erosion may have impacted reservoir evolution through additional meteoric diagenesis (grain cementation or dissolution), dolomitization (Sarg, 1988), dedolomitization (Manni, 1985), or karstification (Matthews, 1992; Fritz and Medlock, 1995). The relationship between paleo-drainage patterns and production is evident when the pre-Woodford topography is compared to the distribution of Hunton oil and gas fields (Fig. 44).

Pre-Woodford paleotopography and drainage patterns were analyzed on regional to local scales. Woodford thickness maps of the Anadarko basin define major north-south-trending drainages (Fig. 45). Many Hunton fields in the central and western parts of the basin (Custer, Dewey, and Ellis Counties, Oklahoma) are adjacent to these drainages. These fields all lie in a fairway (Fig. 46) where intertidal facies in the Henryhouse Formation were dolomitized (Al-Shaieb and others, 1993). Many of these dolomitized reservoirs were subjected to additional dissolution to form type 2 reservoirs (Matthews and Al-Shaieb, 1993). Blubaugh (1999) compared flowing and shut-in pressures from drillstem tests to evaluate permeability by using a gauge called the permeability index. Many high-permeability reservoirs (index values approaching 1.0) lie within the dolomite fairway in the Henryhouse and Chimneyhill (Fig. 46). Comparing the permeability in-

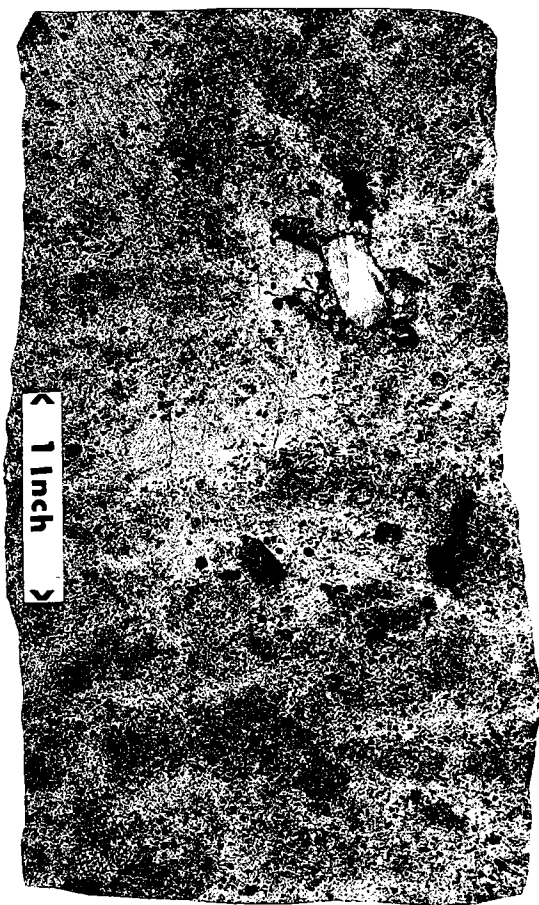


Figure 43. Enlarged moldic porosity in dolo-wackestone with vugs that are greater than twice the average grain size. Vugs are partially filled with calcite (Amax Hickman core, 13,525 ft).

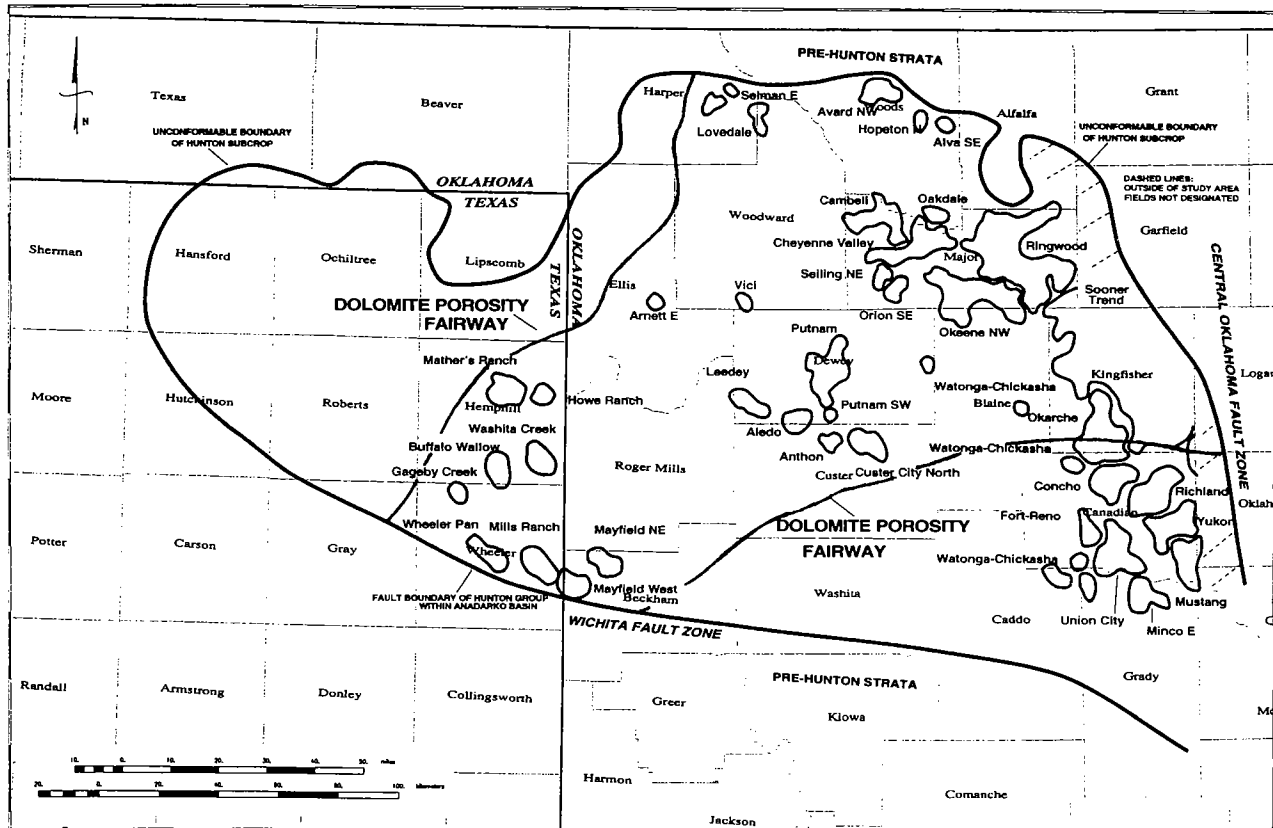


Figure 44. Map showing Hunton oil and gas fields in the Anadarko basin, and the dolomite porosity fairway.

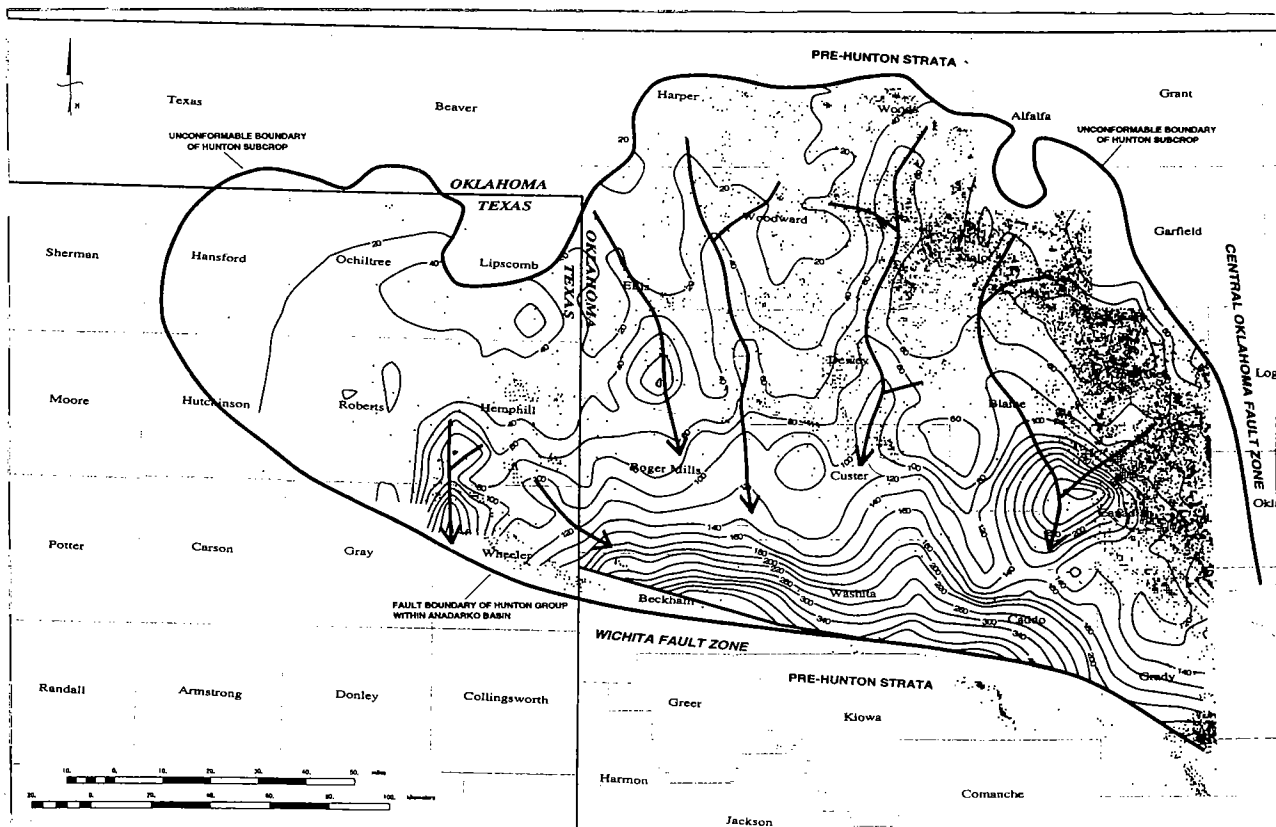


Figure 45. Map showing Woodford Shale thickness in the Anadarko basin, major paleodrainage patterns, and Hunton penetrations.

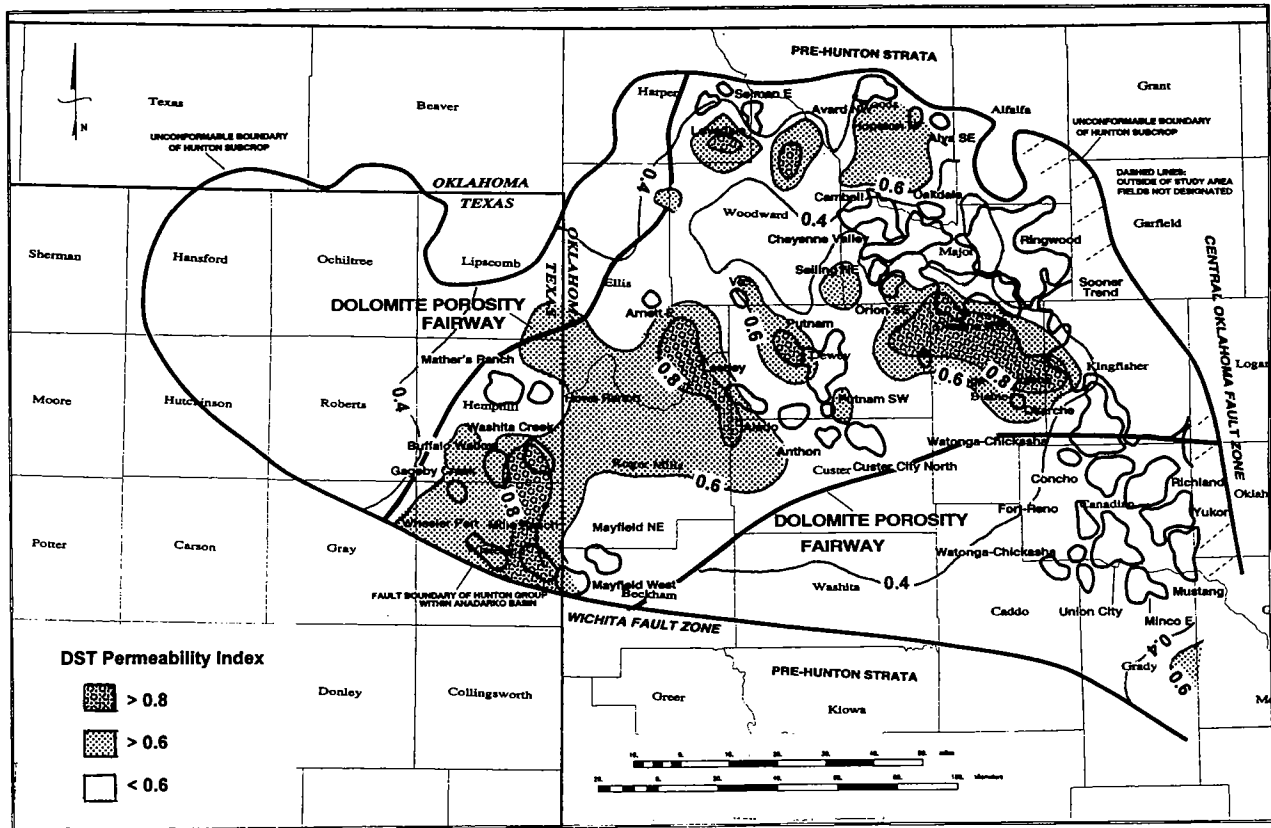


Figure 46. Map showing Hunton dolomite porosity fairway in the Anadarko basin, with drillstem-test (DST) permeability indexes.

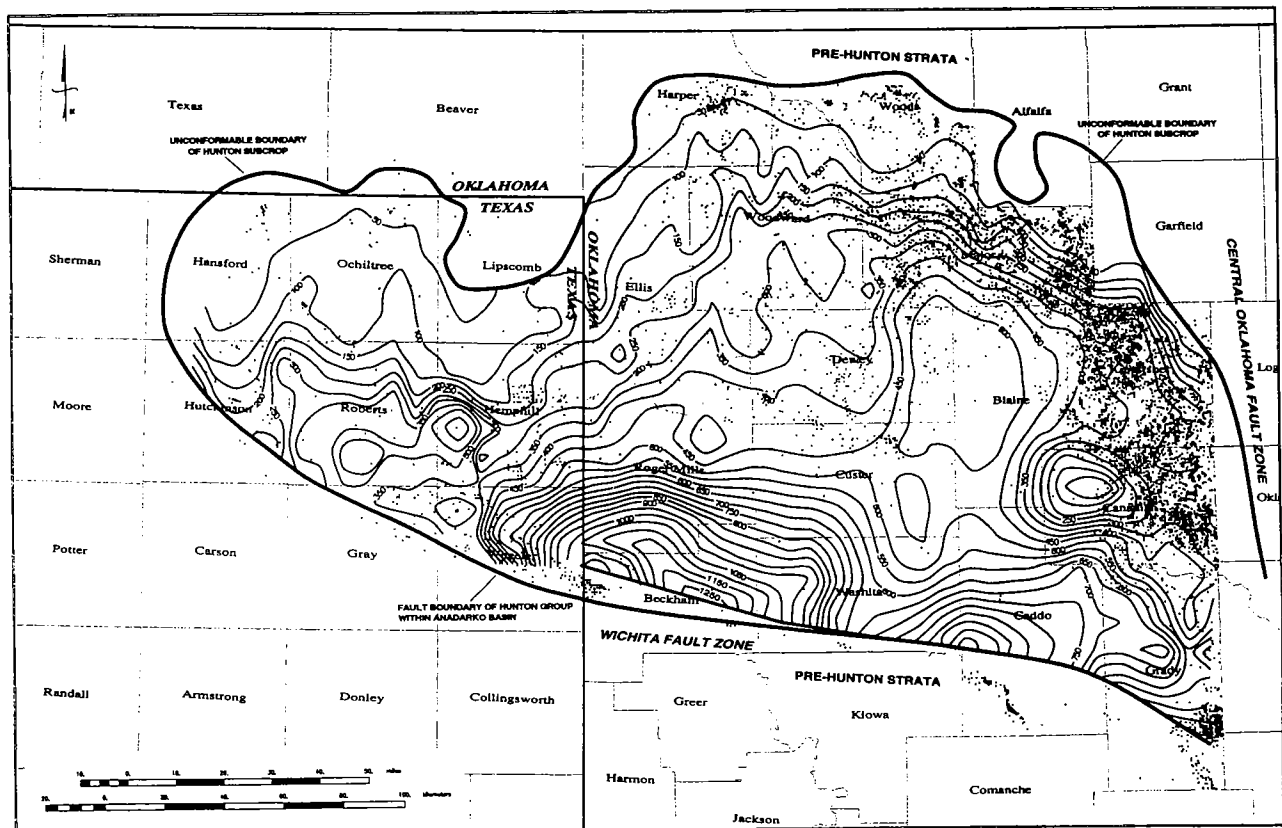


Figure 47. Map of Hunton Group thickness in the Anadarko basin, showing relationship between thinning or truncation of the Hunton and productive trends.

dex, dolomite fairway, and field locations summarizes the importance of dolomitization to reservoir evolution. On the northern shelf (Blaine and Major Counties, Oklahoma) production is concentrated along a northwest–southeast trend where pre-Woodford erosion thinned the Hunton (Fig. 47) but did not remove dolomitic type 2 reservoirs in the Henryhouse. North of this trend, type 2 reservoirs are generally absent, and production is sparse.

Type 2 reservoirs in the Chimneyhill Subgroup are responsible for the production trend in Harper and Woods Counties, Oklahoma (Figs. 44, 45). Type 2 reservoirs are also found in the deep Hunton fields in Beckham County, Oklahoma, and Wheeler and Hemphill Counties, Texas. Here, vuggy and intercrystalline dolomitic porosity in the Chimneyhill are preserved below 20,000 ft.

IMPLICATIONS

The identification of depositional facies and post-depositional diagenesis in the Hunton Group is an essential parameter in determining potential reservoir

rocks. It is most evident that the intertidal facies (facies II) is the major reservoir rock in the Henryhouse–Hargan/Bois d’Arc Formations. In this facies, grain-rich zones provided a fabric that was susceptible to dissolution. Dolomitization preserved pathways for corrosive fluids to move through the carbonate. Therefore, exploration programs for the Hunton in the Anadarko basin should consider the location of the prospect with respect to the position of facies trends and the dolomite fairway. Subaerial exposure associated with hiatuses (sequence boundaries) impacted reservoir evolution through meteoric diagenesis, dolomitization, and karstification. Consequently, the spatial relationship of the target reservoir to unconformities can be critical. Paleotopography may be useful in predicting areas of increased meteoric flow and porosity enhancement below the pre-Woodford unconformity. Therefore, any exploration strategy should include a precise understanding of stratigraphy, facies analysis and distribution, dolomitization and other diagenetic overprints (karst), and the position of unconformities with respect to the proposed reservoir.

PART VI

Leedey Field Hunton Reservoir Study (T. 16 N., R. 20 W., Dewey County, Oklahoma)

Kurt Rottmann

INTRODUCTION

The Leedey Hunton field lies in the southwestern corner of Dewey County, Oklahoma. Figure 48 is a generalized location map for the Leedey Hunton reservoir study area, showing the discovery well and the well in which the type log was run. The discovery well is the Hoover and Bracken No. 1-6 Anderson, in the E½W½ E½ sec. 6, T. 16 N., R. 20 W. The well was completed in

July 1977 for 3.08 MMCFG/18 hr. Figure 49 is a well-information map showing producing zones and is a key to well tabulations in Table 5, giving operators, lease names, and well numbers. The field is in the deeper part of the Anadarko basin, which contains overlying overpressured Springer and Morrow (Pennsylvanian) deposits. Owing to the presence of these upper overpressured formations, drilling in the underpressured Mississippian and Silurian-Devonian sections has been sparse and usually confined to structurally defined prospects.

Production from the Hunton Group in this field is from the Silurian sequence. The Hunton, as described earlier in this report, is a series of limestones, marlstones, and dolomites sandwiched between the Upper Ordovician Sylvan Shale and the Upper Devonian-Lower Mississippian Woodford Shale.

This field study was selected for several reasons. First, Leedey field is an example of Hunton production in the deep Anadarko basin that is structurally controlled. A knowledge of the types of structures necessary for entrapment are important for the pursuit of other structurally controlled prospects. (Middle Paleozoic structures are

the primary emphasis for the East Arnett field study, which is discussed next.)

The second reason this field was selected for study is the important stratigraphic relationship between the Hunton and the overlying Woodford Shale. Deposition of the various formations of the Hunton was not continuous. A series of uplifts and erosional events occurred at various times during deposition of this car-

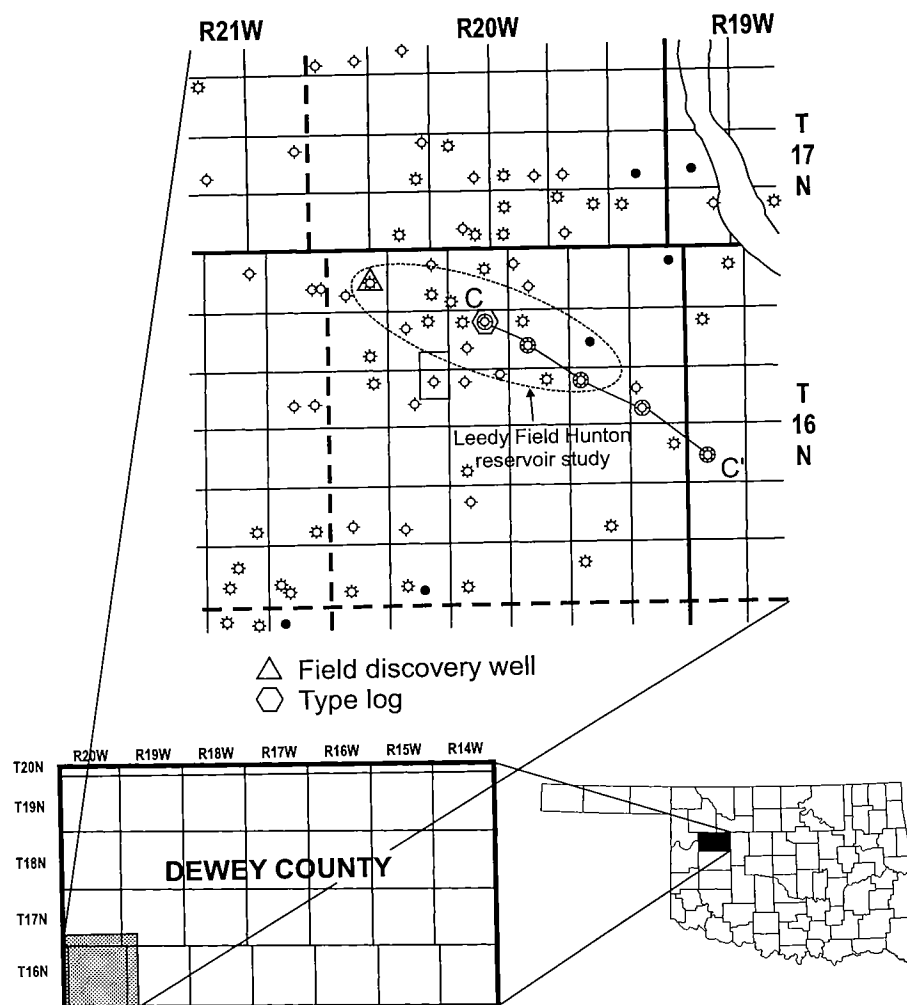


Figure 48. Generalized location map of Leedey field Hunton study area in Dewey County, Oklahoma. Cross section C-C' is shown in Figure 51.

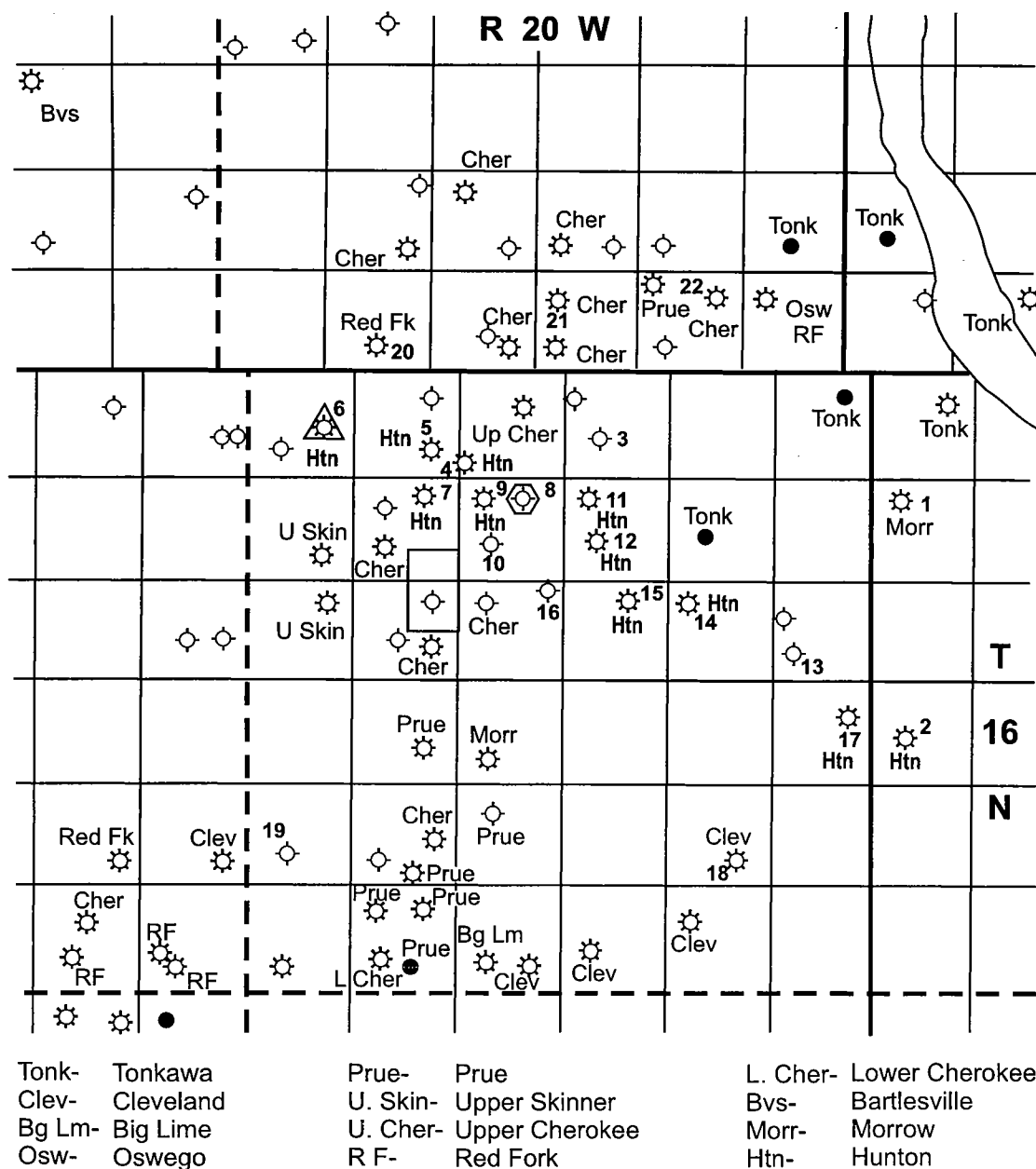


Figure 49. Well-information map showing producing reservoirs for wells in Leedey field Hunton study area. Numbers by wells are a key to well tabulation in Table 5.

bonate sequence. Figure 20A,B is a correlation chart giving the times of origin and relationships of these formations, including corresponding unconformities and periods of erosion. Prior to deposition of the Woodford Shale, a significant period of uplift and erosion occurred during Middle Devonian time that dramatically altered and modified the Hunton paleotopographic surface. This modified surface influenced and controlled deposition of the Woodford Shale. During this time, Hunton strata were uplifted and exposed to sub-aerial erosion. This erosional event is probably best known for the morphological features produced on the Hunton surface more than any other such event, ex-

cept for the pre-Frisco unconformity discussed previously. During this erosional event, dissolution of the exposed Hunton surface produced relatively deep crevices and karst features in addition to well-developed but immature surface-drainage systems or erosional channels. It is the goal of this field study to understand the role these channels play in an explorationist's interpretation of a reservoir's thickness, geometry, and distribution. Furthermore, understanding the extent of these channels and the relationship they have to reservoirs contained within them creates a new venue for Hunton stratigraphic traps in the deeper part of the Anadarko basin.

TABLE 5. — Well Tabulation Keyed to Figure 49, Showing Well Locations, Operators, and Lease Names for Leedey Field, Dewey County, Oklahoma

Map no.	Location	Legal	Operator	Lease
1	sec. 7, T. 16 N., R. 19 W.	C NW¼	Ports of Call Oil Co.	#1-7 Leedy
2	sec. 19, T. 16 N., R. 19 W.	2,440 ft FSL & 1,445 ft FWL	Getty Oil Co.	#1-19 Hall
3	sec. 3, T. 16 N., R. 20 W.	1,980 ft FSL & 1,980 ft FWL	McCulloch Oil Corp.	#1-3 Williams
4	sec. 4, T. 16 N., R. 20 W.	SW¼SW¼	Bracken Exploration Co.	#1-4 Benjamin Stout
5	sec. 5, T. 16 N., R. 20 W.	C SE¼	Hoover & Bracken, Inc.	#1-5 Hazel Crane
6	sec. 6, T. 16 N., R. 20 W.	1,150 ft E of C	Hoover & Bracken, Inc.	#1-6 Anderson
7	sec. 8, T. 16 N., R. 20 W.	300 ft SW of C NE¼	Hoover & Bracken, Inc.	#1 South Unit
8	sec. 9, T. 16 N., R. 20 W.	1,320 ft FNL & 1,980 ft FEL	McCulloch Oil Corp.	#1-9 South
9	sec. 9, T. 16 N., R. 20 W.	C NW¼	Hoover & Bracken, Inc.	#1-9 Martin Unit
10	sec. 9, T. 16 N., R. 20 W.	NE¼SW¼	Humble Oil Co.	#1-9 Boswell
11	sec. 10, T. 16 N., R. 20 W.	N½N½S½NW¼	Bracken Exploration	#1-10 Williams
12	sec. 10, T. 16 N., R. 20 W.	NE¼SW¼	McCulloch Oil Corp.	#1-10 Harrell
13	sec. 13, T. 16 N., R. 20 W.	C SW¼	Getty Oil Co.	#1-13 Hall
14	sec. 14, T. 16 N., R. 20 W.	C NW¼	Hoover & Bracken, Inc.	#1-14 Gamble
15	sec. 15, T. 16 N., R. 20 W.	1,320 ft FNL & 1,920 ft FEL	Union Oil Co.	#1-15 Gamble
16	sec. 16, T. 16 N., R. 20 W.	C NE¼NE¼	Hoover & Bracken, Inc.	#1-16 Joe Craig
17	sec. 24, T. 16 N., R. 20 W.	1,980 ft FNL & 1,320 ft FEL	Getty Oil Co.	#1 Barnitz
18	sec. 26, T. 16 N., R. 20 W.	1,420 ft FSL & 1,720 ft FEL	Helmerich & Payne Co.	#1-26 Hale
19	sec. 30, T. 16 N., R. 20 W.	NE¼SW¼	Samedan Oil Corp.	#1 Walton
20	sec. 32, T. 17 N., R. 20 W.	C S½	Nova Energy Corp.	#1-32 Craig
21	sec. 34, T. 17 N., R. 20 W.	C NW¼	Dyco Petroleum Corp.	#1-34 Moore
22	sec. 35, T. 17 N., R. 20 W.	C NE¼	Inexco Oil Co.	#1 Fariss

STRATIGRAPHY

Figure 50 is the type log for the Leedey Hunton field study. Although this well contains a significantly thick section of Hunton, these strata represent only a small part of the overall Hunton Group. Biostratigraphic studies in the vicinity of the field study are limited. However, the Hunton sequence can be reasonably inferred to belong to the Chimneyhill Subgroup, on the basis of correlation from this area to areas where the biostratigraphy is better known.

The Sylvan Shale is a green to greenish-gray calcareous shale. Based upon graptolite studies (Decker, 1935) and chitinozoan studies (Jenkins, 1970, p. 284–285), the Sylvan is assigned to the Ashgillian Stage of the Late Ordovician Epoch. The Sylvan is remarkable for its uniformity in the character of individual bed sequences, and correlation is possible for considerable distances. This implies that the paleotopographic surface upon which each of these beds was deposited must have been exceedingly flat and featureless. Amsden alludes to the fact that the shallow Anadarko basin may have been restricted, with circulation in parts of it being at a mini-

mum (Amsden, 1988, p. 60). This minimum circulation could have contributed to the Sylvan's widespread homogeneity. Well 1 of cross section C–C' (Fig. 51, in envelope) shows a complete Sylvan section. The lower part grades into limestone or dolomitic limestone. This sequence is typical for this area, and the gradual gradation from shale to limestone increases to the west and northwest as distance from the southeastern source area increases (see Fig. 23).

Deposition of the carbonate sequence of the Hunton Group in the Leedey field area probably represents a continuous period of deposition. The Hunton here is composed predominantly of strata from the Chimneyhill Subgroup, which comprises three formations, in ascending order: Keel, Cochrane, and Clarita. As mentioned previously, this sequence of strata can be correlated to those areas where biostratigraphic control confirms an Early Silurian age.

The type log (Fig. 50) for the Leedey field study area suggests the possible presence of Late Silurian (Pridolian–Ludlovian) Henryhouse strata. This inference was made because of the the marly nature of the upper 30

or 40 ft of Hunton rocks, and marlstone is typical of the Henryhouse Formation. The possible presence of this formation is also based upon the subcrop position of the Henryhouse as seen on the pre-Woodford subcrop map of Plate 6.

Most of the Henryhouse, if present, and any subsequent Hunton formations were removed by several Late Silurian and Early and Middle Devonian erosional events. The Woodford Shale of Late Devonian–Early Mississippian age was then deposited upon the exposed surfaces of the Hunton within the study area. This shale is highly organic and serves as a source rock for many of the hydrocarbons in the Anadarko basin. The shale is easily recognizable owing to its extreme gamma-ray response on geophysical logs and is an easily recognizable regional correlation marker. Above the

Woodford Shale lies the Kinderhook shale of Mississippian age. This shale is a gray to dark-gray shale in western Oklahoma that probably represents a transition from the highly organic shale of the Woodford to the argillaceous and organic limestones of the Mississippian.

ISOPACH MAPPING

Figure 52 is a gross-isopach map of the Hunton Group. This map represents a reasonable interpretation of the geometric configuration of the Hunton thickness within the field study area. The Hunton isopach is basically nondescript and uniform, ranging from approximately 400 to 425 ft in thickness. However, in secs. 10 and 13, three Hunton wells encountered thicknesses of 56, 332, and 265 ft, respectively. The inclusion of these wells in the gross isopach forces

a “thin” to be mapped in secs. 10, 11, 12, 13, 14, 15, 22, 23, 24, 25, and 26. Based upon the mapping, the source or cause of the “thin” cannot be determined.

Cross section C–C' (Fig. 51) is a stratigraphic section incorporating wells flanking the “thin,” including those wells that drilled the “thin.” It is readily apparent in this cross section that the vertical scale of the Woodford Shale is greater than that of the Sylvan Shale and Hunton Group. The Woodford, when deposited, was a shale with a high water content. Twenhofel (1950, p. 279), referring to compaction of shales with water content, wrote: “This water from the moment of deposition begins to be expelled, and compaction results, which is thought gradually to increase as the sediments accumulate. After the sediments have been buried to depths of 1,000 feet or more, the water is thought to be largely expelled, and sediments originally with 50% or more of water would decrease to half the original thickness.” This implies that the highly water-saturated Woodford Shale would have compacted to approximately 50% of its original thickness upon burial and subsequent deposition and overburden pressure of additional sediments. This general relationship holds true for many areas of Oklahoma (Rottmann, 2000). The equation should include the Kinderhook, where present. The depositional and stratigraphic relationship between the Woodford Shale

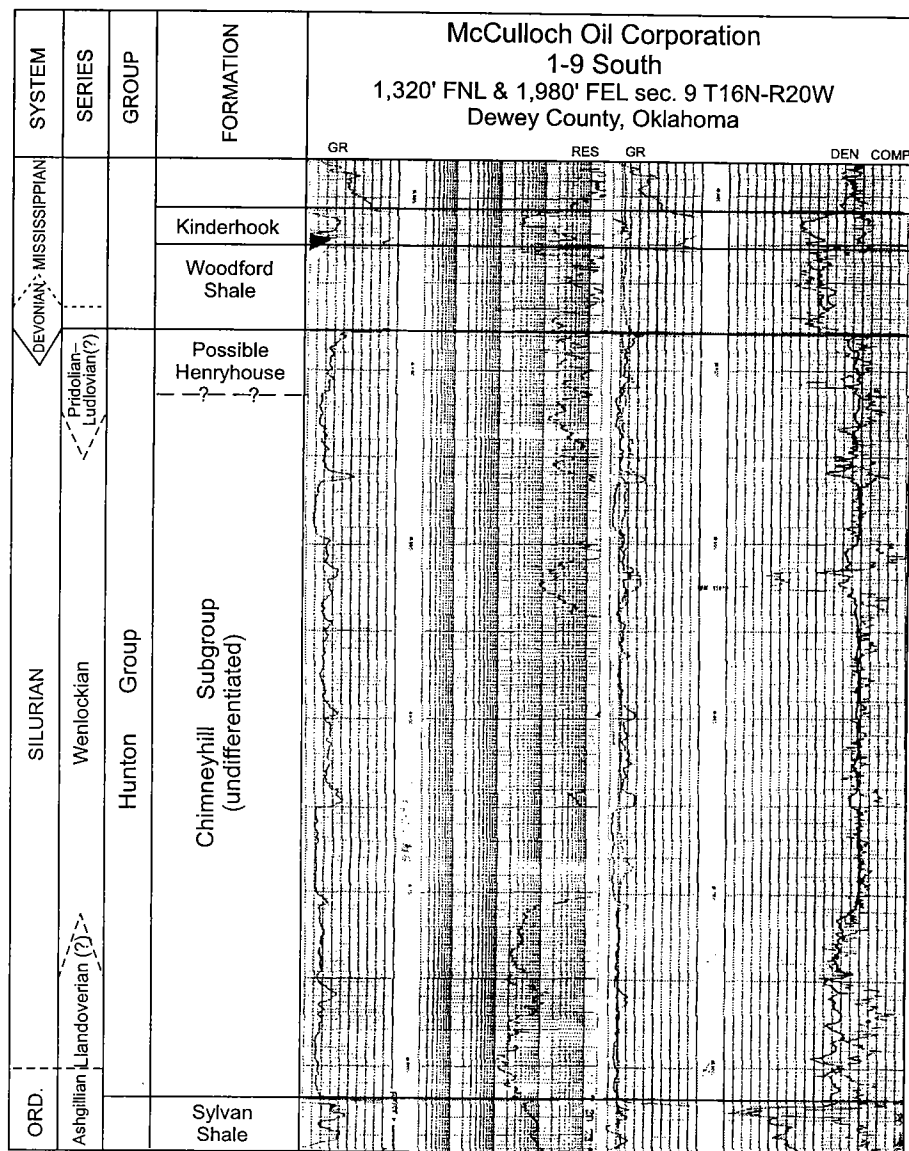


Figure 50. Type log for Leedey field, showing Hunton units represented and characteristic geophysical-log signatures. Dashed lines indicate uncertain but probable stratigraphic identification. GR = gamma ray; RES = resistivity; DEN COMP = density compensated.

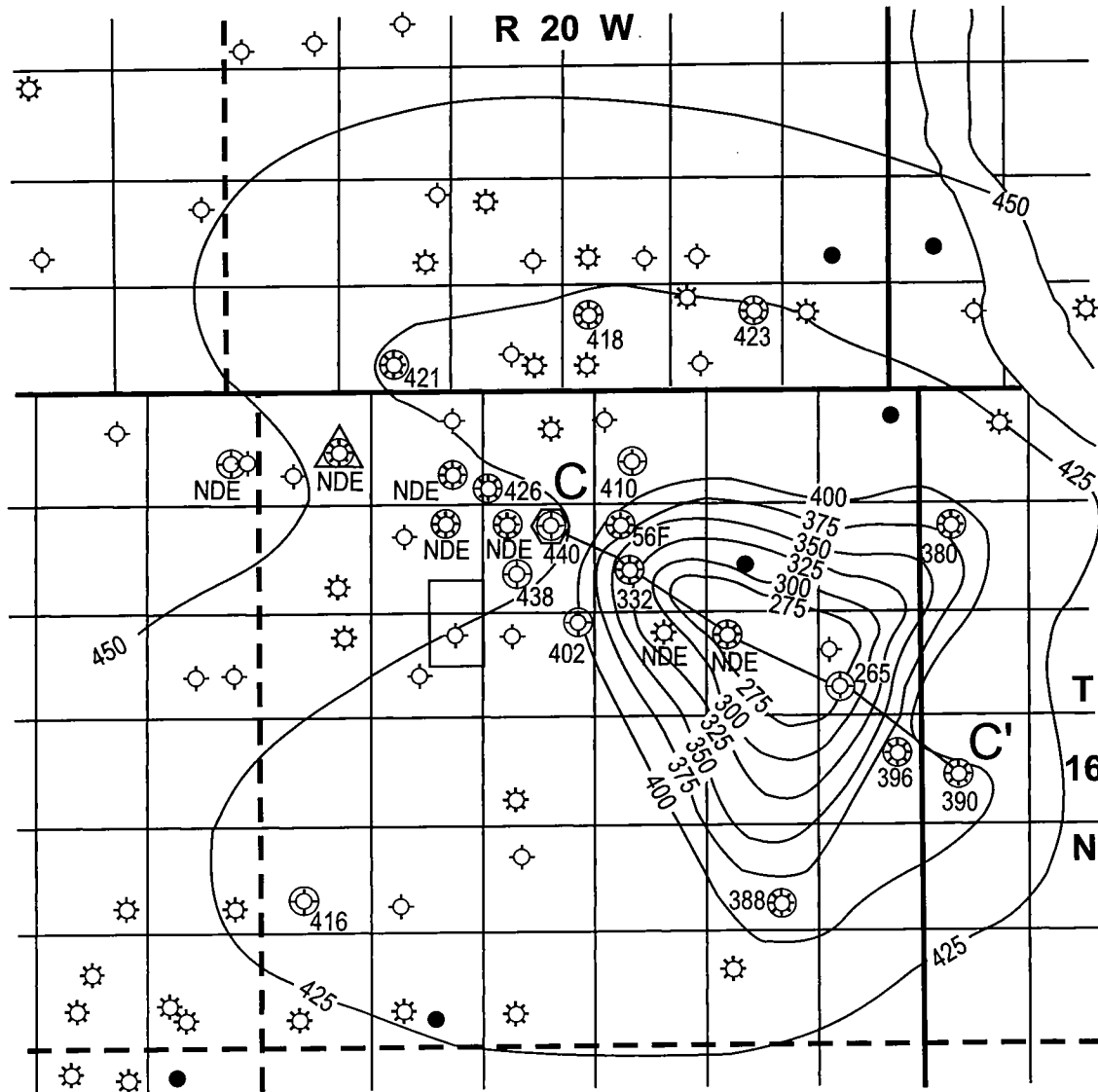


Figure 52. Gross-isopach map of Hunton Group in Leedey field study area. Contour interval is 25 ft. *NDE* = not deep enough. See text for further explanation.

and the Hunton can be recreated for that period immediately after deposition of the Woodford by modifying the current thicknesses of Woodford strata with respect to compaction. This has been done in cross section C–C' (Fig. 51) by doubling the thickness of the Woodford Shale to account for this compaction. Notice that the top of the Kinderhook shale, which is the datum for the cross section, is essentially parallel to the Sylvan in spite of the varying thicknesses of the Woodford and Hunton. This implies that during the depositional period from Late Ordovician to Early Mississippian time, structural movement was minimal (Rottmann, 2000). The increased isopach interval observed between wells 1 and 2 in Figure 51 is accounted for by regional dip.

As mentioned several times in this text, the various beds of the Sylvan, Hunton, and Woodford are extremely uniform, both horizontally and vertically, and these beds are practically identical in this configuration

over wide areas of the Anadarko basin. A hint of this uniformity is illustrated on cross section C–C' (Fig. 51) by observing the identical geophysical-log patterns of beds 1, 2, and 3 of the Woodford Shale. An examination of logs from wells a considerable distance away would show similar correlative beds. These beds essentially represent parallel time lines and are referred to as time-stratigraphic markers. This implies that the surface of such a bed is everywhere time equivalent—in other words, deposition would have taken place everywhere at the same time. The tops of the Kinderhook, Woodford, and Sylvan are excellent examples of time-stratigraphic surfaces.

Amsden refers to the boundary between the Woodford and Hunton as being diachronous (see Freeman and Schumacher, 1969; Amsden and Klapper, 1972, p. 2330–2331). By definition, this means that the boundary “is of varying age in different areas or that cuts

across time planes or biozones; e.g., ... a marine sand that was formed during an advance or recession of a shoreline and becomes younger in the direction in which the sea was moving" (Jackson, 1997). Figure 53 is a set of two schematic cross sections that illustrate these two principles.

Sandstone A in Figure 53A is an eroded surface. With transgression, sandstone B is onlapping; within sandstone B is found faunal assemblage 1, which is specific to a certain time period. As transgression continues, sandstone B continues to onlap. Faunal assemblage 3 is also a unique faunal assemblage. Notice how faunal assemblage 3 is at the top of the shale on the west side of the cross section, but its stratigraphic position decreases in height toward the east until it eventually disappears by onlap. The same situation occurs to faunal assemblage 4. To the west it is at the top of the formation, but its position descends in an easterly direction. Because the boundary between sandstone A and sandstone B is not coincident with time, it is termed *diachronous*, and Sandstone B would be termed a *rock-stratigraphic unit*.

Figure 53B illustrates a similar scenario, but in this case faunal assemblages 1, 2, and 3 maintain their stratigraphic positions with respect to the facies they were deposited in. These strata would be termed *time-stratigraphic units* with parallel time lines.

Understanding the time-stratigraphic nature of the Woodford and Sylvan and the diachronous boundary between the Woodford and the Hunton are essential when attempting to explain how the Woodford was deposited. It is generally accepted that the pre-Woodford unconformity surface was subaerially exposed, creating a drainage system upon the Hunton surface. Examination of the Woodford isopach from Plate 2 illustrates a pronounced drainage system in central and western Oklahoma. Figure 54 is a series of schematic cross sections illustrating what the pre-Woodford Hunton surface might have looked like

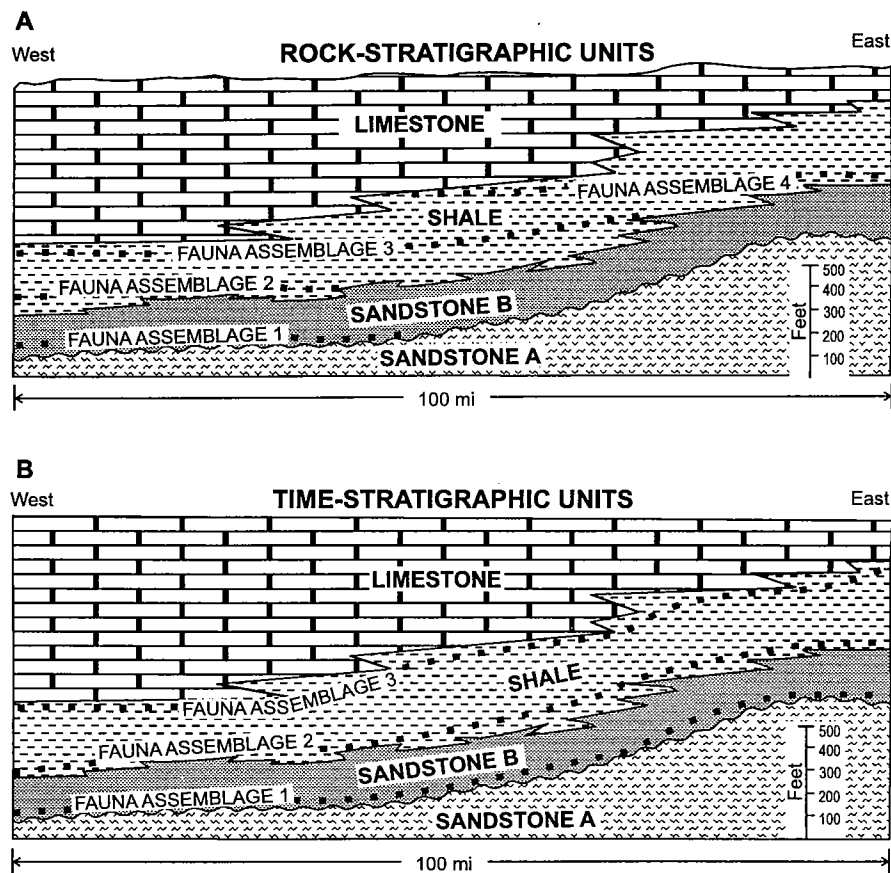


Figure 53. Hypothetical stratigraphic sections, showing (A) rock-stratigraphic units and (B) time-stratigraphic units. Dots represent time lines. See text for explanation.

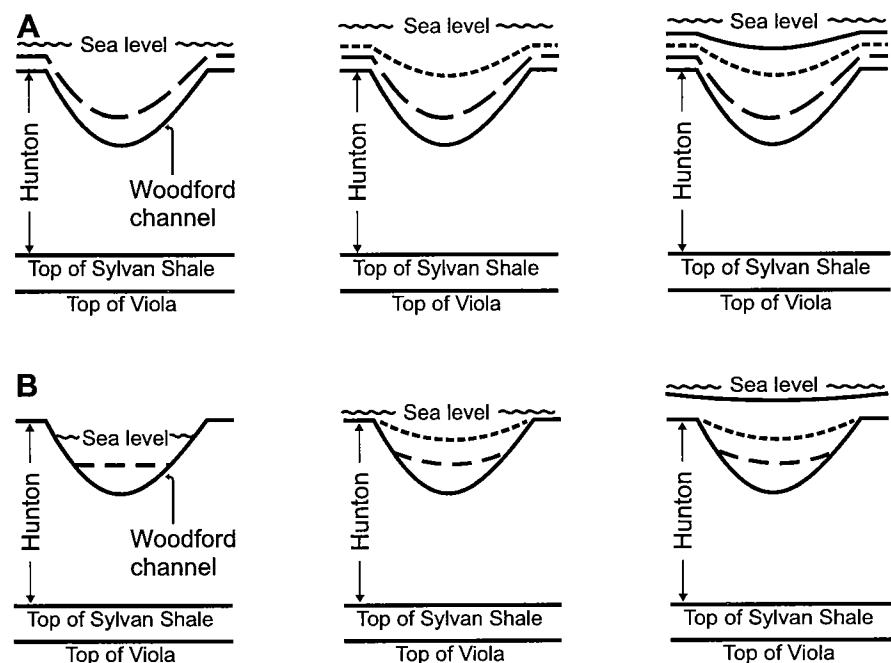
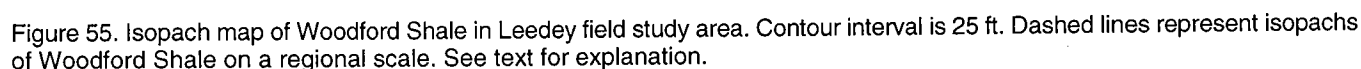


Figure 54. Two hypotheses for Woodford Shale deposition. (A) Regional seas deposit shale by settling. (B) Channels fill with shale; after filling, seas become regional. See text for further explanation. From Rottmann (2000, fig. 5).



nel fill” are not present to any degree in wells 1, 3, and 5. Furthermore, the model of Figure 54A is contrary to Amsden’s interpretation, and other interpretations, of this boundary as being diachronous.

Figure 54B is a second model used to explain Woodford deposition. This version implies a gradual initial inundation by the transgressive Woodford sea. Owing to the slow advance of the sea from the basin to the south, the sea would have been initially confined to the channels. Deposition was probably consistent with burial, resulting in the channels becoming filled and choked with sediment (Fig. 54B, center). These Woodford channels were essentially filled with shale and clastic material prior to any regional Woodford deposition. Ultimately, with the continuing rise in sea level,

the Woodford sea would have emerged from the channels and inundated the remaining Hunton surface. With the sea now covering the Hunton surface regionally, clastic material would have been deposited on the previously exposed Hunton highs as well as in the choked and filled Hunton channels. These regional deposits would then have been widespread and correlative, both over the paleotopographic highs and over the choked erosional channels (Fig. 54B, right). This could have occurred only if the Woodford channels were filled with detritus and the surface of this detritus was parallel to the exposed adjacent Hunton paleosurface of the channel fill at the time of regional Woodford deposition. Thus, the facies of the Woodford Shale within the channel would not be present or correlative with any facies deposited on nonchannel Hunton surfaces, as illustrated in Figure 54B (right) and as apparent from the well-to-well correlation of the Woodford in cross section C-C' (Fig. 51). This scenario would fit the interpretation of the boundary between the Woodford and Hunton as being diachronous. For the purpose of this report, that portion of the Woodford Shale thought to have been deposited on the nonchannel Hunton surface is informally termed "regional Woodford Shale." That portion of the Woodford Shale thought to have been deposited in and confined to the post-Hunton channels is informally termed "Woodford channel fill."

Figure 55 is an isopach map of the Woodford Shale in the Leedey field study area. The Woodford ranges in thickness from about 35 ft in this area to 108 ft in the SW $\frac{1}{4}$ sec. 13, T. 16 N., R. 20 W. By incorporating a regional overview of the Woodford isopachs, the presence of two erosional channels within the field area becomes apparent. The regional Woodford isopach map of Plate 2 suggests the presence of these channels as well as others in central and western Oklahoma. The channels drained from north to south. The southwestern part of Oklahoma near the depocenter of the Anadarko basin may have been a basin into which these channels drained. The silty shales and siltstones of the Misener in southwestern Oklahoma may have been the remainder of the terrigenous material from this post-Hunton-pre-Woodford erosional period.

The dashed lines of Figure 55 are the isopach contours for the regional Woodford Shale described previously. These contours suggest a south dip at the time of Woodford deposition within the field study area. These same regional Woodford Shale contours can

be inferred from the Woodford isopach map of Plate 2. Outside of the influence of the erosional channels, the contours illustrate the orientation of the strike and dip of the basin during this time interval.

A plausible observation could be made at this point. I have observed that many wells in a general locality will usually have uniform or nearly identical Woodford thicknesses. Figure 55 illustrates this observation to a degree. The Woodford isopach, which is composed of regional Woodford facies, is similar to identical over fairly large areas. In the Leedey field proper, the isopach between the channels averages 50 to 55 ft in thickness. Farther north, it averages 35 ft or so. In areas of greater control, this pattern still holds true. Amsden speaks of dissolution, deep crevices, and even small caverns at the top of the subaerially exposed Hunton carbonate sequence prior to Woodford deposition (Amsden, 1980, p. 14). In almost all cases, these solution fractures or other erosional features were filled with either Misener sand or brecciated limestone or dolomite fragments prior to Woodford Shale deposition. Thus, there seems to have been a relative uniformity in topographic relief (almost a peneplain) on the Hunton surface away from the erosional channels at the time of Woodford deposition. This seems odd, especially in light of the great period of time during which the Hun-

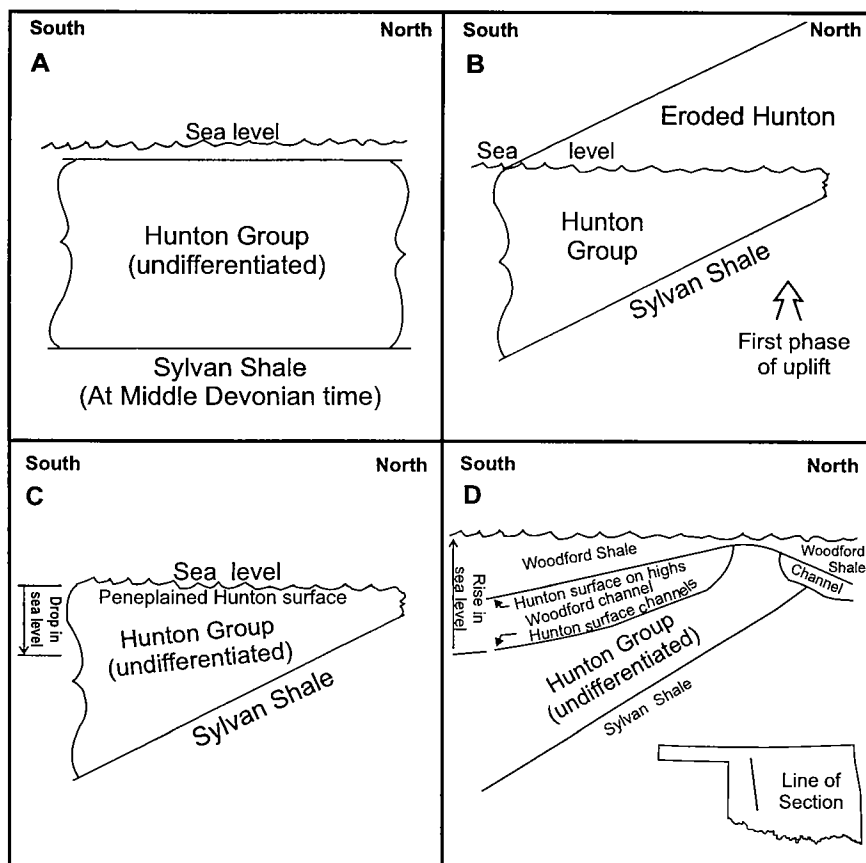


Figure 56. Schematic cross sections showing two stages of post-Hunton erosion and subsequent deposition of Woodford Shale. Not to scale. See text for description.

ton was exposed prior to Woodford deposition. Figure 56 is a series of schematic cross sections that may offer a reasonable explanation for this anomaly. Figure 56A illustrates Hunton deposition during Sawkillian time. Regional uplift and tilting of the basin (Fig. 56B) introduced the first phase of erosion, resulting in complete truncation of the exposed Hunton surface (Fig. 56C). At this point, the overall geometry of the Anadarko basin was established.

Following peneplanation, a lowering of sea level possibly occurred, exposing the peneplained Hunton surface to a second phase of erosion, resulting in the immature drainage systems seen today (Fig. 56D), as suggested by the Woodford isopach map of Plate 2. This second phase of erosion could explain the relatively uniform topographic relief of the Hunton paleosurface outside the area of influence of the erosional channels.

ISOPACHING THE HUNTON NEAR PRE-WOODFORD EROSIONAL CHANNELS

Examination of cross section C-C' (Fig. 51) illustrates two types of Woodford facies, a Woodford chan-

nel-fill facies and a regional Woodford Shale. The thickness of the Woodford channel-fill facies should represent the amount of Hunton removed prior to Woodford deposition. Figure 57 is a regional isopach map of the Woodford channel-fill deposits restored to pre-Woodford depositional thicknesses. This was done by using the factor discussed previously to allow for compaction. Figure 58 shows the same isopach method for the Leedey Hunton field study area. The dashed regional Woodford contours can be used to estimate the thickness of both the Woodford channel-fill facies thickness and the regional Woodford shale thickness. The contours of Figure 58 represent the reconstructed (de-compacted) thickness of the Woodford channel-fill isopach, which also estimates the amount of Hunton strata removed prior to Woodford deposition. As explained earlier, the isopach values for the Woodford channel fill were doubled to allow for compaction and restoration of sediment thickness to original conditions.

Taking the isopach map of Figure 58 one step further, it stands to reason that if the isopachs represent the amount of strata removed prior to Woodford depo-

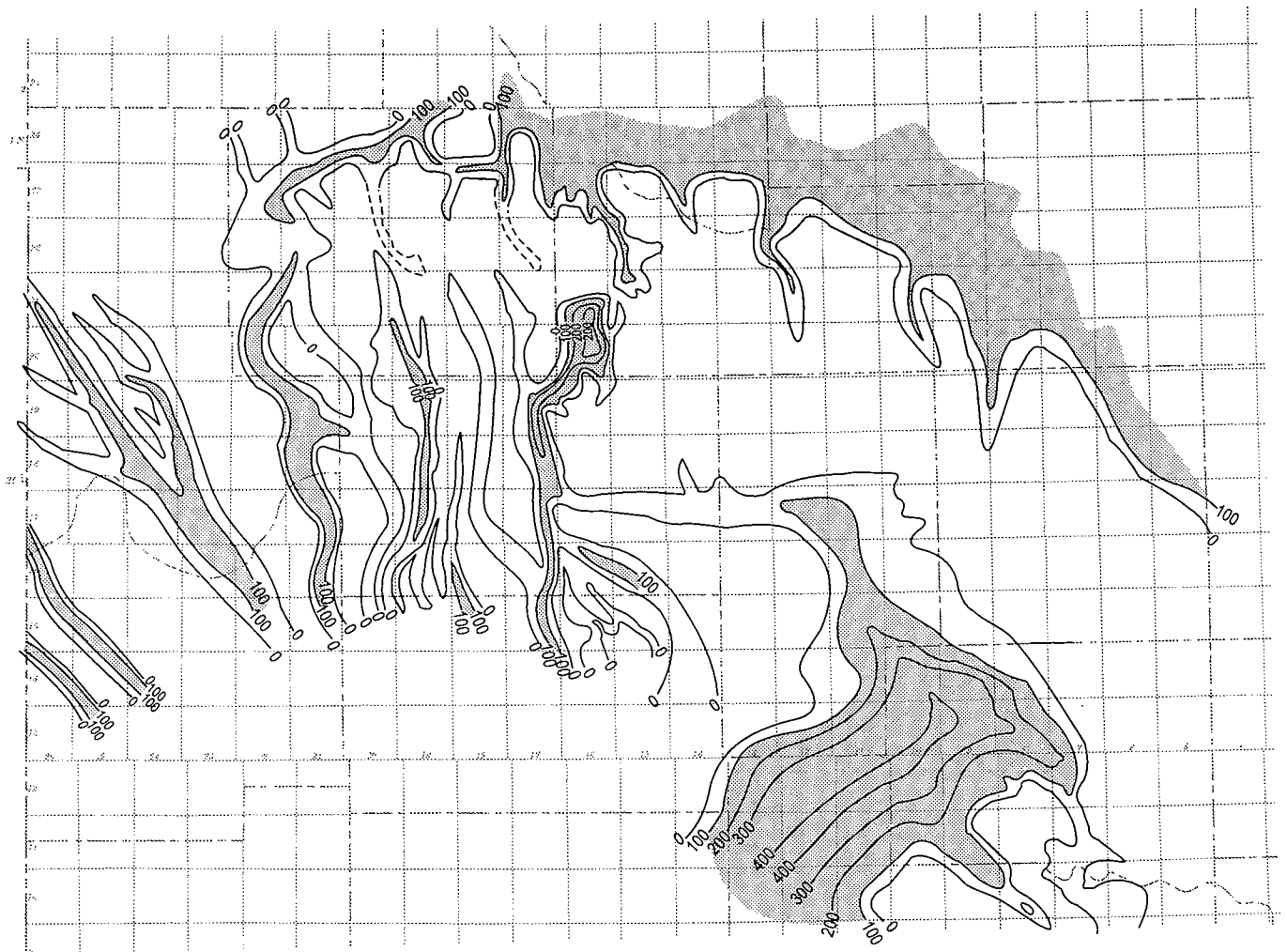


Figure 57. Isopach map of Woodford channel-fill facies, restored to original thickness by multiplying current thickness by a compaction factor of approximately 2 in the area of Ts. 10–24 N., Rs. 5–26 W., Oklahoma. Dashed lines indicate facies probably composed of sandstone. Contour interval is 100 ft.

sition, then adding the thickness of the restored Woodford channel to the affected Hunton erosional surface would restore the Hunton thickness to pre-channel conditions. The isopach values of Figure 59 represent this concept. Those wells that encountered no pre-Woodford channeling retain their original isopach values. Those wells that encountered a Woodford channel facies have their original thicknesses restored by adding a doubled Woodford channel facies (restoring the channel fill to original thickness) to the thickness of the Hunton, thus restoring the Hunton to its pre-channel thickness. The preparation of this kind of map is critical when attempting to isopach present-day Hunton thickness, because it gives an orientation of strike and dip prior to channeling, which could not be recreated by any other method.

Reconstructing the present-day Hunton isopachs can now be accomplished by overlaying the restored pre-Woodford channel isopachs of Figure 58 on the reconstructed pre-Woodford Hunton isopachs of Figure 59 (see Fig. 60) and by subtracting the Woodford channel-fill isopach values, essentially restoring the erosional drainage system that was present prior to Woodford deposition (Fig. 61). Figure 61 illustrates the correct isopach values and geometry of the Hunton for the Leedey field study area, because it incorporates the isopach orientation of the eroded Hunton paleosurface with the thickness and orientation of the pre-Woodford drainage system.

Figure 62 is a regional isopach map of the reconstructed thickness of the Hunton prior to the exposure and formation of the regional erosional drainage sys-

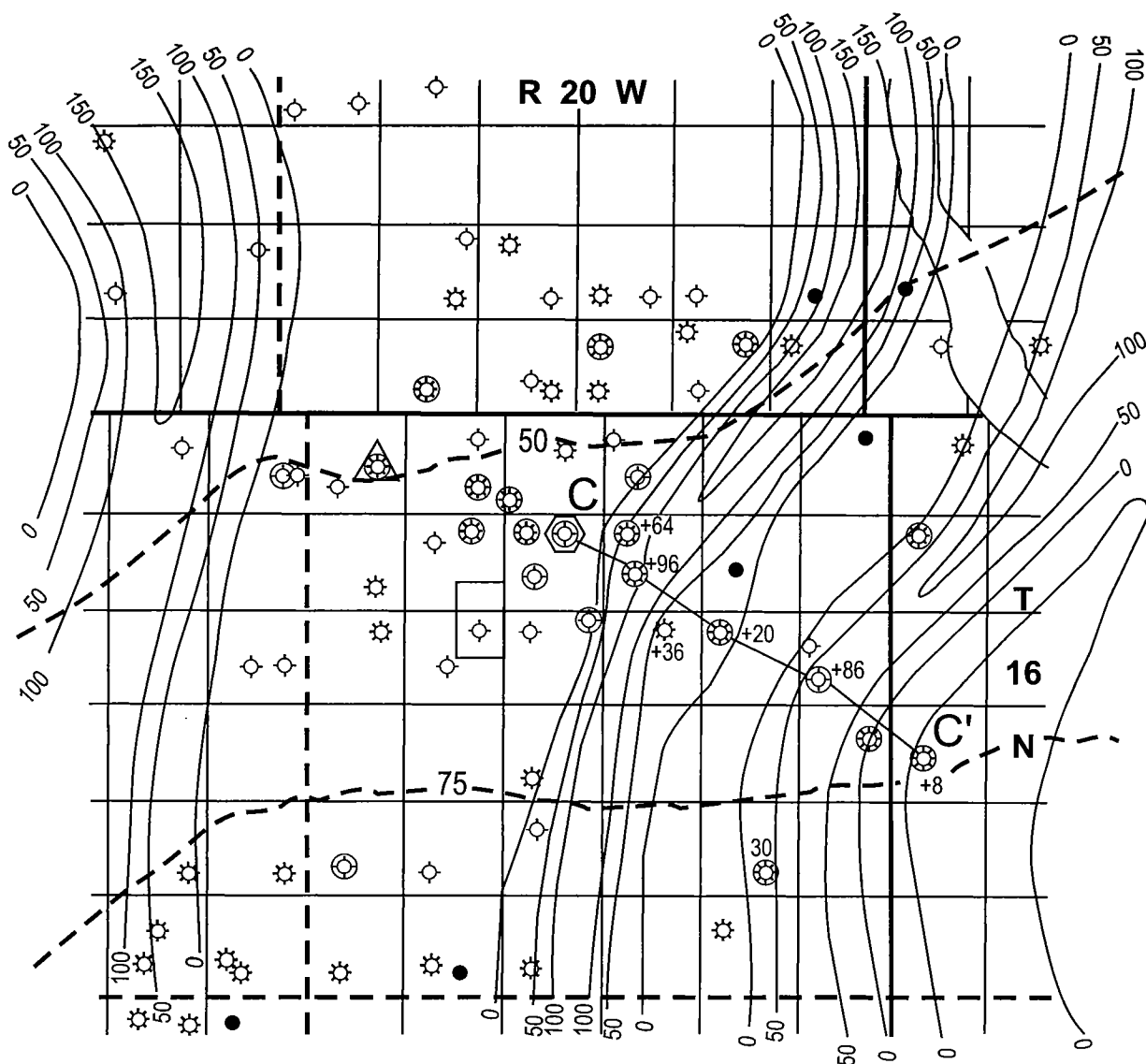


Figure 58. Isopach map of Woodford channel-fill facies in Leedey field study area, restored to original thickness by multiplying current thickness by a compaction factor of approximately 2. Contour interval is 50 ft. Dashed lines represent isopachs of Woodford Shale on a regional scale. See text for explanation.

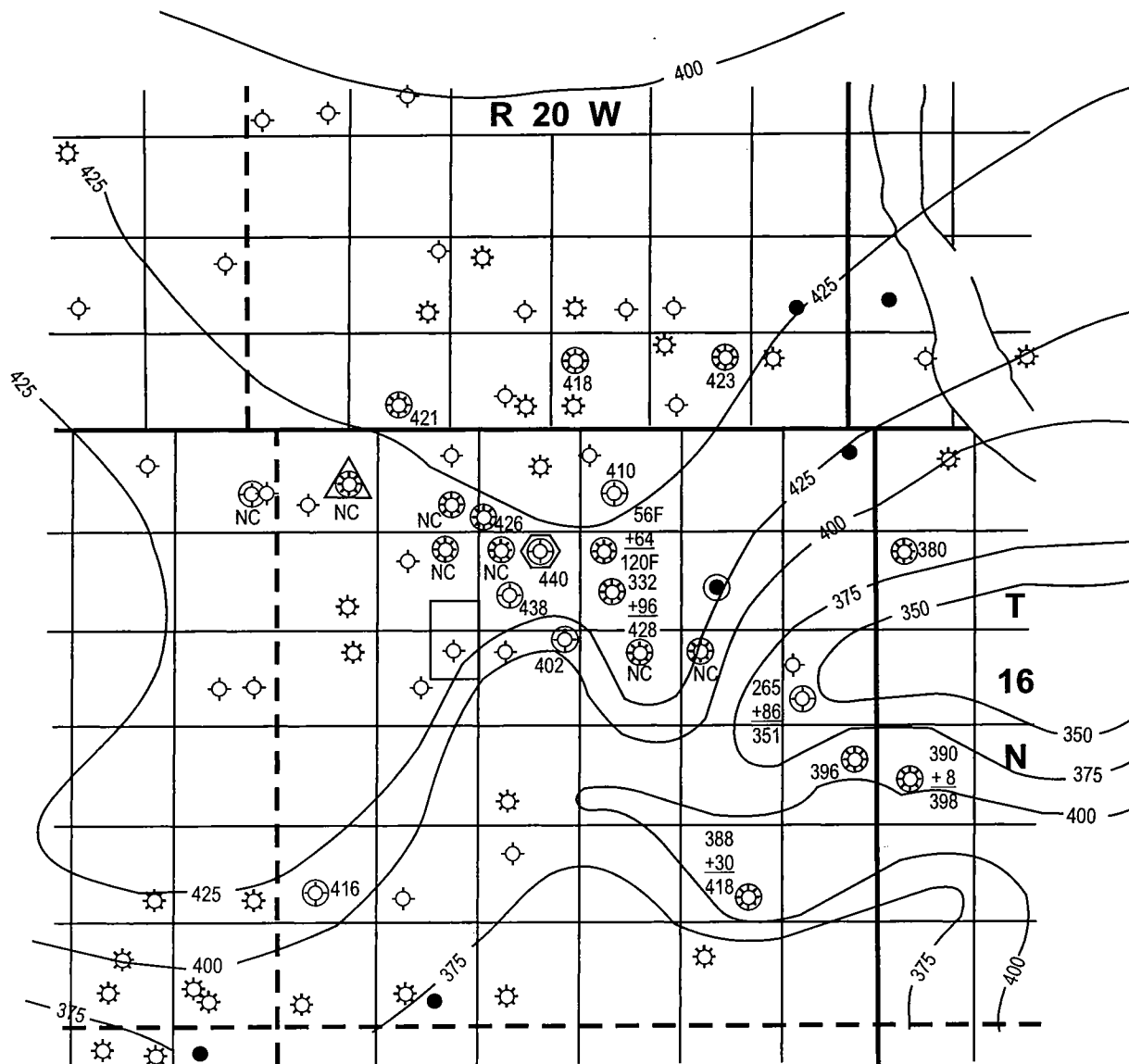


Figure 59. Isopach map of restored Hunton thickness, derived by adding thickness of Hunton to eroded Hunton, as suggested by thicknesses of Woodford channel-fill deposits. NC = no control. Contour interval is 25 ft. See text for explanation.

tems inferred from Figure 57. The process for creating this isopach map is identical to that just described for the Leedey field study area. Those Woodford channel-fill thicknesses recognized were doubled to reconstruct the thicknesses of the channels. Overlaying Figure 57 on Figure 62, and subtracting the contour values, result in the current Hunton isopach map for western Oklahoma, which was incorporated in the Hunton isopach map of Plate 1.

STRUCTURAL IMPLICATIONS OF THE SILURIAN-DEVONIAN ISOPACHS

As mentioned earlier, in those areas of continuous deposition devoid of structural influences, the surfaces of the Sylvan Shale, and the Woodford Shale and/or Kinderhook shale, represent time-stratigraphic horizons. Similar lithofacies were deposited in uniform

moments of time regionally. Cross section C-C' (Fig. 51) illustrates the almost parallel nature of these two surfaces with respect to each other. The method of doubling the Woodford and/or Kinderhook thicknesses, and adding them to the Hunton thicknesses for local areas, generally results in uniform isopach thicknesses where structure (other than regional dip) was not active during this depositional interval (Rottmann, 2000). Figure 63 is just such an isopach map, which is featureless and represents an approximation of the thickness of the original sequence prior to Meramecan time. This map shows that the strike at this time was essentially east-west, with dip to the south at a rate of 25 ft per mi. An anomalous well with a discordant isopach interval was drilled in the NW¼ sec. 10, T. 16 N., R. 20 W. This well encountered a thickness of 240 ft, less than half that of all other wells in the vicinity. The anoma-

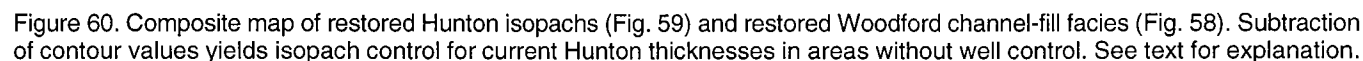


Figure 64 is a map showing the structure at the top of the Hunton Group in the Leedey field study area. The contours generally portray a regional southwest dip but are interrupted by a northwest-southeast up-to-the-basin normal fault. The throw of the fault is approximately 400 ft. Closure against the upthrown surface of the fault created the reservoir for the Leedey

Figure 65 is an isopach map of the Woodford Shale and Kinderhook shale restored to their original thicknesses by doubling present thickness values to account for post-depositional compaction and added to the respective Hunton well-bore thicknesses. The top of the Woodford is considered to have been a flat, featureless, time-stratigraphic surface. Several prominent structural features are readily obvious in Figure 65. These features are labeled A through G and represent several kinds of structural features that affected the Hunton-Woodford/Kinderhook isopachs. These features are

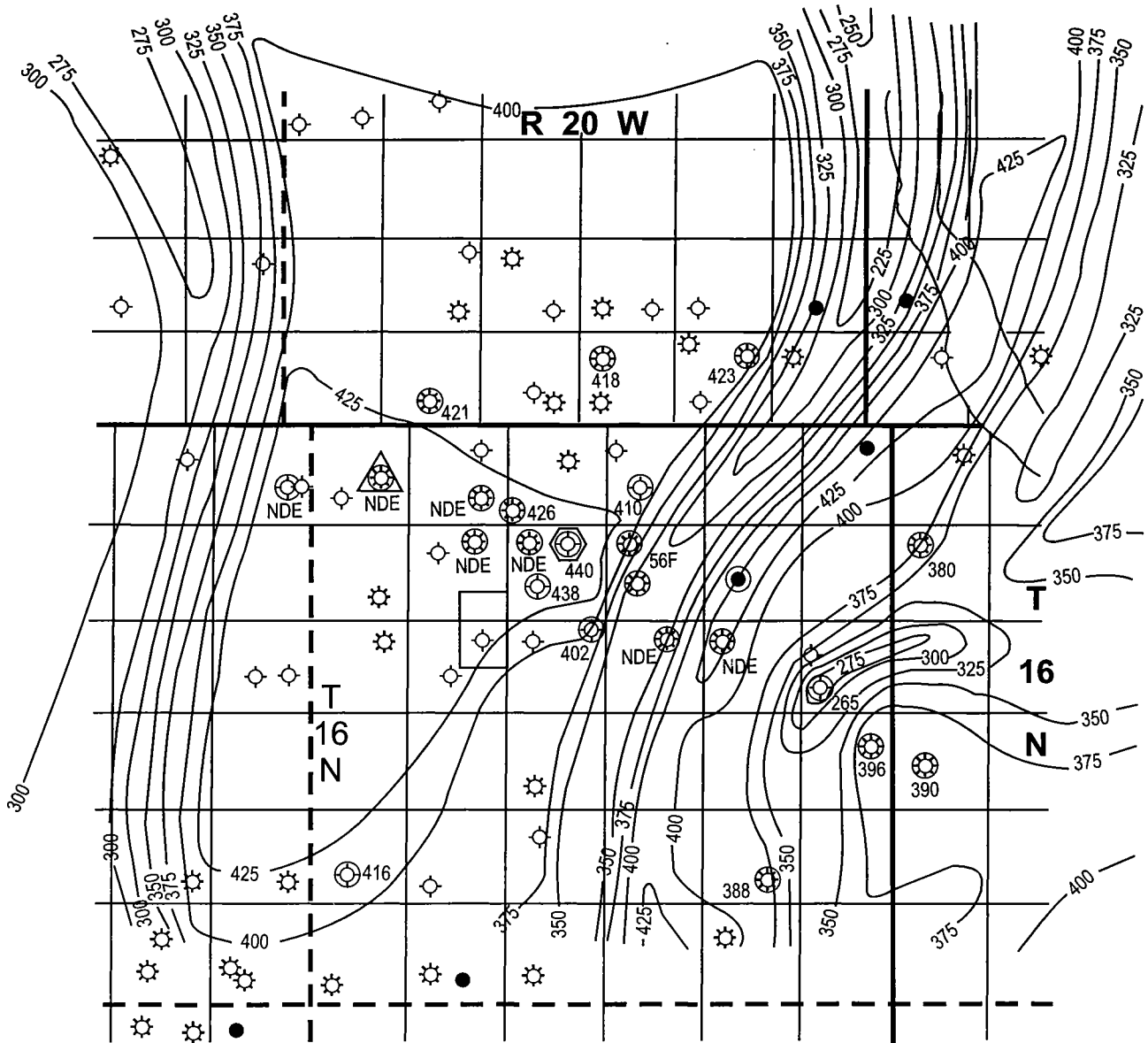


Figure 61. Isopach map of Hunton Group in Leedey field study area. Geometry of contours derived from subtraction of restored Hunton isopachs and restored Woodford channel-fill deposits. Contour interval is 25 ft. NDE = not deep enough. See Figure 60 and text for details.

discussed in some detail later in this publication. Figure 64 gives a good indication of the strike and dip of the basin prior to Meramecan deposition. The dip in the eastern part of the area shown in Figure 65 was to the west-southwest, and the dip in the western part, essentially to the south.

PRE-WOODFORD-CHANNEL HYDROCARBON SEALS

One characteristic of shales in general is their non-permeability to fluid flow after compaction unless, of course, shale contains permeable strata or fractures that create permeability. More often than not, however, shales are nonpermeable. Thus, the Woodford Shale in particular acts as a hydrocarbon seal for many reservoirs in Oklahoma. Such seals can form in two

basic ways: (1) as a sealing boundary against a porous and permeable stratigraphic unit that has been faulted adjacent to the Woodford, and (2) as a stratigraphic boundary in which the Woodford forms a natural overlying barrier to underlying porous and permeable strata. The channeling of the Hunton paleosurface and subsequent deposition of impermeable Woodford channel fill is a unique reservoir stratigraphic trap not generally seen in other strata in Oklahoma. But, as previously mentioned, the compaction of the Woodford Shale, when not taken into account, is a potential pitfall for explorationists seeking to interpret Woodford-Hunton trap geometries.

As an example, consider Figure 66. This cross section (D-D') is of the West Campbell field in Major County, Oklahoma. Well 2 penetrated a deeply incised

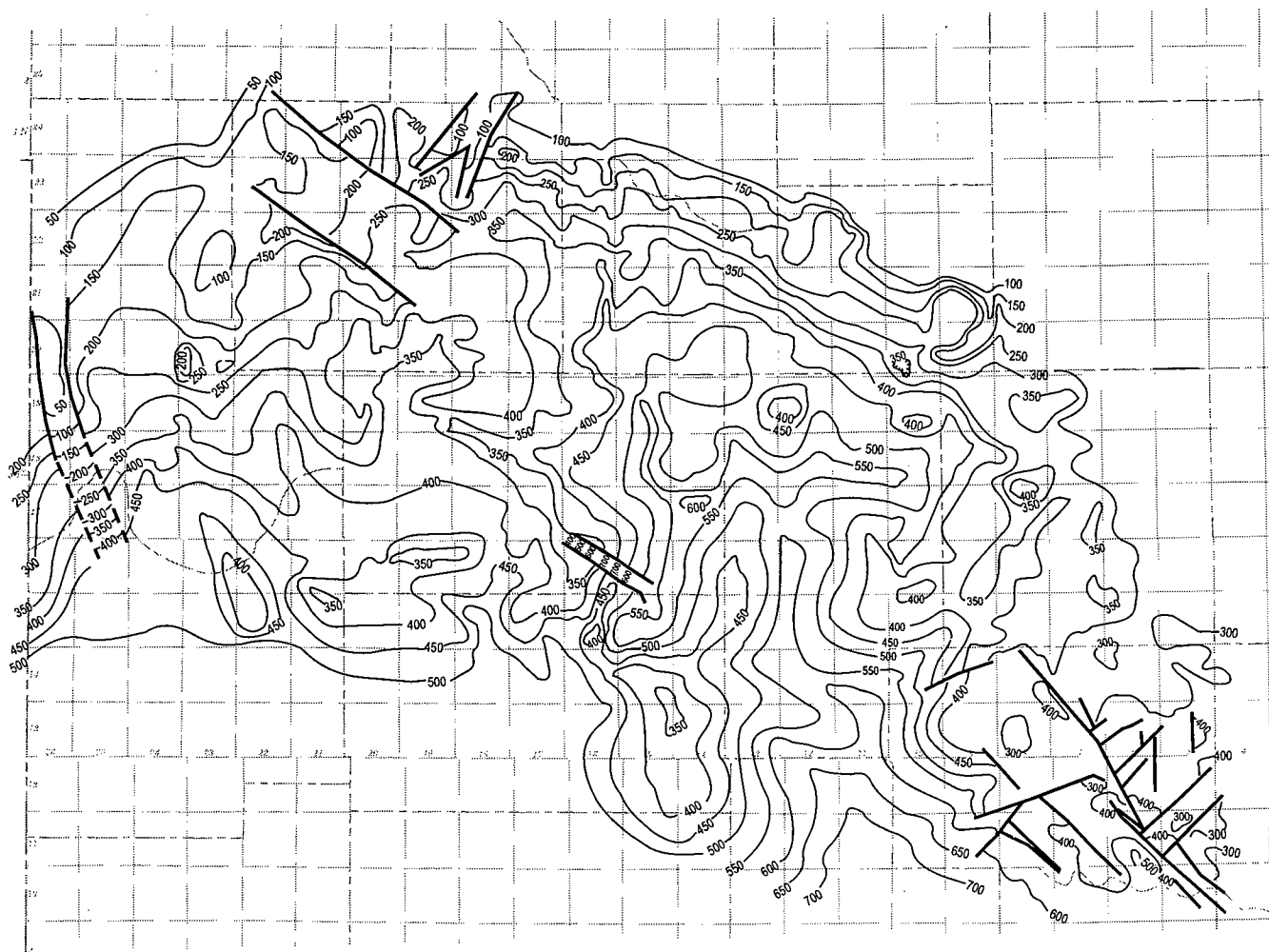


Figure 62. Isopach map of restored Hunton sequence in area of Ts. 10-24 N., Rs. 5-26 W., Oklahoma. Isopach interval derived by adding Hunton thickness to restored Woodford channel-fill facies to derive Hunton pre-erosional thickness. Contour interval is 50 ft.

channel filled with Woodford deposits. This well is between two adjacent, nonchannel wells, 1 and 3. The datum for this cross section is the top of the Woodford Shale. Post-depositional compaction of the Woodford has not been accounted for in this section, with all stratigraphic sequences having been treated equally. What is immediately apparent is the structural high at the Sylvan level in well 2. The cross section is technically correct, because the datum at the top of the Woodford Shale is time stratigraphic, and the stratigraphic relationships, as shown in the well log, were valid at the time of deposition. However, the presence of unequal Woodford thicknesses in adjacent wells requires the decompaction of the Woodford to original thicknesses.

Figure 67 illustrates why the Woodford thickness needs to be decompacted prior to incorporating the unit in a stratigraphic cross section representing original depositional conditions. Figure 67A represents the Hunton and Woodford stratigraphic relationship at the time of deposition. The Hunton was approximately 400 ft thick at the start of post-Hunton uplift, tilting, and

erosion. Subsequent erosion incised a 150-ft channel in the top of the Hunton. This channel was filled with Woodford channel deposits until the channel was completely filled, at which time the Woodford sea spread over the nonchannel paleosurface, depositing the regional Woodford Shale. Subsequent Mississippian deposition created overburden pressure on the underlying Woodford Shale, which expelled water from the shale, essentially compacting the shale to approximately one-half its original thickness and distorting the top of the Woodford time-stratigraphic datum (Fig. 67B). Figure 67C illustrates the pitfall that could occur by creating a stratigraphic cross section using the compacted surface of the Woodford as a datum. By flattening this datum, the surface of the Sylvan appears as an artificial high (see also Fig. 66).

Cross section D-D' (revised) of Figure 68 is identical to that of Figure 66, except the datum is now the top of the Kinderhook Shale. Both the Kinderhook and Woodford have been restored to their original thicknesses by doubling. This cross section (Fig. 68) is quite different from the first interpretation (Fig. 66). The apparent

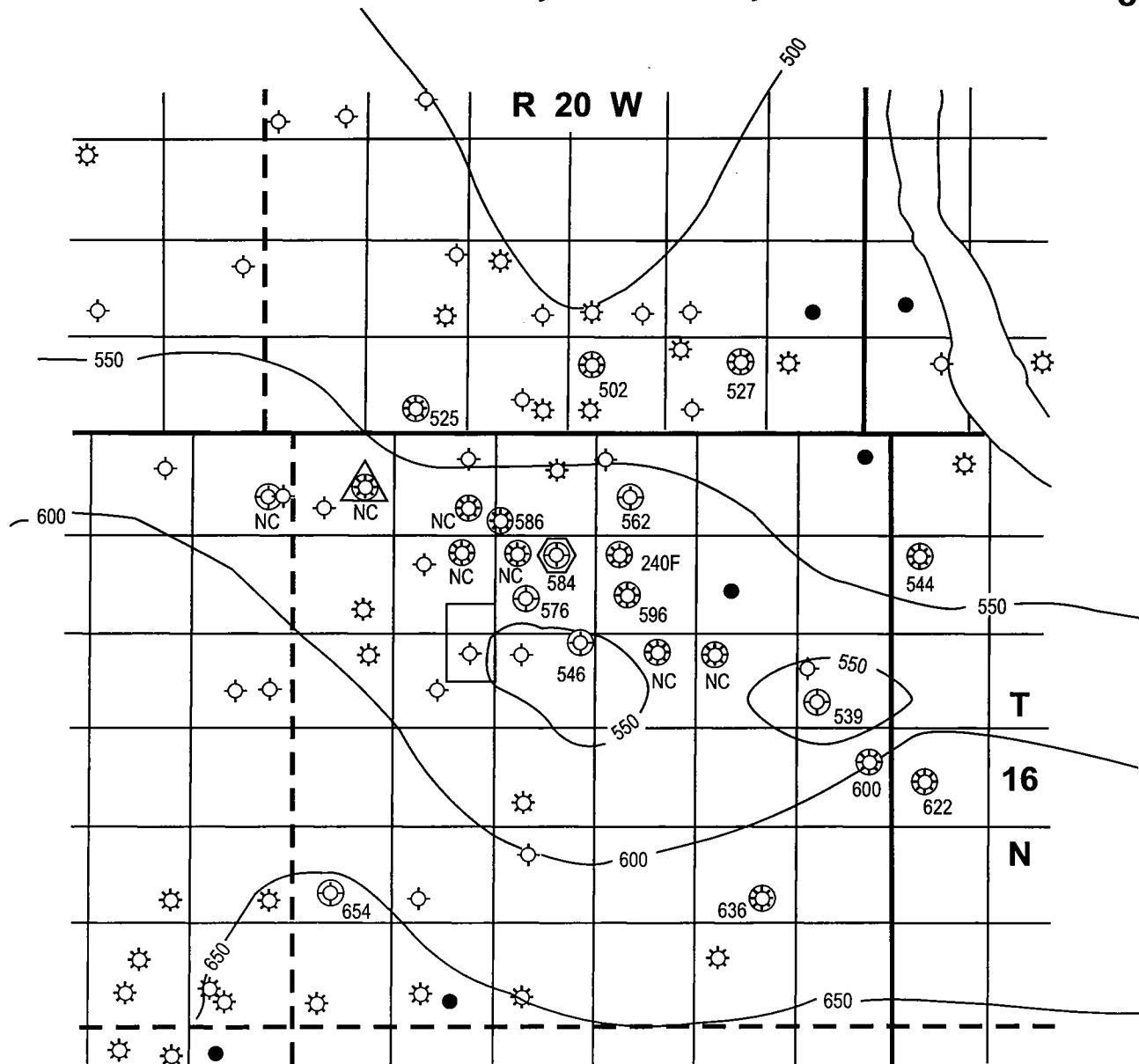


Figure 63. Isopach map of Hunton thickness plus uncompacted thickness of Woodford Shale and Kinderhook shale to derive an isopach interval from the top of the Sylvan Shale to the top of the Kinderhook shale for Leedey field study area. Contour interval is 50 ft. NC = no control. See text for explanation.

structure centered near well 2 has disappeared. The time-stratigraphic surfaces of the Sylvan Shale and Kinderhook shale are now almost parallel, suggesting a complete lack of structural influence during deposition. Also, the relationship of the porosity zone to the sealing channel-fill deposits of the Woodford can be correctly interpreted. The trap for this porosity zone is stratigraphic rather than structural as implied by Figure 66.

Cross section D-D' (Fig. 68, revised) also reveals how the Woodford Shale must have rapidly dewatered. The Woodford in well 2 is considerably thicker, and its net compaction therefore would have been larger than at wells 1 and 3. Thus, with increased overburden pressure from deposition of the Kinderhook shale, the paleosurface at well 2 would have been lower than at wells 1

and 3 at the top of the Woodford. In response to this lowering of the paleosurface, a greater thickness of Kinderhook would have been deposited than at wells 1 and 3. Figure 69 is an isopach map of the Kinderhook shale in western Oklahoma. The isopachs suggest north-south thickening in trends that parallel the pre-Woodford channels shown in Figure 57. These Kinderhook thickening trends resulted from differential compaction of the Woodford in both the channel and non-channel areas.

A second reason for interpreting and restoring Woodford channel and nonchannel thicknesses can be illustrated by the schematic cross sections of Figure 70. Suppose, as an example, that we recognize a Woodford channel-fill sequence by geophysical-log correlation, and that its present-day thickness is 150 ft and the re-

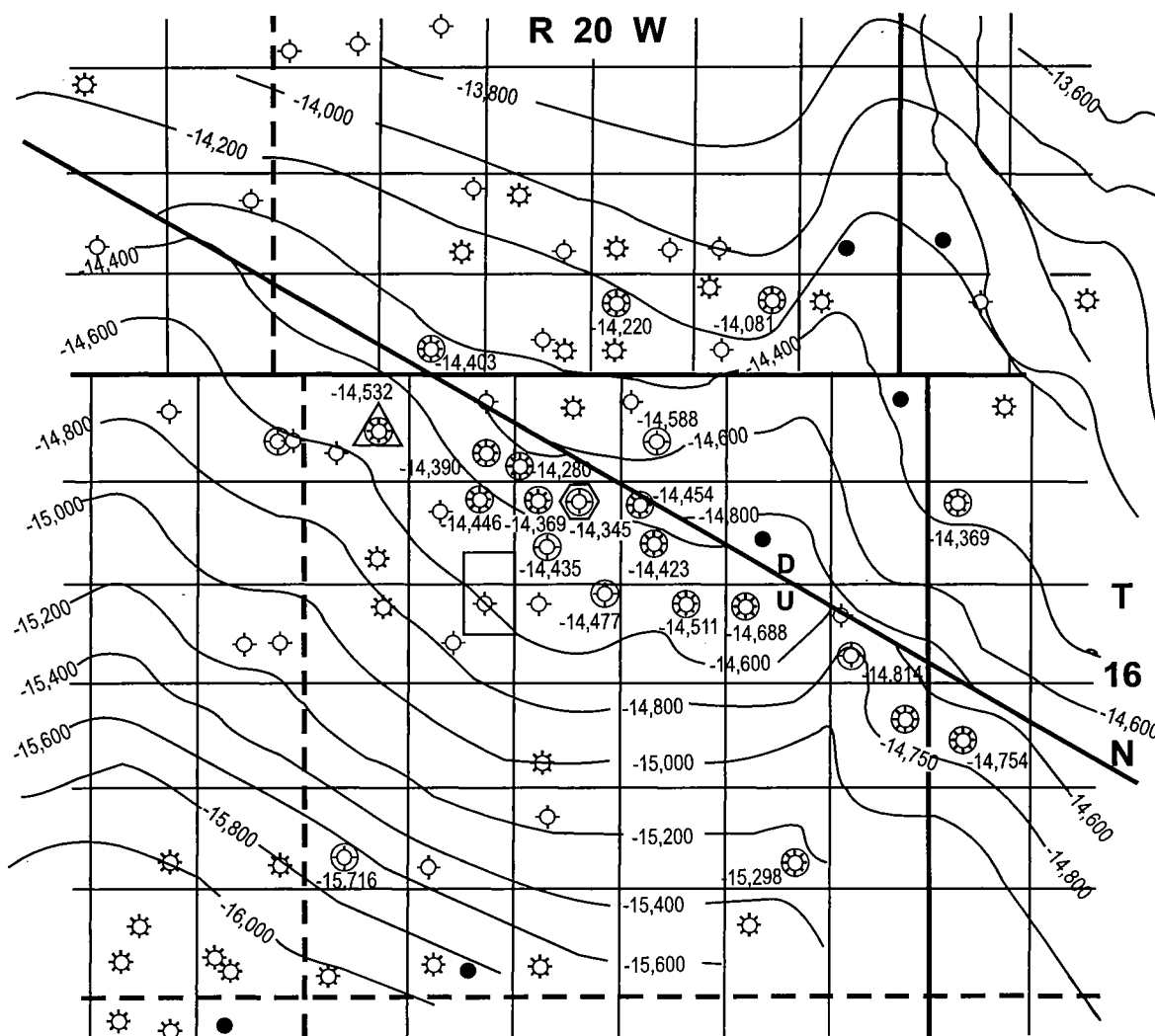


Figure 64. Structure-contour map depicting top of Hunton Group in Leedey field study area. Contour interval is 200 ft.

gional Woodford thickness 25 ft (Fig. 70A1). A pitfall would be to project the present-day thickness of 150 ft for the pre-Woodford channel on an isopach map and to hang the top of the present-day pre-Woodford channel so it is flat to the top of the adjacent nonchannel Hunton surface (Fig. 70A2). Doing this would arbitrarily flatten the distorted time-stratigraphic surface of the Woodford channel fill. By using the compacted present-day thickness, the porosity zone (Fig. 70A2) would not be sealed by the impermeable channel-fill facies. By assuming that the compacted surface of the Woodford channel-fill deposit is flat, the distortion that occurred after compaction is not accounted for, as illustrated and defined in Figure 67. It would also appear that only 150 ft of the Hunton was eroded and that the base of the Woodford channel fill would have only cut and potentially sealed 150 ft of the 250-ft Hunton porosity zone (Fig. 70A2).

The correct way to interpret the pre-Woodford channel is, first of all, to recognize that it is compacted

and to restore the current thickness of the Woodford Shale to its original thickness at the time of deposition (Fig. 70B1). By multiplying the channel thickness by an approximate compaction factor of 2, the thickness of the Woodford channel fill is restored to its original thickness of 300 ft. Now, the top of the pre-Woodford channel surface can be hung parallel to the top of the surface of the nonchannel Hunton adjacent to the channel, as illustrated in Figure 70B2. Note that the restored pre-Woodford channel thickness of 300 ft does cut the base of the porosity zone, creating a seal for a potential Hunton stratigraphic trap.

Cross section C-C' (Fig. 51) incorporates the foregoing principle in its creation. The thicknesses of the Kinderhook and Woodford strata having been doubled to account for compaction, the true thicknesses of the channel systems with respect to the Hunton can now be observed. There appear to be three primary porosity zones (A, B, and C) on the cross section. Porosity zones A and B are sealed by Woodford channel-fill deposits,

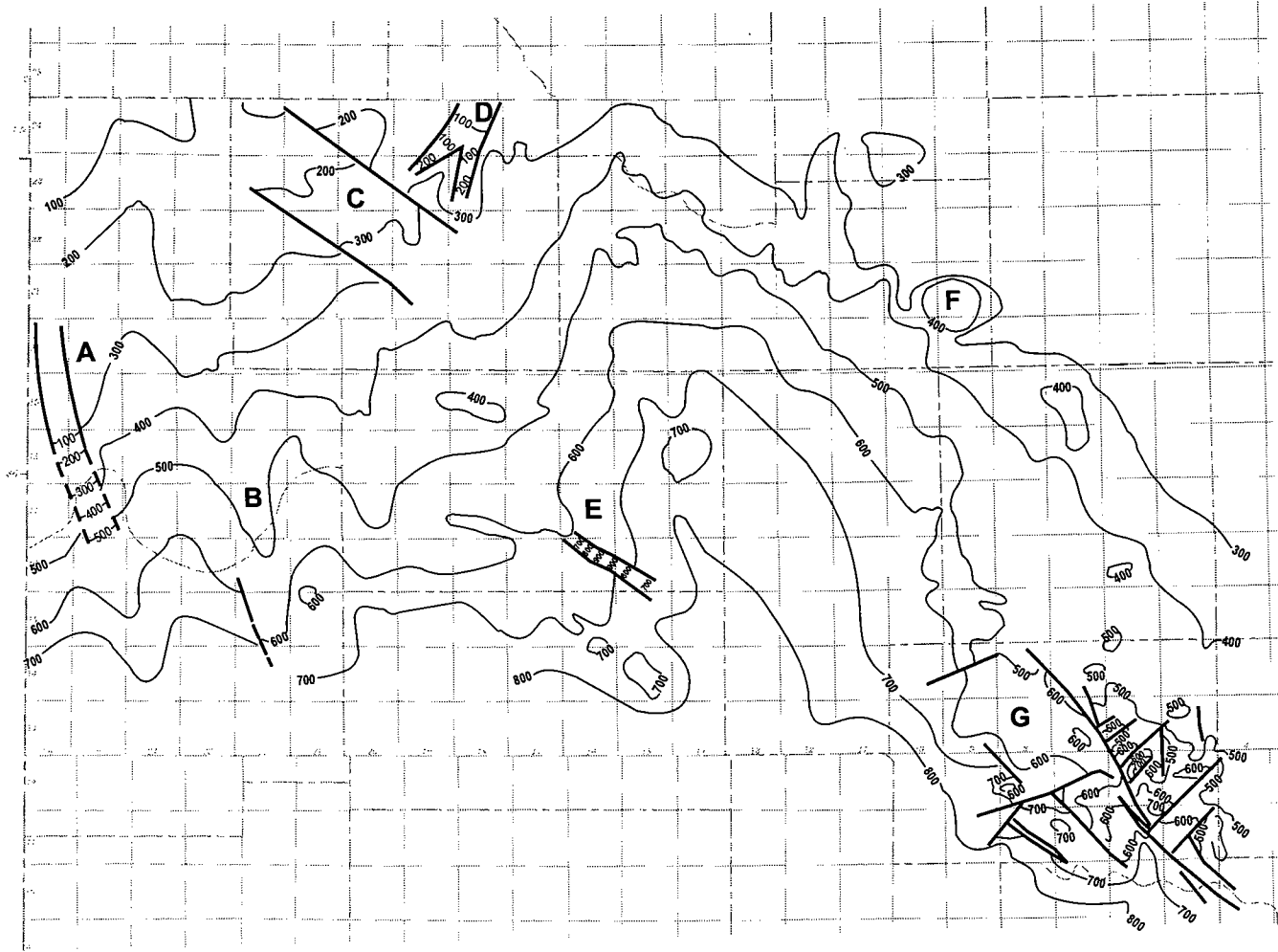


Figure 65. Isopach map of Hunton thickness plus uncompacted thickness of Woodford Shale and Kinderhook shale to derive an isopach interval from the top of the Sylvan Shale to the top of the Kinderhook shale in area of Ts. 10–24 N., Rs. 5–26 W., Oklahoma. Letters A through G represent areas of Hunton thickness affected by structural influences. Contour interval is 100 ft.

identified in wells 2 and 3. Porosity zone C appears to be unaffected by the presence of the pre-Woodford channels.

CORES

None of the wells in the Leedey field study area cored the Hunton. The nearest wells that did core the Hunton are too far away to be representative.

RESERVOIR PARAMETERS AND PRODUCTION

Table 6 lists reservoir parameters for the Hunton in the Leedey field study area. The field was drilled on 640-acre spacing. The average porosity is assumed to be 10%, although it appears from porosity logs that many intervals may be fractured. Thus, it is not known

how much production might have been attributed to fracture porosity versus matrix porosity.

Figure 71 shows the gas-production curve for the field. Production was established in 1973. To date, the field has a cumulative production of more than 32 BCFG. Of interest is the Hunton production in sec. 19, T. 16 N., R. 19 W. The Getty Oil Co. No. 1-19 Hall well had an initial flowing potential through perforations of 1.7 MMCFGPD. This well has a cumulative production of more than 2.2 BCFG. The Hunton production is probably coming from a thick sequence bounded by channeled Hunton on its east and west flanks and sealed by the normal fault to the north. This well also serves as an excellent example of how pre-Woodford erosion can modify Hunton reservoirs.

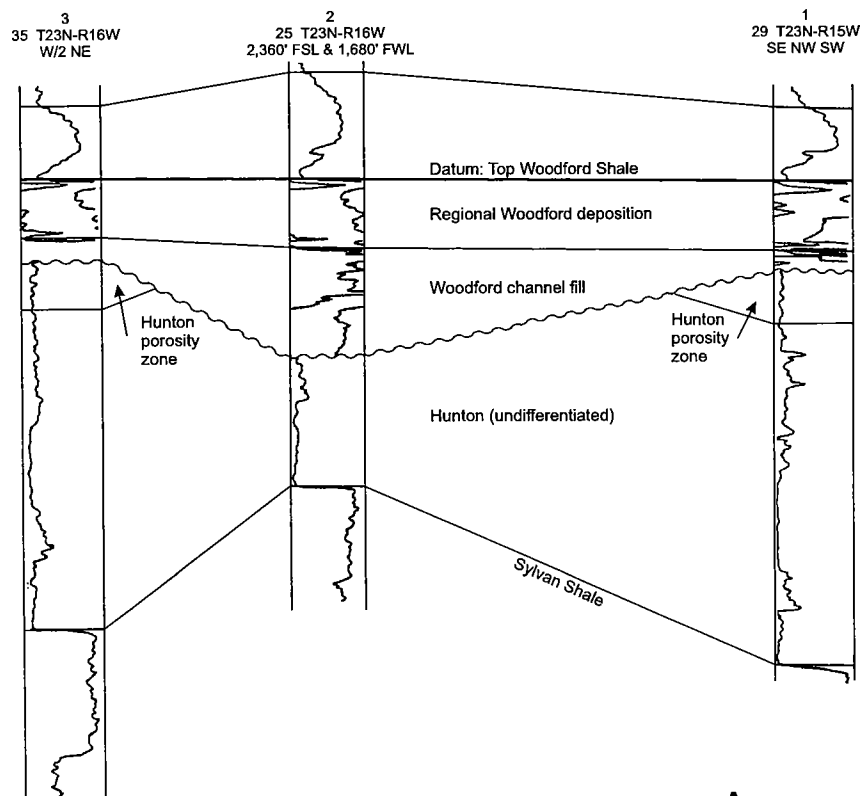


Figure 66. Cross section D-D', constructed by using compacted present-day Woodford Shale thicknesses. Apparent structure is created in center well. Datum is top of Woodford Shale.

TABLE 6. – Geological/Engineering Data for Hunton Limestone, Leedey Field Study Area, Dewey County, Oklahoma

Hunton limestone	
Reservoir size (oil)	Not applicable
Reservoir size (gas)	~2,000 acres
Well spacing (gas)	640 acre
Oil–water contact	Not applicable
Gas–water contact	Unknown
Porosity	10%
Permeability	Unknown
Water saturation	~20%
Gas/oil ratio	Not applicable
Thickness (net sand) ($\phi > 8\%$)	~20 ft
Reservoir temperature	285°F
Oil gravity	Not applicable
Initial reservoir pressure	6,800 psia
Initial gas formation volume factor	0.0035
Original oil in place (volumetric)	Not applicable
Cumulative condensate	182,860 BC
Recovery efficiency (oil)	Not applicable
Cumulative gas	32.48 BCF

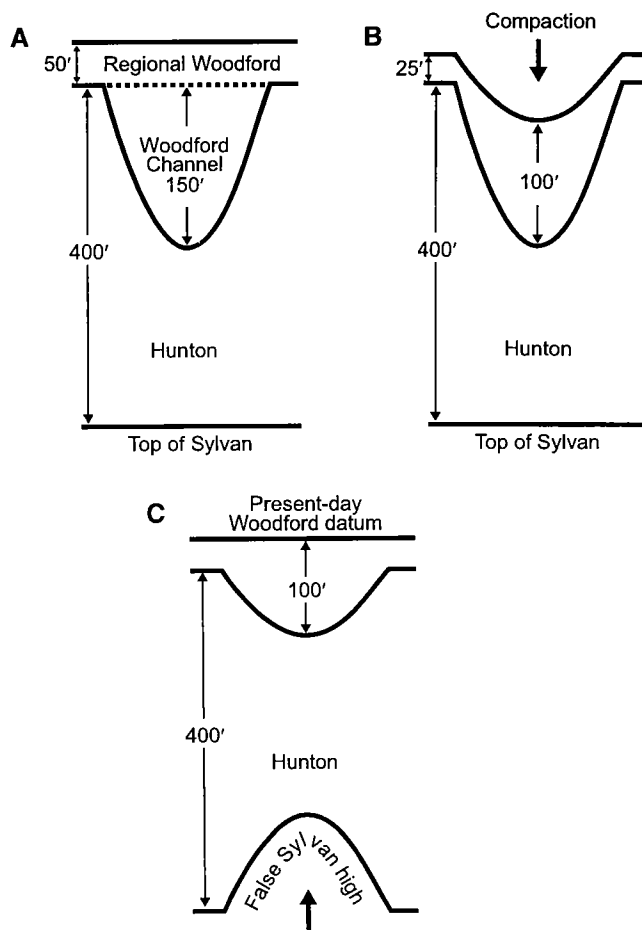


Figure 67. Schematic cross sections interpreting Woodford Shale compaction, and the pitfall of using a compacted Woodford section when considering the present-day Woodford surface as a stratigraphic datum (C). From Rottmann (2000, fig. 6).

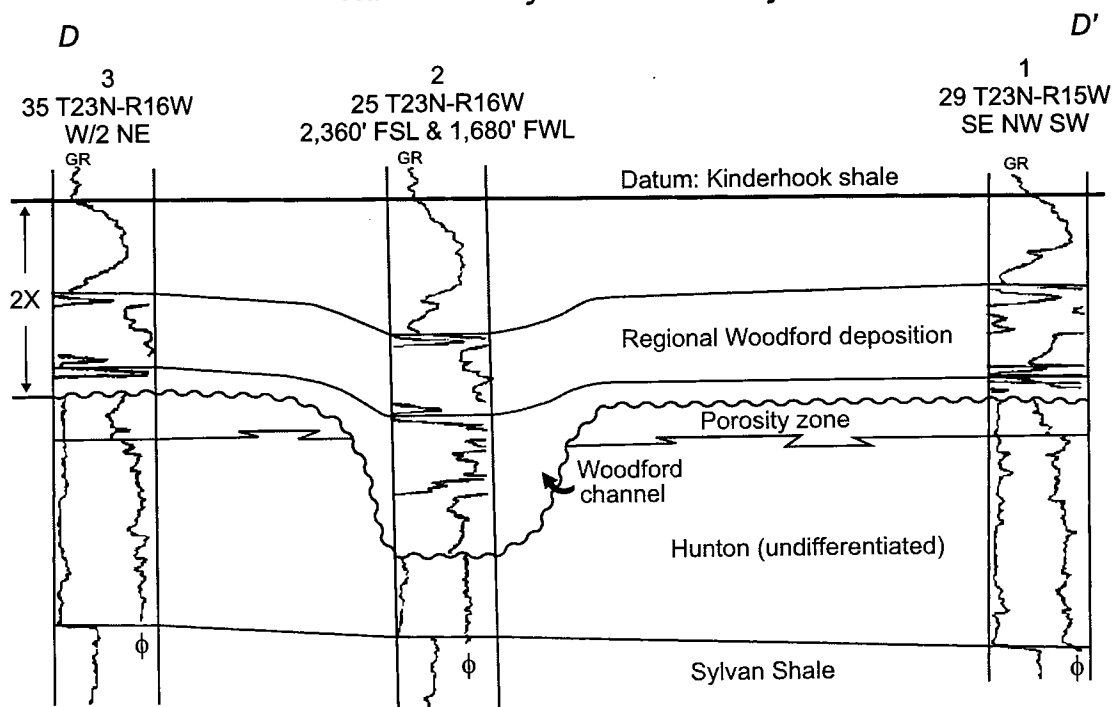


Figure 68. Revised cross section D-D', constructed by using restored Woodford Shale thicknesses. The Woodford Shale and Kinderhook shale have been doubled in thickness to account for compaction. From Rottmann (2000, fig. 8).

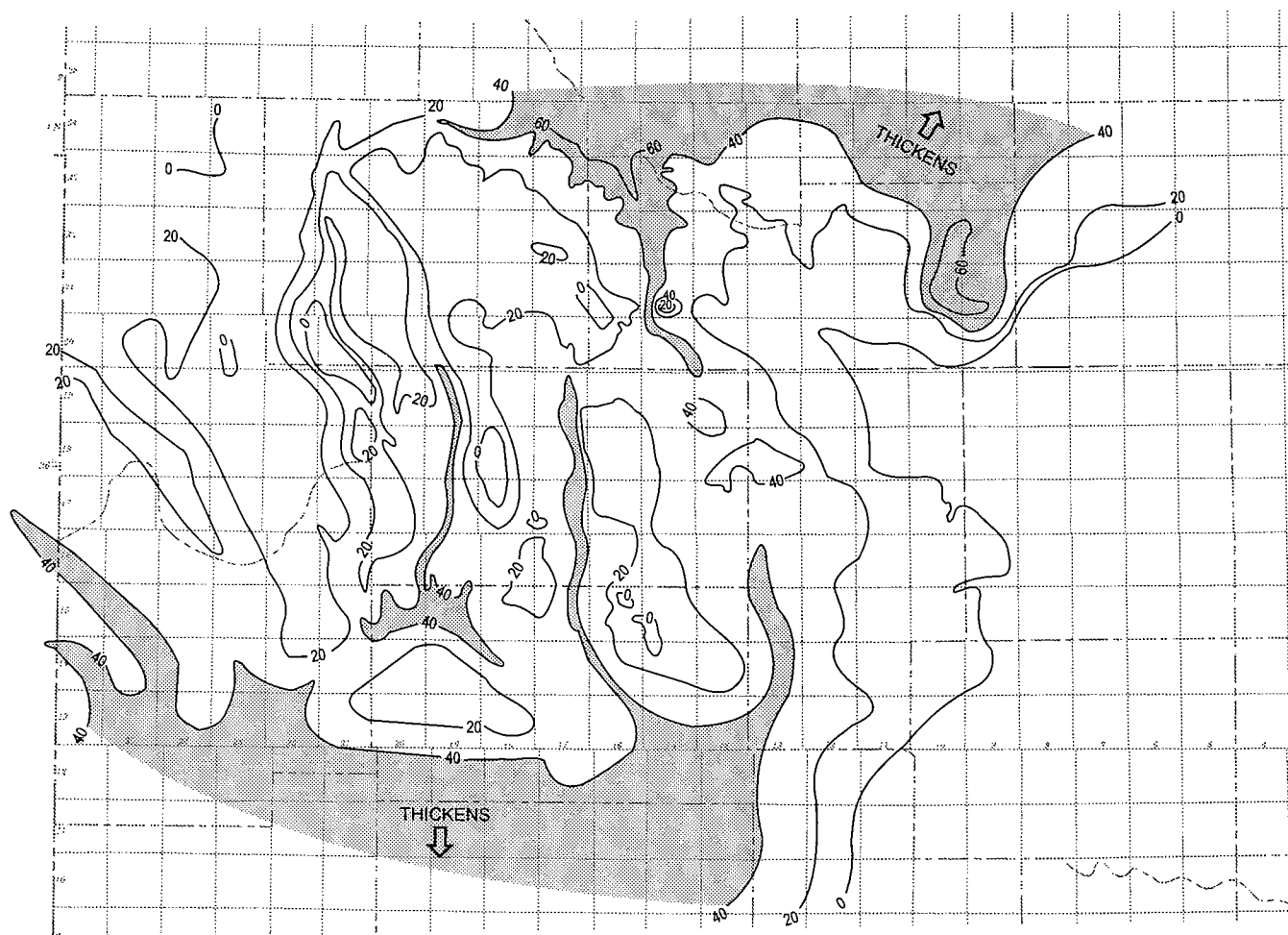
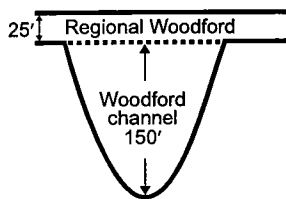
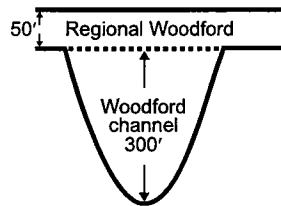


Figure 69. Isopach map of Kinderhook shale in area of Ts. 10-24 N., Rs. 5-26 W., Oklahoma. Contour interval is 20 ft.

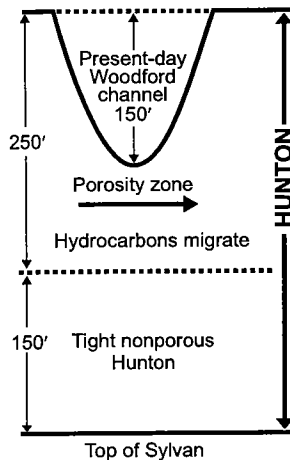
A1



B1



A2



B2

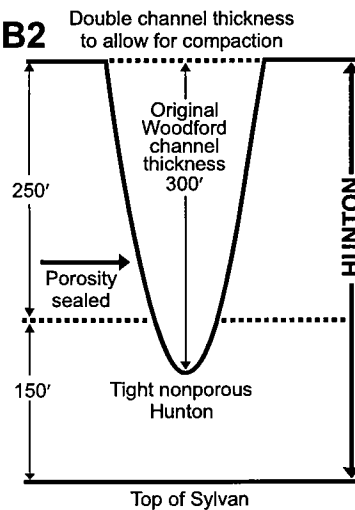


Figure 70. Schematic cross sections, illustrating incorrect method of using present-day Woodford Shale thicknesses (A1 and A2), and correct method of using restored Woodford Shale thicknesses (B1 and B2), when exploring for Hunton Group porosity seals from Woodford Shale channel deposits. From Rottmann (2000, fig. 16).

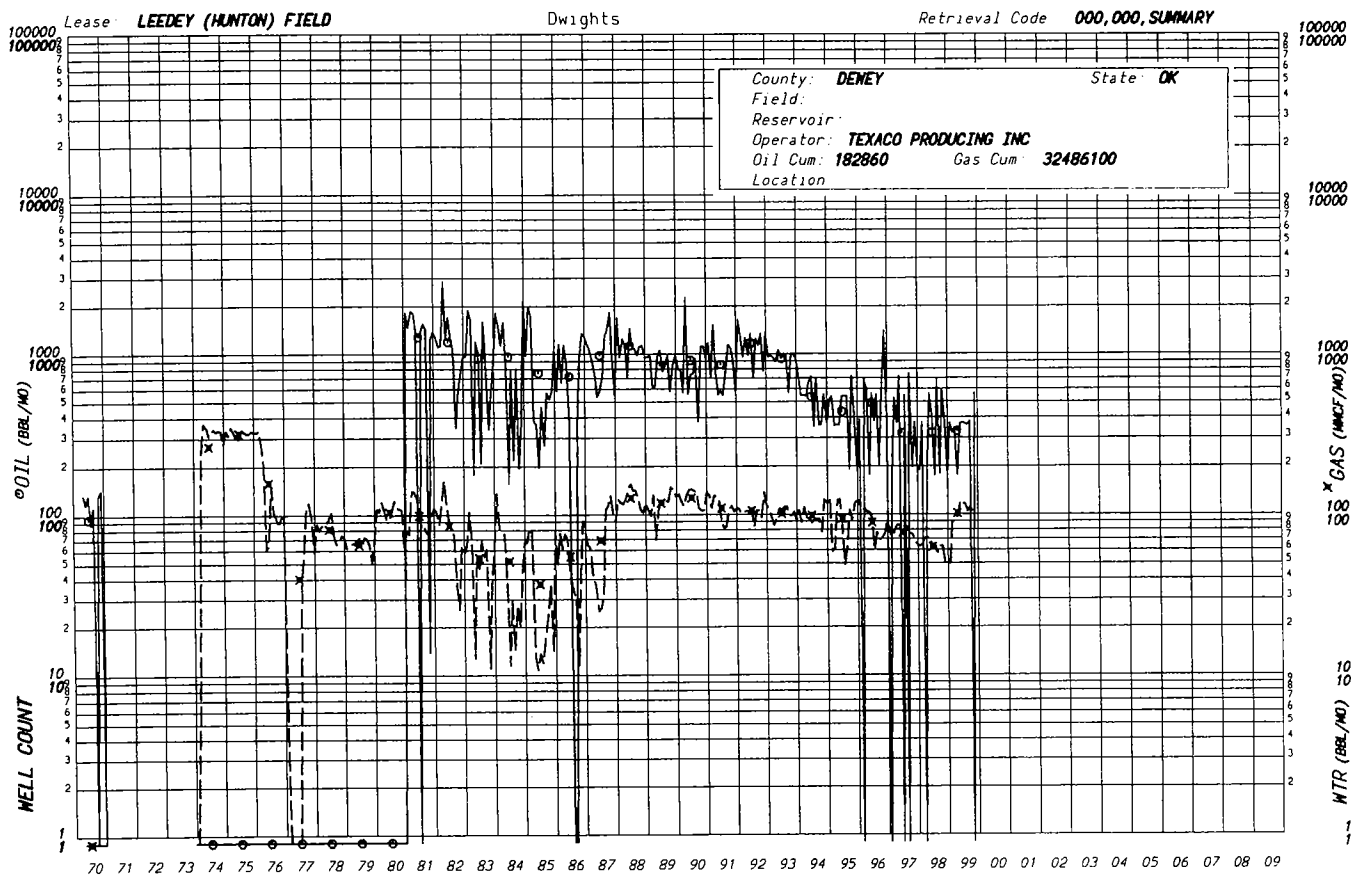


Figure 71. Graph showing gas-production curve for Leedey field Hunton study area.

PART VII

East Arnett Field Hunton Reservoir Study (T. 20 N., R. 23 W., Ellis County, Oklahoma)

Kurt Rottmann

INTRODUCTION

The East Arnett Hunton field is in central eastern Ellis County, Oklahoma. The field was discovered in 1965 by the Pan American Petroleum No. 1 Boyd Unit, in the SW¼NE¼ sec. 32, T. 20 N., R. 23 W., with an initial flowing potential from the Hunton of 7.1 MMCFGPD.

The field was expanded to include four additional wells in 12 years. Figure 72 is a generalized location map of the East Arnett Hunton field study area. Three lines of stratigraphic cross sections—E-E' (Fig. 73), F-F' (Fig. 74, in envelope), and G-G' (Fig. 75, in envelope)—are shown, as well as the type log and discovery well (the same well) for the field.

The field is in the Anadarko basin, underlying typically overpressured Atoka, Morrow, and Springer deposits. However, in the vicinity of this field study, the high-pressure zones can be drilled through without blow-out or lost-circulation problems, as their pressures are lower and approach pressures typical of a normal vertical pressure gradient. Information from many of the well-completion cards, supplied by Petroleum Information, indicate only an initial surface casing and a final completion casing for many of the Hunton penetrations or producers.

Production from this field primarily is from the Silurian sequence of the Hunton Group. This is a sequence, locally, of dolomitic limestones and dolomites underlying the Devonian–Mississippian Woodford Shale and overlying the Ordovician Sylvan Shale. However, in the area of this field study the Sylvan has changed laterally from calcareous shale to heavily dolomitized shale and argillaceous dolomite, grading toward the overlying and underlying cherty carbonates. This gradational lithologic character suggests that the sequence from Viola to Sylvan to Hunton may have undergone continuous

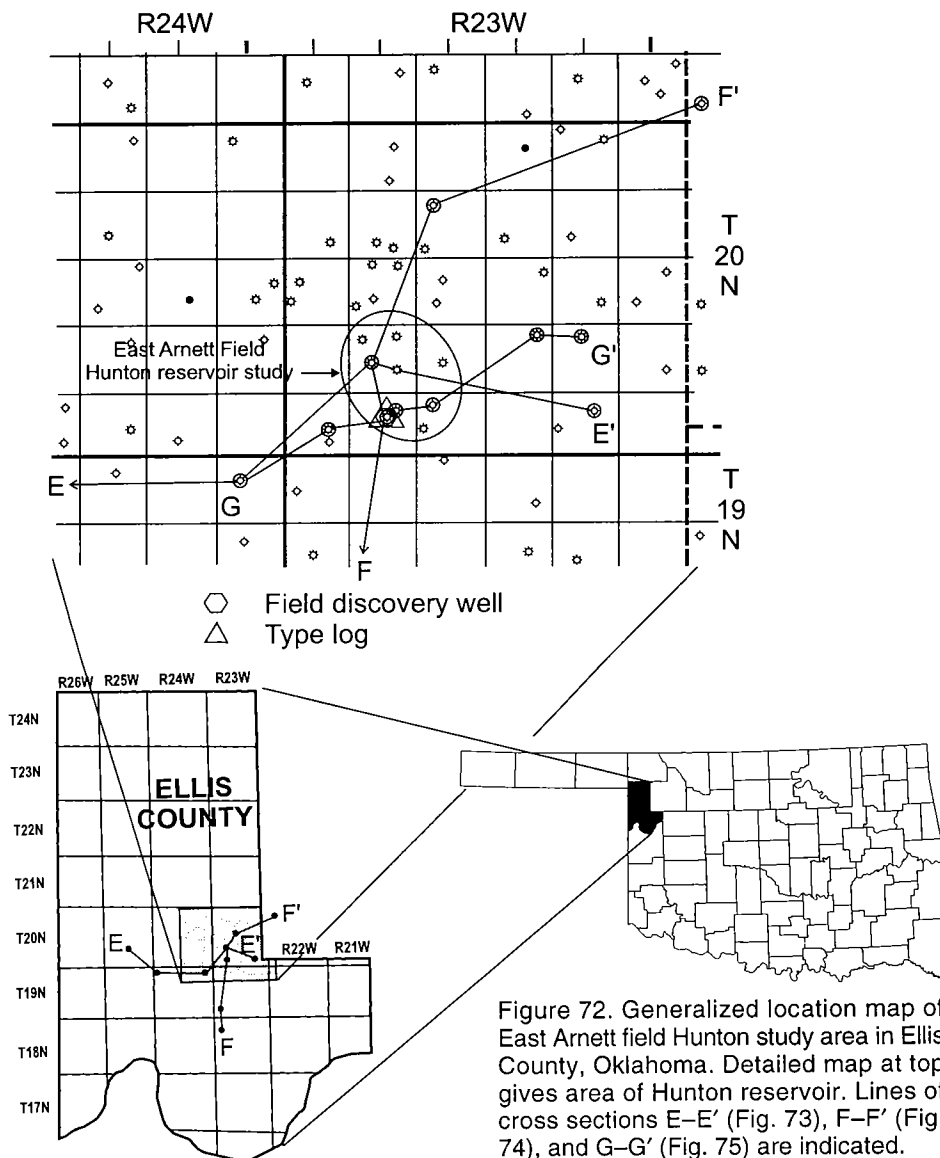


Figure 72. Generalized location map of East Arnett field Hunton study area in Ellis County, Oklahoma. Detailed map at top gives area of Hunton reservoir. Lines of cross sections E-E' (Fig. 73), F-F' (Fig. 74), and G-G' (Fig. 75) are indicated.

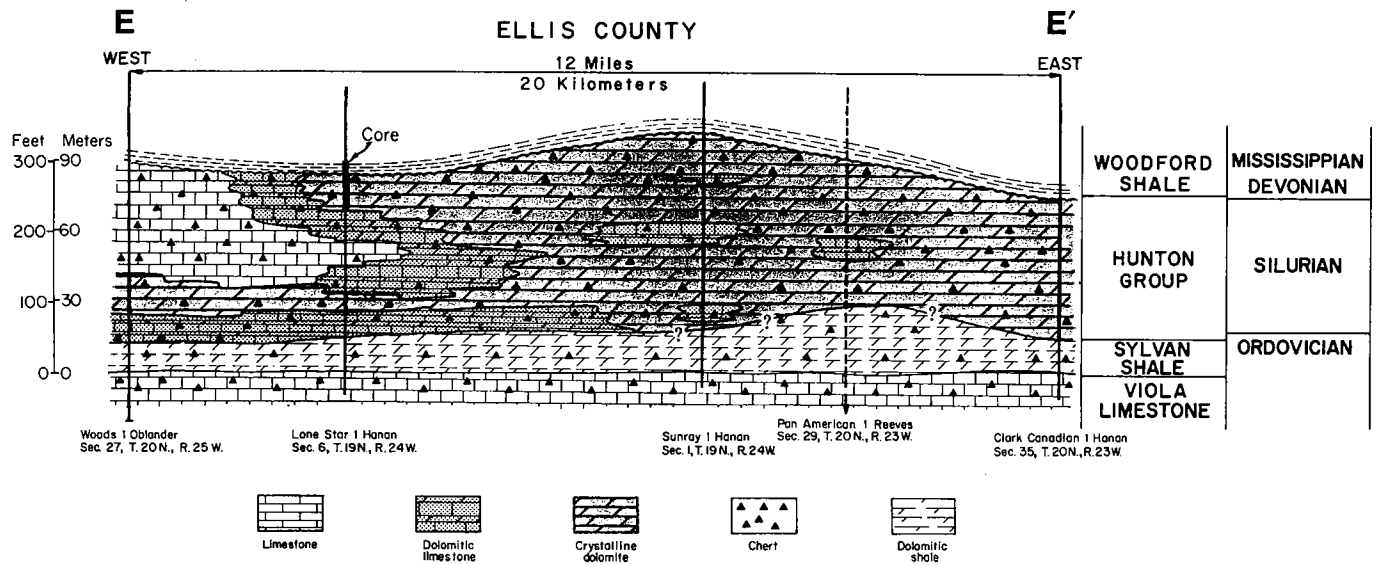


Figure 73. Stratigraphic cross section E-E', showing inferred relationships of Viola-Sylvan-Hunton-Woodford strata. Datum is base of Sylvan Shale. Interpretation of strata based mainly on thin-section and core analysis by Amsden. Line of section shown in Figure 72. Modified from Amsden (1980, p. 42).

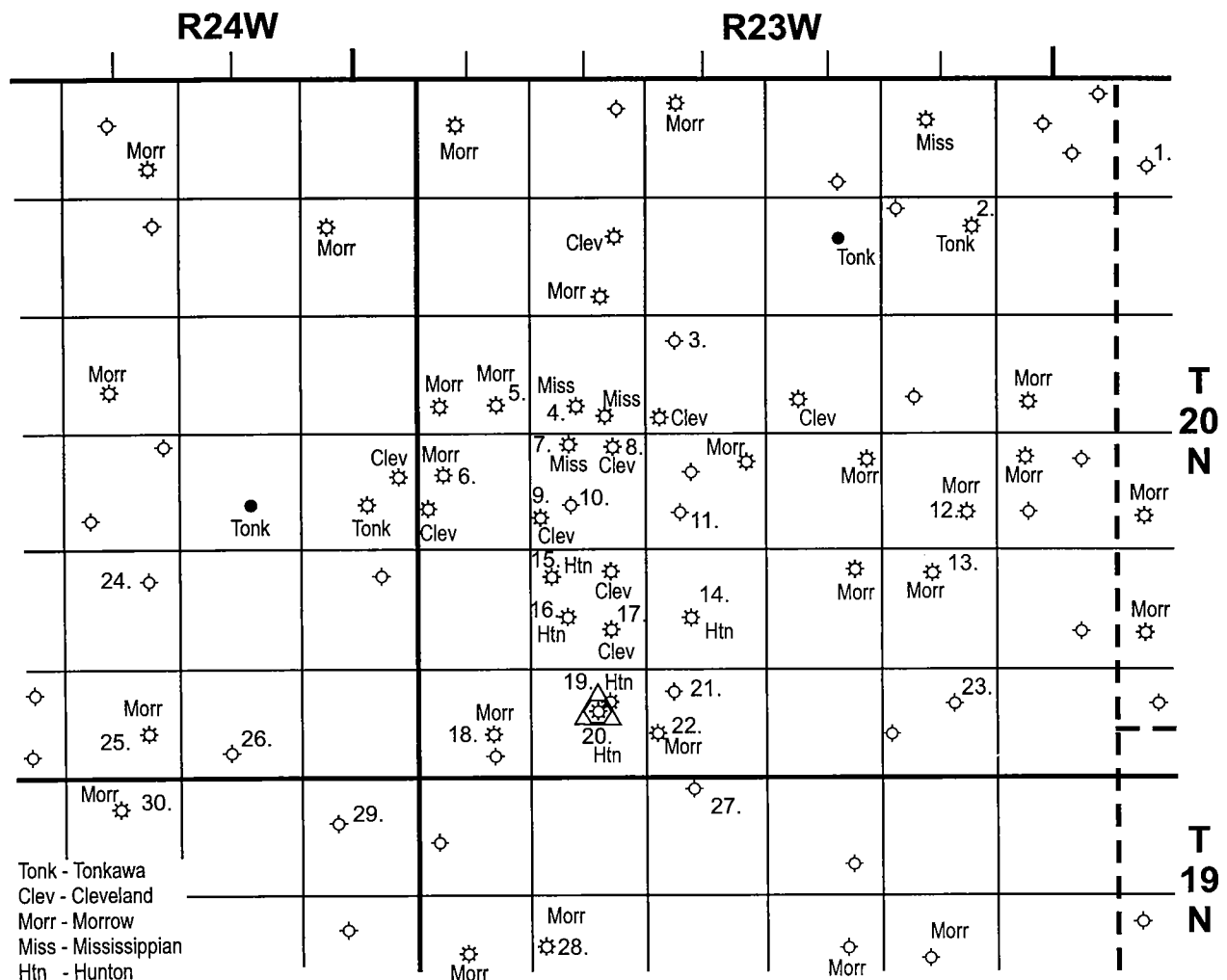


Figure 76. Well-information map showing producing reservoir(s) for wells in East Arnett Hunton field study area. Numbers by wells refer to listing in Table 7, which gives locations, operators, well numbers, and lease names.

TABLE 7. — Well Tabulation Keyed to Figure 76, Showing Well Locations, Operators, and Lease Names for East Arnett Field, Ellis County, Oklahoma

Map no.	Location	Legal	Operator	Lease
1	sec. 6, T. 20 N., R. 22 W.	C SW¼	Anadarko Land & Exploration	#1-6 Hamilton
2	sec. 11, T. 20 N., R. 23 W.	NE¼	Citation Oil and Gas Co.	#1-11 Hamilton
3	sec. 16, T. 20 N., R. 23 W.	C NW¼	Argonaut Energy Corp.	#1 State
4	sec. 17, T. 20 N., R. 23 W.	SW¼NE¼SE¼SW¼	Petro Energy Exploration	#1-17 Josephine
5	sec. 18, T. 20 N., R. 23 W.	C SE¼	Hanover Management Co.	#1-18 Guy
6	sec. 19, T. 20 N., R. 23 W.	S½NW¼	C. F. Braun Co.	#1-19 Guy
7	sec. 20, T. 20 N., R. 23 W.	660 ft FNL & 1,980 ft FWL	NO-EN-CO	#1-20 Peters
8	sec. 20, T. 20 N., R. 23 W.	N½NE¼	Woods Petroleum Corp.	#20-1 Griffith
9	sec. 20, T. 20 N., R. 23 W.	W½SW¼	Hanover Management Co.	#1 Sober
10	sec. 20, T. 20 N., R. 23 W.	1,920 ft FSL & 1,920 ft FWL	Samadan and Wolfe	#1 Sober
11	sec. 21, T. 20 N., R. 23 W.	SW¼NE¼SW¼	GHK Oil Co.	#1-21 Thompson
12	sec. 23, T. 20 N., R. 23 W.	S½S½N½SE¼	C. F. Braun Co.	#1 Lowery
13	sec. 26, T. 20 N., R. 23 W.	100 ft E of C N½	ESCO	#1-26 Hanan
14	sec. 28, T. 20 N., R. 23 W.	NE¼SW¼	Pan American Petroleum	#B-1 Thompson
15	sec. 29, T. 20 N., R. 23 W.	C NW¼	Hanover Management Co.	#1 Taylor
16	sec. 29, T. 20 N., R. 23 W.	NE¼SW¼	Pan American Petroleum	#1 Reeves
17	sec. 29, T. 20 N., R. 23 W.	C SE¼	Jones and Pellow Oil Co.	#1-29 Reeves
18	sec. 31, T. 20 N., R. 23 W.	1,370 ft FEL & 1,980 ft FSL	Magness Petroleum Co.	#1-11 Hanan
19	sec. 32, T. 20 N., R. 23 W.	NE¼SW¼NE¼	Amoco Production Co.	#2 Boyd Unit
20	sec. 32, T. 20 N., R. 23 W.	SW¼NE¼	Jennings Petroleum Co.	#1 A. H. Boyd
21	sec. 33, T. 20 N., R. 23 W.	C NW¼	Cleary Petroleum Corp.	#1-33 State
22	sec. 33, T. 20 N., R. 23 W.	NW¼SW¼	Ricks Petroleum Corp.	#33-2 Cherokee Strip
23	sec. 35, T. 20 N., R. 23 W.	SW¼NE¼	Clark Canadian Exploration	#1 Hanan
24	sec. 27, T. 20 N., R. 24 W.	NE¼	Woods Petroleum Corp.	#1 Roper
25	sec. 34, T. 20 N., R. 24 W.	N½N½SE¼	Southport Exploration	#1-34 H. D. Shields
26	sec. 35, T. 20 N., R. 24 W.	E½E½E½SW¼	Southport Exploration	#1 Mann
27	sec. 4, T. 19 N., R. 23 W.	NE¼NE¼NW¼	Ricks Petroleum Corp.	#4-A Eddie Max
28	sec. 8, T. 19 N., R. 23 W.	SW¼SW¼NW¼	Brigham Oil and Gas	#8-1 Paige
29	sec. 1, T. 19 N., R. 24 W.	SE¼NW¼	Sunray Oil Corp.	#1 Hanan
30	sec. 3, T. 19 N., R. 24 W.	W½W½W½NE¼	Southport Exploration	#1 Rollin

deposition and that the area of the field study may have been beyond the depositional limit of terrigenous material prevalent in Sylvan deposits to the east and south.

This field study was selected as an example of a structurally controlled reservoir in the deeper part of the Anadarko basin. The type of structure controlling closure for this reservoir is one of several similar ones in western Oklahoma that also affect or influence production from other formations. The goal of this field study is to examine the structural influences that occurred during Hunton deposition and to understand the nature of residual or recurrent structural movement during Paleozoic time. Figure 76 is a well-information map showing producing formations, and is a

key for Table 7, which is a listing of well locations, operators, lease names, and well numbers in the East Arnett field study area.

STRATIGRAPHY

The stratigraphic section (Fig. 77) for the East Arnett Hunton field study is illustrated by the log from the Jennings Petroleum Corp. No. 1 Boyd well, in the SW¼ NE¼ sec. 32, T. 20 N., R. 23 W., Ellis County, Oklahoma. The Hunton is generally a carbonate sequence sandwiched between the Ordovician Sylvan Shale and the Devonian–Mississippian Woodford Shale. However, as mentioned previously, the shales of the Sylvan have graded laterally to argillaceous limestone and dolomitic

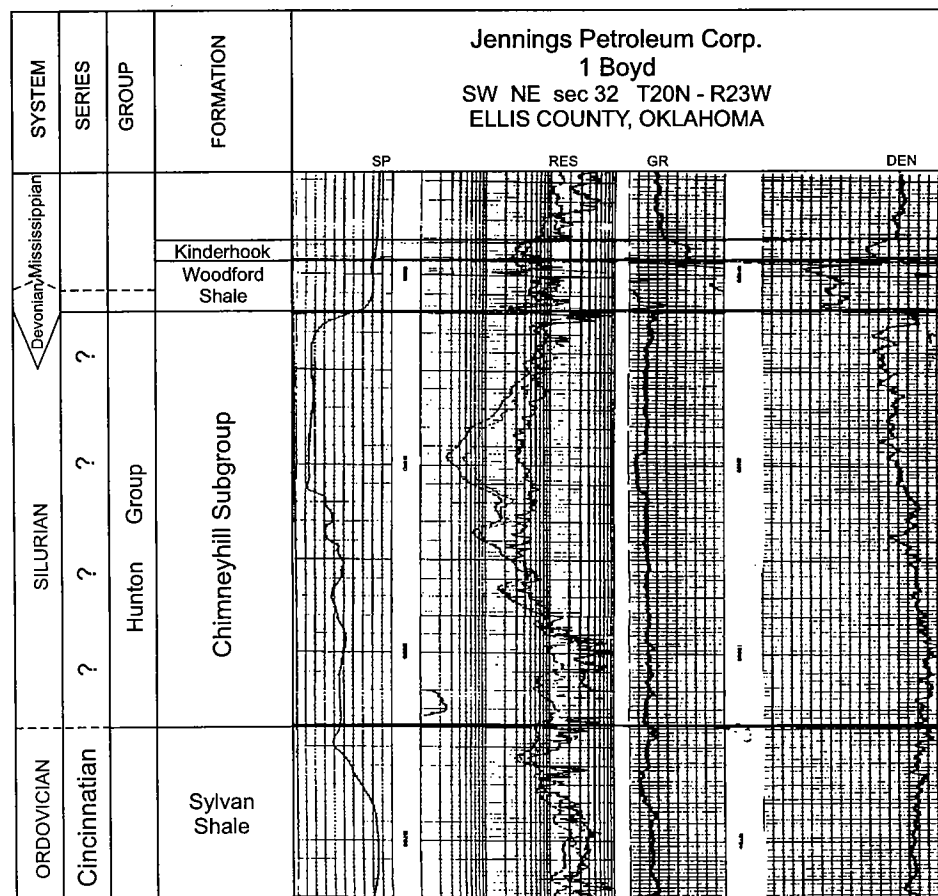


Figure 77. Type log for East Arnett field, showing Hunton section and characteristic geophysical-log signatures. Dashed lines indicate uncertain but probable stratigraphic identification. *SP* = spontaneous potential; *RES* = resistivity; *GR* = gamma ray; *DEN* = density.

shale in the vicinity of this field study. This presence of carbonate strata from Viola through basal Hunton may indicate continuous deposition. The lack of sufficient detrital materials to form true shales may have been the result of this area's location far from the source of these materials. Amsden (1980, p. 43) points out that thin-section studies from both core and well samples easily determine the Viola–Sylvan and Sylvan–Hunton boundaries. As shown in the type log (Fig. 77), the entire Hunton section is composed of Silurian strata. Five wells in the vicinity of this field study were described by Amsden and offer some lithostratigraphic and biostratigraphic control. These wells are identified by number on Plate 6 as follows: (1) no. 104, Clark Canadian Exploration Co. No. 1 Hanan; (2) no. 105, Sunray Oil Corp. No. 1 Ralph Hanan; (3) no. 107, Lone Star Producing Co. No. 1 V. Hanan Unit; (4) no. 186, Woods Petroleum Corp. No. 1 Oblander; and (5) no. 207, Pan American Petroleum Corp. No. 1 Reeves Unit.

Amsden (1980) published a schematic cross section that illustrates the lithology of the Hunton Group in the East Arnett field study area (Fig. 73). The line of this section is shown in Figure 72. The strata in and around the study area are composed primarily of crystalline dolomite. To the west, the dolomite grades into a cherty limestone in the upper half of the Hunton section of the Oblander well (see Fig. 72). Amsden considers this a lateral gradation. The significance of this gra-

dation is discussed in greater detail in the Prairie Gem field study. The Cochrane Formation of the Chimneyhill Subgroup is noted for chert deposits, but Amsden does not address the chert as being an indicator of a lithostratigraphic unit in these wells.

In the type log (Fig. 77), the Hunton section is attributed to the Chimneyhill Subgroup, with no further distinctions being made. The contact between the Ordovician and the Silurian is shown as a dashed line on the type log. No biostratigraphic or lithostratigraphic evidence supports the presence of the Ordovician Keel Formation. If this formation were present, this systematic boundary would need to be adjusted accordingly. Previously in this text, I made reference to the case for correlating the Clarita Formation and the marlstones of the Henryhouse. It was mentioned that in the western part of the Anadarko basin these correlations become indistinct and subjective. This is true for the Hunton strata in this study area.

Overlying the Hunton Group is the Late Devonian–Early Mississippian Woodford Shale. This shale in the study area is generally a persistent and uniformly thin shale ranging from 5 to 30 ft in thickness. The Woodford is composed predominantly of regional Woodford deposits as described in the study of the Leedey Hunton field. Overlying the Woodford Shale is the Mississippian Kinderhook shale. This shale probably represents a transition from the organic shales of the Wood-

ford to the arenaceous limestones of the Meramec, which overlie the Kinderhook shale.

Cross section F-F' (Fig. 74) is a south-north stratigraphic section. The datum for the section is the top of the Woodford Shale. In the previous study of the Leedey field, the importance of reconstructing Woodford thicknesses was stressed when interpreting Woodford-Hunton stratigraphic relationships at the time of deposition. This cross section does not employ that principle for this reason. Wells 1 through 4 illustrate a Woodford Shale thickness that is essentially uniform. Compacting strata of equal thickness results in equal thickness. Therefore, in those areas devoid of significant differences in Woodford Shale thickness, reconstructing the thickness to original conditions is an unnecessary step. The Woodford in wells 5 and 6 is thicker and does contain 30 ft of lower Woodford, which probably consists of channel-fill deposits. Wells 4 and 5 are 6.5 mi apart, and this cross section is not meant to

show accurate Woodford-Hunton stratigraphic relationships.

Cross section F-F' (Fig. 74) also illustrates the regional south-north truncation of the Hunton. This gradual truncation is readily apparent from the Hunton isopachs of Plate 1. I have observed that many of the Hunton wells in western Oklahoma contain a fractured or porous zone approximately 150 ft above the Sylvan Shale. This zone is shown on this cross section. Many of the wells whose thickness is less than 150 ft are generally tight. Although Amsden points out that dissolution is prominent on the pre-Woodford erosional surface, I have observed from geophysical-log interpretation that many wells in this vicinity have little indication of porosity at the top of the Hunton.

ISOPACH MAPPING

Figure 78 is a gross-isopach map of the Hunton Group in the East Arnett Hunton field study area. The

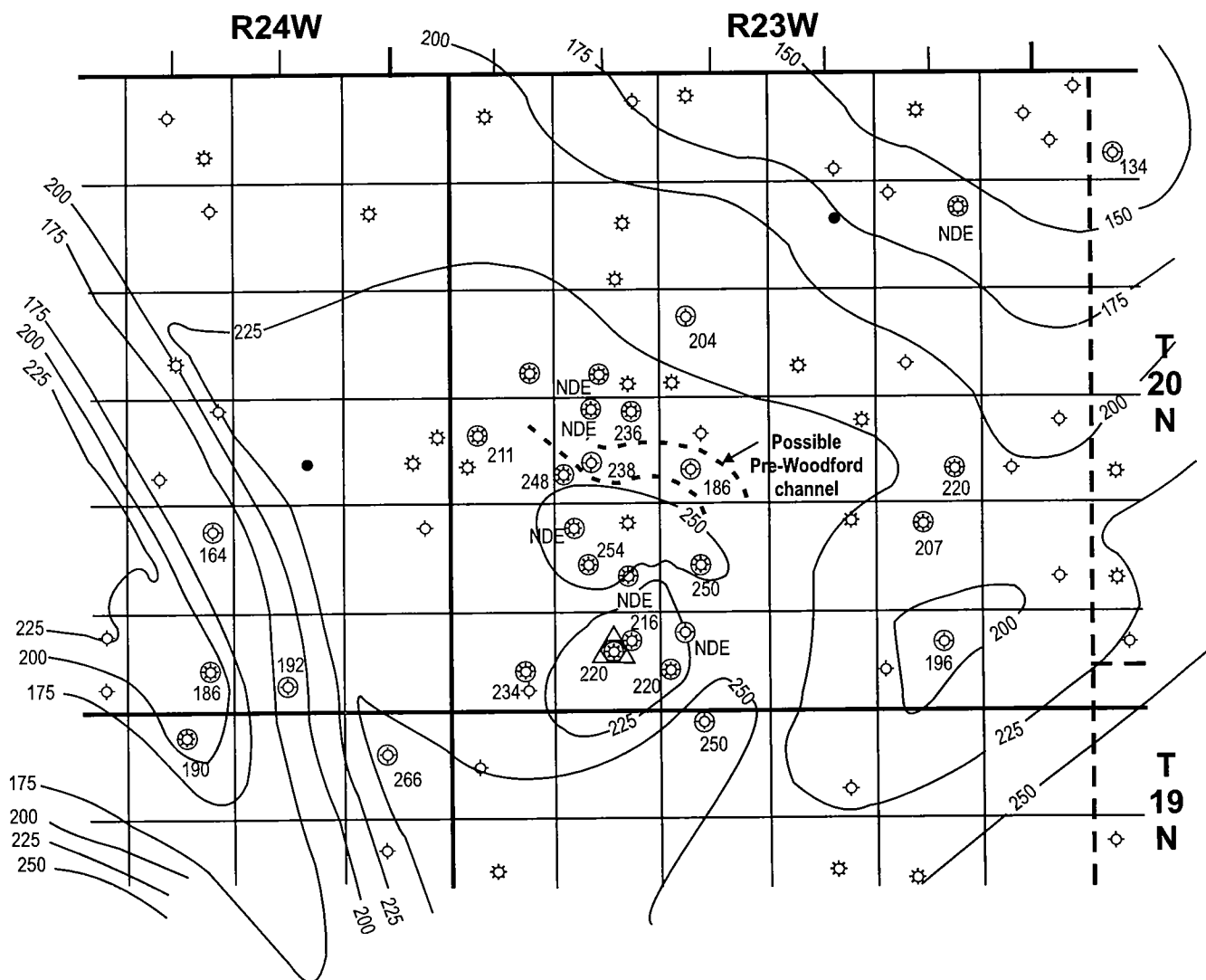


Figure 78. Gross-isopach map of Hunton Group in East Arnett field study area. Contour interval is 25 ft.

Hunton isopach ranges in thickness from 150 ft in the northeast corner of the study area to 250 ft in the south part. The Hunton isopach on the west side of the study area indicates a channel geometry. Examination of the wells in secs. 22 and 34, T. 20 N., R. 24 W., confirms a lower Woodford facies consistent with Woodford channel-fill deposits. The technique for incorporating Woodford channel geometry into the gross Hunton isopach, as explained in the Leedey field study, was incorporated when this isopach map was created. However, owing to space constraints, these maps were not incorporated. In the East Arnett field, two isopach "thins" are apparent. The first is centered about sec. 20, T. 20 N., R. 23 W., and the second is centered about sec. 32, T. 20 N., R. 23 W. A third "thin" is centered about sec. 35, T. 20 N., R. 23 W.

Figure 79 is an isopach map of the Woodford Shale in the study area. Here, the Woodford is uniformly thin, ranging from 15 to 30 ft thick, and is areally persistent.

The Woodford channel, mentioned previously, is clearly apparent from this isopach map.

Figure 80 is a net-porosity map for the Hunton Group in the study area. As mentioned previously, Hunton porosity seems to be confined to those strata at least 150 ft above the base of the Hunton. This is not a hard and fast rule, but it is consistent enough to warrant mentioning. The Hunton control for deriving the porosity map is sparse, and increased control could markedly alter the interpretation.

Figure 80 suggests two primary areas of porosity development. The first, and larger of the two, is an elongate pod in secs. 16, 17, 20, 21, 28, 29, 31, 32, and 33, T. 20 N., R. 23 W. The porosity thicknesses in this trend range from 20 to 80 ft.

Determining the porosity from available porosity logs was difficult. Many zones appeared washed out, which is a possible indication of fracturing, and these zones were included in the isopachs (Fig. 80). Another

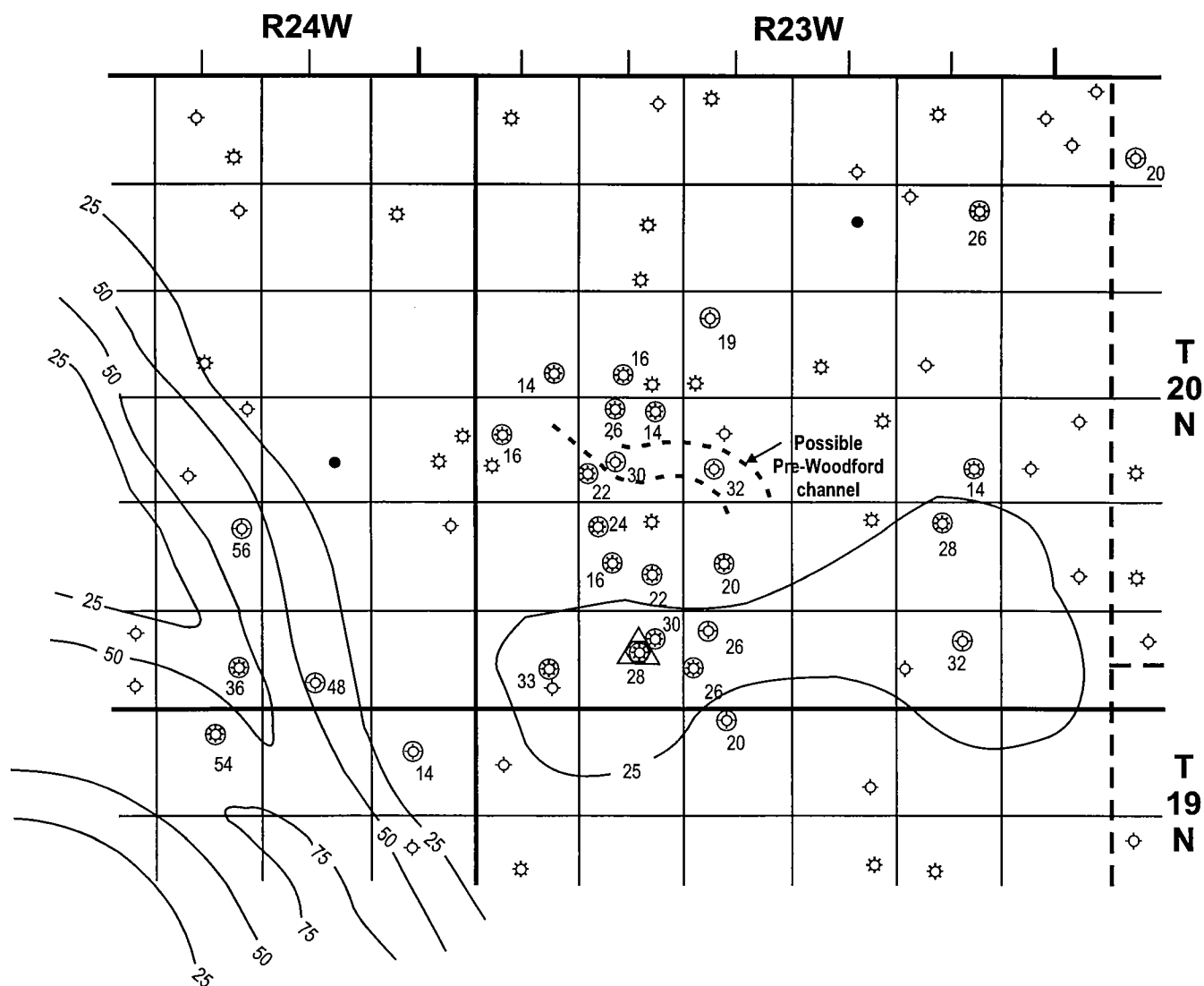


Figure 79. Isopach map of Woodford Shale in East Arnett field study area. Contour interval is 25 ft.

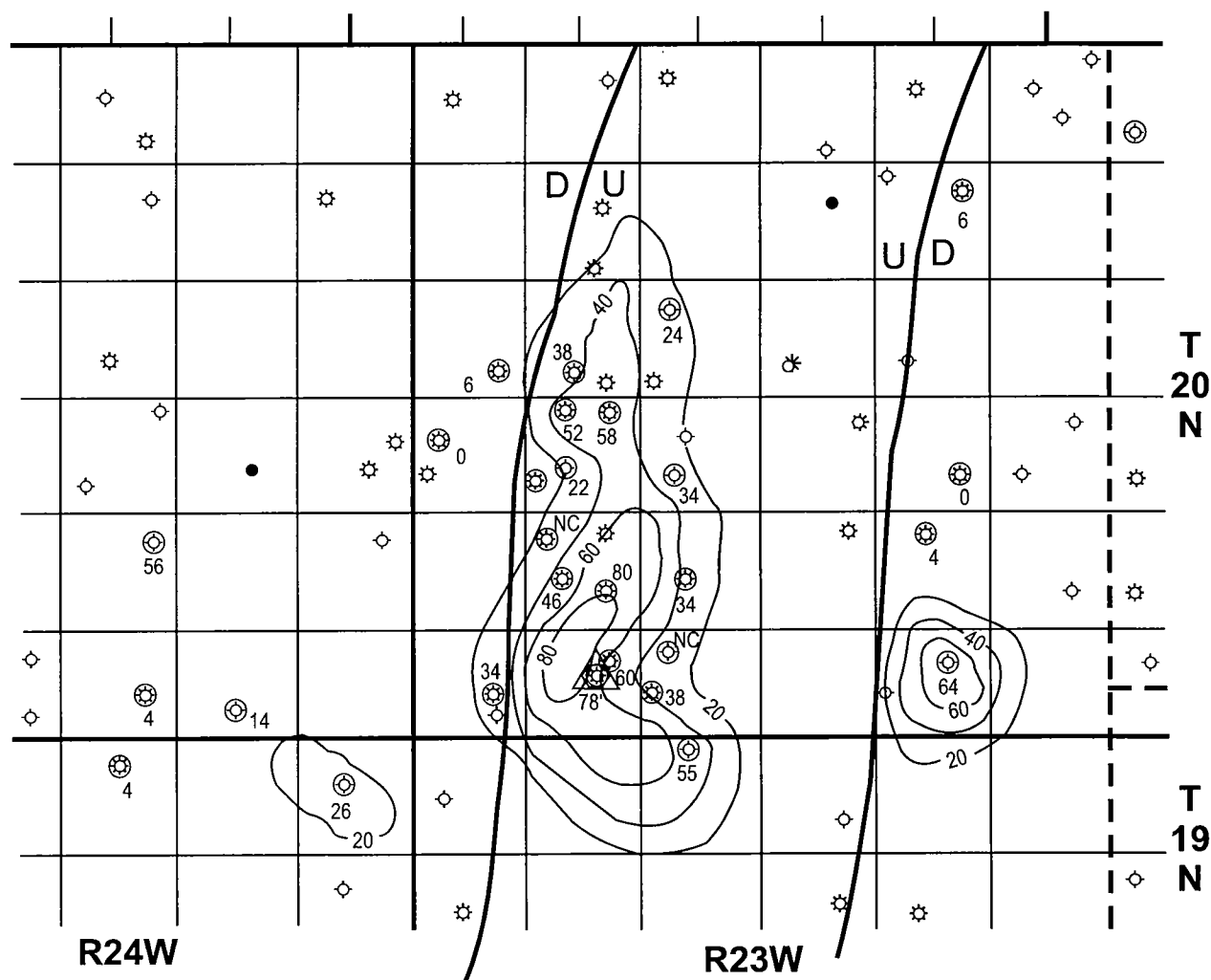


Figure 80. Isopach map of net porosity in East Arnett field study area. Contour interval is 20 ft; contours represent thickness, in feet, of porous strata.

problem for determining a porous layer was interpreting the matrix density of the layer. Most of the density-porosity logs are calibrated on a limestone-matrix density of 2.71. Any dolomite or dolomitic zones would appear to be below the porosity cutoff and thus would appear as negative porosity. Without a core to accurately determine the matrix density of the section, it is up to the geologist to estimate the type of strata and adjust porosity scales accordingly.

Of primary interest is the location of the thickest porosity zone in relation to the Hunton gross-isopach "thins" in Figure 79. These porosity zones are congruent with the "thins," an indication that post-Hunton erosion may have selectively eroded the Hunton in these areas, modifying the porosity and/or permeability in the process. Figure 80 also shows two faults, which are discussed in the next section.

STRUCTURE

Figure 81 is a structure-contour map of the East Arnett field study area, depicting the top of the Hunton Group. This map suggests a current east-west strike in

this part of the basin, with dip to the south at approximately 200 ft per mi. The contours suggest a regional homocline, except for a 3-mi-wide, north-south horst block. The throw on the west side is about 300 ft, and on the east side about 100 ft, suggesting that the horst block may be tilted. A structural closure is present in sec. 32, T. 20 N., R. 23 W. This apparent closure has approximately 150 ft of relief. The closure is the primary controlling factor for the productive reservoir in sec. 32. The Hunton also produces in other sections, including secs. 20 and 29. The 200-ft contour interval may mask smaller closures.

The two faults defining the horst block are shown on the porosity isopach map of Figure 80. It is possible that displacement of the west block fractured the Hunton adjacent to or near the fault to enhance the porosity and permeability of the wells in the first pod of porosity that was mentioned.

Examination of the Hunton structure map of Plate 3 reveals a more extensive presence of the horst block from Figure 81. A second horst block is also present to the west, along the Oklahoma-Texas border. These

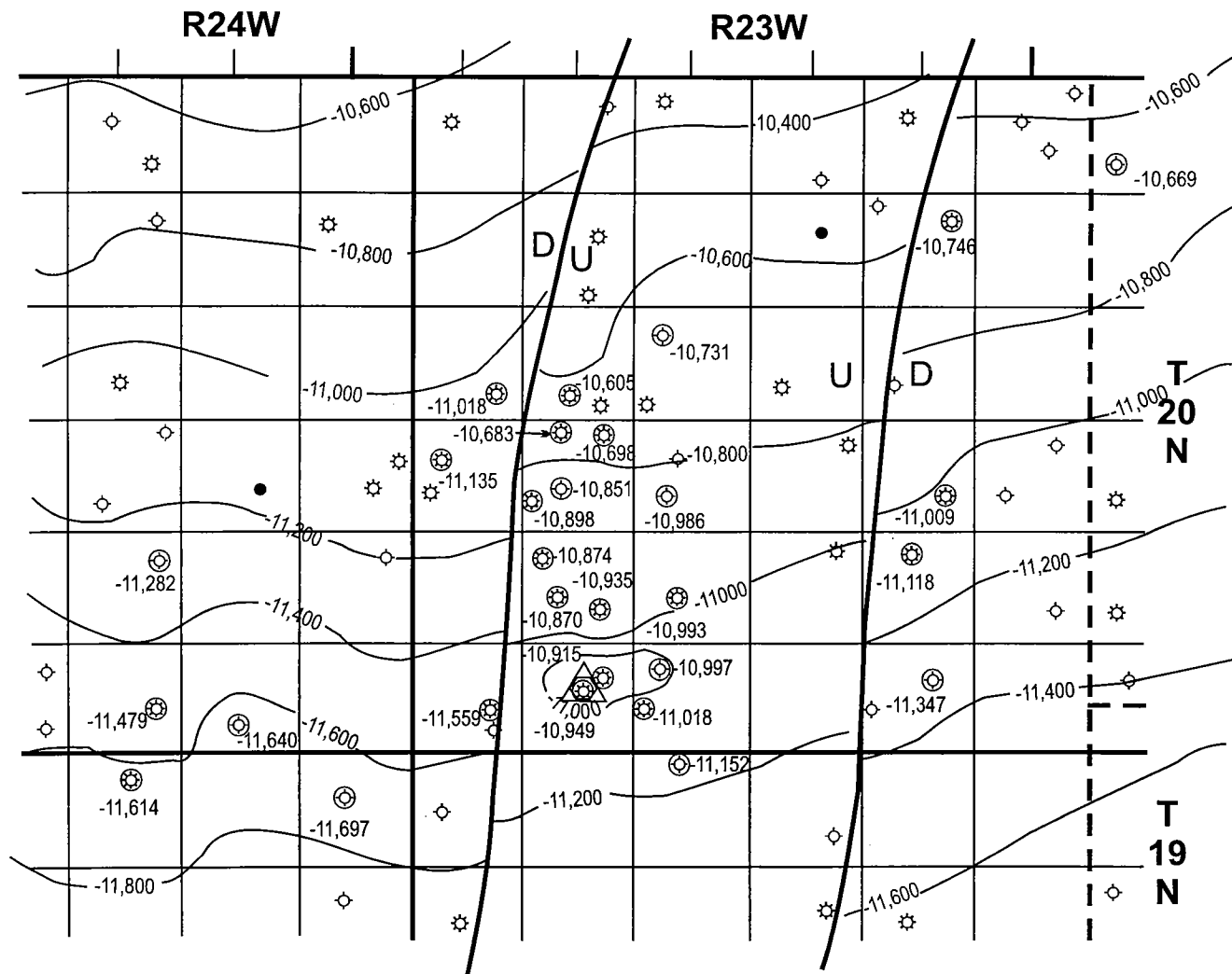


Figure 81. Structure-contour map of top of Hunton Group in East Arnett field study area. Contour interval is 200 ft.

basement-controlled features are prevalent at the top of the Hunton horizon. In 1964, Schramm spoke of observing depositional-thickness irregularities from Simpson (Middle Ordovician) isopach maps that resulted in the identification of Simpson tectonic features in central and western Oklahoma. These tectonic features were positive regional trends that influenced overlying deposits. It appears from a map in Schramm's 1964 publication that several of these features may be congruent with those suggested on the Hunton structure map of Plate 3, although it might be noted that the scale of Schramm's map is small and that it is not possible to accurately locate those features he mentioned.

It is my experience that prominent structural features commonly exhibit multiple periods of activity or movement. I have informally coined the term *remnant structure* to define persistent movement through time of these basement-oriented active structures. The horst block illustrated in Figure 81 is no exception. Periods of structural activity manifest themselves at several horizons. Figure 82 is a well log showing the interval isopached in Figure 83. The isopached interval extends

from a zone referred to as the Chester "B" to the top of the Woodford Shale. The Chester "A" sequence shown on the log may in fact be Springeran limestone, which would be equivalent to a lateral sandstone facies in the deeper part of the Anadarko basin. The Chester "A" sequence is not a desirable unit for isopach purposes, because its contact with the overlying strata is an erosional angular unconformity, as illustrated on cross section G-G' (Fig. 75). I have chosen the Chester "B" as the upper isopach zone within the Chesterian section because it has not been affected by erosion. Three prominent south-trending noses are readily apparent in Figure 83. The noses represent a thin isopach interval. This thinning is due either to onlapping of the strata of this isopached interval onto a recurring structure or to minor uplift and erosion of strata within the isopached interval over the structure.

The isopach map of Figure 83 represents a second distinct period of structural activity, with structural movement and thinning at the Hunton horizon having been the first period (Hunton structure map, Pl. 3; Hunton isopach map, Pl. 1). Three structural features

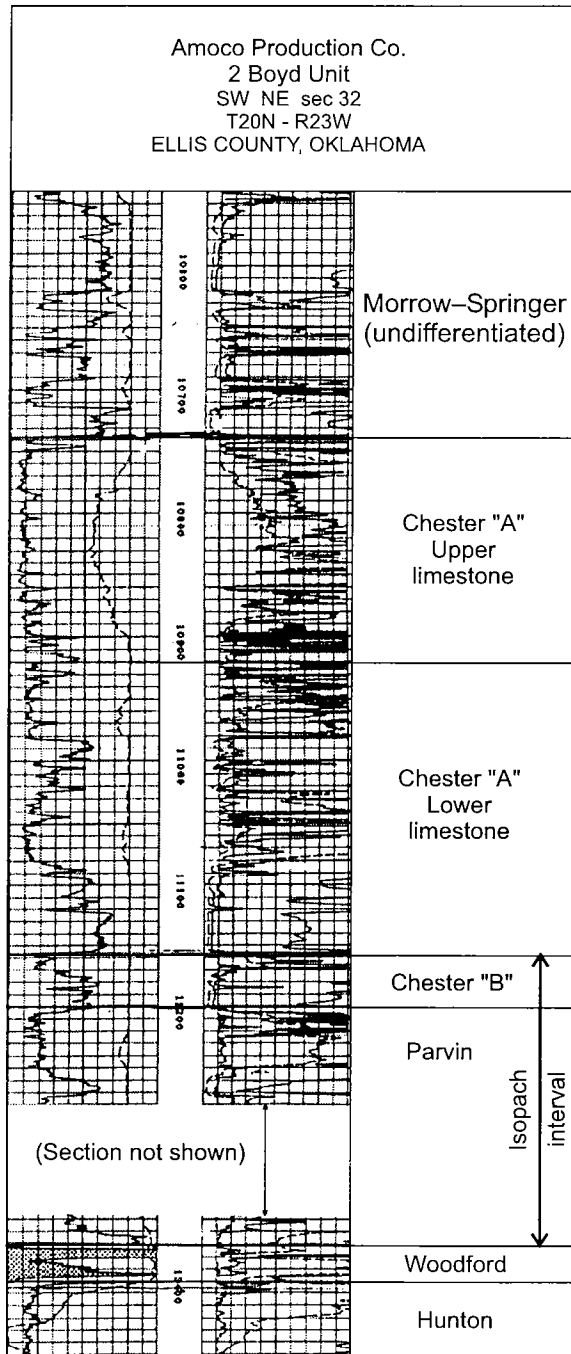


Figure 82. Type log indicating section isopached in Figure 83.

are shown in Figure 83: from west to east, they are the Ellis, Woodward, and Pratt anticlines. The Ellis and Woodward anticlines are informally named and are original to this study. The Pratt anticline is a well-recognized structural feature in south-central Kansas. Figure 84 illustrates these three features as well as other features that affected Paleozoic deposition. The Mobeetie and Sayre anticlines (Wroblewski, 1967, p. 135) and the Corn-Eakly-Fort Cobb anticline (Clement, 1988, p. 913) were previously recognized. The Ca-

nadian flexure is unique to this study and is discussed in a following section.

A third period of structural activity between the lower Morrow and the Chester "A" sections is illustrated on cross section G-G' (Fig. 75). Two intervals informally named by the author, the "Cunningham" and "White," thin dramatically in wells 4 and 5. This thinning appears to be the result of uplift and erosion rather than onlap of the two sequences. Correlation of the shale section in the "White" interval in wells 6 and 7 does not suggest onlap but erosion.

The point should be made that most of the significant accumulations of gas are associated with these structural features. These structural features are not productive at the Hunton level, but local structural anomalies along these features may contain producible hydrocarbons. Also of importance is the influence

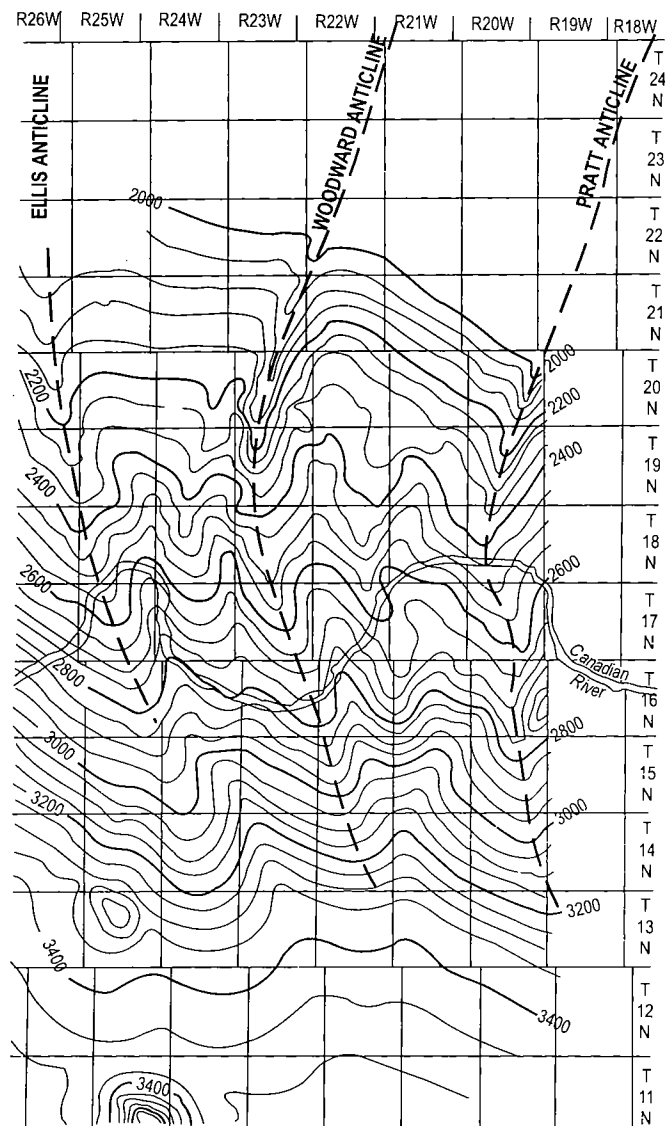


Figure 83. Isopach map of interval from top of Chester "B" zone to top of Woodford Shale. Chester "B" zone is defined on type log (Fig. 82). Contour interval is 50 ft.

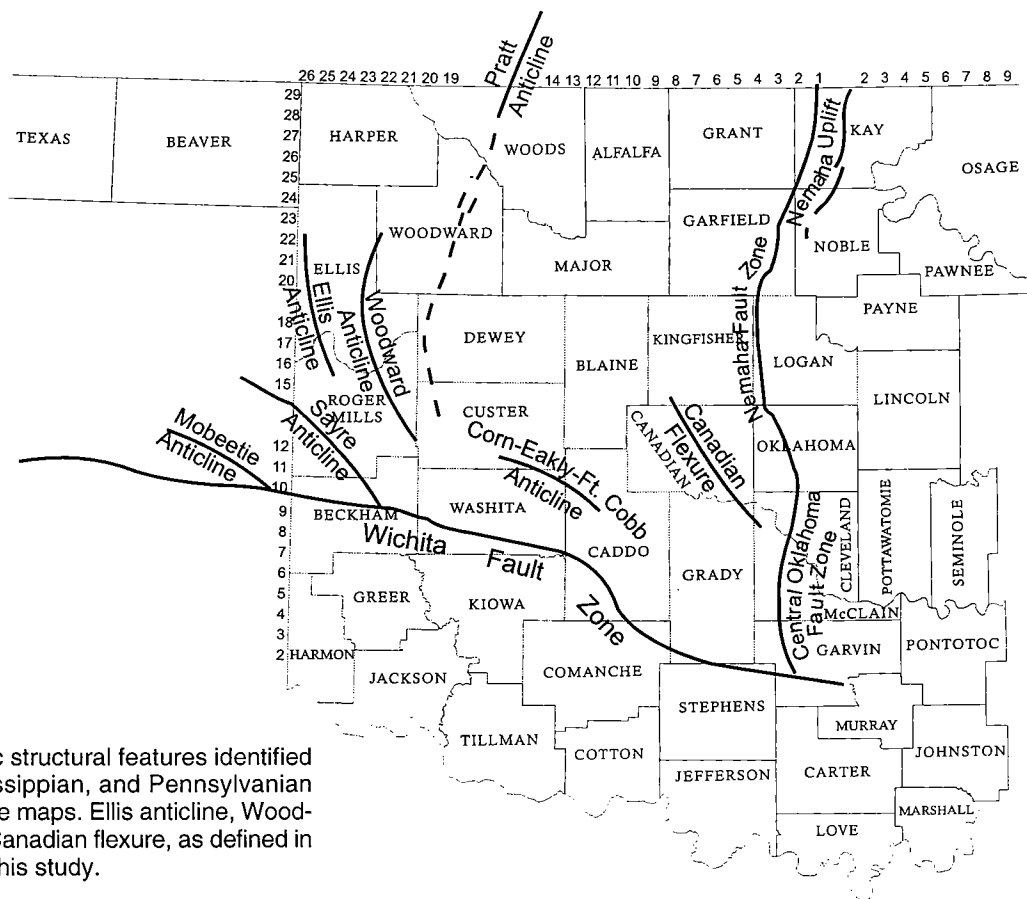


Figure 84. Paleozoic structural features identified from Hunton, Mississippian, and Pennsylvanian isopach and structure maps. Ellis anticline, Woodward anticline, and Canadian flexure, as defined in text, are original to this study.

these features have on other potentially productive zones. Fracturing as the result of periodic movement should be expected and may be a significant source of permeability in other reservoirs. For example, productive Mississippian wells within the East Arnett field study area may be draining a larger area because of the natural fracturing that may have occurred. Indications of fracturing are mentioned in the section on coring.

The following is a brief description and justification for recognizing the three structural features original to this workshop—the Ellis anticline, the Woodward anticline, and the extension of the Pratt anticline into Oklahoma.

Pratt Anticline Extension

The Pratt anticline is a regional Paleozoic structural feature extending southward from the central Kansas uplift to the Oklahoma border (Brown and Banta, 1993, p. 104). It is oriented south-southwest, and current publications suggest that the feature dies out at the Oklahoma border. I have studied the Simpson Group in Woods County, Oklahoma, and have long suspected that the anticline continues farther to the south, at least midway into Woods County. If the trend of the Pratt anticline is projected southward from Kansas, it would intercept a prominent horst block in T. 24 N., R. 18 W., in Woodward County, Oklahoma. A continuation of this trend to the south-southwest would intercept and coincide with the structurally controlled isopach “thin”

observed in the isopach interval from the Chester “B” to the top of the Woodford in Figure 83. The Pratt anticline manifests itself at the Ordovician level, although, if the extension of this feature is justified, periodic structural movements in the Silurian–Devonian sequence, as well as in the Mississippian sequence, seem probable.

Woodward Anticline

The Woodward anticline is named for the structural feature responsible for the horst block identified in the East Arnett field study area. Examination of the isopach interval from the Chester “B” to the top of the Woodford in Figure 83 verifies the congruence of the thinning at the Mississippian level with structural uplift and thinning observed at the Hunton level. Further evidence of subsequent uplift is interpreted from the thinning of the “Cunningham” and “White” intervals in wells 4 and 5 on cross section G–G’ (Fig. 75). The presence of this anticline can readily be observed on the Hunton structure map of Plate 3.

Ellis Anticline

The Ellis anticline is another horst-block feature that was uplifted and eroded prior to Woodford deposition. The Hunton isopach map of Plate 1 illustrates the pronounced thinning over this feature. Typical Hunton thicknesses of wells drilled in the anticline are 30–50 ft thick, whereas wells drilled in the adjacent down-

thrown blocks approach 250 ft in thickness. The anticline is projected to the southeast on the basis of the nosing apparent on the isopach map of Figure 83.

CANADIAN FLEXURE

The Canadian flexure is informally termed and original to this study for that area characterized by folding and faulting in Canadian County, Oklahoma. This flexure is evident in Ts. 10–14 N., Rs. 5–8 W. The scale of the Hunton isopach map (Pl. 1) and the Chimneyhill isopach map (Pl. 5) make it hard to visualize the persistent but subtle movement that must have occurred during deposition of the Chimneyhill Subgroup in that area. The same situation is true with the Hunton structure map (Pl. 3), although the major faults associated with this area are shown. The map that shows structural influence on Hunton deposition is the restored

Woodford–Kinderhook plus Hunton isopach of Figure 65. This is the isopach map of the Hunton Group plus the Woodford Shale and Kinderhook shale. The shale units were restored to their original thicknesses by multiplying their current thicknesses by a decompaction factor of 2. Area G in Figure 65 suggests that large differences in isopach thicknesses are associated with the Canadian flexure.

Figure 85 is a Sylvan structure map of an area centered about T. 12 N., R. 7 W., Canadian County, Oklahoma. The control for this map and that for Figure 86 is approximately 1 to 2 wells per section. This control is considered adequate for displaying the faulting and thickening of the Chimneyhill Subgroup in the Canadian flexure area. Cross section H–H' (Fig. 87, in envelope), illustrates stratigraphic relationships of the Chimneyhill. The contour interval of the Sylvan structure

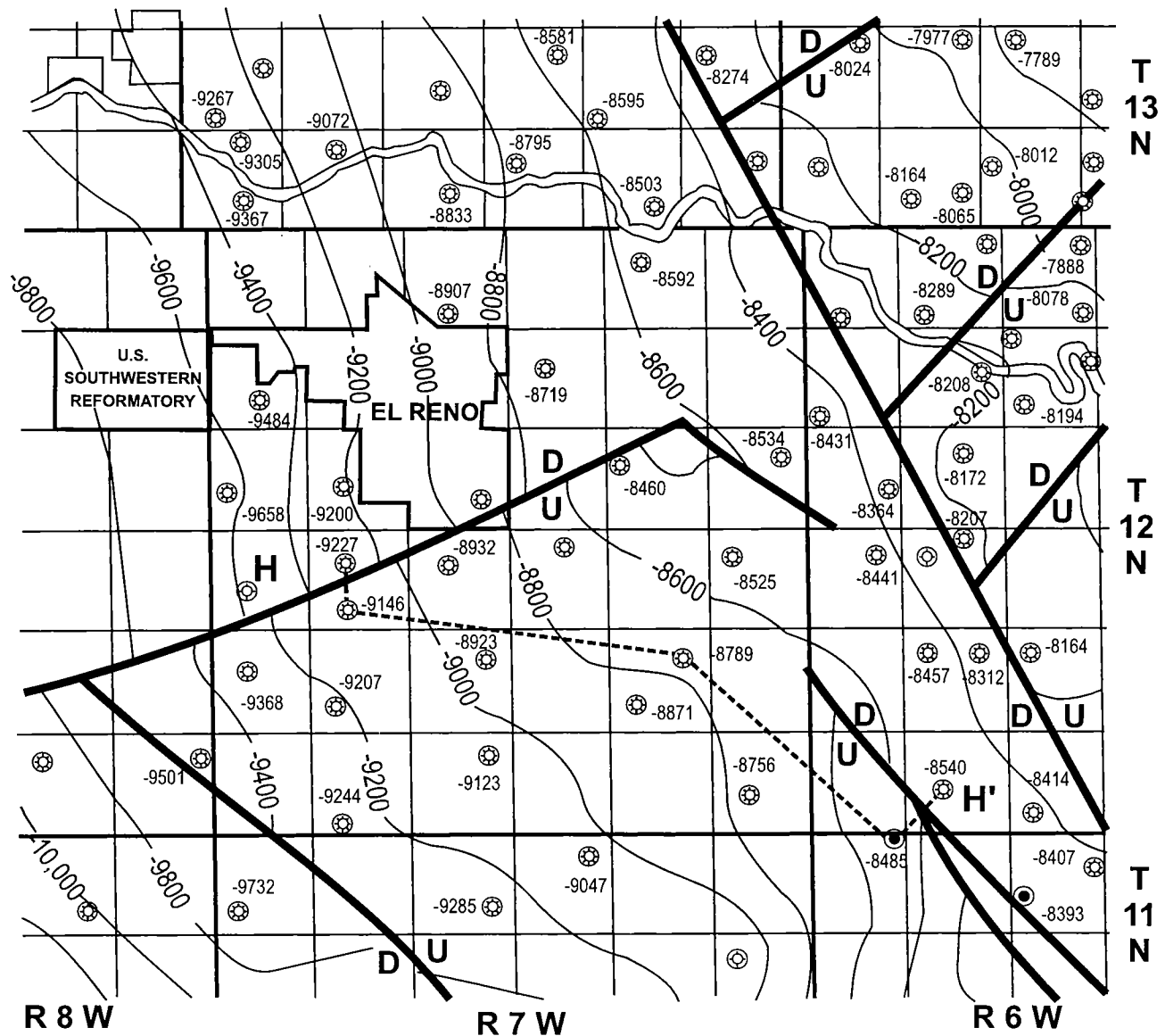


Figure 85. Structure-contour map of top of Sylvan Shale in Canadian County, Oklahoma. Contour interval is 200 ft.

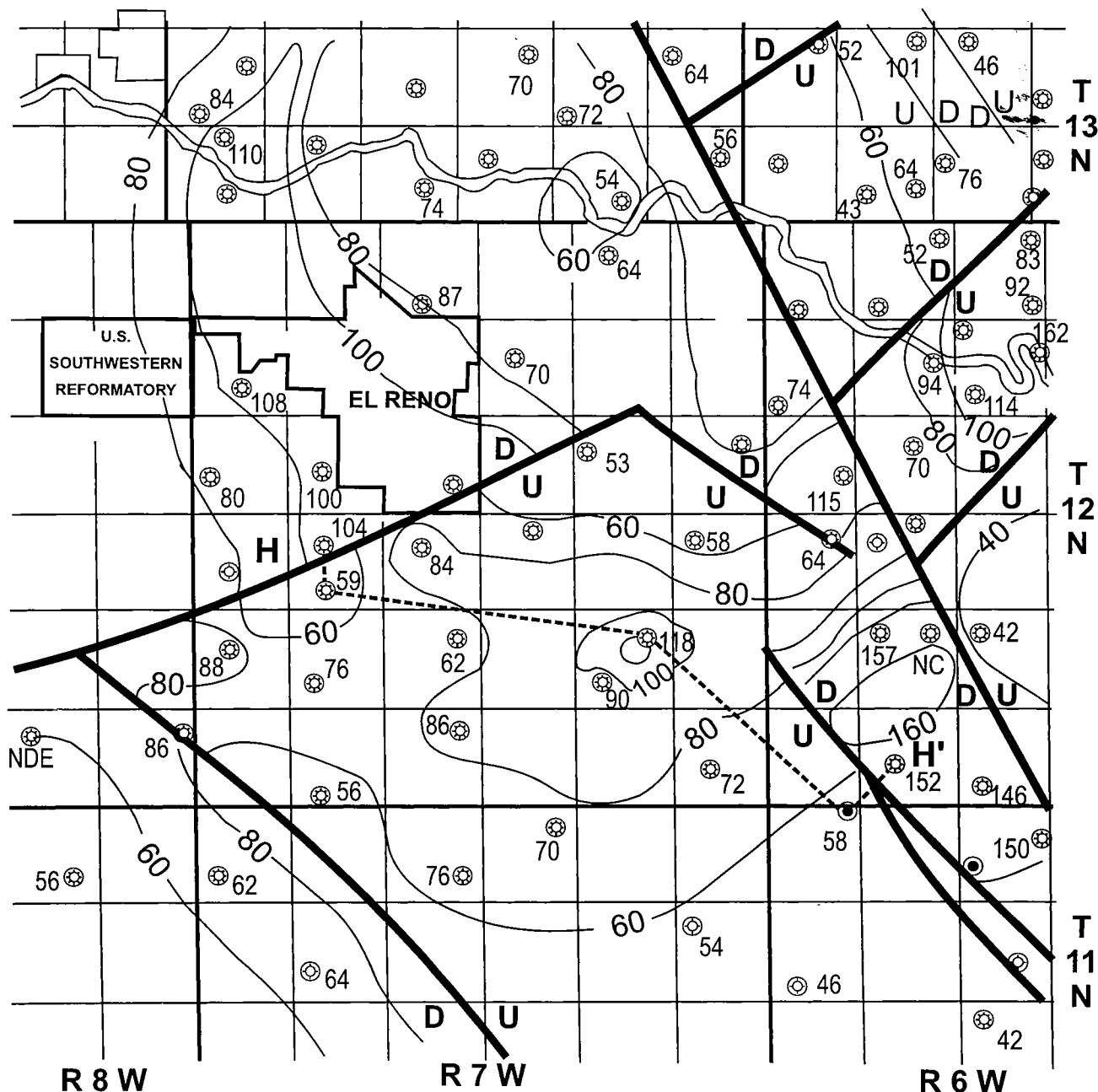


Figure 86. Isopach map of Chimneyhill Subgroup in Canadian County, Oklahoma. Contour interval is 20 ft.

map (Fig. 85) is 200 ft. The area includes a number of normal faults whose throws range from <50 ft to >200 ft. The rate of dip within the blocks is almost 300 ft per mi. Cross section H-H' (Fig. 87) is a stratigraphic cross section whose datum is the top of the Chimneyhill Subgroup, which is the same as the base of the regional Henryhouse marlstone lithofacies described in previous sections. What is apparent from this section is the virtual parallelism between the top of the uncompacted Woodford Shale and the datum. Wells 1 and 5 suggest minor thickening in this interval. Both wells are on the downthrown side of normal faults, and this increase in thickness may be due to increased movement

of the downthrown block during Henryhouse deposition. The dramatic thickness changes of the Hunton as seen in Figure 65 evidently occurred during Chimneyhill deposition. The Hunton type log (Fig. 21) for this workshop was selected partly because it demonstrates the zones that are present in the thick Chimneyhill sequence.

The depositional history of the Chimneyhill Subgroup in this area is similar to that in other areas except for the presence of faulting and gentle folding. I have examined samples from many wells in this vicinity. The Keel and Cochrane Formations may be present and observable, but only if those wells circulated samples

to the surface after penetrating the Sylvan. However, without core data, the thickness of these zones is speculative. The Keel and Cochrane on cross section H-H' (Fig. 87) are shown to be in their usual lithostratigraphic positions. The Keel appears to be present in every well except for well 2. This well has the thinnest Chimneyhill section, and the absence of the Keel may be due to the post-Keel unconformity, with removal by erosion. The indication of thickening and thinning is apparent in the Cochrane Formation, as wells 1, 3, and 5 reflect a thicker Cochrane section than do wells 2 and 4. The geometry of the gamma-ray response appears similar in all wells, although the relative thicknesses change. This same relationship is even more evident in beds 1, 2, and 3 of the Fitzhugh Member of the Clarita Formation. Again, each bed appears to be present, but the thickness of each bed depends on the overall thickness of the Chimneyhill. If the Chimneyhill Subgroup is a thick unit, its formations, beds, and correlative zones are thicker than their equivalents in thinner Chimneyhill sections.

This thickening and thinning, with no erosion, implies continuous deposition, which was probably made possible by growth faults. Two growth faults are indicated on cross section H-H' (Fig. 87). The first is between wells 1 and 2, and the second is between wells 4 and 5. These growth faults of Chimneyhill age have similar positions and displacements as the faults illustrated in Figure 85. Owing to the parallel relationship between time-stratigraphic intervals in the Henryhouse and the Woodford, this episode of fault movement probably ceased in post-Chimneyhill time. In Figure 86, an isopach map of the Chimneyhill Subgroup, thin Chimneyhill strata are on the upthrown sides of the fault blocks, and thick strata are on the downthrown sides, as also illustrated on cross section H-H' (Fig. 87).

Of major interest to operators and explorationists is the presence of shallow stratigraphic markers that indicate deeper structure. The isopach map of the Chimneyhill Subgroup (Fig. 86), coupled with the Sylvan Shale structure map (Fig. 85), should indicate upthrown fault blocks at depth. Figure 88 illustrates those wells currently producing from the Upper Ordovician Viola and from the Middle Ordovician Simpson. Note the amount of Simpson production

in the south half of T. 12 N., R. 7 W. The upthrown fault block probably created a structural closure for deeper production, as shown in this figure. Those Simpson producers not associated with apparent closures could be the result of closures that may not be apparent from existing well control.

STRUCTURAL HIGHS VERSUS TOPOGRAPHIC HIGHS

In the Leedey field study, it was pointed out that the Woodford and Hunton have a stratigraphic relationship. I published a paper (Rottmann, 2000) devoted to determining the relationship between the Hunton and the Woodford that included examples and guidelines to use in determining if a thick or thin Woodford sequence was structurally or stratigraphically controlled. In all cases, though, this structural or stratigraphic relationship cannot be determined without considering the overall Hunton thickness—that is, by including the top of Sylvan Shale in determining the total Hunton thickness. Structural interpretations cannot be made by using only a Woodford isopach interval or a Hunton isopach interval unless, of course, the zone is cut by a fault.

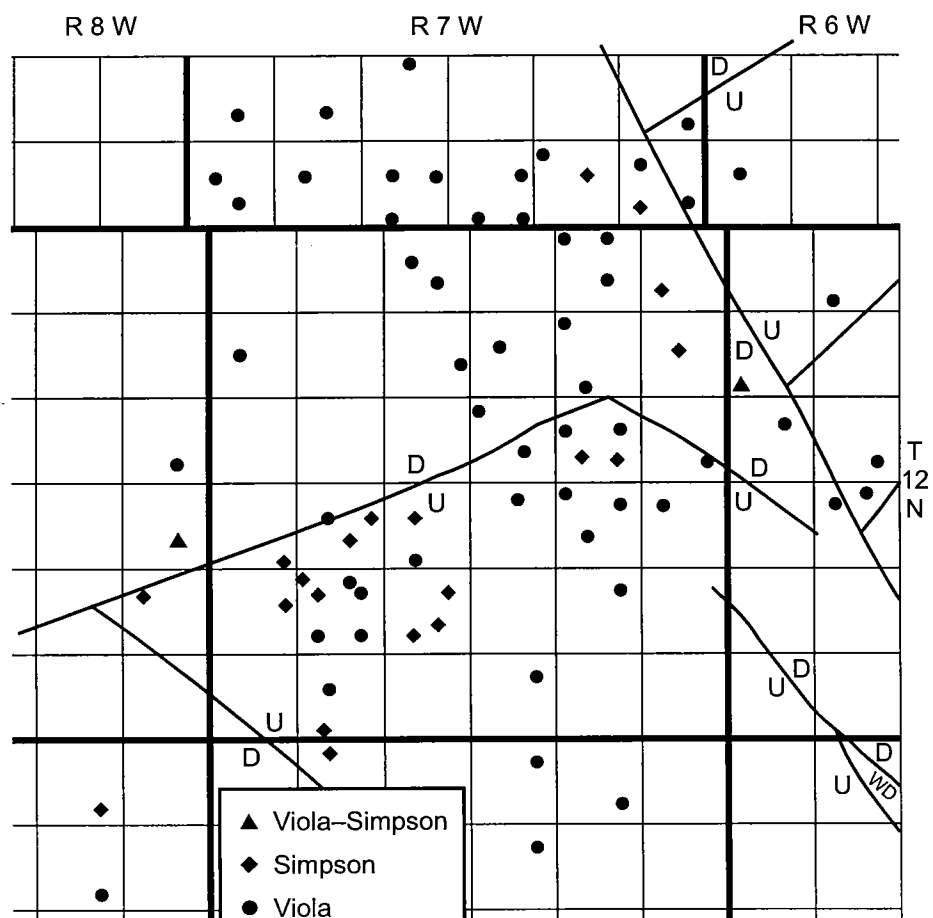


Figure 88. Relation of Viola and Simpson production to faults as determined by Chimneyhill isopach map of Figure 86 and Sylvan structure map of Figure 85.

The following example illustrates how a potential structural interpretation could just as easily be a purely stratigraphic one. Figure 89 is a Woodford isopach map (Hester and Schmoker, 1993, fig. 1) of western Oklahoma. The Woodford was deposited upon the post-Hunton erosional surface. The Woodford isopach of Figure 89, as well as the Woodford isopach of this report (Pl. 2), suggest two possible Woodford depocenters. One is in the structurally deep part of the Anadarko basin, and the other is in Woods, Alfalfa, and Grant Counties, Oklahoma. These two depocenters are separated by a positive northwest-southeast feature (Fig. 89). Figure 90 illustrates the drainage system incised into the Hunton paleosurface, and the direction of drainage for each of these depocenters as interpreted by Hester and Schmoker (1993). The restored Woodford channel isopach map (Fig. 57) supports this interpretation. Drainage on the south side of the positive feature was to the south, and on the north side, to the southeast. These interpretations are based on reconstructing the geometry of the paleodrainage system of the Woodford channel-fill deposits (Fig. 57).

The question is, what is the nature of the positive feature separating deposition of the Woodford into two drainage systems? Hester and Schmoker consider this feature to be a paleotopographic high and that the thin upper Woodford deposits indicate that this feature was rising during the pre-Woodford episode of regional erosion (Hester and Schmoker, 1993, p. 75). The positive feature is considered to be a forebulge, rising prior to and throughout Woodford deposition in response to subsidence of the southern Oklahoma aulacogen (Hester and Schmoker, 1993, p. 78). This uplift would imply basement structural involvement; if this is correct, it could be an attractive focal point for an exploration effort.

Figure 91 is a schematic cross section from Hester and Schmoker (1993, fig. 2) used to show the three informal divisions of the Woodford Shale, as described by them, and to suggest the presence and position of the positive feature mentioned previously. The original figure from Hester and Schmoker used a Woodford thickness that represented only the compacted present-day thickness of the Woodford Shale. Figure 91 has been

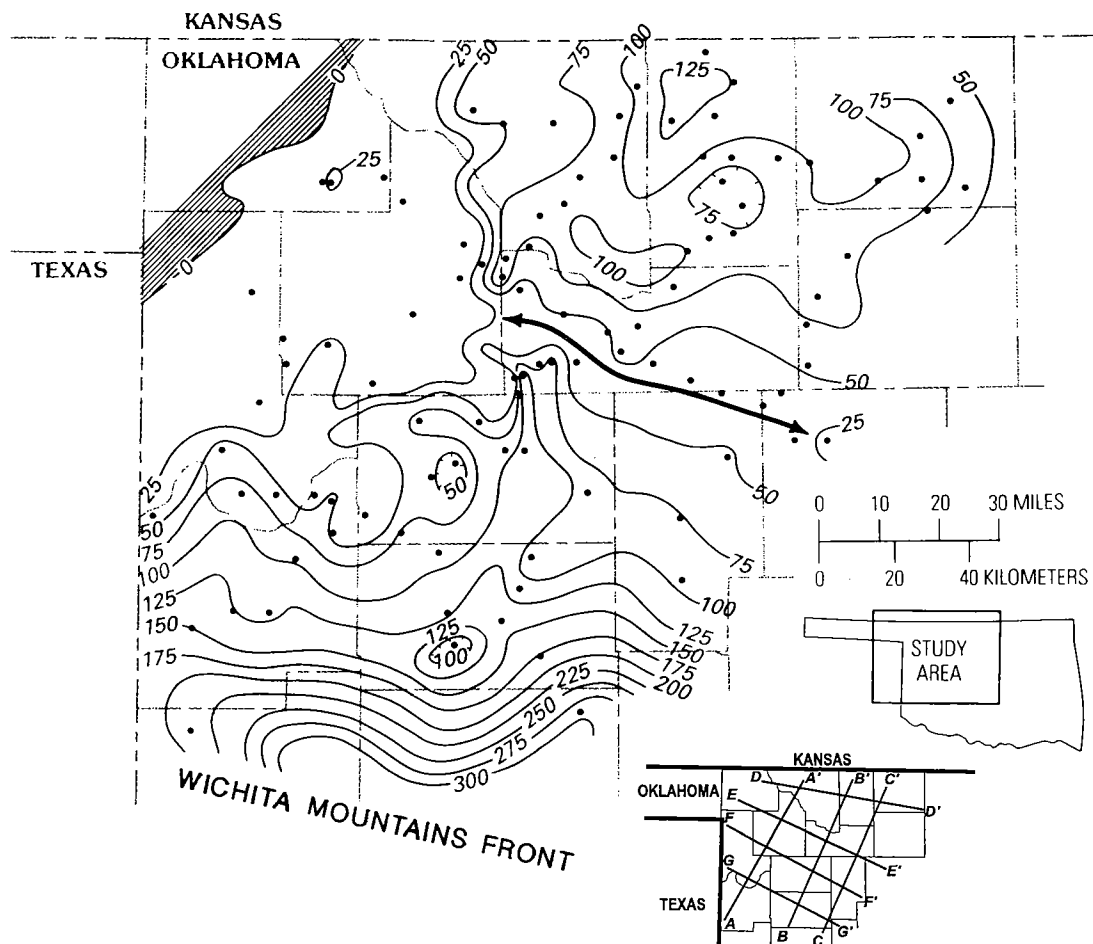


Figure 89. Isopach map of Woodford Shale. Heavy line with arrows marks axis of paleotopographic high that separates Woodford into northeast and southwest depocenters. Dots show wells from which data were obtained. Area where Woodford Shale is absent is hatched. Contour interval is 25 ft. Modified from Hester and Schmoker (1993, fig. 1).

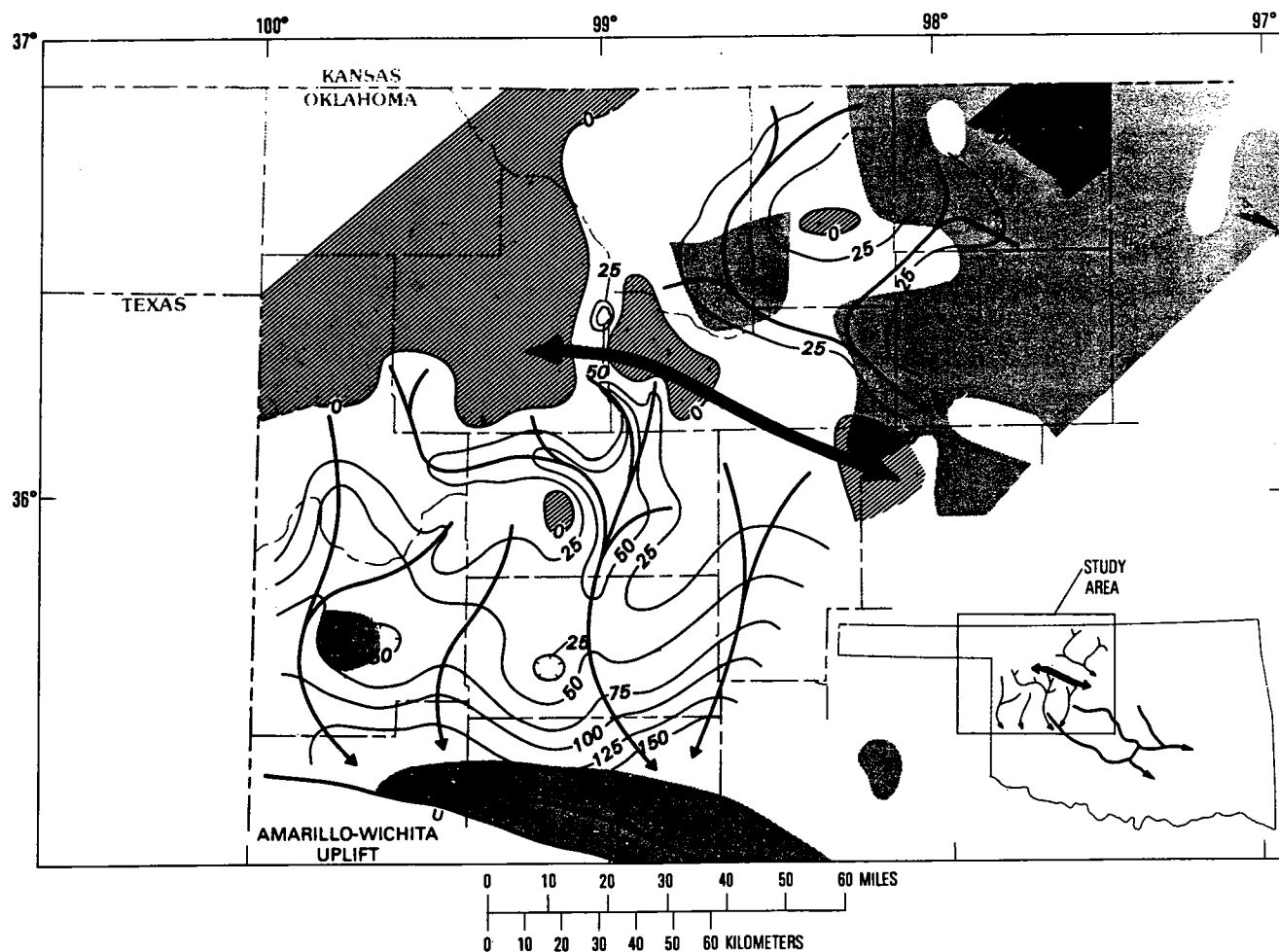


Figure 90. Isopach map of lower member of Woodford Shale (see Hester and Schmoker, 1993). Major erosional channels on pre-Woodford surface (thin lines with arrows) are inferred from thickness of lower member. Areas where lower member is absent are hatched. Distribution of Misener sandstone (shaded) as depicted by Amsden (1975) from Hester and others (1992). Heavy line with arrows marks axis of paleotopographic high. Contour interval is 25 ft. From Hester and Schmoker (1993, fig. 3).

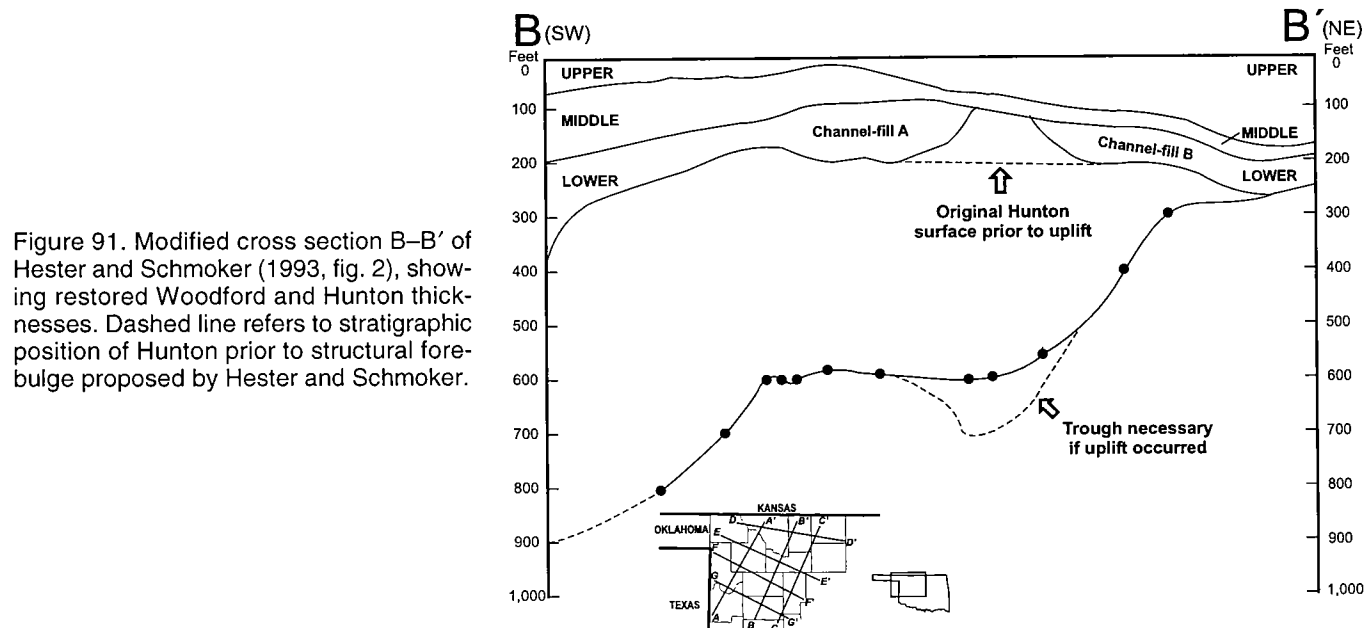


Figure 91. Modified cross section B-B' of Hester and Schmoker (1993, fig. 2), showing restored Woodford and Hunton thicknesses. Dashed line refers to stratigraphic position of Hunton prior to structural forebulge proposed by Hester and Schmoker.

modified by decompacting the Woodford Shale to represent the actual thickness at deposition and to add the stratigraphic position of the Sylvan Shale (bottom). The dashed line at the base of the Woodford represents the approximate position of the Hunton paleosurface prior to a forebulge uplift, as described by Hester and Schmoker. By lowering the Hunton topographic surface to its pre-structural position, it is also necessary to lower the Sylvan–Hunton boundary by equal increments as shown by the dashed line at the Sylvan Shale horizon. This means that a trough would have been in place prior to any structural movement. If such a trough had been present, additional deposition either of the Chimneyhill Subgroup or of the Henryhouse Formation would have had to occur. Unfortunately, core information necessary to resolve this question is not available.

Another scenario to explain this positive feature would be simply a paleotopographic high present during the second stage of erosion, as suggested in the Leedey field study and presented in Figure 56. Figure 56 suggests three steps in the erosion of the post-Hunton surface and deposition of the Woodford Shale. The first step involves the uplift and tilting of the Hunton surface regionally. A northwest–southeast hinge line may have developed at this time approximately in the position of the positive feature shown in Figure 90. Amsden (1980, p. 61) also mentions the formation of an arcuate hinge line, up to the north and down to the south. This uplift would correspond to Figure 56B. I suggest that peneplanation of the exposed Hunton surface occurred prior to the formation of a channel drainage system. (Fig. 56C). Following peneplanation, a drop in sea level may have occurred, re-exposing the Hunton surface. The immature drainage system that formed did not have time to dissect the Hunton surface completely, thus failing to connect the southern depocenter of the Woodford with the northern depocenter. With the rise in sea level and subsequent deposition of Woodford channel-fill deposits and regional shale deposits, the drainage system was effectively preserved. The resulting geometry of a stratigraphic section perpendicular to this positive feature would be identical to that of Figure 56D and Figure 91.

CORES

A number of cores were obtained and described by Amsden (1975, 1993). However, none of the core reports were available for this publication. An indication of the intense fracturing that may have resulted from the uplift of the Woodward anticline is suggested by the

TABLE 8. – Geological/Engineering Data for Hunton Limestone, East Arnett Field Study Area, Ellis County, Oklahoma

<u>Hunton Limestone</u>	
Reservoir size (oil)	Not applicable
Reservoir size (gas)	~900 acres
Well spacing (gas)	640 acre
Oil–water contact	Not applicable
Gas–water contact	Unknown
Porosity	10%
Permeability	Unknown
Water saturation	~20%
Gas/oil ratio	Not applicable
Thickness (net sand) ($\phi > 8\%$)	~30 ft
Reservoir temperature	220°F
Oil gravity	Not applicable
Initial reservoir pressure	4,100 psia
Initial gas formation volume factor	0.0044
Original oil in place (volumetric)	Not applicable
Cumulative condensate	Not applicable
Recovery efficiency (oil)	Not applicable
Cumulative gas	18.42 BCF

core descriptions of wells 4 and 6 of cross section F–F' (Fig. 74).

PRODUCTION AND RESERVOIR PARAMETERS

Table 8 gives the reservoir parameters of the East Arnett Hunton field. As mentioned previously, the reservoir size is not readily apparent, but 900 acres would seem reasonable, given the state of decline of production and other parameters. The 30 ft of average porosity is an estimate; actual porosity varies considerably from well to well. It is not known how much of this net porosity is represented by fractures or by matrix porosity.

The gas-production curve for the East Arnett field Hunton reservoir is shown in Figure 92. The field has a cumulative production of more than 18 BCFG. Most of this production is probably attributable to the No. 1 Boyd discovery well, discussed previously.

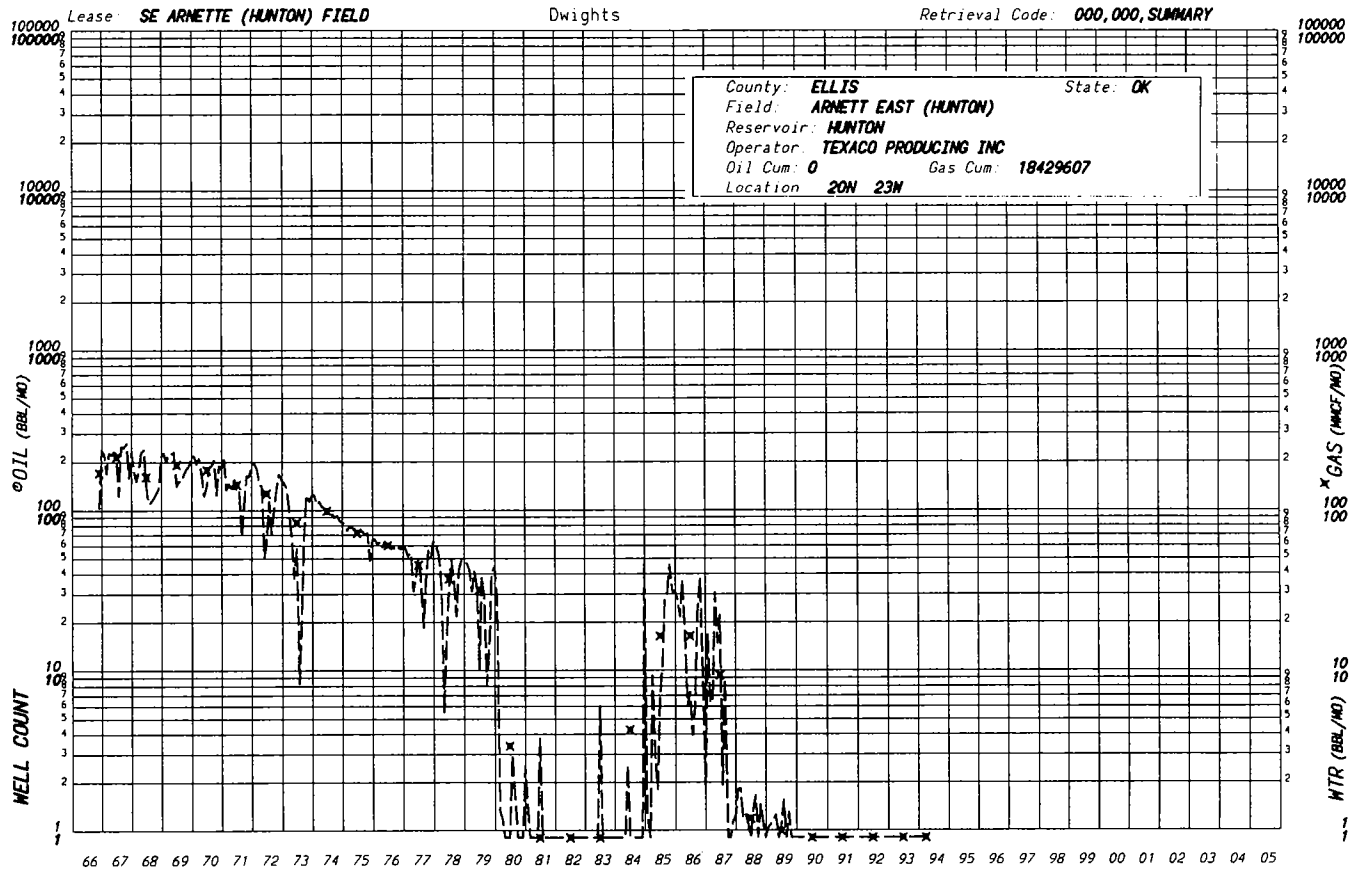


Figure 92. Graph showing gas-production curve for East Arnett Hunton field study area.

PART VIII

Prairie Gem Field Hunton Reservoir Study (T. 16 N., R. 2 E., Lincoln County, Oklahoma)

Kurt Rottmann

INTRODUCTION

The Prairie Gem field Hunton reservoir study area is in northwestern Lincoln County, central Oklahoma. The field is on the Cherokee platform, which is north of the Arkoma basin and east of the Nemaha fault zone. Figure 93 is a generalized location map for the field study and shows the line of cross section P-P' (Fig. 94, in envelope), which illustrates the stratigraphy. The discovery well was the Berry No. 1 Wilkins, in the SE $\frac{1}{4}$ NE $\frac{1}{4}$ sec. 11, T. 16 N., R. 2 E. The well was completed in 1959 for an initial flowing potential of 14 MMCFGPD with 16 BO per MMCFG. Two additional wells were completed in the Hunton the following year. Figure 95 is a well-information map showing operators, well numbers, lease names, and producing reservoirs for wells in the study area.

The Prairie Gem Hunton reservoir was selected for two reasons. First, the producing Hunton reservoir appears to be part of an environment of deposition that is unique in comparison to that of typical deposits of the Chimneyhill Subgroup. Interpretations of the regional correlations of this sequence of Hunton strata may introduce new possibilities for the origin of Hunton Silurian dolomites. Regional correlations and stratigraphic sequences within the Chimneyhill are uniform and correlatable from this field westward into the deeper part of the Anadarko basin, and it is hoped that concepts and correlations for this field study can also be applied to the Chimneyhill in other shelf areas.

The second reason this field study was selected is its proximity to an active play currently in progress near Carney, Oklahoma, which is approximately 4 mi south of this field. There,

many operators are developing the Hunton reservoir. Any information for a field study within the Carney Hunton play would be difficult to obtain, as many operators feel that contributing such information would compromise their exploration efforts. I am familiar

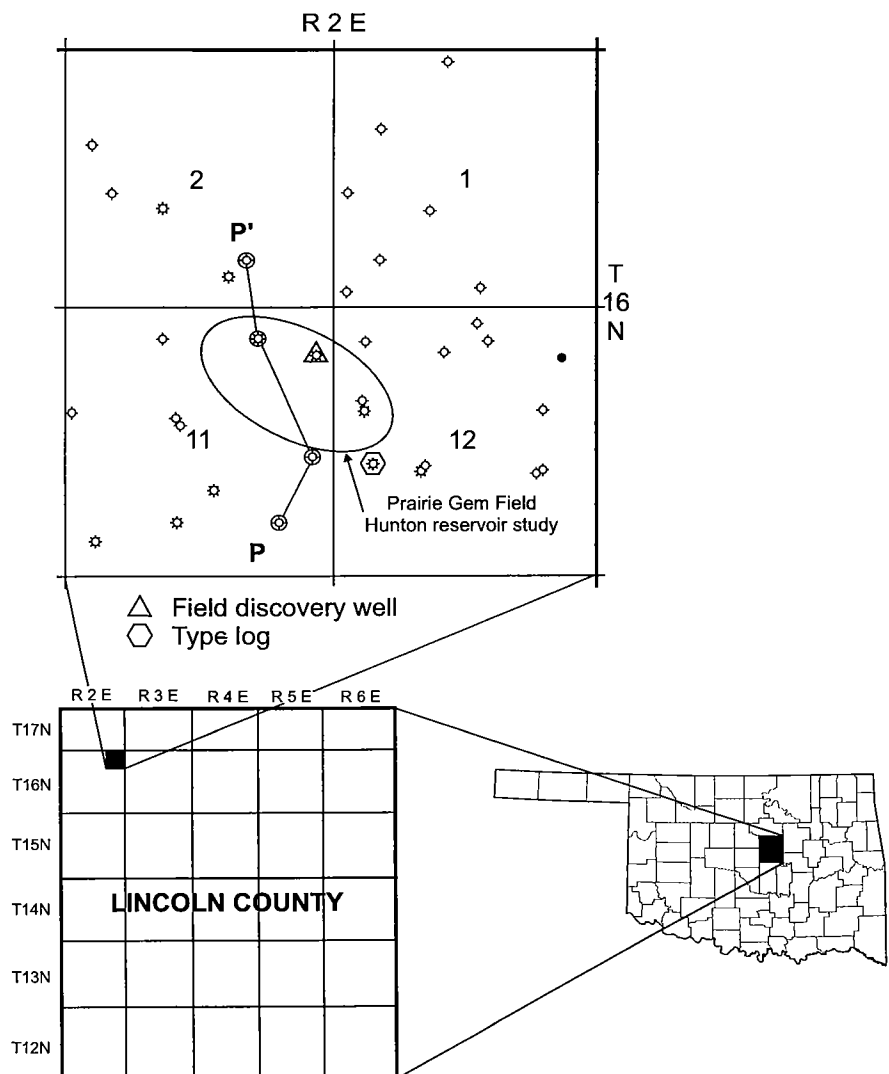


Figure 93. Generalized location map (below) of Prairie Gem field Hunton study area in Lincoln County, Oklahoma. Upper map shows location of Prairie Gem Hunton reservoir. Cross section P-P' shown in Figure 94.

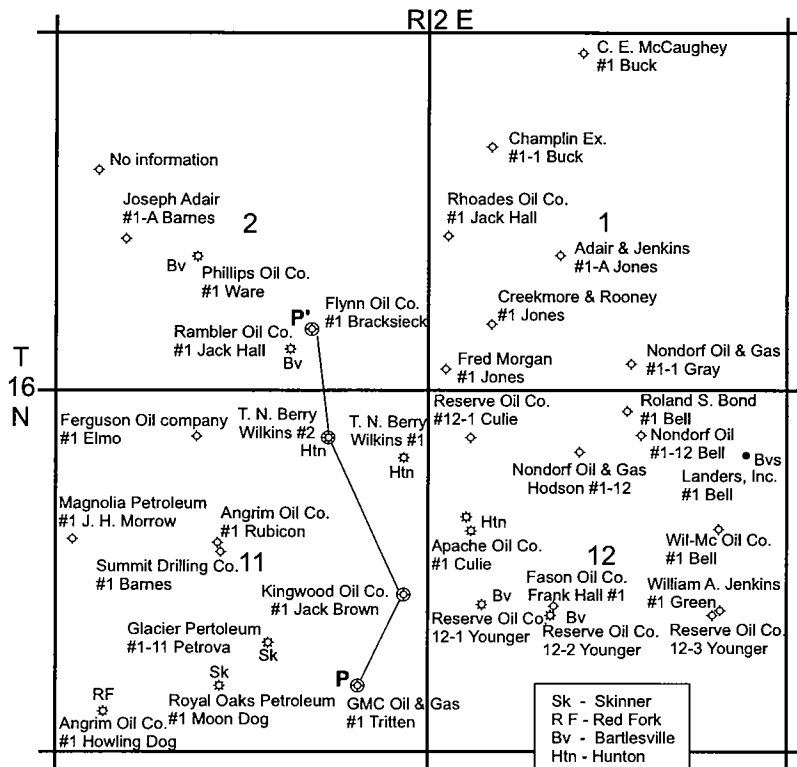


Figure 95. Well-information map showing operators, lease names, well numbers, and producing reservoirs for wells in Prairie Gem Hunton field study area.

with this active area, and I previously published preliminary studies about the play (Rottmann, 1993, p. 83). The Prairie Gem Hunton field has similar stratigraphic and facies relationships to those of the Carney area. Thus, this study serves as an analogy to the prolific Carney trend without compromising confidential information. Also, enough reservoir data are publicly available to draw reasonable preliminary conclusions as to the type and method of production from high-water-cut Hunton oil reservoirs.

STRATIGRAPHY

The type log for the Prairie Gem field Hunton study is the Reserve Oil, Inc., No. 12-1 Younger, 2,130 ft FSL and 825 ft FWL sec. 12, T. 16 N., R. 2 E., Lincoln County, Oklahoma (Fig. 96). Many of the logs for the field study area are older logs, with electric, microlog, and SP logs being the predominant open-hole wireline logs run. Other wells were drilled only through the upper few feet of the Hunton out of concern for entering a water leg below any possible oil column. The Younger well fits three requirements for a type log: (1) the well penetrated the entire Hunton se-

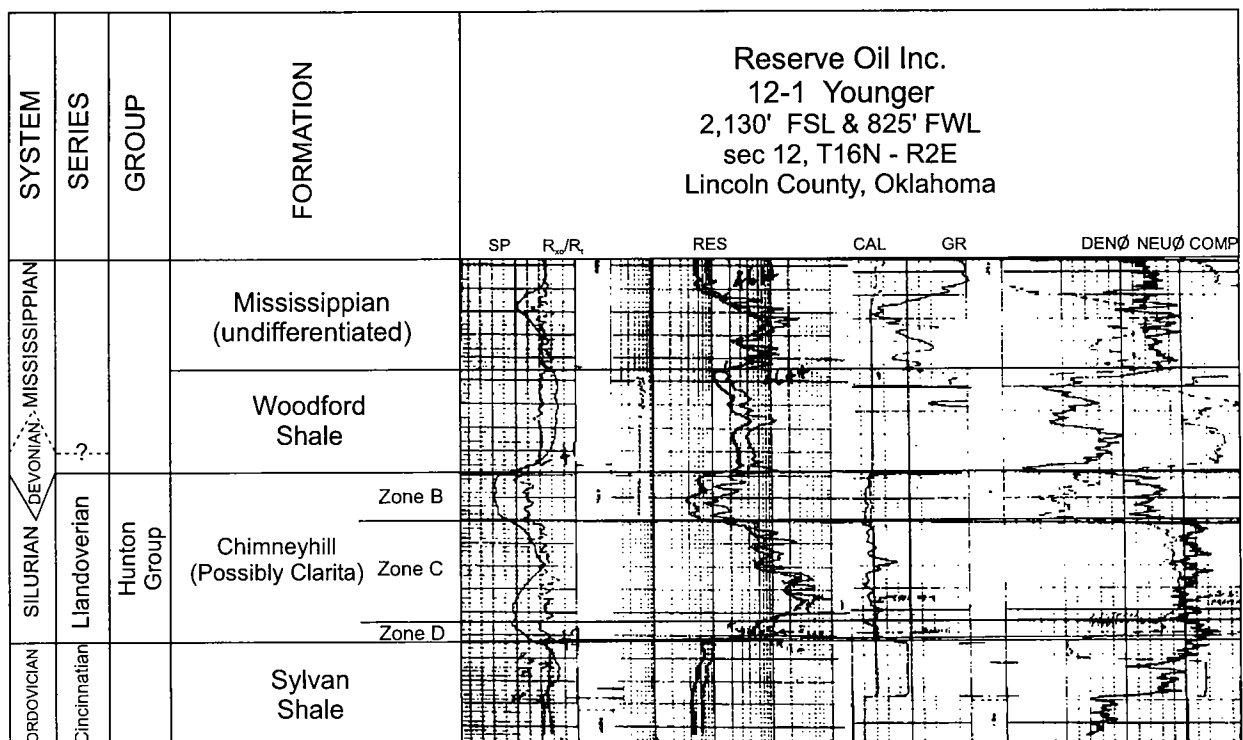


Figure 96. Type log for Prairie Gem Hunton field, showing Hunton Formations represented and characteristic log signatures. Dashed lines indicate uncertain but probable stratigraphic identification. SP = spontaneous potential; R_{xo}/R_t = ratio of resistivity of flushed zone to resistivity of uninvaded zone, or true resistivity; RES = resistivity; CAL = caliper; GR = gamma ray; $DEN \phi$ = density porosity; $NEU \phi$ = neutron porosity.

quence, (2) a complete modern log suite was run, and (3) the well is a good representative of the productive facies in the field.

The underlying Sylvan Shale is consistently uniform in thickness in the field study area, averaging 90 ft. Overlying the Sylvan is the Hunton section of early Late Silurian age. Biostratigraphic control from cores is not available in the vicinity, although correlation with those wells supplying biostratigraphic control suggests that the section probably is composed entirely of the Chimneyhill Subgroup, with the Clarita Formation being the predominant component. A number of cores have been recovered in the Carney area for a study of this producing interval that was funded by the U.S. Department of Energy, but the core analyses have not been released. The Hunton is overlain by the Late Devonian–Early Mississippian Woodford Shale, which is uniform in thickness and probably consists of regional Woodford deposits, as described previously. The Woodford Shale is overlain by undifferentiated Mississippian limestones.

In examining annotations on well logs and scout tickets, I have noticed that many geologists label various distinctive beds of the Hunton in the study area as (in ascending order) Chimneyhill, Henryhouse, and Bois d'Arc. It is easy to understand why this is so, and the confusion inherent in sorting out the stratigraphic relations. The overall shape of the SP curve for a Hunton section containing the Silurian Chimneyhill Subgroup and Henryhouse Formation, and the Devonian Bois d'Arc–Frisco Formations, is usually similar and easily recognizable on a regional basis because of the distinctive lithologies. The sequence is composed of an organo-detrital limestone (Chimneyhill Subgroup)/marlstone (Henryhouse)/organo-detrital limestone (Bois d'Arc–Frisco), with the SP curve for this sequence commonly being “clean”/shaly/“clean.” The SP signature for the type log of this workshop (Fig. 21) is shown in Figure 97A. This “clean”/marly/“clean” sequence of the Hunton Group takes on a distinct sigma-shaped character, which is the general shape for the Silurian–Devonian sequence described previously and which is recognizable for many wells in the subsurface of central and western Oklahoma. However, this generally sigma-shaped curve can lead to misidentification or miscorrelation of strata, owing to the familiar and recognizable SP shape. Figure 97B illustrates the SP curve for two wells to the west of the Prairie Gem field study area and the corresponding sigma-shaped SP curve. The characteristic SP sigma shape in this area has led some geologists to believe that the Hunton Group here comprises several formations because of the similarity of the SP curve (Fig. 97B) to the sigma-shaped SP curve for those strata deeper in the basin (Fig. 97A).

Figure 98 is a cross section (I–I') of the two wells shown in Figure 97B. These wells are approximately 7 mi apart. Notice the apparent ease of correlation between zones 1, 2, and 3. The correlations appear to be identical, even to the detail of point 2 appearing on

both SP curves. Figure 99 is a location map showing the line of this cross section in the Prairie Gem field study area, and lines of four additional cross sections, J–J', K–K', L–L', and M–M'.

Cross sections J–J', K–K', and L–L' are illustrated in Figure 100. Well 1 of cross section I–I' (Fig. 98) is an offset to well 3 of cross section J–J'. Well 2 of cross section I–I' is repeated as well 9 of cross section J–J'. In cross section I–I', zone 1 is in the upper part of both wells. However, the interval identified as zone 1 in well 1 on cross section I–I' is not correlative with the same interval on cross section J–J' (Fig. 100). The interval identified as zone B in well 3 descends westward until, at well

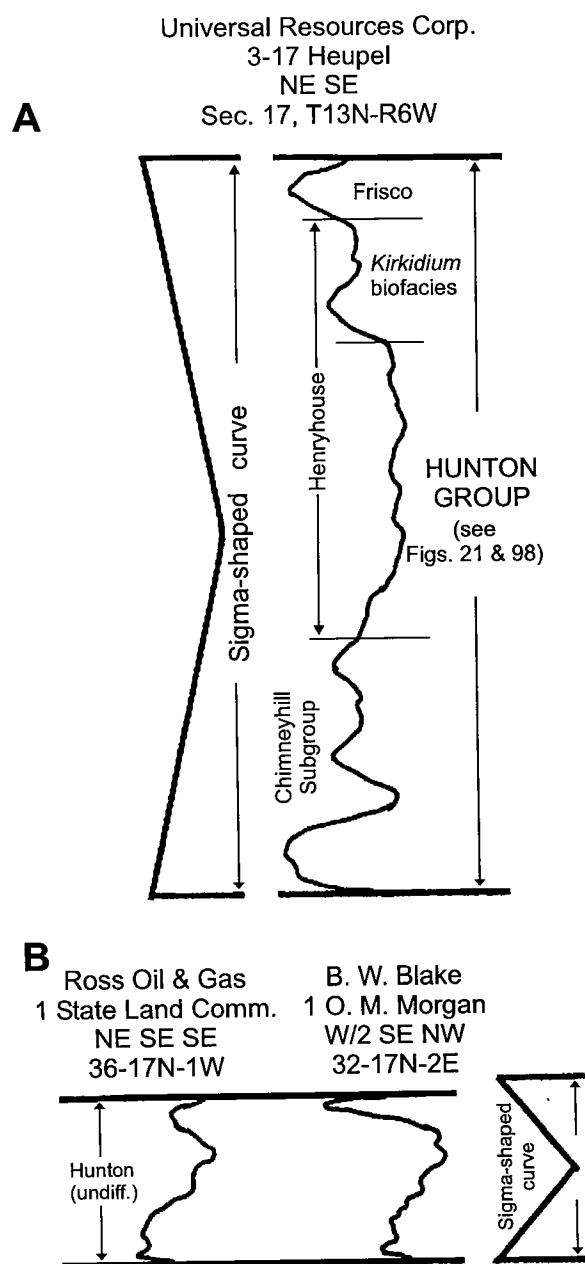


Figure 97. Comparison of sigma shape (S) of SP curves for wells listed. See text for explanation. From Rottmann (1993, fig. 9).

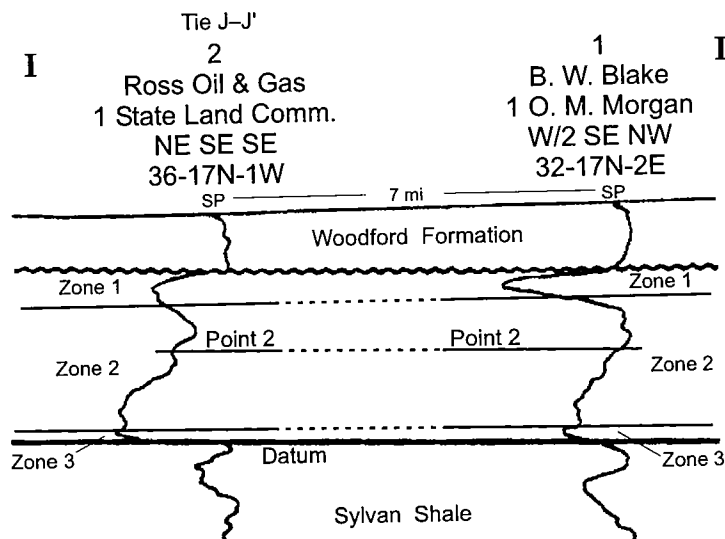


Figure 98. Stratigraphic cross section I-I'. Line of section shown in Figure 99. From Rottmann (1993, fig. 4).

9, it is near the bottom of the sequence. This same relationship is true for zone B in cross sections K-K' and L-L'. Therefore, the apparent correlation of zones 1, 2, and 3 in cross section I-I' is completely erroneous, so the corresponding sigma-shaped curve (Fig. 97B) could not possibly represent strata from the Chimneyhill, Henryhouse, and Bois d'Arc-Frisco as annotated on many logs. Cross sections J-J', K-K', and L-L' all suggest a progradational foreslope or fan depositional environment for zone B.

A revised version of cross section I-I' (Fig. 101) illustrates the correct correlation of zones A, B, C, and D, based upon the regional correlations of cross sections J-J', K-K', and L-L' (Fig. 100). As the sequence represented by zone B is identical in shape and character to the sequence of zone C in Figure 101, it can be assumed that the depositional environment for zone B is identical to that of zone C and has been repeated. Furthermore, zone D is the trailing end of a third sequence, and zone A is the beginning of a fourth sequence. The regional pre-Hunton unconformity has modified the thicknesses of these zones and should be taken into consideration when interpreting depositional environment. Notice the similarity of the SP shape of both wells 1 and 2 of cross section I-I' (Fig. 101) to that of the type log (Fig. 96).

The correlation of the Hunton illustrated in Figure 101 also offers a correlation central to the environment of deposition for the producing facies of the Prairie Gem Hunton field and for the developing Hunton play in the Carney area. The depositional environment for the sequences represented by cross section I-I' (Fig. 101) is examined later, but

a few observations and considerations can be made about the depositional environments for zones A, B, and C of cross section I-I' from isopach mapping.

Figure 102 shows a gross-isopach map of the Hunton strata for the area outlined in Figure 99. The isopachs show the regional thinning of the Hunton to the northwest and northeast (see Pl. 1). The Hunton thickens to the southeast, where it approaches 150 ft in thickness. Several pre-Woodford erosional channels modify the Hunton thickness locally in the southern part of the map. Overall, the complex internal geometry illustrated in cross sections J-J', K-K', and L-L' (Fig. 100) is not apparent from this Hunton gross-isopach map.

Figure 103 is an isopach map of zone C as identified on cross section I-I' (Fig. 101) and on sections J-J', K-K', and L-L' (Fig. 100). The zone is thick at the east end of the mapped area and gradually thins to the west. The heavy dashed line approximates the point where zone C completely pinches out. The east end of the mapped area is characterized by a series of east-west-trending thick and thin deposits of zone C. The thicker sections approach 130 ft in thickness, with the thinner areas being 10–30 ft thick. On the basis of the SP character of the well logs reflecting a thick zone C sequence, a characteristic decrease in "clean" SP response from bottom to top is evident, which could mean a gradation to a tighter matrix, shalier conditions, or a finer grain size, or a combination of these factors, in the upper part of zone C. In the isopached area, porosity and permeability in zone C seem to be limited, based on log character. However, the influence of fractures cannot be discounted but is not recognizable from the SP-log response. The overall SP shape of zone C is uniform and easily correlatable

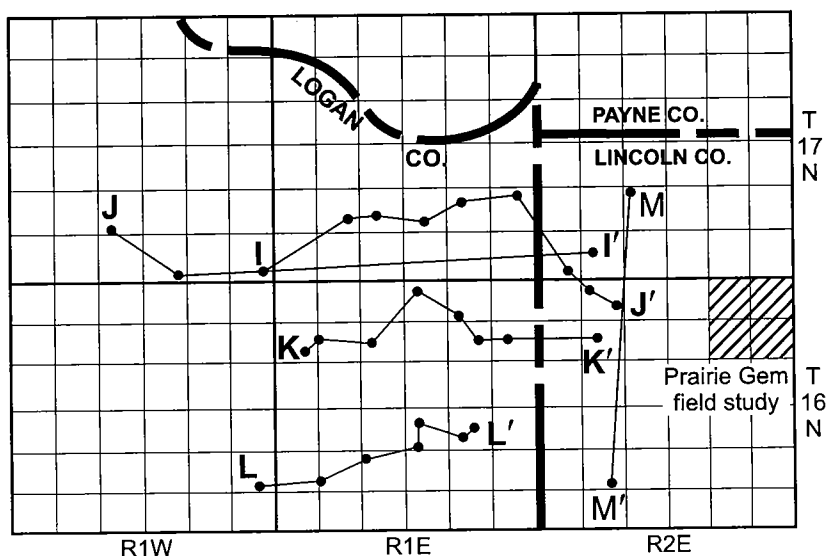


Figure 99. Location map for cross sections I-I' (Fig. 98), J-J' (Fig. 100), K-K' (Fig. 100), L-L' (Fig. 100), and M-M' (Fig. 108).

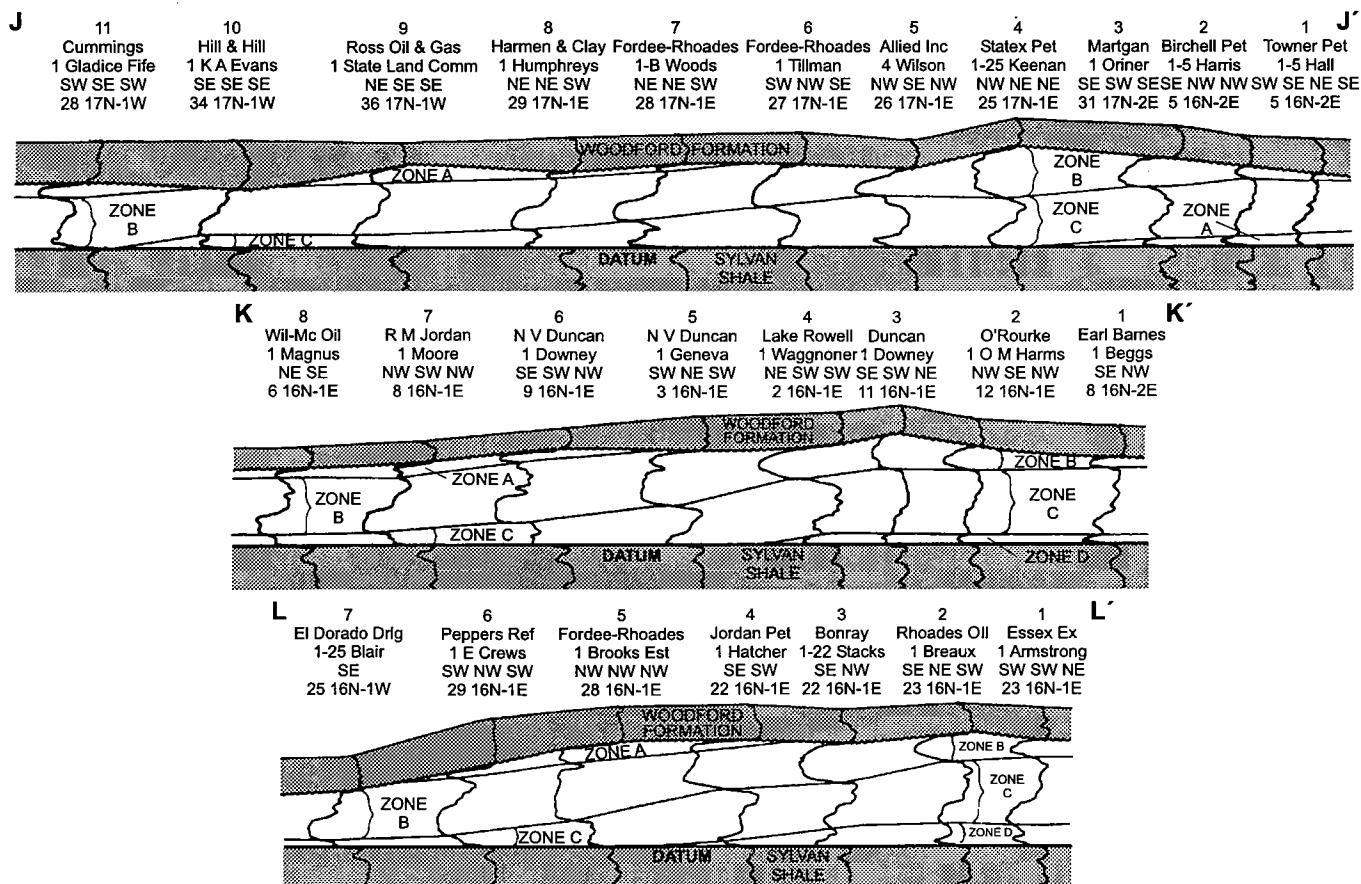


Figure 100. Cross sections J-J', K-K', and L-L'. Lines of sections shown in Figure 99. From Rottmann (1993, fig. 10).

between closely spaced wells. The gradual thinning and eventual pinch-out of zone C appears to be a function of sediment starvation rather than erosion. Without core control to discern the boundary relationship, however, the observation is speculative. There seems to be a common line of demarcation from the abruptly thickening and thinning area (east-central part of Fig. 103) to the area characterized by beds of uniform but

gradually thinning strata (west-central part of Fig. 103), even though well density and control are about equal for both parts.

Figure 104 is an isopach map of zone B, which overlies zone C. This isopach is also characterized by two geometries of deposits. In the east-central part of the isopached area, zone B also exhibits an east-west orientation of alternate thick and thin deposits. The isopach thickness ranges from 0 to 50 ft. The relationship of zone B to zone C is as follows. The thick sections of zone B occupy and overlie the thin sections of zone C. Conversely, the thin sections of zone B overlie the thick sections of zone C. The cumulative effect of this relationship is manifested in the gradual thinning of the Hunton to the northeast, as shown in Figure 102. Unlike zone C, zone B does not exhibit a gradual thinning and eventual pinch-out of strata; instead, it seems to maintain a relatively uniform thickness over most of the mapped area. The thickness of zone B is modified by subtle channeling of the Woodford in the

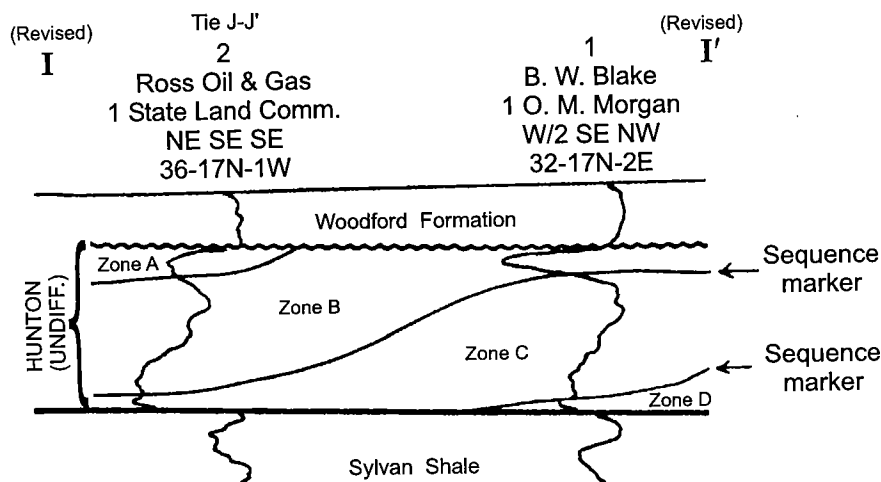


Figure 101. Revised cross section I-I' (see Figs. 98 and 100). From Rottmann (1993, fig. 12).

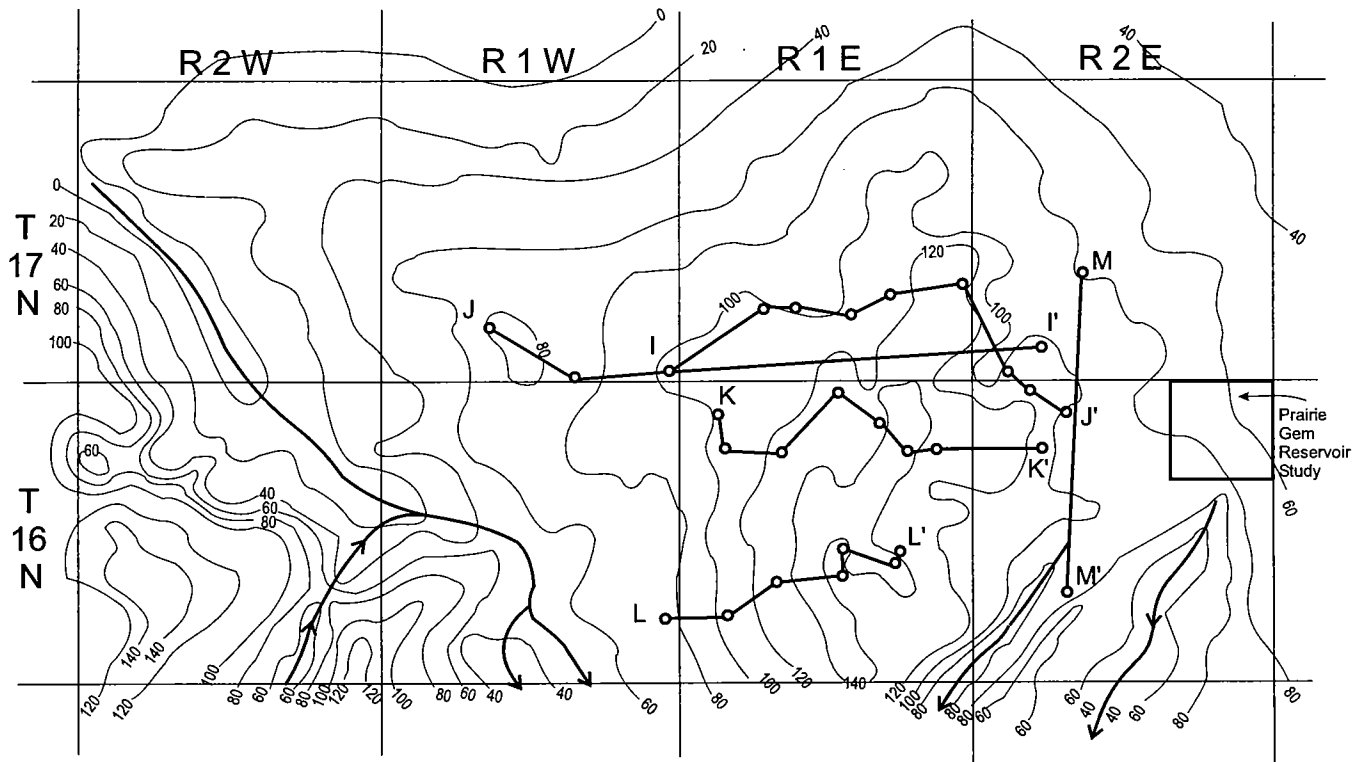


Figure 102. Gross-isopach map of Hunton Group in Lincoln, Logan, and Payne Counties, Oklahoma. Arrows indicate axis of pre-Woodford channels. Contour interval is 20 ft. Cross section M-M' shown in Figure 108.

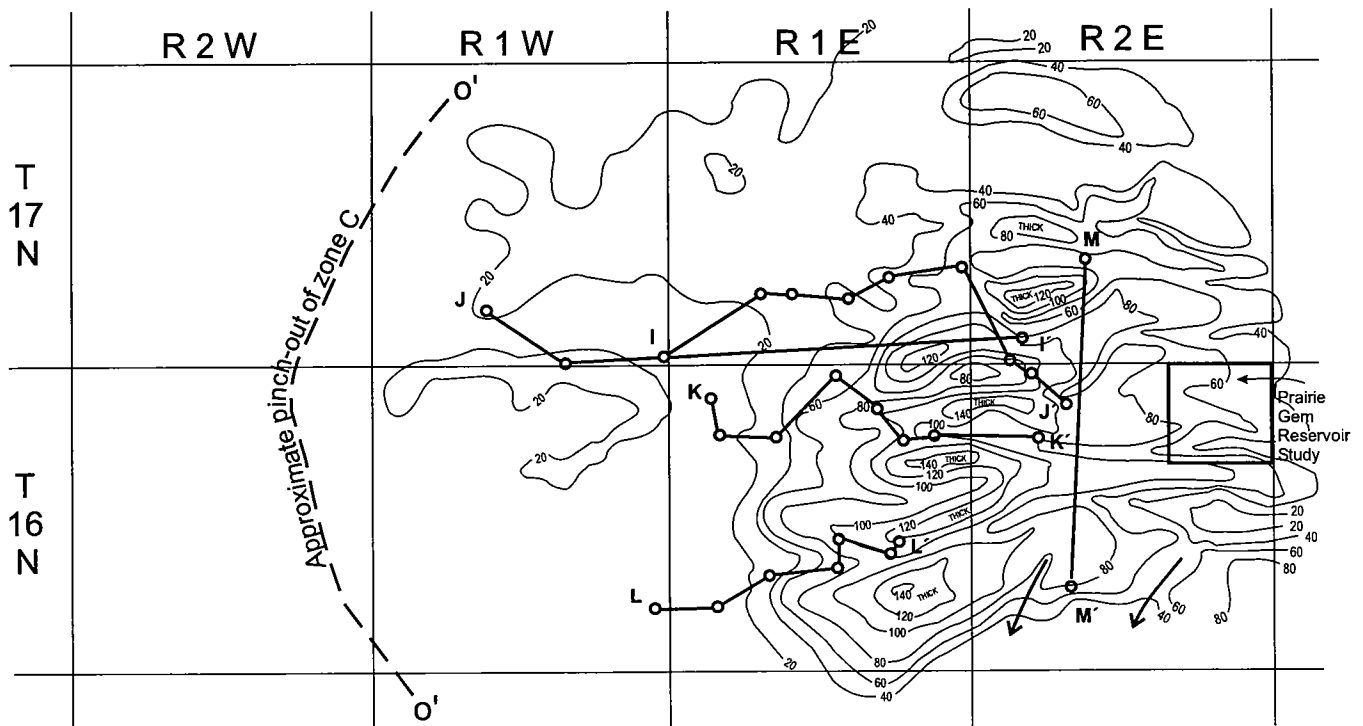


Figure 103. Isopach map of zone C of Hunton Group in Lincoln, Logan, and Payne Counties, Oklahoma. Arrows indicate axis of pre-Woodford channels. Contour interval is 20 ft. See Figures 100 and 101 for zone identification. Cross section M-M' shown in Figure 108.

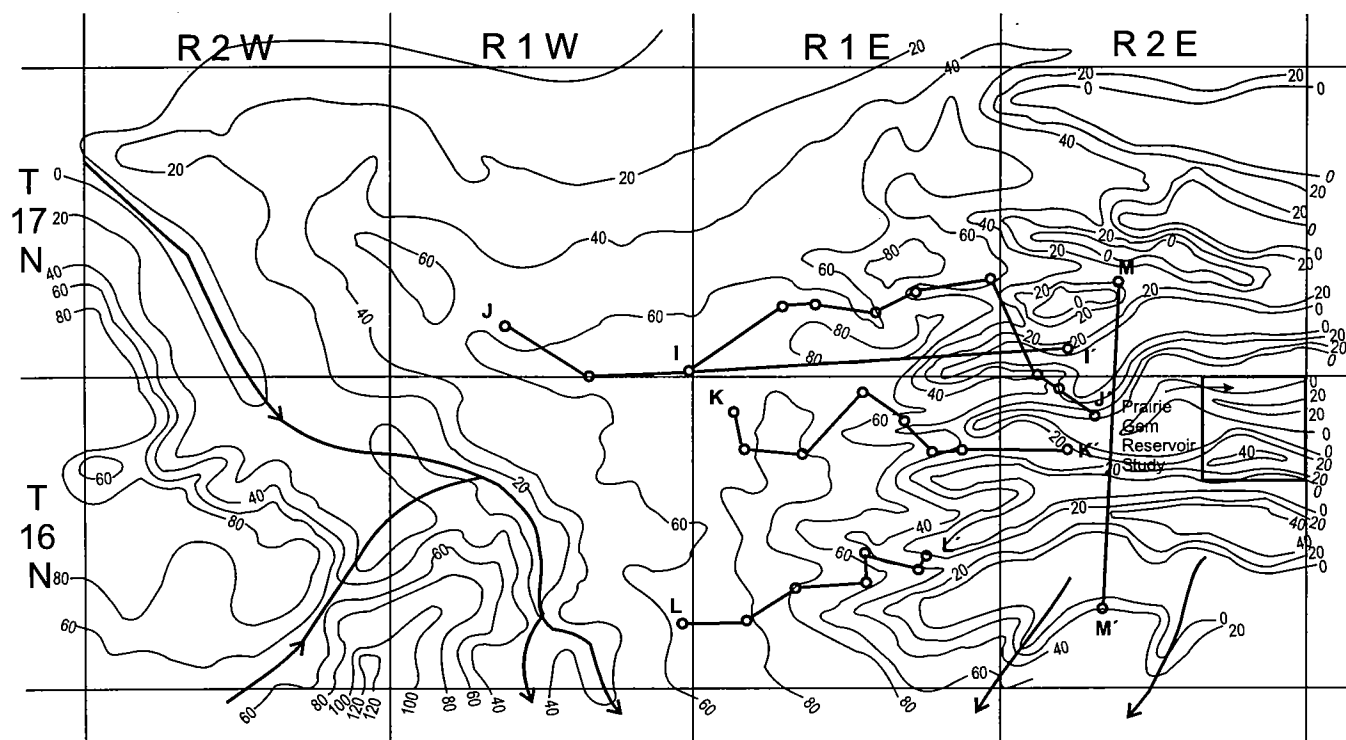


Figure 104. Isopach map of zone B of Hunton Group in Lincoln, Logan, and Payne Counties, Oklahoma. Arrows indicate axis of pre-Woodford channels. Contour interval is 20 ft. See Figures 100 and 101 for zone identification. Cross section M-M' shown in Figure 108.

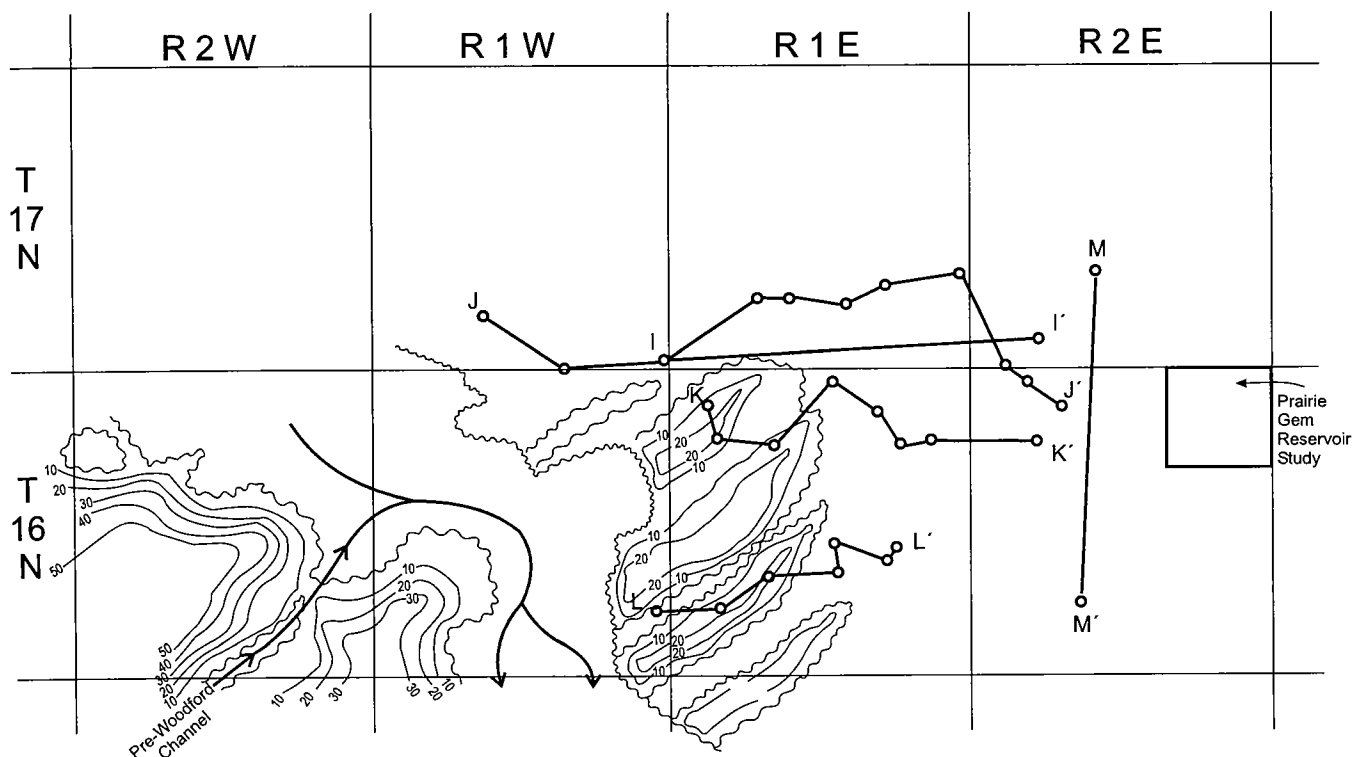


Figure 105. Isopach map of zone A of Hunton Group in Lincoln and Logan Counties, Oklahoma. Arrows indicate axis of pre-Woodford channels. Contour interval is 10 ft. See Figures 100 and 101 for zone identification. Cross section M-M' shown in Figure 108.

southeastern part of the mapped area, which is a result of post-Hunton regional uplift, tilting, and erosion to the northwest. Zone B approaches 120 ft in thickness in the southwestern part of the mapped area.

Various SP profiles of zone B suggest a presence and an absence of porosity. In the eastern part of the mapped area, the SP deflection is pronounced, and many of the wells are characterized by good porosity and permeability. Drillstem tests indicating flowing oil or salt water from this interval are common, as bottom-hole flowing pressure almost equals bottom-hole shut-in pressure. The zone is characterized by a strong water-drive capability with a substantial aquifer base. It is unclear how post-Hunton erosion, dissolution, and dolomitization affected these good porosity and permeability values. As the porous section of zone B occurs lower in the section (east to west), reservoir parameters tend to be less favorable. Many wells exhibit low porosity values, and drillstem tests commonly suggest a limited reservoir. It is not known how much secondary mineralization affected this porosity-permeability reduction. As the "clean" SP signature of zone B occurs lower in the section, a sequence of strata appears within the zone that is identical in log shape, lithology, reservoir parameters, and probably depositional environment to the entire zone C sequence. It is this repetition of identical sequences of strata that is unique in this area. The general line of demarcation from alternating east-west thick and thin deposits in the east-central part of the isopached area to a uniform thickness in the west-central part is at the approximate point observed in Figure 103.

Figure 105 is an isopach map of the uppermost layer, zone A. Owing to post-Hunton erosion and subsequent channeling of Hunton strata, this interval is thin in the mapped area. The isopach ranges in thickness from 0 to >50 ft in the extreme southwest corner of the mapped area. Based on the SP shape, the strata seem to be similar in lithology and texture to those of the underlying B and C zones; however, a few completion cards indicate that this interval may be composed of fine-grained sandstone. The Misener Sandstone is probably present in this area but would be difficult to discern by wireline-log interpretation alone.

I have known of this unique stratigraphic relationship in this area for many years (see Rottmann, 1993). However, I had not previously derived a model for the depositional environment that I feel satisfies the geom-

TABLE 9. — Characteristics of Hunton Strata in the Prairie Gem Field Study Area

1. Repetition of sequences of identical geometries of strata, suggesting repeated identical environments of deposition for multiple zones. This cyclicity of geometry is uniformly present in almost all wells.
2. Basal part of a sequence is commonly characterized by coarser strata and commonly exhibits good porosity and permeability.
3. Sharp basal contact between zones; the strata exhibit a fining-upward profile as interpreted from SP and gamma-ray logs.
4. Distal part of zone C exhibits an arcuate shape. A common demarcation point exists between alternating thick and thin deposits and those exhibiting uniformly thick strata.
5. Seems to be an absence of terrestrial deposits—i.e., clays and silts and/or sandstones.
6. Old drillers' logs and scout tickets refer to porous zones as "Hunton Detrital."

etries, trends, and characteristics of these deposits. After taking everything into consideration, however, I feel that one of two uniquely different environments of deposition may explain the origin of these deposits. Table 9 lists some of the characteristics of these strata and sequences of strata in the study area. Any interpretation of depositional environments would need to include these observations.

The first possible depositional model for this area is that of a progradational shallow-shelf carbonate environment that exhibits a sequence-stratigraphic interpretation, as described by Beaumont and by Al-Shaieb, Puckette, and Blubaugh in earlier sections of this publication. Figure 106 is a depositional model for illustrating details of sequence stratigraphy (Fritz and Medlock, 1993). Those deposits associated with intertidal and subtidal environments would certainly be appropriate for shallow-water carbonates in the Prairie Gem field study area. However, detailed core descriptions would be necessary to interpret the texture and lithofacies necessary for the determination of this environment. Such sequence-stratigraphic relationships have not been observed for the Chimneyhill Subgroup in outcrop, although this may be a function of the thick-

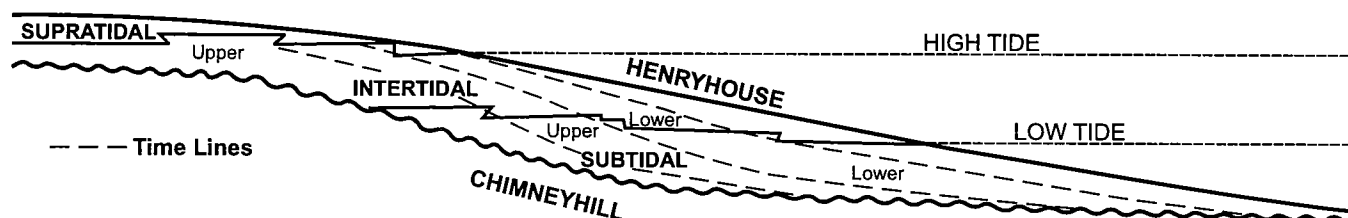


Figure 106. Depositional model showing details of progradation and aggradation. Modified from Fritz and Medlock (1993, p. 174).

ness of the interval present. I tend not to accept this model for depositional environment, because the strata in the field study seem to have taken on characteristics of a clastic deposit within marine influences. The apparent channeling of zone B into zone C suggests to me that clastic sedimentary processes may have dramatically influenced the depositional environments of this area.

The second depositional model, which I favor, within the scope of available information, is that of the influence of a local submarine fan on otherwise typical shallow-marine shelf deposits. Figure 107 is a schematic drawing showing many of the characteristics listed in Table 9 for various wells in the field study area. Figure 107A illustrates the stratigraphic relationship of zones D, C, B, and A, in ascending order. All of the characteristics listed in Table 9 apply to this repeated sequence of strata, except for item 4. Both zones D and C pinch out within the study area. Zones A and B continue to the west, well beyond the study area. Item 5 is

a typical characteristic for alluvial-fan or submarine-fan deposits. However, if, as I suspect, the source area was composed principally of carbonate material, the normal fine- to coarse-clastic relationships of fan deposits would be composed of different materials and possibly would involve different geometries.

Figure 107B shows current stratigraphic relationships of Mississippian, Woodford, Hunton, and Sylvan strata, following regional uplift and tilting of the Cherokee platform. The SP profiles for five wells within this schematic section are shown.

Figure 108A,B illustrates characteristics and a depositional model for a submarine fan (Walker and Mutti, 1973). Figure 108C,D,E,F represents the depositional history for that area defined by cross section M-M' through time. Figure 108C illustrates the distal extent of zone D. The thickness of zone D was not mapped for this study, but the zone exhibits identical characteristics to those of the distal limit of zone C (Fig. 103). Zone D thins to the west and eventually pinches out (Fig.

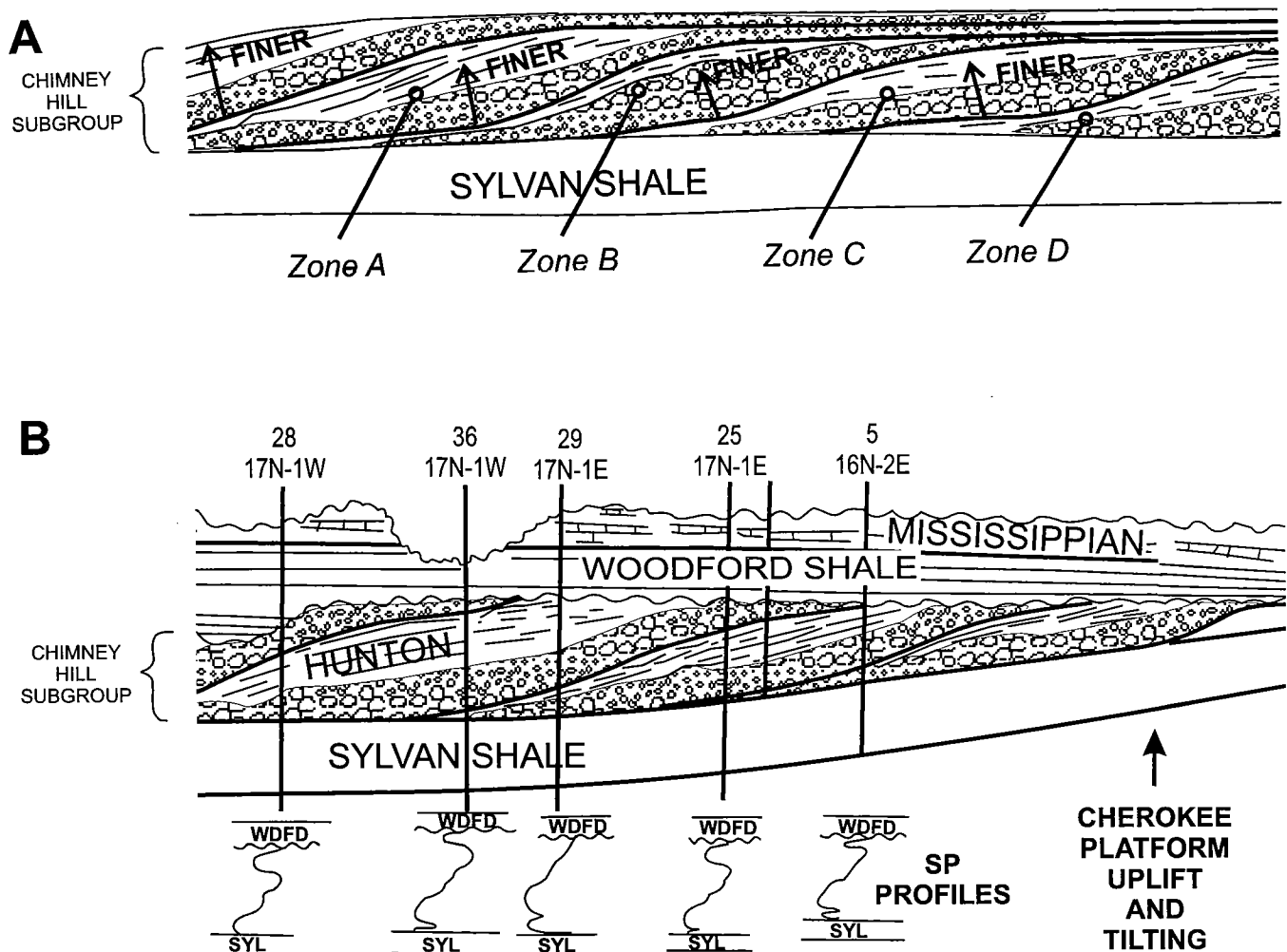


Figure 107. (A) Schematic cross section showing texture and fining-upward profile for various zones illustrated in Figures 100 and 101. (B) Schematic cross section showing current Hunton-Woodford-Mississippian stratigraphic relationships. Various SP curves are shown in line of section to compare Hunton strata and geophysical-log response.

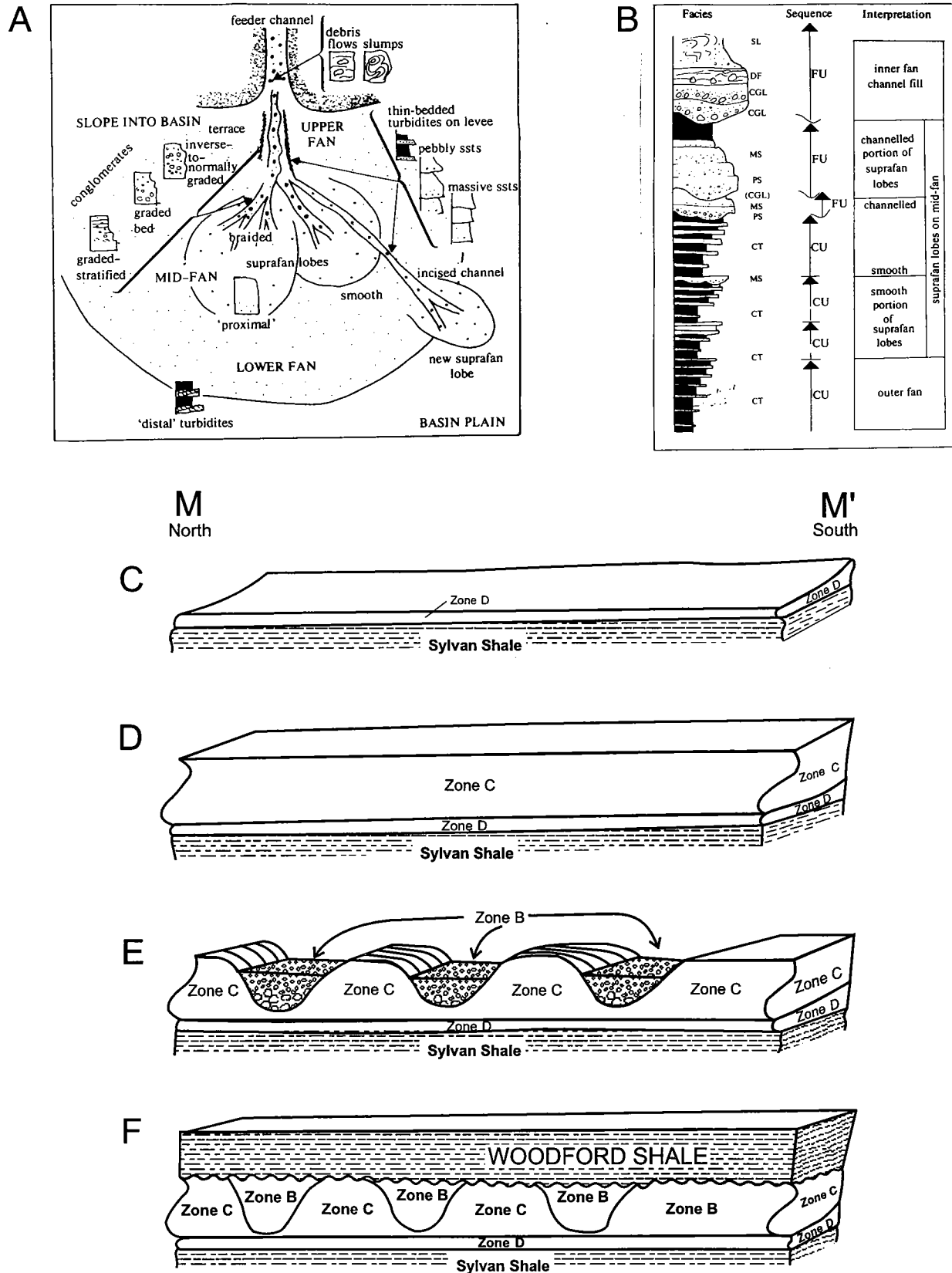


Figure 108. (A) Schematic environmental model of a submarine fan (from Walker and Mutti, 1973). (B) Hypothetical submarine-fan stratigraphic sequence produced by fan progradation (from Walker and Mutti, 1973). *FU* = fining upward; *CU* = coarsening upward; *SL* = slump; *DF* = debris flow; *CT* = classic turbidite; *MS* = massive sand; *PS* = pebbly sand; *CGL* = conglomerate. (C–E) Schematic north–south cross section M–M', illustrating deposition of zones D, C, and B. (F) Peneplanation, followed by deposition of Woodford. Line of section shown in Figures 99, 102, 103, 104, and 105.

100); the zone is thin and is generally composed of tight, impermeable strata as interpreted from porosity logs (see Fig. 96). Figure 108B suggests that deposits of the outer fan consist of fine silt and shale. These lithologies are not generally present in strata of the field study area. The absence of fine silt and shale would dramatically alter the distal geometry of a fan deposit. Fans composed of carbonate material probably would have a smaller areal extent and would not exhibit a coarsening-upward texture, as would be expected from sediments suspended in the transporting fluid. The lower fan is characterized by uniformly thick sheet deposits. The distal ends of both zones D and C fit these criteria.

Figure 108D represents suprafan lobes of zone C, which overlie and prograde westward over zone D. Owing to its position in the lobe, zone C is fairly thick. Figure 108B suggests that suprafan deposits exhibit a fining-upward profile, which is most evident for every well containing zone C deposits in the field study area.

Figure 108E illustrates the incision of the zone C suprafan lobe by the progradation of zone B deposits. These channels may have brought in new carbonate clastic material to form a new prograded suprafan lobe westward of that of zone C. The demarcation line mentioned previously is that area where the channels cease and uniformly thick sheet deposits of the distal portion

of the middle fan and lower fan begin. Eventually, as these channels became choked with sediment, new channels carried zone A deposits seaward. However, because of post-Hunton uplift and erosion in this vicinity, the geometry of zone A is not apparent.

A submarine-fan model for the environment of deposition requires certain characteristics. Those characteristics of Table 9 seem to fit this depositional model better than any other. I interpret this detritus to be composed of localized detrital material, including possible carbonate detritus from regional uplifts of carbonate strata to the northeast, perhaps the Ozark uplift. I feel that the cyclicity may have involved repeated periods of periodic uplift and erosion of these landward deposits. Where carbonate clastic material was not introduced, organo-detrital debris from normal-marine depositional environments may have been the case, as described by Amsden and others for the Clarita Formation. Two analogies for this model are found in the literature. A possible modern analogy (Davies, 1970) for this channel model is at Shark Bay, Western Australia. At Shark Bay, more than 50 tidal channels are cut into the shallow bank structure and the Wooramel-Gladstone flat on the eastern margin of the bay. The channels are as much as 0.3 mi wide, 8 mi long, and 32 ft deep. These channels are spaced at intervals from 0.2 to 2.5 mi apart. Sediments in the channels are well-

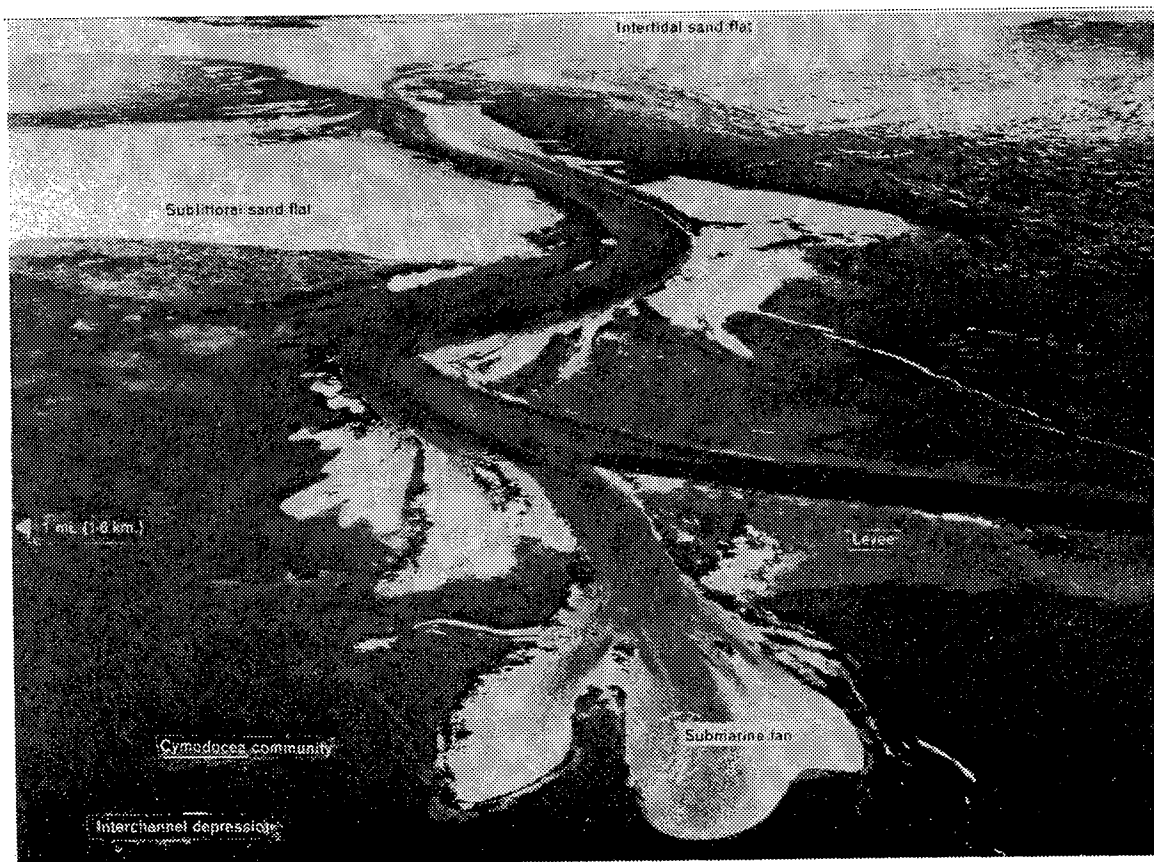


Figure 109. Submarine fan at Shark Bay, Western Australia. From Davies (1970). Reprinted by permission of American Association of Petroleum Geologists.

sorted quartzose skeletal calcarenites, derived mainly from intertidal sand flats. Davies interprets these channels as tidal drainage characterized by a net seaward transport of land-drainage siliciclastic sediment with which carbonate sediment is mixed. Figure 109 illustrates a submarine fan developing from a crevasse splay formed by the breaching of the levee of channel 21. The fan is prograding into the deeper water of the inter-channel depression and the gulf floor.

A possible ancient analogy (Fig. 110) for the depositional model for the study area is that interpreted for the Ste. Genevieve Limestone in the Bridgeport field area of Illinois (Choquette and Steinen, 1980). Three channels of sandy pellet- and ooid-rich calcarenite and calcarenitic sandstone were deposited, trending northeast-southwest across the La Salle anticline which influenced development of the La Salle shoal of Figure 110. Cores from these channels suggest they consist of a basal conglomerate with clasts of lime or (dolomitized) mudstone or wackestone and slightly cemented oolite. This conglomerate is overlain by 6–19 ft of cross-stratified fine- to medium-grained calcarenite, which, in turn, is overlain by fine- to very fine-grained calcarenite. These channel-fill calcarenite lenses are up to 21 ft thick, 0.6 mi wide, and 6 mi long. The model presented by Choquette and Steinen (Fig. 110) implies extension of the channels to the northeast. These channels are inferred to approach tens of kilometers in length and in fact may have been associated with a positive land area.

BASINWARD DISTRIBUTION OF PRAIRIE GEM PRODUCING FACIES

The previous discussion of the possible depositional environments of Hunton strata within the Prairie Gem field study area suggests that submarine fans may have been deposited in conjunction with shallow-water marine deposits. It was mentioned, but not expanded upon, that Hunton Group zones A and B did not thin and pinch out as did zones C and D, but the strata continued to the west. I believe that the submarine-fan concept is limited to areas mostly east and northeast of Prairie Gem field, and that normal shallow-water shelf deposits were laid down to the west.

Cross section N–N' (Fig. 111, in envelope) is a west-east regional cross section that ties the depositional patterns and facies of the Prairie Gem field area (wells 1 and 2) to wells in the deeper part of the Anadarko basin that exhibit greatly expanded thicknesses of Chimney-

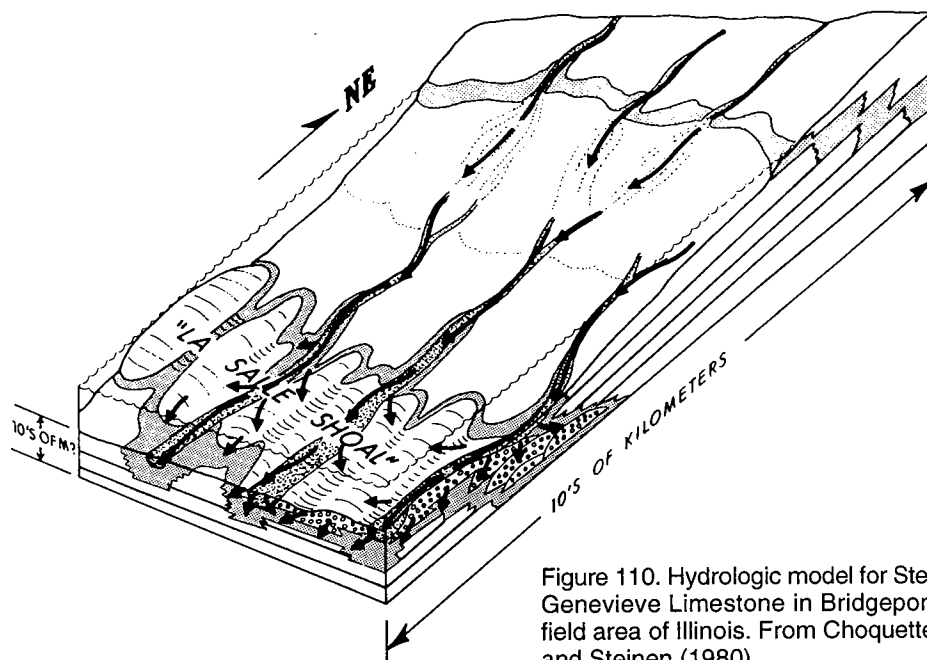


Figure 110. Hydrologic model for Ste. Genevieve Limestone in Bridgeport field area of Illinois. From Choquette and Steinen (1980).

hill strata. The revised correlations of cross section I–I' (Fig. 101) are shown for wells 1 and 2. I do not doubt that zones D and C pinch out and that zone B becomes contiguous with the Sylvan Shale, at least east of the Nemaha fault zone. The limestone of zone B is readily correlatable and basically uniform in thickness and can be easily traced to the west, southwest, and northwest. South of Prairie Gem field, the nature of the deposits is repetitious, and correlations can be questionable. At some point west of the Nemaha fault zone, a basal limestone appears, underlying zone B between wells 2 and 3 (Fig. 111). On the basis of regional correlations of this basal zone and of zone B with wells supplying biostratigraphic control, these zones appear to be the Keel–Cochrane and Clarita Formations, respectively.

As the correlation of zone B proceeds basinward, the zone can be subdivided into two distinct facies, described earlier in this report, beds 2 and 3 (cross sections A–A' and B–B', Pl. 4; cross section H–H', Fig. 87). The extension of zone A into the basin appears to correlate with bed 1. Beds 1 and 3 in the basin are primarily the organo-detrital fossiliferous limestones of the Fitzhugh Member of the Clarita Formation. Bed 2, which appears marly to slightly marly in the basin, correlates with the finer grained, shaly to marly deposits of the fining-upward texture of the suprafan deposits of the submarine-fan environment interpreted for the Prairie Gem field study area.

Beds 1 and 3 are the main Chimneyhill sequences that contain porosity and that commonly contain dolomite. The porous zones of wells 4, 5, and 6 are dolomitic limestones that grade to crystalline dolomite and illustrate the general confinement of dolomite to beds 1 and 3, commonly present in the Hunton dolomite province. Where dolomitization is widespread, bed 2

and the overlying Henryhouse Formation may have become dolomitized as well as "clean" beds of the Cochrane and Keel Formations. Cross section N-N' (Fig. 111) illustrates a dramatic thickening of Chimneyhill strata into the basin. However, what is obvious is the invariable presence of beds 1, 2, and 3 in the basin; the thickness of these beds is proportional to the overall

thickness of the Clarita, as was discussed for the Canadian flexure of the East Arnett field study. I feel there may be a link between the channel, possibly the submarine-fan, deposits at the margin of the basin and the continuation of similar and uniform bed deposition (albeit under different environments) in the basin, and the close association of dolomite with the original pre-

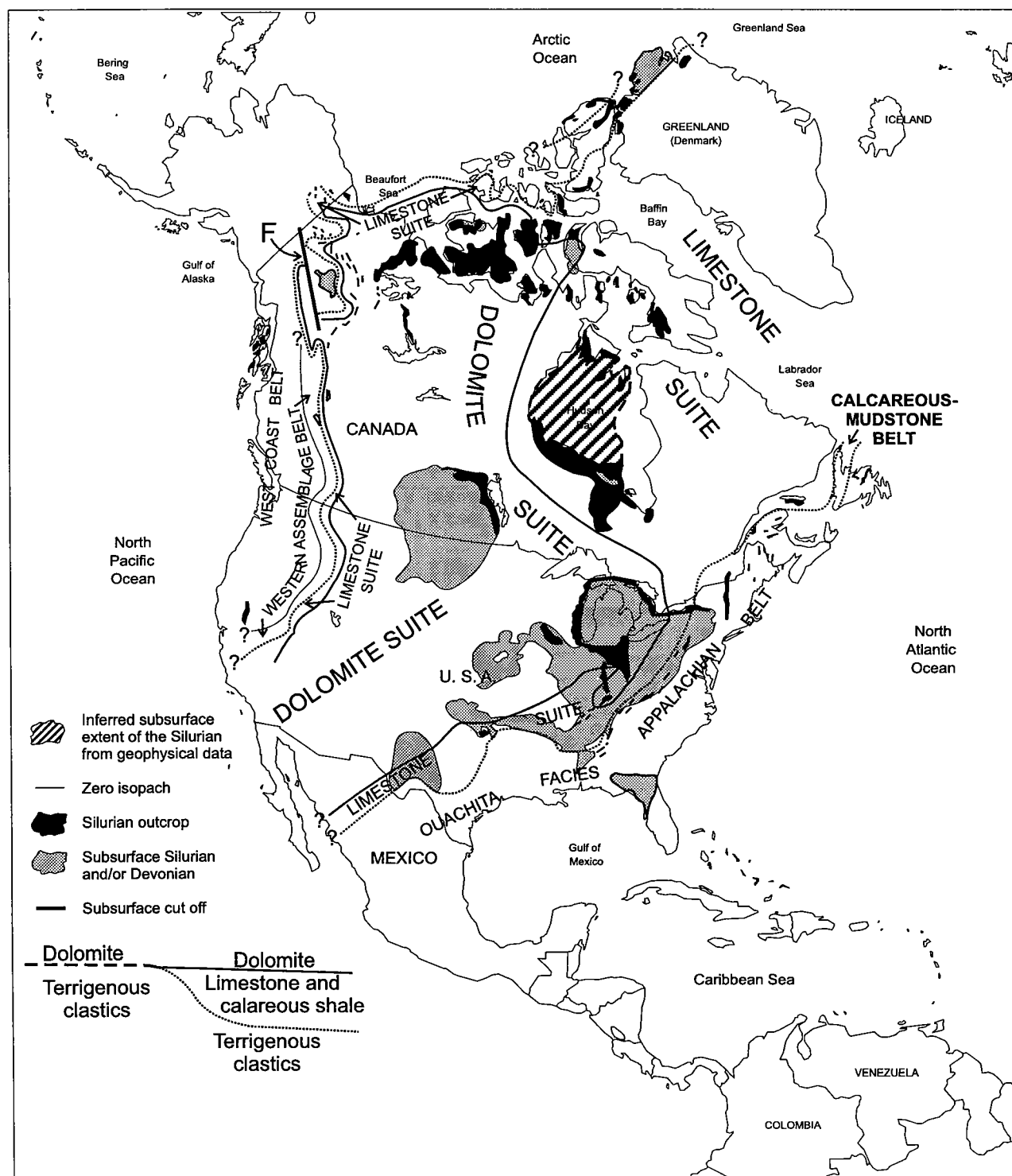


Figure 112. Geologic map of North American craton, showing Silurian surface and subsurface deposits. Modified from Berry and Boucot (1970).

dominantly porous and permeable beds 1 and 3. To further illustrate this concept, a review of dolomitization in the Hunton is necessary and appropriate.

DOLOMITIZATION OF HUNTON STRATA

Figure 27 illustrates the position of the Henryhouse marlstones with respect to the Marathon–Ouachita province. This figure also shows a boundary between limestone facies and dolomite facies that divides Oklahoma and northern Arkansas into these two provinces. North of this line, dolomitization is prevalent and occurs throughout the Silurian section. South of this line, dolomitization rarely occurs. This boundary between dolomite and limestone is actually only a part of a much larger cratonic feature. Figure 112 is a geologic surface and subsurface map, illustrating Silurian deposits and their relationship to this dolomite–limestone boundary. In the center of the craton in Silurian time were deposits containing dolomite called *dolomite suite*. Fringing this suite is a band of predominantly limestone strata called *limestone suite*. Continuing outward from the center of the craton are two provinces, the one to the west called the Western Assemblage belt (Berry and Boucot, 1970) or Cordilleran belt, and the two to the south and east, the Ouachita facies (or as Amsden calls it, the Marathon–Ouachita province; see Fig. 27) and the Appalachian belt. These orogenic belts were positive features, involving uplift and erosion of older sedi-

ments and volcanics that supplied terrigenous material for deposition. The Anadarko basin and the northern part of the Arkoma basin are separated by this lithologic boundary, with dolomite facies (dolomite suite) being to the north and limestone facies (limestone suite) to the south. It is not completely understood how the process of dolomitization occurred and what might have been the source for the tremendous amounts of Mg needed to replace limestone with facies ranging from dolomitic limestone to crystalline dolomite.

Amsden (1975, 1980) intensively studied the effects of dolomitization on strata in well cores from the Anadarko and Arkoma basins. A prudent method for addressing the possible origin of dolomitization and the methodology of its origin would be to review five conclusions that Amsden derived from his studies (Amsden, 1980, p. 55) and the bearing these observations have on the Prairie Gem field Hunton reservoir study:

1. Silurian dolomites were emplaced before middle Early Devonian (Siegenian) time. Figure 113 shows lithologies of two wells in the Arkoma basin as described by Amsden (1980) and Amsden and Rowland (1965). The Frisco Formation is present in both wells and lies between dolomites of the underlying Quarry Mountain Formation of Silurian (Wenlockian) age and the overlying Sallisaw Formation of Early Devonian (Emsian) age. If late dolomitization had occurred, it is unlikely that the Frisco would have remained every-

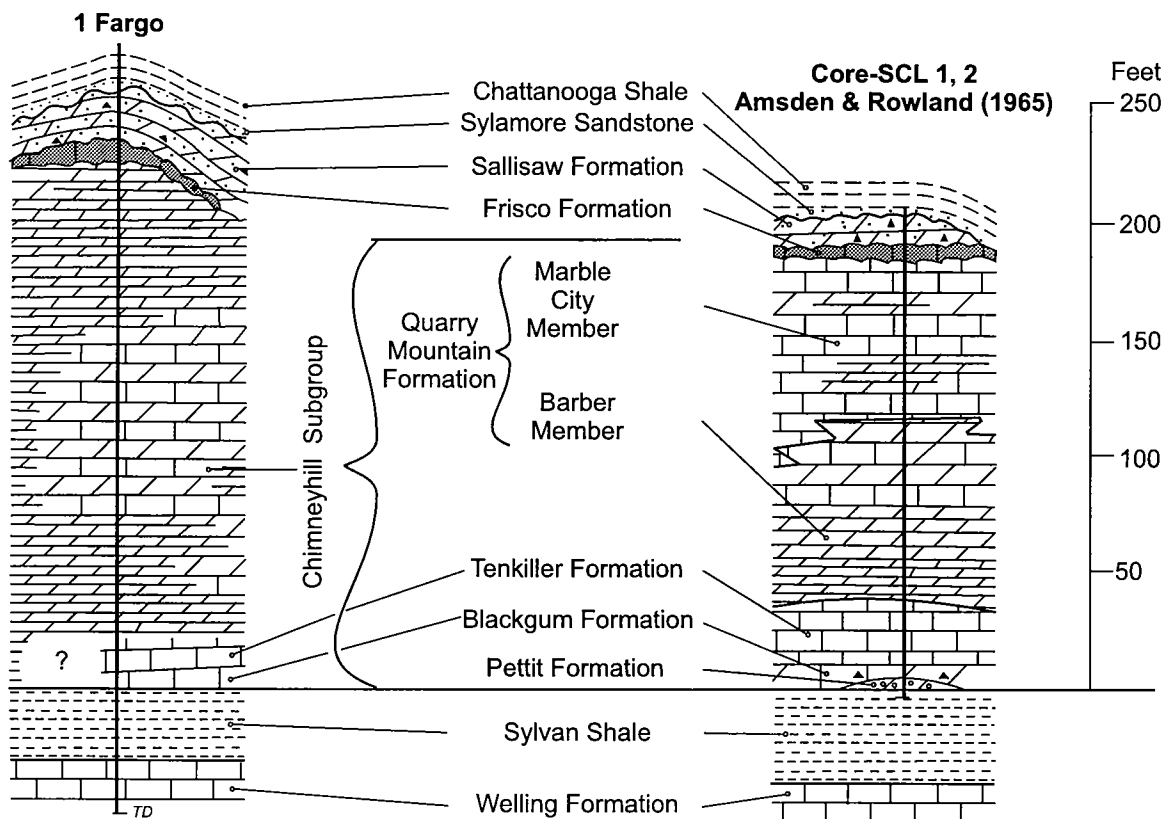


Figure 113. Schematic section of two wells in eastern Oklahoma, showing relationship of Frisco Formation to dolomites of Quarry Mountain Formation and Sallisaw Formation. Modified from Amsden (1993).

where a low-Mg carbonate (see Fig. 31 for analysis). This observation enforces the concept that dolomitization was penecontemporaneous with deposition. Amsden also notes that the dolomitization is independent of tectonic activity or unconformity relationships.

2. All of the late Ordovician–Silurian limestones, dolomitic limestones, calcitic dolomites, and crystalline dolomites bear marine fossils. Amsden's study of the biostratigraphy suggests that the quantity and type of fauna observed in outcrop and cores are independent of the magnitude of dolomitization. This implies that environmental conditions—water temperature, salinity, depth, and dissolved CO_2 levels—must have been essentially uniform to support similar life forms in both carbonate suites.

3. The limestones are a lithofacies of the dolomites, and all data support both a lateral and vertical gradation from limestone to dolomite. Amsden's outcrop and core evaluations resulted in the observation that the amount of dolomite increased from outcrops in the Arbuckle Mountains to the dolomite province. The Henryhouse Formation in the outcrop area consists of a low-Mg marlstone in which the fossils retained their microtexture. Scattered minor grains of euhedral dolomite crystals are present. Into the subsurface, detritus decreases, and the rock grades into an organo-detrital, grain-supported carbonate. The fossil boundaries are impinged upon by dolomitization and exhibit corrosion as dolomite content increases. Well into the dolomite suite, the matrix becomes almost entirely dolomite crystals, and fossils appear as corroded remnants with the microtexture still present. The final stage of dolomitization occurs where the matrix is composed of interlocking dolomite crystals. Some of the fossils are completely obliterated, and those that remain are preserved as molds. Figure 114 illustrates the distribution of MgCO_3 , seen as the percentage of total rock volume in Silurian rocks from the Arbuckle Mountains–Criner Hills region and from cores in the Anadarko basin. This figure suggests a bimodal character, with limestone and crystalline dolomite being the two principal components of the carbonate strata.

4. There is much geographic and stratigraphic variation in the degree of dolomitization, but all formations from the Keel Oolite (Late Ordovician) through the Henryhouse (Late Silurian) are affected by the dolomitization. The presence of dolomite in the pre-Devonian Hunton sequence is of economic importance, as it is highly

important to reservoir quality. Figure 115 is a chart showing the relationship of porosity to the MgCO_3 content from 22 wells in western Oklahoma. The chart shows that Silurian strata that contain less MgCO_3 generally have a lower matrix porosity than those that contain $>35\%$ MgCO_3 . Porosity development in carbonates can be complicated. Original porosity may be affected by solution and recrystallization after deposition (Choquette and Pray, 1970); dolomitization may increase the original porosity (Al-Hashimi, 1972). Amsden suggests that dolomitization and solution may occur together and that they may be related (Amsden, 1975, p. 64).

5. Hunton Silurian dolomites have a distinct geographic concentration in Oklahoma, and are part of the North American dolomite province. I believe that Amsden implied that the dolomites are concentrated in a band from eastern Oklahoma through central Oklahoma and into western Oklahoma approximately parallel to the limestone–dolomite boundary illustrated in Figure 27. He also stated that, in his opinion, Silurian thickness and dolomitization were not related (Amsden, 1975, p. 49). However, in my opinion, there is a strong relationship between thickness and dolomitization. The thickness I am referring to is not of the total

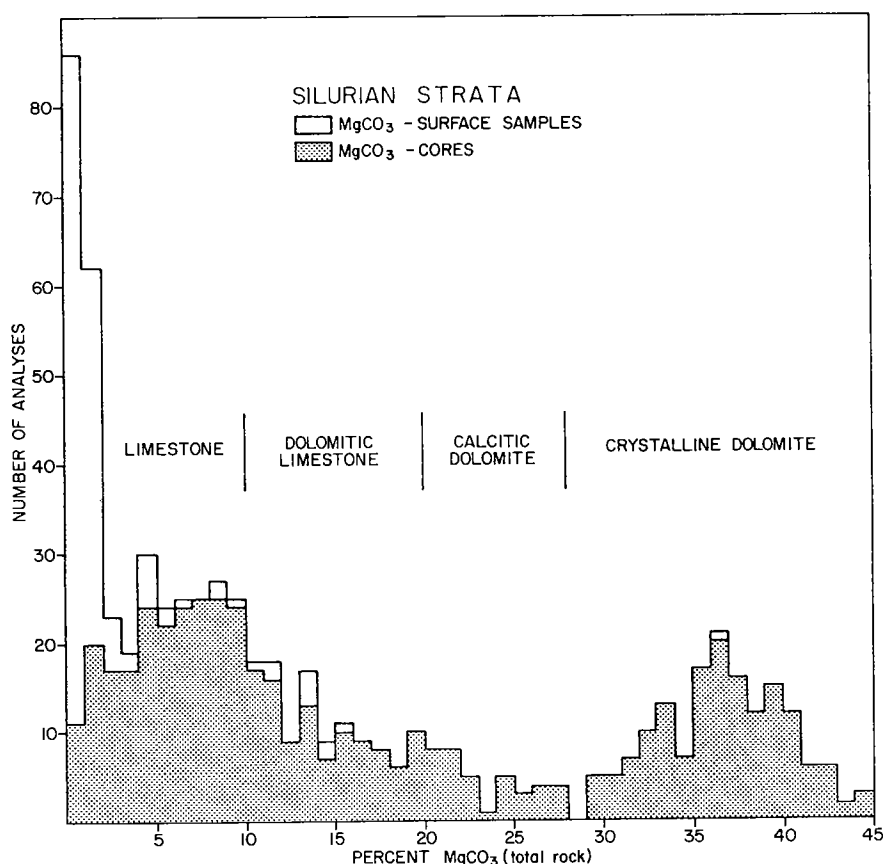


Figure 114. Frequency diagram based on analyses of 148 surface samples and 510 core samples for distribution of MgCO_3 (as percentage of total rock volume) in Silurian rocks from Arbuckle Mountains–Criner Hills region and Anadarko basin (Amsden, 1975, p. 48).

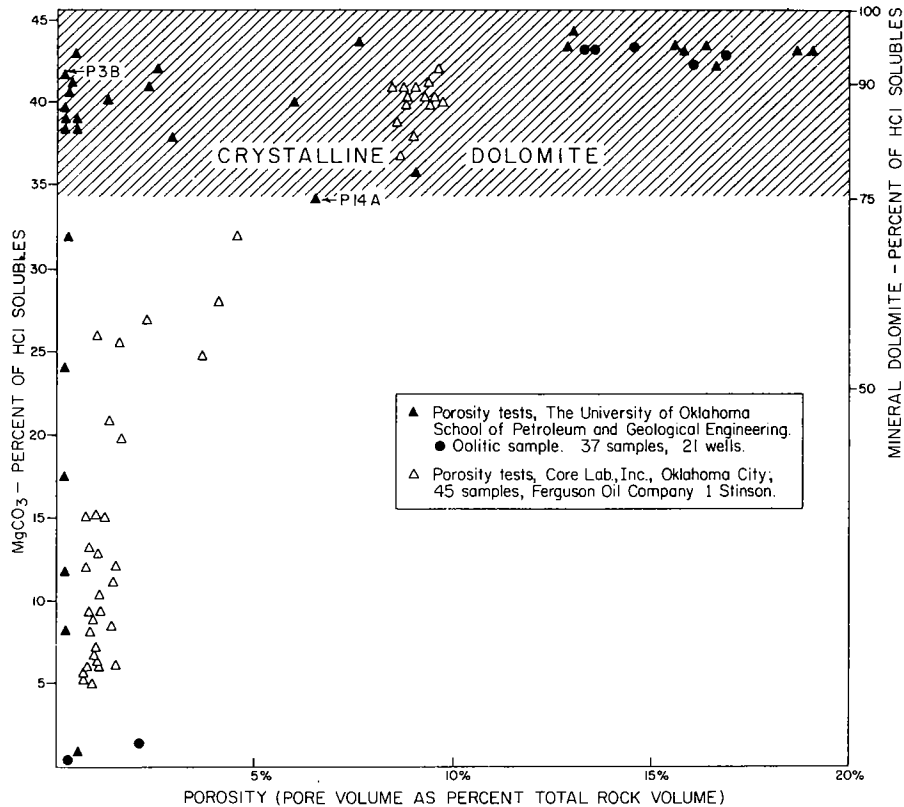


Figure 115. Chart showing relationship of porosity to MgCO_3 , where the latter (and mineral dolomite) are expressed as percentage of acid-soluble parts only. This also shows relation of porosity to crystalline-dolomite texture. From Amsden (1975, p. 63).

Silurian section but of specific beds within it. The shaded parts of Figure 116 show the areas of greatest dolomitization. Dolomitization decreases away from the "thick" axis to the point at which the strata approach low-Mg limestone. The boundary of the shaded area approximates the 100-ft contour that outlines the area of an abrupt Chimneyhill thickness change in central and west-central Oklahoma (see Chimneyhill isopach map, Pl. 5). Cross section N-N' (Fig. 111) extends from the channel and apparent fan deposits in Lincoln and Logan Counties basinward through these thick Chimneyhill deposits. This cross section shows that the abrupt increase in Chimneyhill thickness occurs mainly in the Clarita Formation. As mentioned before, beds 1, 2, and 3 seem to increase proportionately with an increase in thickness of the Chimneyhill. The organo-detrital sequences of beds 1 and 3 and those of the Cochrane Formation are also the sequences in which dolomitization is greatest. Bed 1 in wells 4, 5, and 6 of cross section N-N' (Fig. 111) is highly dolomitized. A gradual decrease in dolomitization probably extends vertically from this bed.

Cross section O-O' (Fig. 117, in envelope) is a stratigraphic section normal to the thick isopach trend of the Chimneyhill. Wells 1 and 7 are on either side of the Chimneyhill "thick," illustrated in Figure 116, and represent the stratigraphic section of typical Chimneyhill

and Henryhouse wells outside the shaded, thick Chimneyhill area of Figure 116. The darkened area in wells 1, 6, and 7 is that section of strata termed the "marlstone" interval, which is isopached in Figure 27 and discussed under Henryhouse stratigraphy. My observation is that the Chimneyhill and Henryhouse strata in wells on either side of the shaded thick Chimneyhill interval of Figure 116 are almost identical in correlation. This implies that the depositional environment of the Chimneyhill, Henryhouse marlstone, and upper Henryhouse was also identical on either side of this regional thick interval. Correlatable beds of the Henryhouse may have existed in the shaded thick interval of Figure 116, but dolomitization may have altered the interval, rendering it almost uncorrelatable.

Recreating the stratigraphic relationships for the Chimneyhill Subgroup and Henryhouse Formation can be tricky, and interpretations for the environment of deposition can depend entirely on the correct selection of a datum

for creating stratigraphic cross sections. Cross section O-O' (Fig. 117) provides an excellent example of the contrast in environmental interpretation that can be inferred simply by changing the datum for the cross section. The following are two interpretations for the thick Chimneyhill section as indicated in Figure 116.

The datum chosen for cross section O-O' (Fig. 117) is the Chimneyhill-Henryhouse contact. The "marlstone" sequence of wells 1, 6, and 7 is readily recognizable and easy to correlate. However, wells 2 through 5 have a lower Henryhouse section that does not have the recognizable geophysical-log pattern that is correlatable to wells 1, 6, and 7. Because of this, the datum can be chosen only by the easily recognizable upper limit of the Chimneyhill Subgroup in all seven wells. The problem with this correlation is that it suggests that the strata directly above the Chimneyhill in wells 2 through 5 are probably time stratigraphic and thus time equivalent to the strata in the same vertical position in wells 1, 6, and 7.

The cross section shows that wells 1 and 7 have a thin Chimneyhill interval that thickens toward well 4. If this stratigraphic relationship is correct, Chimneyhill strata would appear to take on the characteristics of having been deposited in a trough. Abrupt thickening on this order would require penecontemporaneous faulting similar to the thickening and thinning interval of the Chimneyhill as interpreted in the vicinity of the

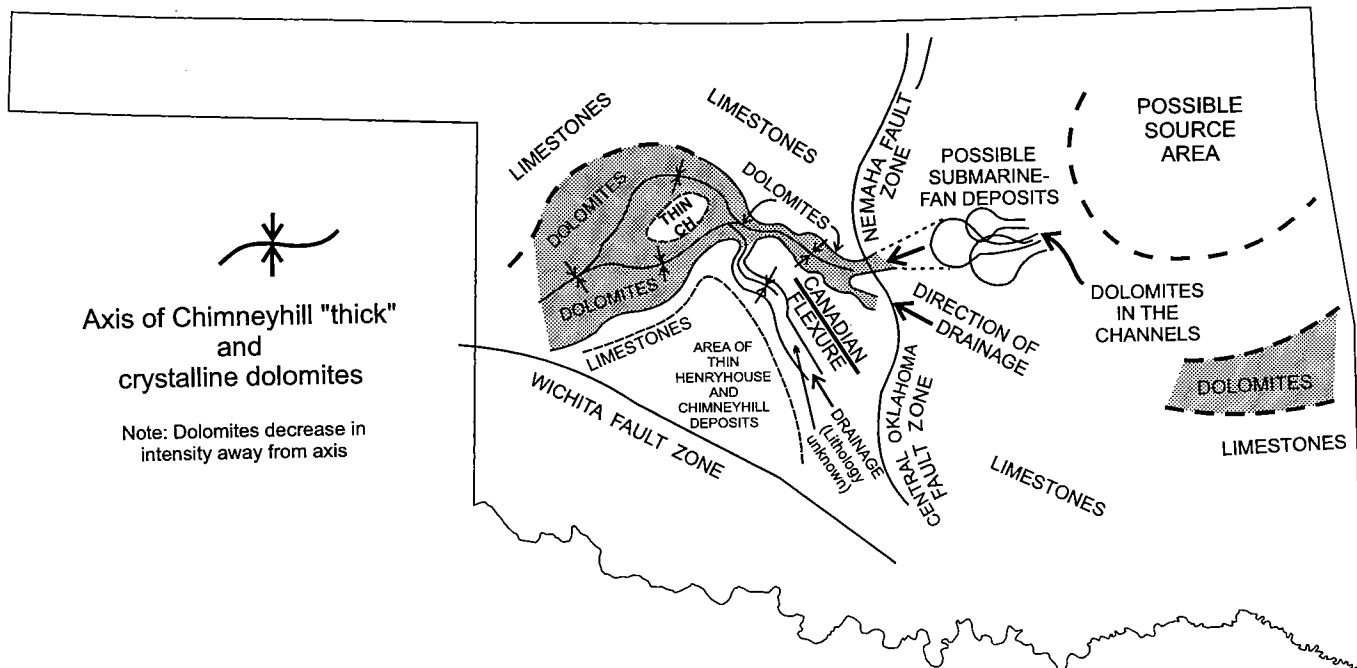


Figure 116. Geologic sketch map showing dolomite and limestone relationships. Shading indicates areas of maximum dolomite in central and western Oklahoma. Heavy arrow indicates direction of flow for possible freshwater aquifer that may have occurred during periods of Chimneyhill exposure. Possible depositional environment and source area for east-central Oklahoma are indicated.

Canadian flexure (described in the East Arnett field study). The difference between the Chimneyhill "thick" in this cross section and that found in the Canadian flexure area is that the overlying Henryhouse is not consistent in thickness here. In fact, the isopach intervals in all wells from the top of the Hunton and from the top of the Woodford to the Sylvan Shale are almost equal in all wells. The concepts derived for the relationships between the Woodford and the Hunton in the Leedey field study area suggest that structural features should not be apparent where these equal-thickness relationships hold true. The time-stratigraphic surfaces of the tops of the Woodford and the Sylvan of cross section O-O' (Fig. 117) are not parallel, because the datum chosen was probably not a flat feature at the time of deposition. Two facts support this conclusion.

First, as the top of the Hunton and the top of the Sylvan are essentially parallel surfaces in this area, structural features would be evident on structure maps for the top of the Sylvan and the top of the Hunton. A structural trough should be apparent on the Hunton structure map (Pl. 3). Such a structure would have the geometry of a meandering trough, as observed in Figure 116. Examination of the structure at the top of the Hunton (Pl. 3) yields no indication of this type of structure. Second is the lack of parallelism between two time-stratigraphic surfaces whose thickness relationships suggest that no structural movement was involved during their deposition.

A revised cross section O-O' (Fig. 118, in envelope) is the same section, but now the datum is the top of the Woodford Shale. Hanging this cross section on a known

time-stratigraphic datum creates a totally different perspective for the Chimneyhill-Henryhouse relationship and the environment of deposition. Almost readily apparent are the lack of any structural features and the almost uniform parallelism between the top of the Woodford and the top of the Sylvan. Minor thickness variations of this isopach are due to thickening into the basin from regional dip.

Revised cross section O-O' (Fig. 118) shows a thickening of the Chimneyhill at the expense of the Henryhouse. This thickening has the characteristics of a stratal buildup. Thus, rather than a trough being responsible for the thick section of Chimneyhill, as seen in Figure 116, it is likely that the thick section is actually a stratal buildup along this meandering trend. I believe there is some merit to this observation, because most of the strata that have dramatically thickened belong to the organo-detrital facies. The arrows in Figure 116 that indicate direction of drainage may in fact be the direction of currents that supplied nutrients or other life-supporting components responsible for a prolific increase in fauna within this thick Chimneyhill trend. Those areas flanking this trend may have been restricted from the introduction of this material, which may have resulted in a thinner, less prolific number of organisms. It is within this thick Chimneyhill section shown in Figure 116, specifically bed 1, that dolomites are predominant. Wells 2, 3, and 4 show porosity zones that are correlative with dolomitic limestones and crystalline dolomites described by Amsden (1975) in similar facies.

Also of importance are the highly dolomitized beds of the Henryhouse Formation. The distribution of the

Chimneyhill "thick" and the Henryhouse dolomite is related. The dolomites of the Henryhouse seem to be confined to the vicinity of this east-west-trending "thick" in central and western Oklahoma. It is possible that the mechanism for dolomitization that may have initially influenced beds 1 and 3 of the Chimneyhill also affected organo-detrital beds (*Kirkidium* biofacies) of the Henryhouse. The dolomitization does not appear to be confined to any sequence of the Henryhouse, as is apparent for the Chimneyhill.

POSSIBLE MODEL FOR SILURIAN DOLOMITIZATION

Dolomite in the geologic record is common and represents tremendous volumes of strata, yet occurrences of primary dolomite precipitation are currently rare. The lack of primary dolomite formation today might lead one to believe that seawater is undersaturated with respect to dolomite. Studies by Hsu (1966) show that seawater is actually saturated with respect to dolomite and that dolomite is more stable in the presence of seawater than either calcite or aragonite. The incompatibility of this theoretical behavior and the observed behavior is the focus of what is called the "dolomite problem." Dolomites may have difficulty precipitating from seawater because of the layered ordering of the Ca and Mg ions in the dolomite crystal lattice. In dolomites, there are alternate layers of Ca and Mg ions, much like layers of paper, and special conditions are required to produce this geometry in the crystal lattice. Dolomitic calcites are more easily formed, owing to a spiral-growth relationship of the Ca and Mg ions (Leeder, 1983, p. 298). Owing to the difficulties of direct precipitation, dolomites are more likely to have been formed by secondary dolomitization processes. Amsden supports this method and refers often to the penecontemporaneous replacement of calcitic carbonate by dolomite.

Leeder (1983, p. 298–300) suggests three methods of secondary dolomitization. The first involves evaporite deposits in broad, flat plains or sabkhas. Widespread dolomitization has occurred in this environment. Amsden discounts the presence of tidal or supratidal deposits from his study of core and outcrops, owing to the total lack of the following sedimentary features: desiccation cracks, algal mats, laminated dolomites, burrows, birds-eye structures, flat-pebble conglomerates, and an evaporite mineral suite (Amsden, 1975, p. 53–54). However, Al-Shaieb and others have referred to supratidal deposits in northwestern Oklahoma (see report in this publication by Al-Shaieb, Puckette, and Blubaugh).

A second postulated model for secondary dolomitization is the formation-water model (Leeder, 1983, p. 300). This model proposes that beds of limestone are receiving Mg^{2+} and Fe^{2+} enriched fluids from the compaction and diagenesis of mudstones. The simple lack of terrigenous materials sufficient to supply the quantity of ions needed would discount this process in the Midcontinent.

A third process, described by Leeder (1983, p. 299) has possibilities for dolomitization in the Midcontinent. This process is known as the ground-water-mixing model. The model is based on the nonlinearity of solubility curves when solutions of different components are mixed. Figure 119 illustrates the results of a study by Badiozamani (1973) for mixing solutions of seawater with fresh water. His results indicated that a mixture of 5–50% seawater and fresh water would cause calcite to be in an undersaturated condition and dolomite to be supersaturated. Thus, if a fluid of this mixture were to come into contact with calcite, either the calcite would alter to dolomite or dolomite would directly precipitate. Leeder states that the advantage of this model lies in the fact that wide-scale dolomitization can occur at the interface of fresh phreatic water and marine ground-water realms. Current examples of dolomites formed by this process can be observed in the Jamaican and Floridan aquifers (Land, 1973; Hanshaw and Harris, 1979; Randazzo and Hickey, 1978). Dolomite formed from this model affords the following conclusions (Leeder 1983, p. 300): (1) the dolomite spar and microspar crystals appear to be perfectly formed, clear and euhedral if precipitated in cavities; (2) they show perfect stoichiometry because of slow precipitation; (3) they dissolve less readily in dilute acid than do sabkha-type dolomites; (4) this process may explain the low Mg^{2+} content often found in formation waters.

The regional paleogeography and depositional environment of the area that includes the Prairie Gem field study area (Fig. 116) seem to be appropriate for the ground-water-mixing model of dolomitization just described. The depositional model of Figure 110, proposed by Choquette and Steinen (1980), was also used to explain the origin of the dolomites in the Ste. Genevieve Limestone in the Bridgeport field area. The calcarenite-filled channels (solid lines) and shallow oolitic

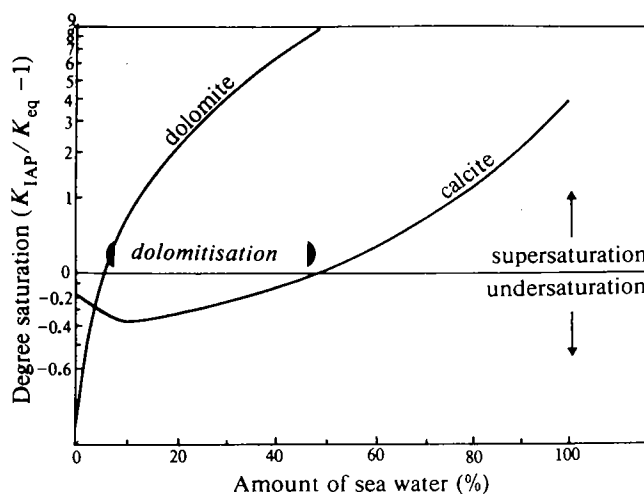


Figure 119. Graph showing that mixing of meteoric fresh water with seawater may cause dolomitization in a zone (5–30% seawater) that is undersaturated with respect to calcite and supersaturated with respect to dolomite. From Badiozamani (1973).

deposits (dashed lines) are shown in Figure 120. The shaded area represents the percentage of dolomite found in the mudstones underlying these deposits. Choquette and Steinen suggest that fresh water may

have been introduced into the highly porous and permeable mudstones from the hydrodynamically developed channel system that may have been supplied fresh water from a recharge area to the northeast. The

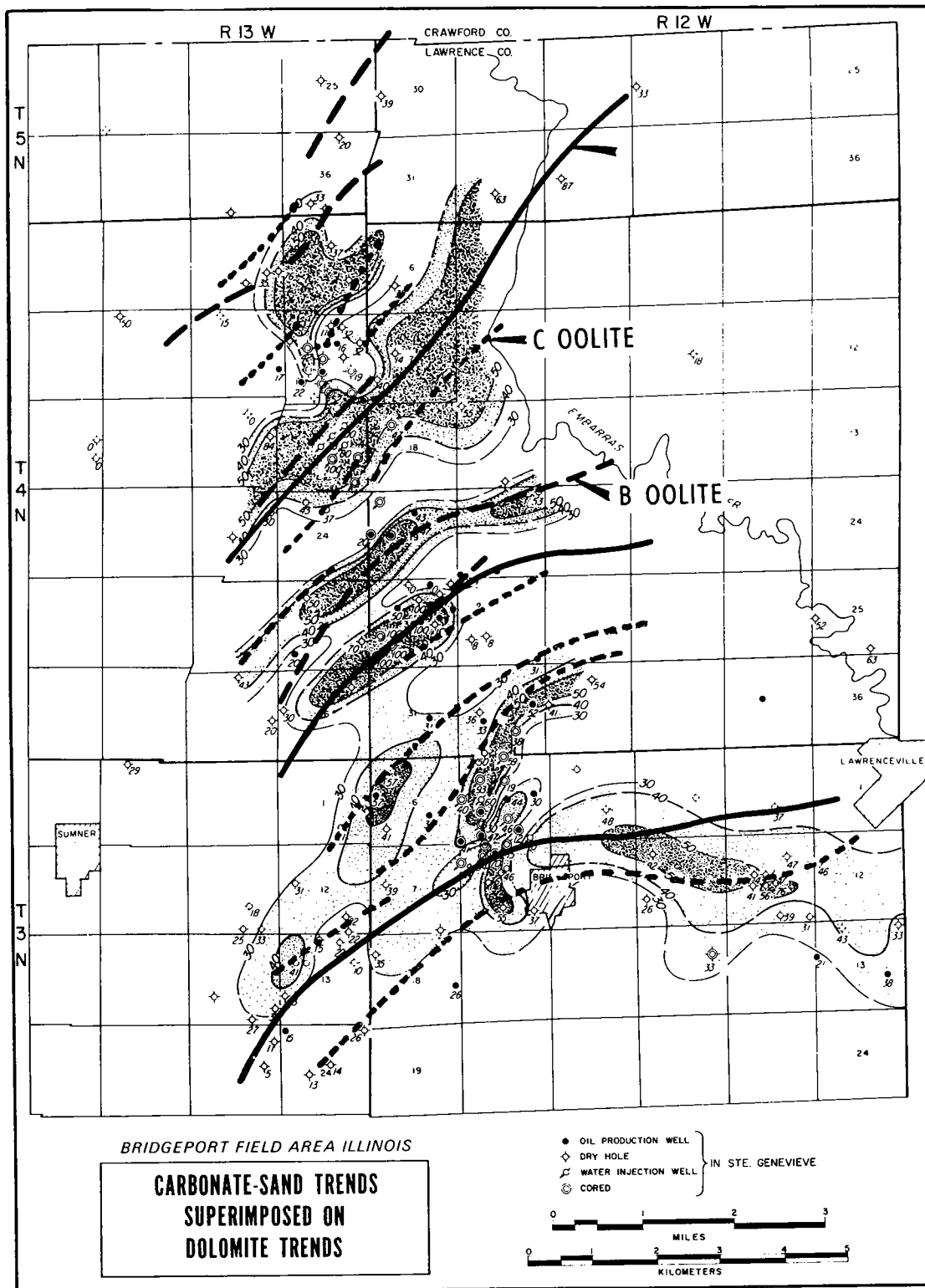


Figure 120. Map showing percentage of dolomite in relation to channel deposits for Ste. Genevieve Limestone in Bridgeport field area, Illinois. Solid lines represent channel-fill calcarenite trends and dashed lines represent oolite trends. From Choquette and Steinen (1980). See text for further explanation.

very shallow oolite-sand aquifers also may have transmitted fresh water. By the time these fresh waters reached this area, they may have mixed with seawater, diluting it enough to form intermediate concentrations favorable for dolomite recrystallization. The strong corollary between the position of the channels and the strongly dolomitized strata suggests this connection. In the Prairie Gem field Hunton reservoir area, the fresh water could have originated from a source area to the northeast. The incised channels in the Prairie Gem field area are predominantly dolomitic in composition; the strata in which the channels were incised are composed of limestone and dolomitic limestone. The knowledge that dolomite occupies the more porous and permeable facies in the channels of the proposed fan model is based on multiple descriptions of dolomite from this zone supplied by scout-ticket information and cable-tool-well descriptions, and is certainly subject to scrutiny. The dolomites of the Prairie Gem field area could have formed under similar circum-

stances. Figure 116 suggests a source area to the northeast of the study area. It is possible that a hydrodynamic system developed and ground water flowed seaward, possibly into and perhaps through this area, diluting connate water and creating a freshwater-seawater mix where dolomites could form, as described by Badiozamani (1973).

Taking this scenario one step further, a regional porous and permeable aquifer could have extended to the west of the Prairie Gem field area in the Chimneyhill Subgroup, owing to the regional and uniform deposition of beds 1 and 3. It stands to reason that fresh water may have been supplied to these beds in central and western Oklahoma from a freshwater source to the east or northeast or from uplift and exposure of the thicker Clarita beds, which may have subjected beds 1 and 3 to freshwater saturation by storms. Whatever may have been the source, the water must have flowed from east to west, on the basis of increasing deposition to the west. It is quite possible that the incursion of fresh wa-

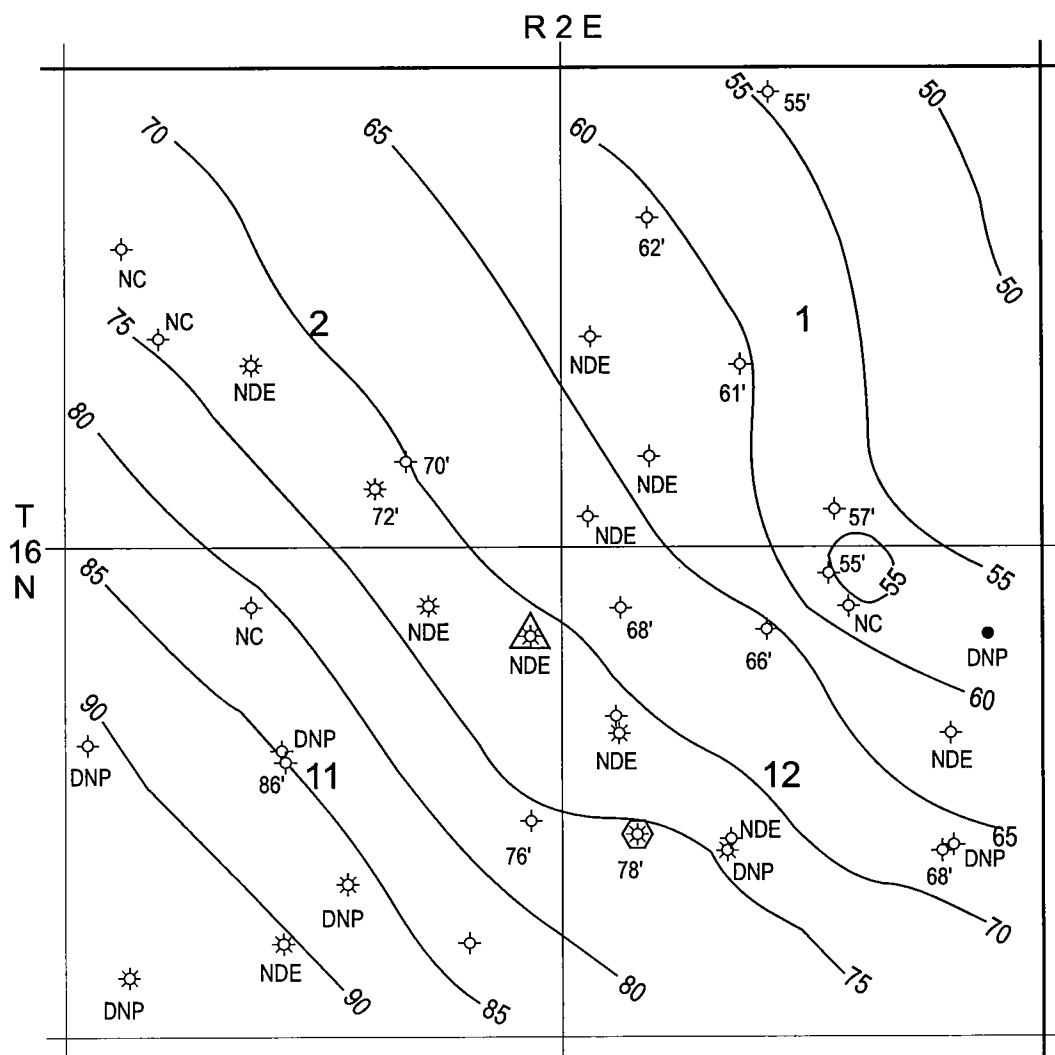


Figure 121. Gross-isopach map of Hunton Group in Prairie Gem field study area, Lincoln County, Oklahoma. Contour interval is 5 ft. DNP = did not penetrate; NC = no control; NDE = not deep enough.

ter may have been limited to the west, as Silurian deposits in far western Oklahoma grade laterally to low-Mg limestones (Amsden, 1975, 1980).

ISOPACH MAPPING

Figure 121 is a gross-isopach map of the Hunton interval for the Prairie Gem field study area. The Hunton isopach is uniform, gradually thinning from 90 ft in the southwest to 50 ft in the northeast. As discussed previously, the gross Hunton isopach does not suggest the complex internal geometry of facies described for Figures 103, 104, and 105.

Figure 122 is a net-porosity isopach map of the producing facies (zone B) in the Prairie Gem field Hunton reservoir. Stratigraphic cross section P-P' (Fig. 94) illustrates the facies relationship described previously. Wells 1 and 4 do not show the incised channel of zone B, and the matrix represents a tight, impermeable seal for the reservoir updip. The isopach map (Fig. 122) illustrates the channel geometry suggested as the model

for the environment of deposition. The two channel deposits are interpreted to be from braided streams in the suprafan of an east-west prograding fan complex as hypothesized earlier. The channel approaches 30 ft in thickness and grades to a wedge edge laterally. The channel is interpreted to be composed of fine to coarse fragmental carbonate material that was called "detrital" on scout tickets from wells drilled with cable tools. If the submarine-fan concept is correct, both the channels and the adjacent nonchannel deposits may contain abundant marine fauna.

STRUCTURE

Figure 123 is a structure-contour map of the Prairie Gem field study area, depicting the top of the Hunton Group. The strike is northwest-southeast, and the dip is to the southwest at approximately 50 ft per mi. A gentle northeast-southwest-dipping nose is apparent from sec. 1 through sec. 11. The nose appears to have a closed structure with approximately 10 ft of closure, as

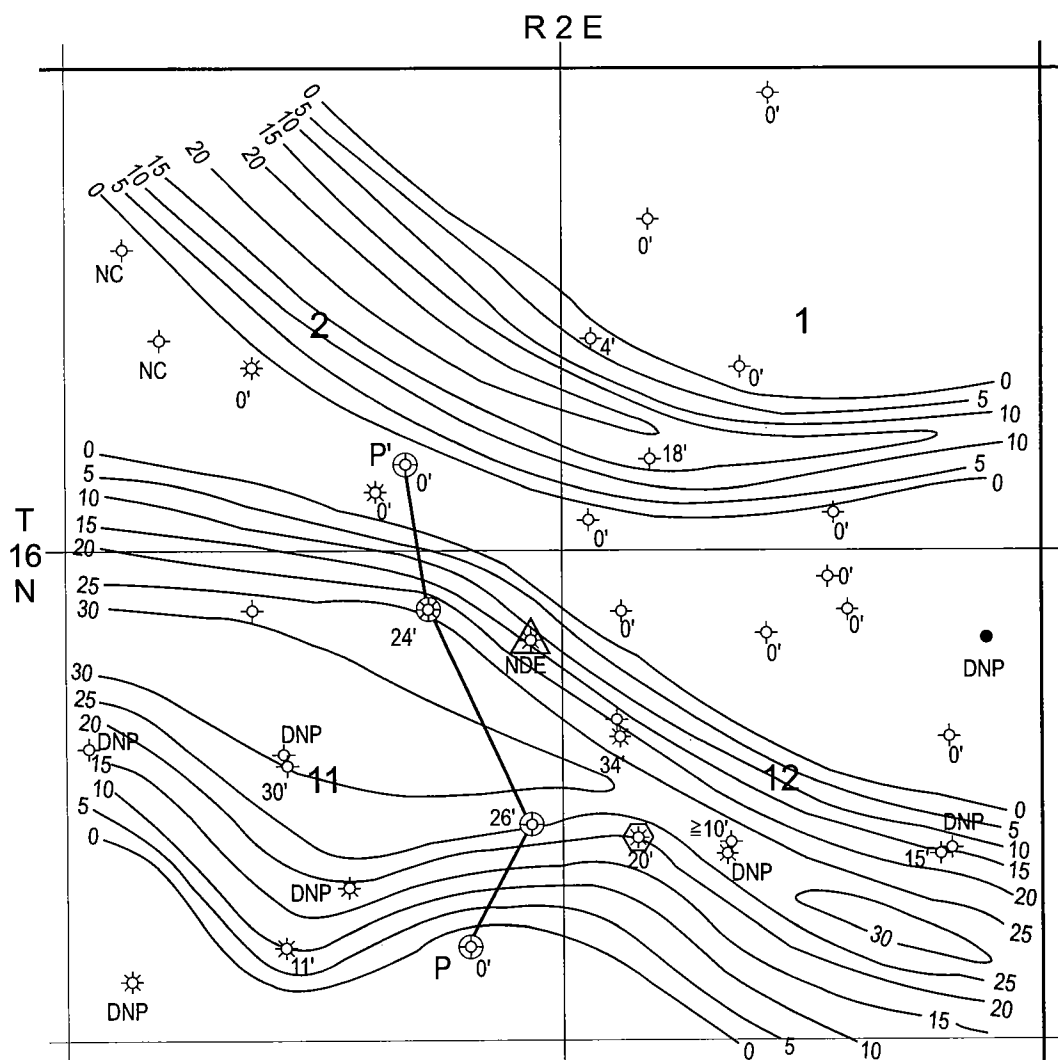


Figure 122. Isopach map of net Hunton zone B porosity in Prairie Gem field study area. Contour interval is 5 ft. See Figure 94 for cross section P-P'. DNP = did not penetrate; NDE = not deep enough.

and represents a significant water-drive energy source. Another characteristic of this zone is its excellent porosity and permeability. T. N. Berry drillstem tested the No. 1 Wilkins discovery well prior to completion. The bottom-hole flowing pressure peaked at 1,575 psia, and the shut-in pressure reached 2,030 psia in 14 minutes. The well flowed gas and oil on the test. Berry set casing at the top of the Hunton and completed the well in open hole for 14 MMCFGPD and 16 BBL of fluid per MMCFG. The production curve of Figure 124 does not show gas, as only oil was reported. The GOR of 71,428/1 clearly indicates the presence of a gas cap at discovery.

PRODUCTION

Figure 124 is the production curve for the Prairie Gem Hunton field. This field has a cumulative production of >350,000 BO, primarily from two producing wells. Well 2 of cross section P-P' (Fig. 94) is an offset producer to the discovery well. This well perforated the top 2 ft of zone B and had a daily initial flowing potential of 600 MCFG, 20 BO, and 140 BW. About 10 ft below the perforations, the resistivity drops, indicating the presence of bottom water. This water leg is present in this and other channel deposits throughout the vicinity

The presence of water-free oil and gas in the discovery well is markedly different than the numerous wells that have been completed to the south near the town of Carney. The production from those wells is characterized by high to very high water volumes, with a small oil cut. Figure 125 is a production curve for two wells in sec. 1, T. 15 N., R. 2 E., Lincoln County, Oklahoma. These wells are approximately 5 mi south of the Prairie

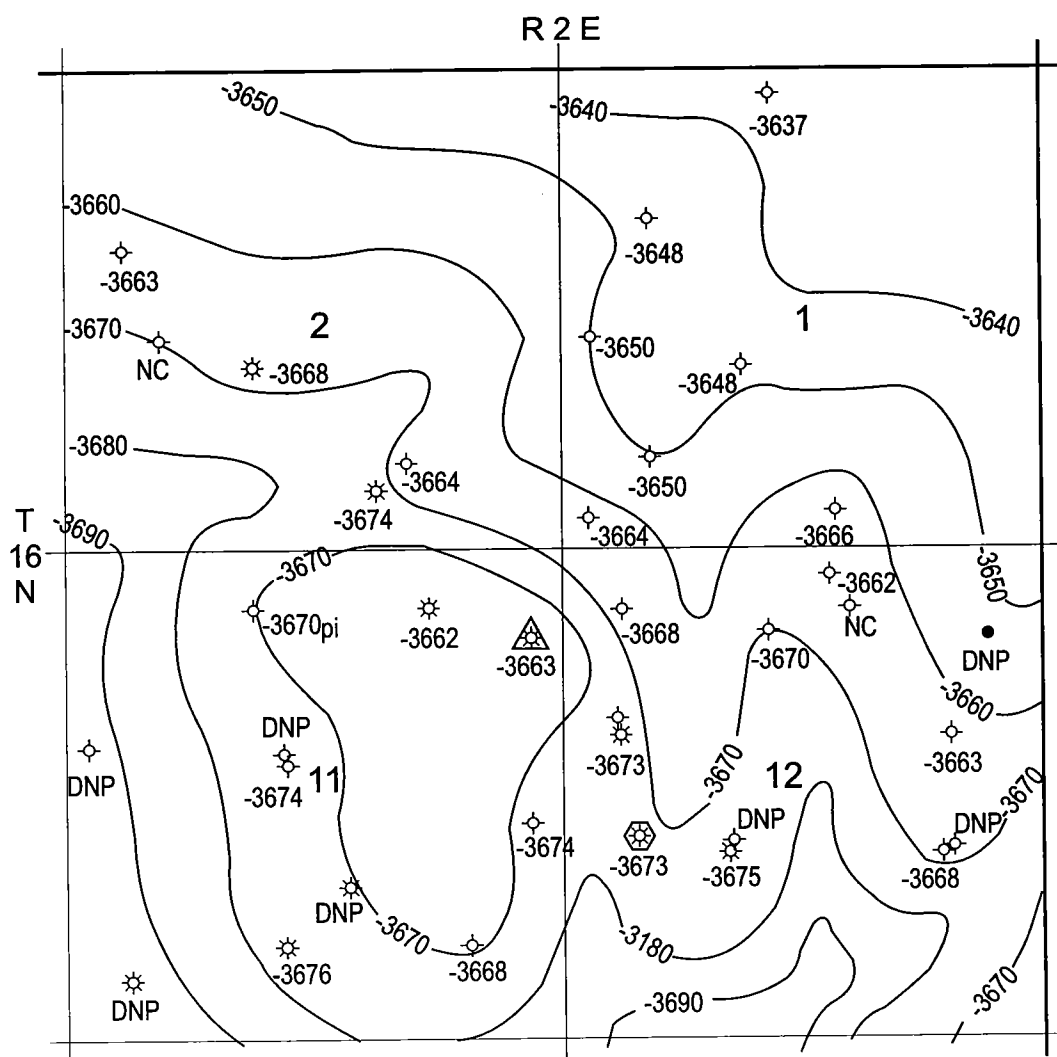


Figure 123. Structure-contour map of top of Hunton Group in Prairie Gem field study area. Contour interval is 10 ft. *DNP* = did not penetrate; *NC* = no control.

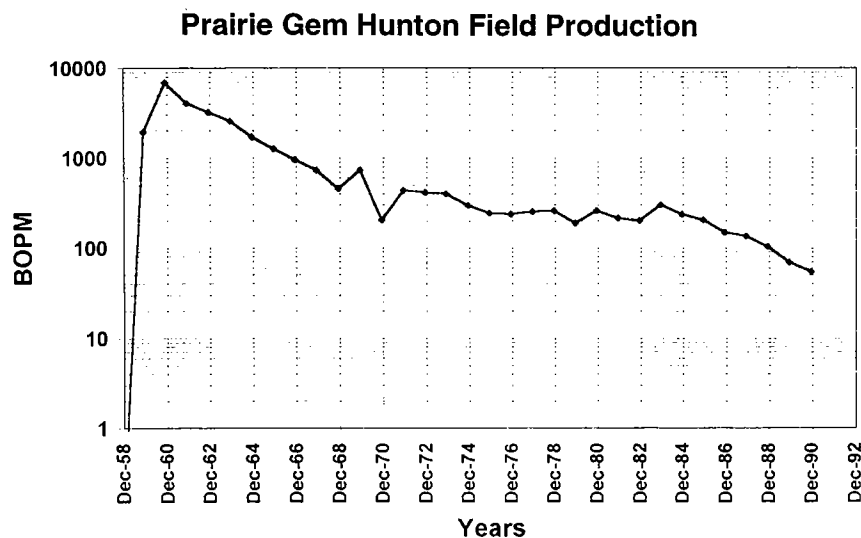


Figure 124. Graph showing oil-production curve for Prairie Gem Hunton field, Lincoln County, Oklahoma. BOPM = barrels of oil per month.

Gem field study area and are producing from the Hunton C and B zones described earlier. These wells have a complicated history, and many specific details are not clear. The No. 1 Decker, in the NE $\frac{1}{4}$ NE $\frac{1}{4}$ NE $\frac{1}{4}$ sec. 1, T. 15 N., R. 2 E., was originally drilled as a dry hole by Arthur Finston in June 1952. FCD Oil Corp. reentered and deepened the wellbore, completing it for 10 BOPD, 110 MCFGPD, and 20 BWPD from the Mississippian and Skinner zones. It is not known exactly when the

Hunton was perforated in this well, but it was probably fairly early in the production history of the well. An indication of this can be inferred from the production curve for December 1979 to September 1985. This period is marked by three increases in average monthly production, which are directly attributable to three increases in the size of the pumping units for this well: the larger the pumping unit, and, correspondingly, the greater the fluid volume produced, the larger the amount of oil that is produced. In August 1986, ST Industries drilled and completed the No. 2 Decker, in the NE $\frac{1}{4}$ NW $\frac{1}{4}$ NE $\frac{1}{4}$ sec. 1, T. 15 N., R. 2 E., from the Viola for 40 BOPD, 60 MCFGPD, and 20 BWPD. Likewise for this well, it is not clear when the Hunton was perforated, but probably it was also fairly early in the productive history of the well. In July 1987, ST Industries went bankrupt, and the wells were shut in until 1990, when Special Energy restarted the Decker lease.

In January 1992, Altex drilled the Pulliam offset leases and completed three wells in the Hunton. The net effect of increased production in the Hunton reservoir from these wells was to increase the oil cut in the two Decker wells. In January 1993, Altex converted the No. 3 Pulliam Hunton producer to a Hunton water-

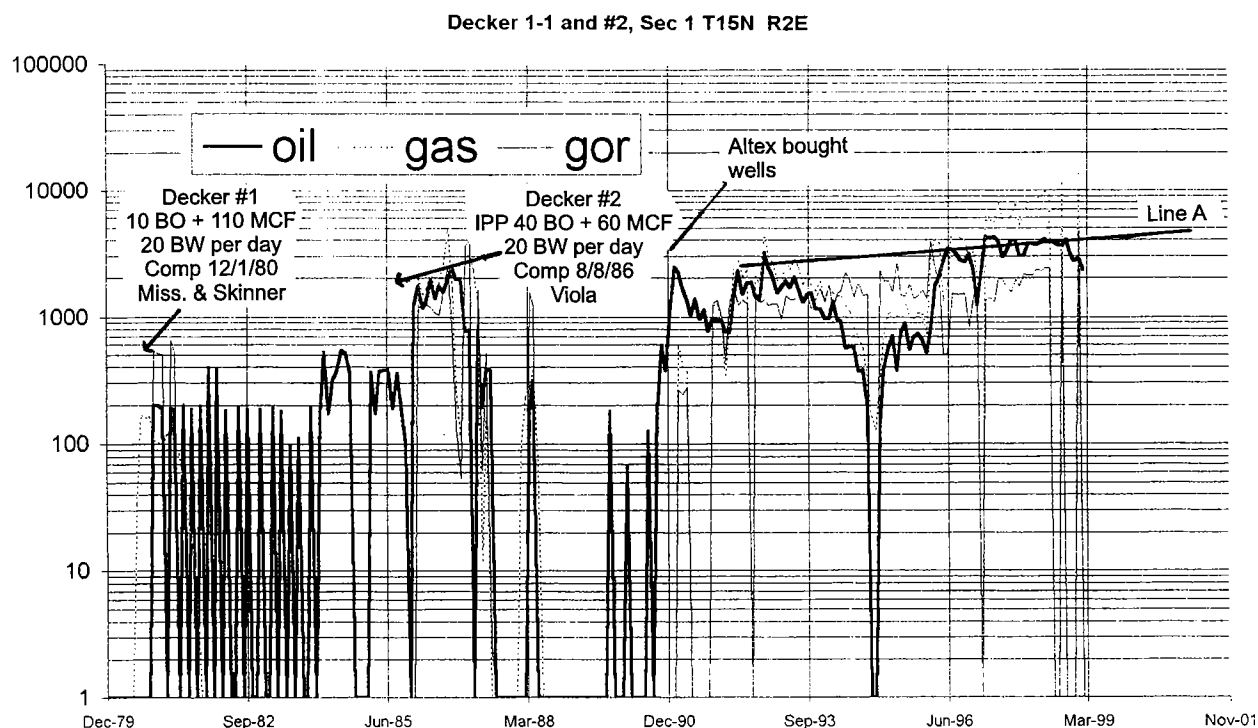


Figure 125. Graph showing oil, gas, and gas/oil-ratio (GOR) curves for two Hunton wells in sec. 1, T. 15 N., R. 2 E., Lincoln County, Oklahoma.

disposal well. This well is a direct offset to the Decker wells. Almost immediately, and for the next 2 years, production from the Hunton dropped dramatically as the direct result of reintroduction of water into the producing portion of the Hunton reservoir. It is thought that in early 1995 water disposal in the Hunton reservoir was abandoned in favor of disposal in rocks of the Arbuckle Group. The oil-production decline ceased, and production stabilized and started to increase. A dramatic increase in production occurred in December 1995, from approximately 700 BO per month (BOPM) to almost 2,000 BOPM. Line A (Fig. 125) represents a best-fit curve for average monthly production for the Decker lease from 1991 to 1999. Notice the overall increase in production with time. This type of production increase does not generally occur with low-volume oil production from reservoirs that are characterized by high water cuts. The introduction of high-volume pumps is responsible for this increasing oil-cut phenomenon with time, and will be addressed in the remainder of this report.

RESERVOIR OBSERVATIONS FOR THE CARNEY HUNTON PLAY

As noted earlier, the Prairie Gem field Hunton reservoir was selected as the field study for this report because of the similarity of the productive-reservoir parameters and depositional environment to those of the developing Hunton play near Carney. I feel that sufficient public information is available from which to draw some observations concerning Hunton production in the Carney play. It should be noted that operators in the play are privy to information not available to me because of confidentiality. This information, once released, may or may not affect the observations of this report.

Figure 126 is an isopach map of Mississippian strata in northwestern Lincoln County, Oklahoma. The Prairie Gem field Hunton reservoir study area is shown, as well as the Carney Hunton play area. A number of faults are present. The faults are probably post-Mississippian or Mississippian in age and generally are normal faults. Prior to deposition of Pennsylvanian strata, this area was exposed to erosion, resulting in a nearly peneplained surface on which Pennsylvanian strata were deposited (Rottmann, 2000). An

isopach map of the Mississippian, therefore, is an ideal means for observing the location of these faults, owing to the varying thicknesses of Mississippian strata contained in the fault blocks on each side of the fault. The upthrown side generally contains thinner Mississippian strata than the downthrown side, where a greater part of the section is preserved.

A significant northeast-southwest-trending normal fault, about 2 mi west of Carney, is apparent from the isopach map of Figure 126. This fault has significant implications for the Carney Hunton play. This fault cuts and seals the underlying porous and permeable

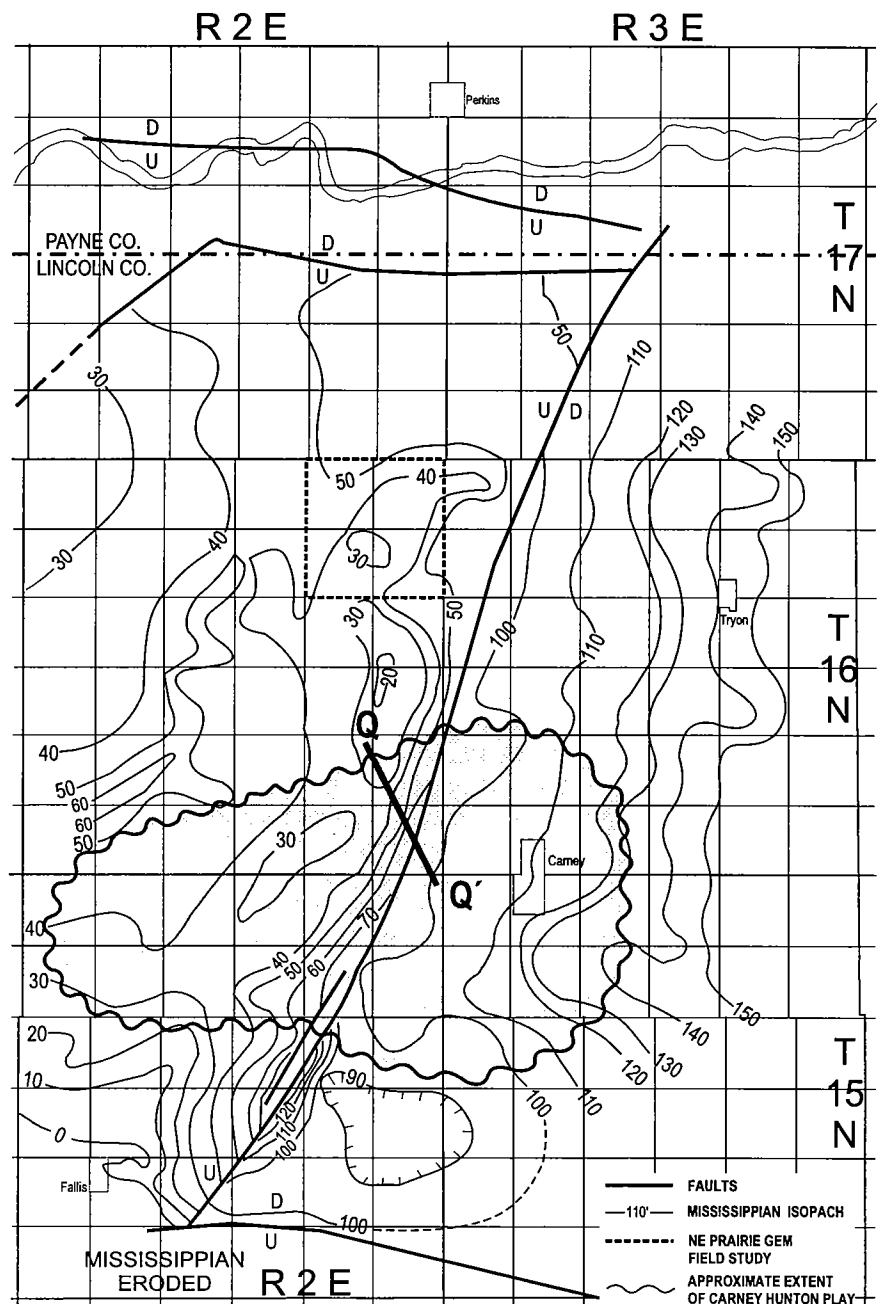


Figure 126. Isopach map of Mississippian strata in northwestern Lincoln County, Oklahoma. Contour interval is 10 ft. Hachures represent isopach "thins." Cross section Q-Q' shown in Figure 127.

Hunton reservoir. It is apparent, after years of production, that the bottom-hole pressures are significantly different on either side of the fault. The reservoirs on the east side of the fault are limited in areal extent, owing to the subcropping Hunton strata to the east and the sealing fault to the west. The various incised channel-fill reservoirs are also sealed laterally. Many of these channels have similar geometries to those mapped to the north, although the east-west channel through Carney may be considerably larger. As of this writing, bottom-hole pressures on the east side of the fault are in the 700–1,000-psia range. Original fluid volumes have decreased, and most wells are on rod pump. The drive mechanism for these reservoirs may have initially been a partial water drive, but with the decrease in pressure and fluid, it is probably now a solution-gas drive. On the west side, pressures are still high, being in the 1,500–2,000-psia range after about a year of production. Fluid volumes are also high. These characteristics suggest a strong water drive for these reservoirs.

Table 10 is a list of the reservoir and engineering data for the Prairie Gem field Hunton reservoir study area and the Carney Hunton reservoir study area. As mentioned previously, not many of the parameters for the Carney area are known, but, with a few exceptions, they should be similar to those of the Prairie Gem field area. The one major difference between the two areas is in reservoir size. Cross section P–P' (Fig. 94) clearly shows a bottom-water component to the Prairie Gem field reservoir. In fact, this reservoir is essentially an oil column above a water column. Water saturations within the oil column are probably very low, except perhaps in close proximity to the water–oil contact, where capillary pressures may create a transition zone.

The Hunton reservoir in and around the Carney area is a completely different matter. Well 2 in Figure 127 (cross section Q–Q') represents an excellent producing section, with the entire section productive, and is one of the two producing wells for the production curve of Figure 125. Resistivities for this well are in the 200–500-ohm range, which equate to a calculated salt-water saturation of approximately 10–25%, with saturations in the more porous streaks approaching 50%. This water saturation should suggest very low water production; however, this is not the case. The Hunton producers offset to this well all averaged >1,000 BWPD. The high volumes of water are probably coming through fractures in the reservoir that are not "seen" by the resistivity log, or from markedly higher porosity and permeability streaks. This is typical of Hunton wells in this play. There may or may not be a low water saturation in the reservoir rock, but there is a high water saturation

TABLE 10. – Geological / Engineering Data for Hunton Limestone, Prairie Gem Oil Field and Carney Hunton Play, Lincoln County, Oklahoma

Hunton limestone	Prairie Gem	Carney Hunton Play
Reservoir size	221.5 acres	Unknown
Well spacing (oil)	40 acre	160–40 acre
Oil–water contact	–3,672	Unknown
Gas–oil contact	Unknown	Unknown
Porosity	15%	6–20%
Permeability	Unknown	Unknown
Water saturation	15%	Varies
Gas/oil ratio	503 SCF/STB	503 SCF/STB
Thickness (net sand) ($\phi > 6\%$)	5 ft	Unknown
Reservoir temperature	120°F	120°F
Oil gravity	42° API	42° API
Initial reservoir pressure	2,100 psia	2,100 psia
Initial formation volume factor	1.31	1.31
Original oil in place (volumetric)	875,000 STBO	Unknown
Cumulative primary oil	375,000 STBO	Unknown
Recovery efficiency (oil)	43%	Unknown
Cumulative gas	Unknown	Unknown

tion in the fracture complex and in the high-permeability streaks within the reservoir. The fracture system may parallel the east–west channel system. The strata flanking the channels probably are impermeable and nonproductive, as seems to be the case in the Prairie Gem field study area. There is no apparent underlying water in the Carney Hunton reservoir area. The channel system in the Carney area is probably wide and may approach several miles. Its length could be measured in tens of miles. The productive channel at Carney could have been one of the primary feeder channels for the submarine-fan model proposed. If introduction of carbonate clastic sediments was sporadic or slow, marine fossils should be present in the rocks and representative of normal shelf assemblages. Cross section Q–Q' (Fig. 127) also illustrates the correlation of the producing channel at Carney with correlated wells to the north. Lithologic distinctions are difficult to discern because of the almost blocky nature of the strata; however, zones B, C, and D can be identified. Zones B and C are isopached in Figures 103 and 104.

OBSERVATIONS ON PRODUCTION FOR THE CARNEY HUNTON PLAY

Examination of the gas/oil-ratio (GOR) curve in Figure 125 suggests a fairly uniform ratio of about 1,500/1 for the period December 1995 through December 1997. A uniform GOR can be indicative of two different drive mechanisms. The first is that of oil expansion. Figure

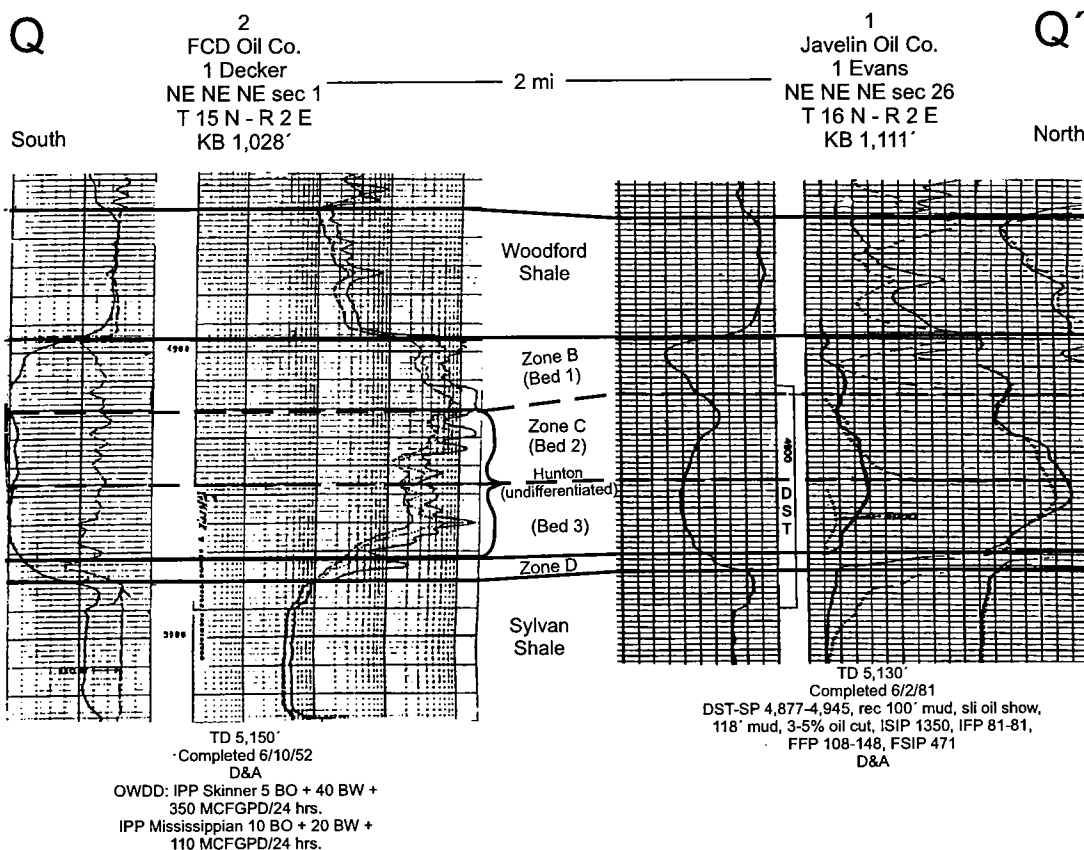
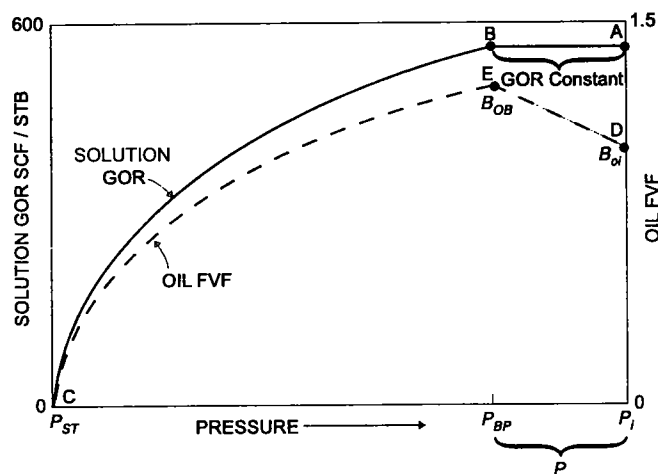


Figure 127. South-north cross section Q-Q', showing stratigraphic relationships and zone identification for wells in the Carney Hutton play, Lincoln County, Oklahoma. Line of section shown in Figure 126.

128 represents a typical GOR curve for a reservoir producing above the bubble point. Production above the bubble point implies that compressed oil is expanding (point D to E), with a corresponding drop in pressure (P_i to P_{BP}). A reservoir that is above the bubble point would have no free gas in the reservoir until the pressure of the reservoir falls below the original bubble-point pressure. If a reservoir is producing above the bubble point, then all gas must be dissolved in the oil; therefore, any produced GOR would come from the produced oil only. The solution GOR curve of Figure 128 illustrates how the reservoir GOR would be constant for production in the pressure ranges of P_i to P_{BP} .

A second drive mechanism that would yield a uniform GOR is a water drive, illustrated in Figure 129. The typical GOR versus the percentage of original oil in place produced for three primary types of drive mechanisms is shown. Only the water-drive mechanism yields a constant GOR. This is because the encroaching water is maintaining pressure and replacing the volume of oil produced. Constant pressure from a water drive would not allow the solution GOR to change because of the uniformity of the pressure. Once the pressure starts to drop, the solution GOR would change in response to gas breaking out of solution, and the resulting solution GOR curve would look like curve C-B in Figure 128.



WHERE: $P_{BP} < P < P_i$
 $B_{OB} < B_{BC} < B_{oi}$

B_{BC} = Current FVF
 B_{OB} = Bubble-point FVF
 B_{oi} = Initial FVF
 P_{BP} = Bubble-point pressure
 P = Current pressure (above the Bubble Point)
 P_i = Initial pressure
 P_{ST} = Pressure at stock tank conditions

Figure 128. Graph showing typical curves for GOR and formation volume factor (FVF) for a reservoir producing above the bubble point. From Rottmann (1999, fig. 22).

The question is, with two possible drive mechanisms that can create similar produced GORs, which one is operating in the Carney Hunton play? Two key pieces of evidence suggest a strong water drive. The Hunton producers on the west side of the fault shown in Figure 126 are producing water volumes in the range of 1,000–2,000 BPD or more and are maintaining a bottom-hole pressure generally >1,500 psia. This is typical of a water-drive mechanism.

A second line of evidence indicating the drive mechanism that is responsible for the uniform GORs of Figure 125 is illustrated in Table 11. This table shows the various reservoir input parameters used to derive output parameters of formation volume factor (FVF), GOR, and bubble-point pressure (P_{BP}). In the input column of cases 1 and 2, all variables are equal except the initial GOR.

Case 1 inputs an initial GOR of 400/1. The output states that the current GOR is also 400/1 and that the bubble-point pressure is 1,648 psia. As the discovery pressure is about 2,100 psia, this scenario would mean that a reservoir having these parameters would be producing above the bubble point by oil expansion, and the uniform GOR value of Figure 125 (point A to point B) is from this drive mechanism. However, a problem exists for this case. Table 12 is a chart of more than 50 wells from the Carney reservoir area, showing the initial-potential production values for oil, gas, water, and GOR. Notice that not a single GOR is in the vicinity of 400/1. In fact, many are 10 to 20 times this value. The fact that not a single well has a low initial-potential GOR indicates that case 1, representing an oil-expansion drive mechanism, is not valid and that the drive mechanism

TABLE 11. — Reservoir Parameters for the Carney Hunton Play, Lincoln County, Oklahoma

Input parameters		Output parameters	
<div>CASE 1</div>			
Pressure:	2,100 psia	Compressibility:	1.14E-05 1/psi
Temperature:	120°F	Form. vol. factor:	1.22 RB/STB
Gas gravity:	0.75	Live oil viscosity:	0.98 cp
Oil gravity:	42° API	Current GOR:	400 SCF/BBL
Sep. temp.:	60°F	Bubble-point press.:	1,546 psia
Sep. press.:	14.7 psia		
Init. GOR (RSI): 400 SCF/BBL			
<div>CASE 2</div>			
Pressure:	2,100 psia	Compressibility:	1.55E-05 1/psi
Temperature:	120°F	Form. vol. factor:	1.31 RB/STB
Gas gravity:	0.75	Live oil viscosity:	0.68 cp
Oil gravity:	42° API	Current GOR:	575 SCF/BBL
Sep. temp:	60°F	Bubble-point press.:	2,100 psia
Sep. press:	14.7 psia		
Init. GOR (RSI): 575 SCF/BBL			

for the Hunton reservoir in the Carney area is a water drive.

Case 2 represents production at the bubble point, at which the produced GOR would increase over time as pressure drops in the reservoir. However, with a water-drive mechanism, pressure would be maintained. The high initial-potential GOR indicated in Table 12 probably suggests that a free-gas state is also present in the Carney field area. To verify that a free-gas state exists, consider case 2 of Table 11. By inputting a value of 575 for the initial GOR, a current GOR of 575/1 will be present at the discovery pressures of 2,100 psia. Thus, 2,100 psia is the bubble-point pressure for the oil at these initial reservoir conditions. However, all of the initial potential GORs for the wells of Table 11 have GORs considerably higher than this. The excess gas being produced would have to be free gas in the reservoir, because the oil is saturated with respect to gas at a GOR of only 575/1. This scenario would still be valid under a water-drive mechanism and probably best describes the high initial-potential GORs for the Carney Hunton play. In this field, not only would the water drive replace the oil being produced, but it also would fill the void created by production of the free gas.

POSSIBLE EXPLANATION FOR "RETROGRADE OIL" PRODUCTION

The history of the Carney area Hunton play has been one of very low oil and gas shows on drillstem tests and of low initial-potential flow rates for oil and gas that gradually increase to higher rates after a period of pro-

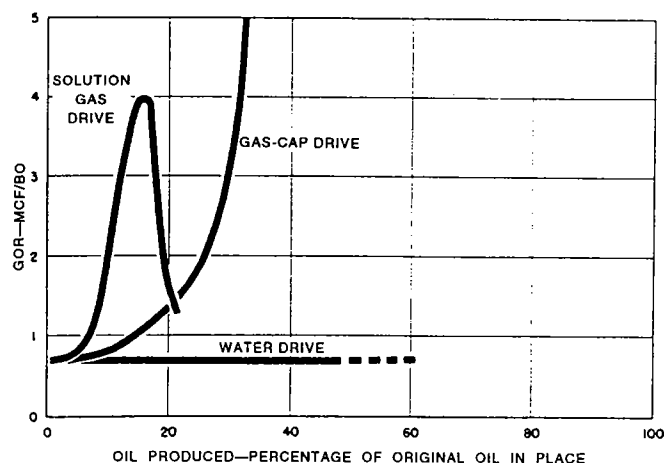


Figure 129. Graph showing general GOR curves for three primary drive mechanisms. Modified from Clark (1969, fig. 70); reprinted by permission of American Petroleum Institute.

**TABLE 12. – Oil and Gas Initial Production, Initial GORs, and Gas/Fluid Ratios (GFR)
for Parts of the Carney Hunton Reservoir Area, Lincoln County, Oklahoma**

Sec	Tnshp	Rge	Location	Operator	Well name	Oil	Gas	Water	WOR	GOR	Total fluid	GFR	Comp. date
1	15N	2E	NE SE NE	Altex	3 Decker	17	37	1,190	70.0	2,176.5	1,207.0	30.7	Feb-96
1	15N	2E	NE SW	Altex	1 Murray	90	180	2,300	25.6	2,000.0	2,390.0	75.3	Apr-98
1	15N	2E	W½SE SE	Altex	2 Pulliam	173	416	1,171	6.8	2,404.6	1,344.0	309.5	May-98
1	15N	2E	S½NW SE	Altex	1 Gray	240	581	1,966	8.2	2,420.8	2,206.0	263.4	Apr-98
2	15N	2E	SW NE SE	Altex	1 Johnny	10	80	480	48.0	8,000.0	490.0	163.3	Oct-97
2	15N	2E	NE NW	Altex	1 Noske	117	547	1,925	16.5	4,675.2	2,042.0	267.9	Dec-98
2	15N	2E	S½NE NE	Altex	1 Chiff	23	285	680	29.6	12,391.3	703.0	405.4	Jun-97
7	15N	2E	SE SE	Special	1 McBride	12	95	3,084	257.0	7,916.7	3,096.0	30.7	Sep-99
7	15N	2E	SE NE	Special	1 Cozene	38	346	4,100	107.9	9,105.3	4,138.0	83.6	Oct-99
8	15N	2E	NW SE	Special	1 Neighbors	60	400	2,600	43.3	6,666.7	2,660.0	150.4	Jan-99
9	15N	2E	SE NW	Special	1 Burnett	52	430	1,256	24.2	8,269.2	1,308.0	328.7	Mar-99
9	15N	2E	W½NE SW	Special	1 Christina	30	20	2,200	73.3	666.7	2,230.0	9.0	Nov-98
9	15N	2E	SW NE	Special	1 Margaret	42	100	501	11.9	2,381.0	543.0	184.2	Oct-98
9	15N	2E	SE NW SE	Special	1 Montgomery a/a comp. 4 days later	43 358	370 623	2,140 2,880	49.8 8.0	8,604.7 1,740.2	2,183.0 3,238.0	169.5 192.4	Dec-98 Jul-00
11	15N	2E	SW NE NE	Marjo	1-11 Ross Alan	120	300	483	4.0	2,500.0	603.0	497.5	Jul-99
11	15N	2E	SW NE SE	Marjo	1-11 Franny	109	273	438	4.0	2,504.6	547.0	499.1	Jul-99
12	15N	2E	SW NE SW	Marjo	1-12 Pearl	7	24	482	68.9	3,428.6	489.0	49.1	Oct-99
12	15N	2E	NE NE	Altex	1 Russell	53	356	1,292	24.4	6,717.0	1,345.0	264.7	Oct-98
12	15N	2E	W½NE NW	Altex	1-12 USA	100	180	430	4.3	1,800.0	530.0	339.6	May-99
5	15N	3E	NW NW SW	Sherman Larry Oil	3 Carney	171	745	1,016	5.9	4,356.7	1,187.0	627.6	Jun-99
5	15N	3E	SW SW SW	Sherman Larry Oil	2 Carney	156	1,132	829	5.3	7,256.4	985.0	1,149.2	May-99
6	15N	3E	SW NW NW	Green Opr	2-6 Gerry	100	300	300	3.0	3,000.0	400.0	750.0	Nov-98
6	15N	3E	SW SW SE	Green Opr	1-6 Patsy	72	700	1,043	14.5	9,722.2	1,115.0	627.8	Jun-98
6	15N	3E	E½SE SE	Green Opr	2-6 Patsy	80	400	450	5.6	5,000.0	530.0	754.7	May-99
6	15N	3E	SW SW	Green Opr	1-6 Bailey	89	1,250	408	4.6	14,044.9	497.0	2,515.1	Jan-98
6	15N	3E	SW SW NW	Green Opr	1-6 Gerry	243	700	360	1.5	2,880.7	603.0	1,160.9	Aug-98
7	15N	3E	SW NW	Altex	2 Harrison	14	118	430	30.7	8,428.6	444.0	265.8	Sep-98
7	15N	3E	SW NE	Altex	2 Dirks	27	279	350	13.0	10,333.3	377.0	740.1	Sep-98
7	15N	3E	W½NE NW	Altex	1 Harrison	55	450	1,800	32.7	8,181.8	1,855.0	242.6	Oct-97
7	15N	3E	NW NE	Altex	1 Dirks	37	320	1,300	35.1	8,648.6	1,337.0	239.3	Nov-97
8	15N	3E	SW NW NW	Altex	1 Thomas	3	30	350	116.7	10,000.0	353.0	85.0	May-99
24	16N	2E	SE SE	Altex	1 Martin	1	14	2,218	2,218.0	14,000.0	2,219.0	6.3	Mar-99
25	16N	2E	NE NE	Altex	1 Williams	2	20	738	369.0	10,000.0	740.0	27.0	Mar-99
25	16N	2E	N½SW SE	Altex	1-A Wolfe Terry	22	60		0.0	2,727.3	22.0	2,727.3	Dec-96
26	16N	2E	SE SW	Special	1 Big Creek	123	180	850	6.9	1,463.4	973.0	185.0	Mar-99
26	16N	2E	SE SE	Special	1 Wassam	43	223	2,200	51.2	5,186.0	2,243.0	99.4	Feb-99
27	16N	2E	NE SW SW	Special	1 Socony	85	149	3,934	46.3	1,752.9	4,019.0	37.1	May-99
28	16N	2E	N½SE SE	Special	1 Westbrook	53	481	1,213	22.9	9,075.5	1,266.0	379.9	Jul-99
28	16N	2E	SW SW	Special	1 Hunt	13	60	1,600	123.1	4,615.4	1,613.0	37.2	Sep-99
33	16N	2E	NE NW	Ancor Petro	1-33 Nossaman	1	450	200	200.0	450,000.0	201.0	2,238.8	May-82
33	16N	2E	NW NW NW	Special	1 Flying J	23	160	980	42.6	6,956.5	1,003.0	159.5	Sep-99
33	16N	2E	NE NE NE	Special	1 Mobil	13	22	1,598	122.9	1,692.3	1,611.0	13.7	Aug-99
33	16N	2E	S½NW NW	Special	1 Carter	30	287	3,207	106.9	9,566.7	3,237.0	88.7	Aug-99
34	16N	2E	S½NW NE	Special	1 Karen	67	375	1,438	21.5	5,597.0	1,505.0	249.2	Apr-99
35	16N	2E	NE NE NE	Altex	1 Crumpler	1	10	2,800	2,800.0	10,000.0	2,801.0	3.6	Apr-96
35	16N	2E	NE SW	Altex	1 Dudley	17	152	931	54.8	8,941.2	948.0	160.3	Dec-98
35	16N	2E	E½SW NW	Greentree Energy	1 Hagar	10	20	40	4.0	2,000.0	50.0	400.0	Sep-81
35	16N	2E	SE NE	Altex	1-A Crumpler	85	275	2,150	25.3	3,235.3	2,235.0	123.0	Jan-98
35	16N	2E	S½NE NW	Altex	1 Hicks-ORR	116	391	1,709	14.7	3,370.7	1,825.0	214.2	Dec-98
35	16N	2E	SW NE SE	Altex	1 Shinn	15	240	1,350	90.0	16,000.0	1,365.0	175.8	Dec-97
36	16N	2E	NE SE SW	S T Industries	36-1 Carney State	15	10	2,000	133.3	666.7	2,015.0	5.0	Dec-86
36	16N	2E	SW SE	Prime Operating	4 Donahoo	130	147	825	6.3	1,130.8	955.0	153.9	Aug-97
36	16N	2E	W½NE SE	Jet Oil	1 Donahoo	65	50	205	3.2	769.2	270.0	185.2	Jan-87
36	16N	2E	W½NE SE SE	Jet Oil	2 Donahoo	22	52	80	3.6	2,363.6	102.0	509.8	Oct-83
36	16N	2E	E½NW SE	Jet Oil	3 Donahoo	63	50	290	4.6	793.7	353.0	141.6	Sep-87
36	16N	2E	N½SW NE	Altex	1A Wilson Ramey	22	70	340	15.5	3,181.8	362.0	193.4	Nov-96
36	16N	2E	NE SW SW	Altex	2 Carney State	88	342	680	7.7	3,886.4	768.0	445.3	May-99
36	16N	2E	SE SE NW	Altex	2 State ORR	28	246	1,630	58.2	8,785.7	1,658.0	148.4	Apr-96
36	16N	2E	NE SW	Altex	1 Carney State	170	230	2,800	16.5	1,352.9	2,970.0	77.4	Nov-96

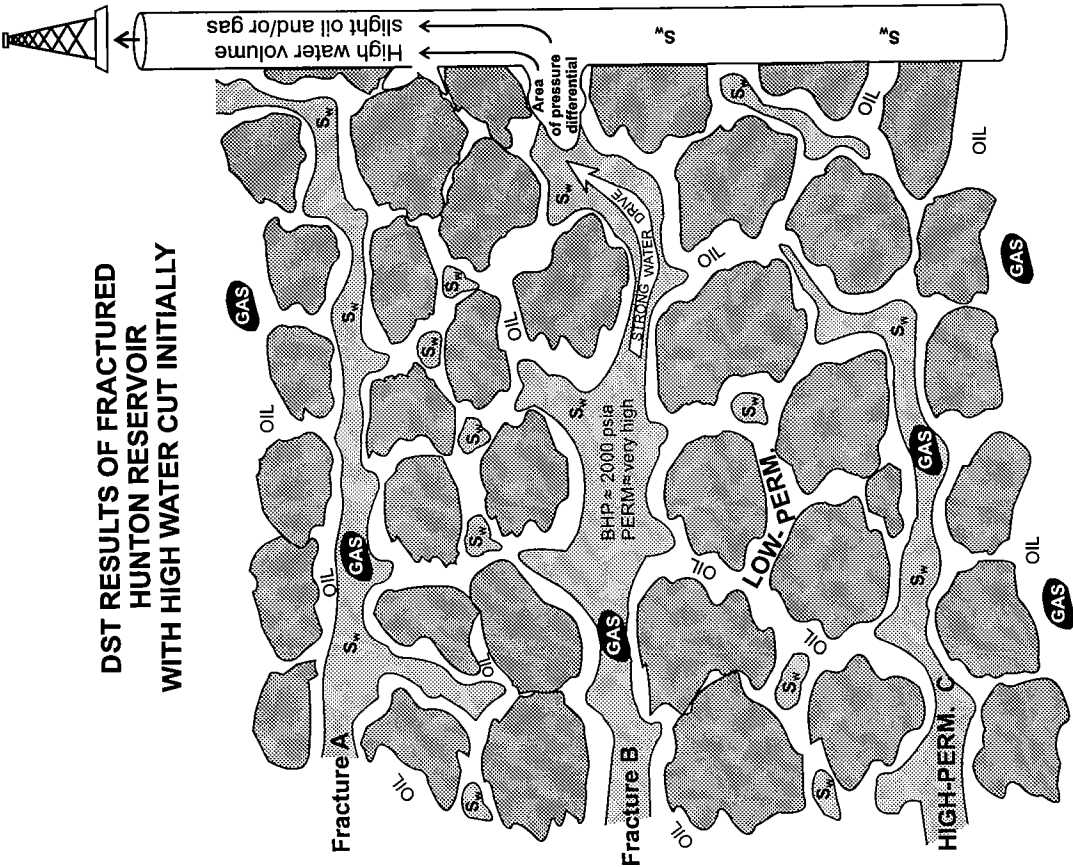


Figure 130. Schematic diagram of Hunton reservoir in contact with drillstem-test (DST) tool. See text for explanation. S_w = water saturation; BHP = bottom-hole pressure.

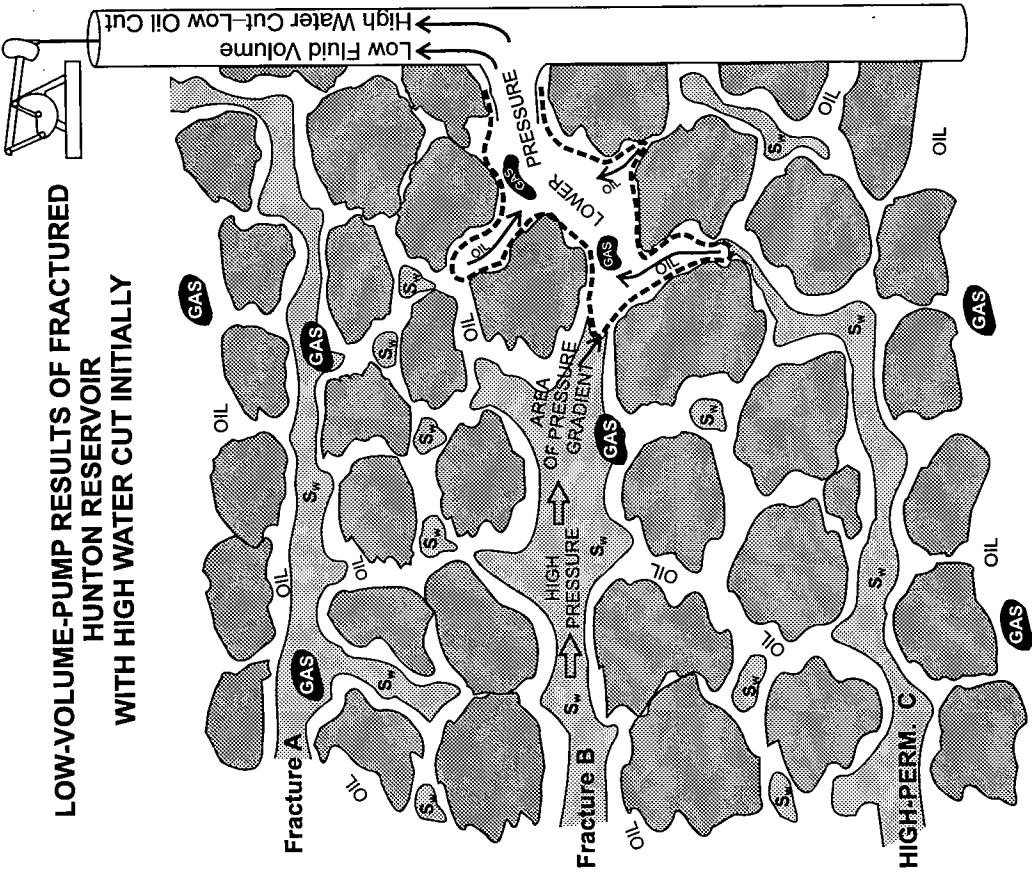
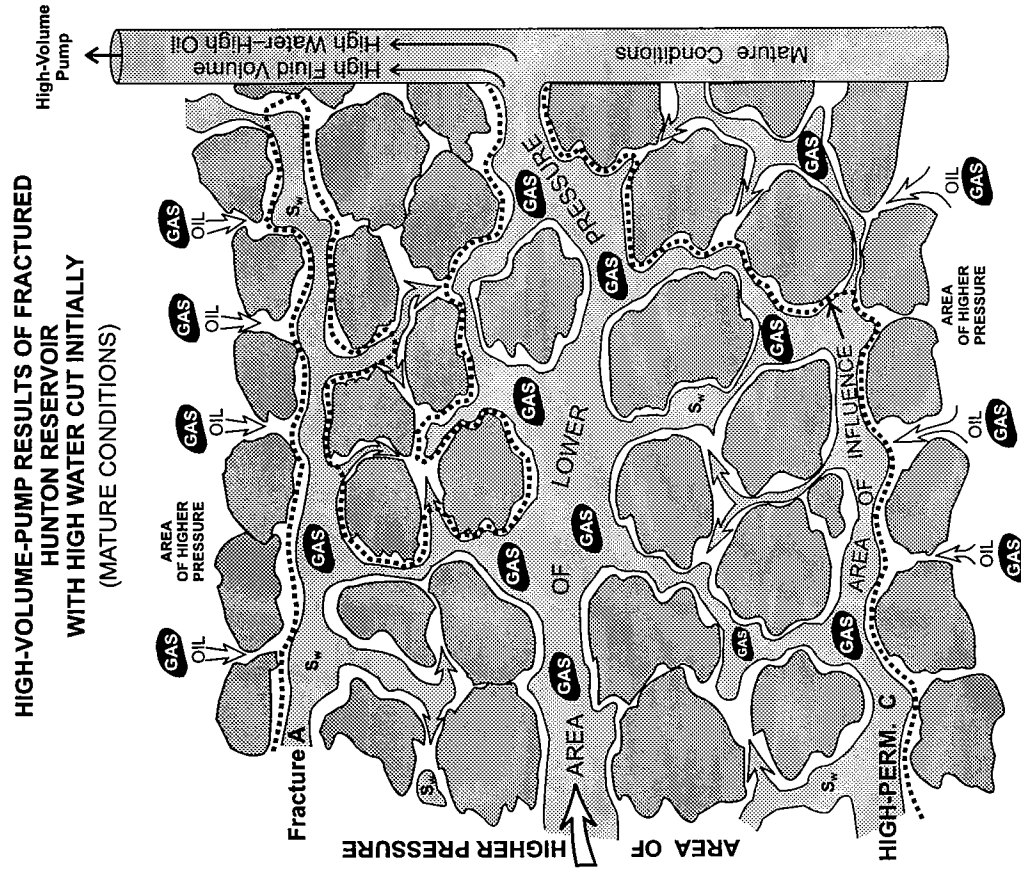
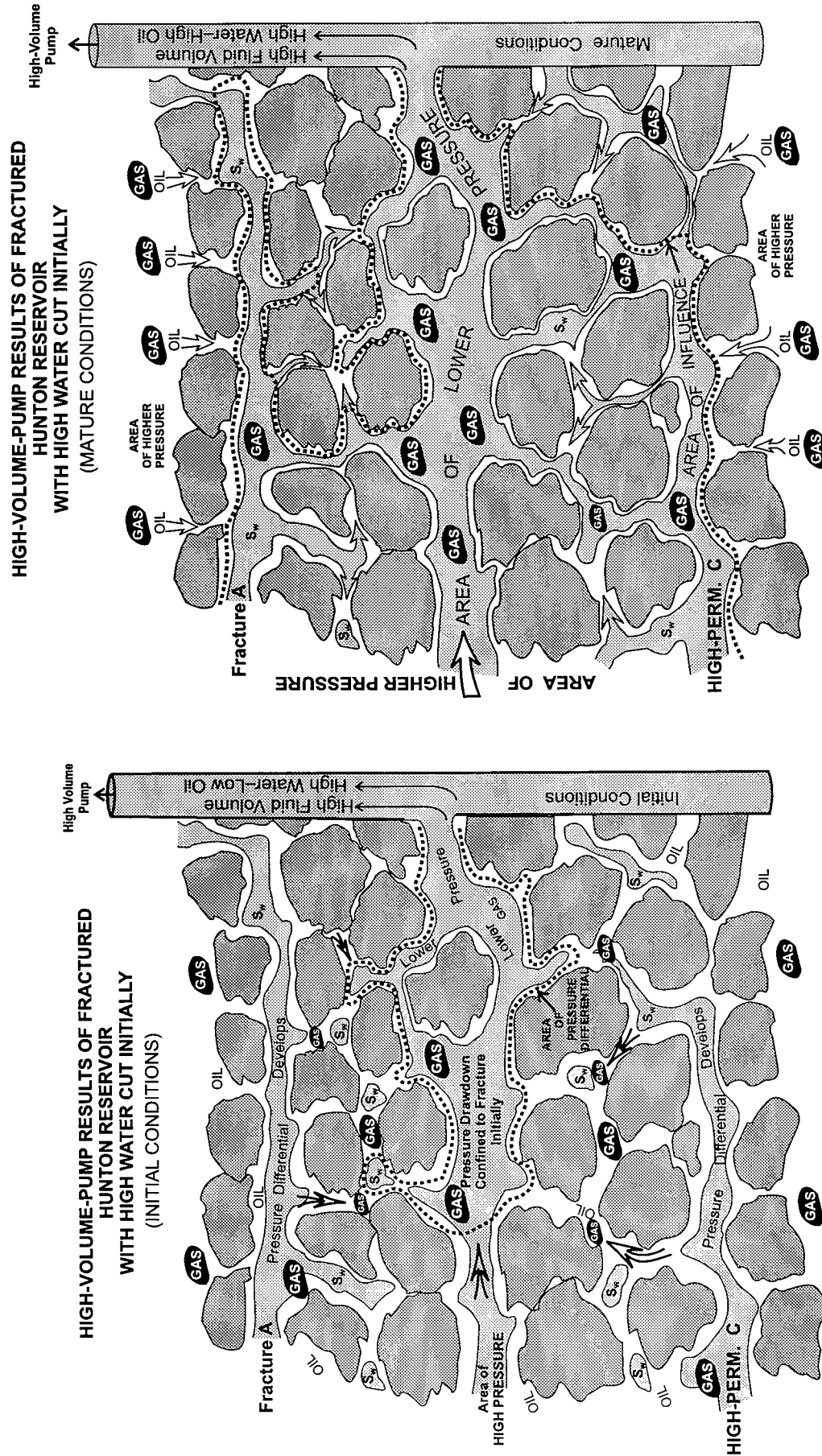


Figure 131. Schematic diagram of Hunton reservoir in contact with completion string and producing with low-volume rod pump. See text for explanation. S_w = water saturation.



duction, especially after installation of high-volume pumps. The term *retrograde oil cut* (ROC) has been informally applied to this producing phenomenon by researchers at the University of Tulsa. Based upon known and assumed parameters, Figures 130, 131, 132, and 133 offer an explanation for the reversal of the oil cut, from low to high, as a function of time.

Figure 130 is a schematic drawing of a vertical cross-sectional area for the producing Hunton reservoir at Carney and the adjacent drill hole (Fig. 130) or completion string of pipe (Figs. 131, 132, 133). The reservoir is assumed to be oil wet, based upon the low formation salt-water-saturation calculations, as observed from the lower section of well 1 and most of well 2 in Figure 127. These resistive profiles are not uncommon for wells in the Carney area. Fractures illustrated in Figure 130 are generally regarded to be vertical in the reservoir. However, for purposes of illustration in Figures 130, 131, 132, and 133, fractures *A* and *B* are considered low angle and intersect the vertical plane of each figure. As postulated for this field, fractures *A* and *B* and high-permeability layer *C* are almost completely filled with water. This interpretation is based on two observations.

First, many porosity logs for the Carney area do not have the porosity (and assumed permeability from the porosity) necessary to sustain flow rates of thousands of barrels per day for sustained periods. Permeability in fractures should be sufficient for this producing rate.

Second, the high resistivities are indicative of low water saturations in the rock matrix. It stands to reason that fractures are the only alternative for areas of high water saturations in many of the wells. It might be prudent to point out that beds or zones of higher water saturation surely exist in the Carney area and that wettability may vary. The correlation of zone B in well 1 of Figure 127 to the north would tie this zone to beds of high primary porosity and undoubtedly excellent permeabilities.

The observation was made that wells of prolific production had or were similar in reservoir characteristics to wells that recovered high water volumes with poor shows of oil and gas on drillstem tests. An example of this scenario can be illustrated by two wells in the SE $\frac{1}{4}$ sec. 2, T. 15 N., R. 2 E. In 1950, Deep Rock Oil Corp. drillstem tested the entire Hunton interval in their No. 1 Johnston well, in the SW $\frac{1}{4}$ SW $\frac{1}{4}$ SE $\frac{1}{4}$ sec. 2. They recovered a slight show of gas in 1 hour and 3,350 ft of salt water in the pipe. The bottom-hole flowing pressure was 1,600 psia, and the bottom-hole shut-in pressure was 2,100 psia in 12 minutes. In 1998, Altex Resources completed the No. 1 Gray in the S $\frac{1}{2}$ NW $\frac{1}{4}$ SE $\frac{1}{4}$ sec. 2. This well is a 40-acre offset to the No. 1 Johnston. Altex completed the Hunton for an initial pumping potential of 240 BOPD, 581 MCFGPD, and 1,966 BWPD. The reservoir in these two adjacent wells would almost have to be in communication, owing to the presence of high permeability, based on flow rates.

The reason the No. 1 Johnston had such a poor show of hydrocarbons could be summarized from the sche-

matic drawing of Figure 130. The area of pressure differential created by the lower pressure in the drillstem-test tool and the formation would have had to be small because of the short time interval of the test and the magnitude of the water drive. I believe that, preferentially, the higher permeability streaks and fractures would have responded to the pressure differential created by the test tool, and because there are predominantly high water saturations, the test yielded significant water with a small show. The influence of the water-drive mechanism also would not have allowed the area of pressure differential to extend any distance into the reservoir.

In the early 1980s, several operators completed Hunton wells in the Carney area with poor results. Typically, they recovered a lot of water and small amounts of oil, rendering the wells marginally economic. I must stress again that these are observations made from my experience in the area and that economic analyses of these wells are not documented here. Figure 131 is a schematic drawing hypothesizing the production scenario for wells producing from the Hunton with rod pumps. It is assumed that the wells pumped lower volumes of water, with marginal production due to the limited pump capacities. As the quantity of oil remains low and does not revert to a high oil cut with time, it is logical to assume that the area of lower pressure created by the pump is confined to the fractures and areas of higher permeability where water is the predominant component. As in the drillstem-test scenario, the fractures and high-permeability streaks would probably have high water saturations and low oil saturations initially. The boundary between the fractures and the rock matrix, or the area of high permeability and lower permeability, would also have been subjected to a pressure differential. With continuing production, areas of lower pressure probably developed in the tighter rock matrix near the perforations in response to the production. As the pressure dropped, gas would have broken out of solution in the oil (which should predominantly have occupied the smaller pore spaces in the rock matrix) and have driven mobile oil toward this pressure differential. Free gas in the reservoir also would have flowed toward the lower pressure area, displacing mobile oil in the process. This process is probably more complicated, as water from the water drive encroached toward the tighter matrix areas affected by production. This could have resulted in oil also being swept to these areas of lower pressure by a water-drive component. I believe that the strength of the water drive will be an overall limit to the area affected by production because of the water drive's makeup capability, which should limit the area of low pressure created by production from the rod pump, rendering the area of influence from the rod pump fairly small. This may explain why production is usually marginal from reservoirs producing by means of such a pumping unit.

The breakthrough for making production economic from this type of reservoir was the introduction of high-

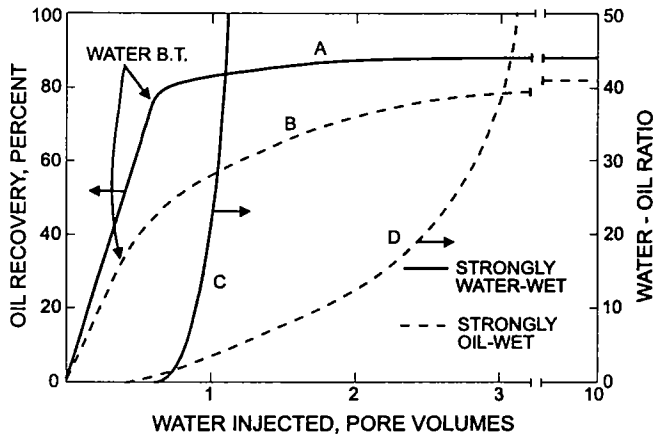


Figure 134. Diagram showing typical waterflood performance in water-wet and oil-wet sandstone cores at moderate oil/water viscosity ratios. Modified from Raza and others (1968). See text for explanation.

volume pumps to produce the fluid. The high-volume fluid production resulted in an exciting revelation. The original low oil cuts reverted to higher oil cuts with time. I would like to clarify the following observations concerning this phenomenon. I am not privy to core analyses or other confidential reservoir information, amount and rates of water production, or any other production peculiarities known by the operators in this play. However, I feel justified in making the preceding and following observations on the basis of detailed discussions of reservoir parameters, production characteristics and trends, and completion techniques with operators, field personnel, service-company personnel, and researchers studying the play. The University of Tulsa and Marjo Oil Co. have received a grant from the U.S. Department of Energy to study and evaluate production characteristics of this trend. This information ultimately will become publicly available, but as of this writing the time of release is not known.

Figure 132 represents what I term the initial conditions of the producing reservoir under influence of a high-volume fluid pump. Because of the large capacities of the pump, I envision the area of influence being greatly expanded in the reservoir initially in comparison to use of the rod pump. The pressure drawdown is probably initially confined to the fractures or high-permeability streaks. The water drive may replace produced fluid, but on the east side of the fault shown in Figure 126, the aquifer is limited, resulting in the current drawdown of pressure as previously described. On the west side of the fault the aquifer is more extensive, and the rate of pressure reduction is considerably slower. The pressure at the working pump is lower than the pressure within the reservoir. A pressure gradient is created from the perforations out into the reservoir. This is the area of pressure differential shown in Figure 132. Because of the high rates of the high-volume pumps, I believe the area of pressure differential or pressure gradient is greater than that of the rod pumps. This in-

crease in areal extent of the pressure gradient increases the boundary area between the fractures and the high-permeability streaks and the oil-saturated rock matrix. Mobile oil from the rock matrix will flow toward this pressure differential, created by the high-volume pump, by solution-gas drive and from displacement by encroaching water from other fractures and higher permeability streaks not directly connected to the perforations. This encroachment by water from other fractures or high-permeability streaks should essentially act as a waterflood and sweep the mobile oil. I believe an oil-wet reservoir is much more likely to be productive under this scenario than a water-wet reservoir. Although, if initial oil saturations are high enough—that is, low primary production—this process should work in a water-wet environment also. As Figure 133 illustrates, once water has communicated with the perforations in certain areas, I would expect incremental oil to be drastically reduced in a water-wet environment.

My reasoning for this statement can be summarized by Figure 134. This figure represents typical waterflood response in a water-wet and oil-wet sandstone cores at a moderate oil/water viscosity ratio (Raza and others, 1968). In a water-wet environment, line A represents percentage of oil recovery as a function of water-injected pore volumes. Once water has broken through, or in this case as fracture A or high-permeability streak C communicates with the perforations, it is possible that very little additional matrix is swept, as evidenced by the amount of additional oil that is recovered after breakthrough on curve A of Figure 134. In an oil-wet environment, recovery of additional oil after breakthrough is very good (curve B). Breakthrough occurs at

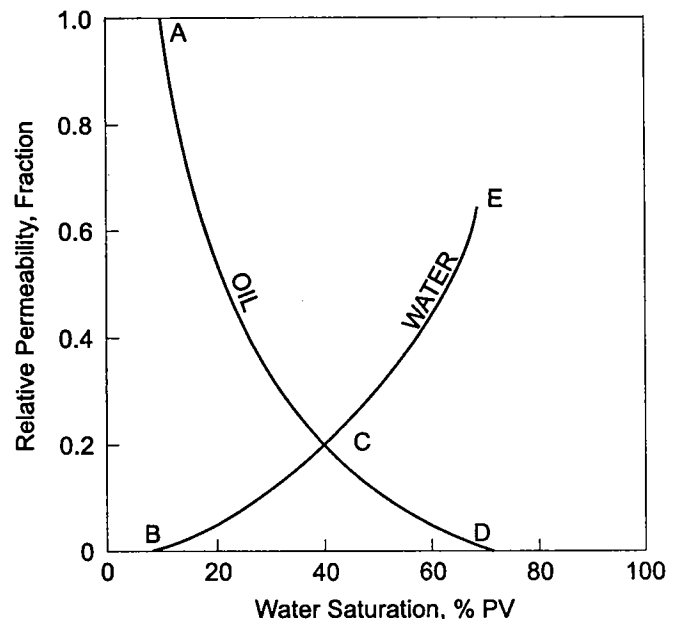


Figure 135. Graph showing water-oil relative-permeability curves for strongly oil-wet rock. (From Craig, ©1971; reprinted by permission of Society of Petroleum Engineers.) See text for explanation. PV = pore volume.

about 30–35% recovery in an oil-wet environment. After this breakthrough, additional matrix is swept, and oil is continually produced. The final percentage of oil recovery for the oil-wet system is 75%. This means that an additional 40–45% of oil was recovered after water initially broke through. For this reason, high water saturation sweeping through the matrix should not hinder production.

Figure 133 represents a more advanced condition in the reservoir with production—where the pressure drawdown has extended horizontally as well as vertically in the reservoir. At the pressure-differential interface, oil and gas are still being driven to the area of influence, and the water, from highly permeable strata or fractures, is approaching the production channels connected to the perforations, sweeping oil in the process.

Figure 135 shows water–oil relative-permeability curves for a strongly oil-wet rock. It is possible that the

relative permeabilities change in the fractures and high-permeability streaks as oil migrates in, changing the water–oil saturations. The end point of this type of production is probably when fluid production decreases, perhaps at the end of the influence from the water drive when more conventional solution-gas-drive mechanics take over.

In summary, it is possible that high-volume pumps create extensive areas of low pressure in the fractures and the highest permeability strata first. Water and mobile oil then migrate from regions of higher pressure to regions of lower pressure. Water or gas may displace mobile oil in its path toward the pressure differential. A retrograde oil cut will occur as the area of influence increases. Eventually, the reservoir will become de-watered (that point when the water drive ceases to have an influence), and more familiar production techniques should be applied.

REFERENCES CITED

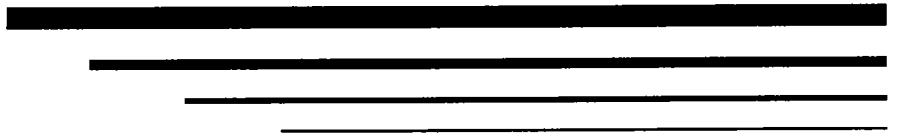
- Adler, F. J.; Caplan, W. M.; Carlson, M. P.; Goebel, E. D.; Henslee, H. T.; Hicks, I. C.; Larson, T. G.; McCracken, M. H.; Parker, M. C.; Rascoe, Bailey, Jr.; Schramm, M. W., Jr.; and Wells, J. S., 1971, Future petroleum provinces of the Midcontinent, region 7, in Cram, I. H. (ed.), *Future petroleum provinces of the United States—their geology and potential*: American Association of Petroleum Geologists Memoir 15, v. 2, p. 985–1120.
- Al-Hashimi, W. S., 1972, A study of dolomitization by scanning electron microscopy: *Yorkshire Geological Society Proceedings*, v. 38, p. 593–606.
- Al-Shaieb, Zuhair; and Puckette, Jim, 2000, Sequence stratigraphy of Hunton Group ramp facies, Arbuckle Mountains and Anadarko basin, Oklahoma, in Johnson, K. S. (ed.), *Platform carbonates in the southern Midcontinent, 1996 symposium*: Oklahoma Geological Survey Circular 101, p. 131–137.
- Al-Shaieb, Z.; Beardall, G.; Medlock, P.; Lippert K.; Matthews, F.; and Manni, F., 1993, Overview of Hunton facies and reservoirs in the Anadarko basin, in Johnson, K. S. (ed.), *Hunton Group core workshop and field trip*: Oklahoma Geological Survey Special Publication 93-4, p. 3–39.
- Amsden, T. W., 1957, Introduction to stratigraphy, *part 1 of Stratigraphy and paleontology of the Hunton group in the Arbuckle Mountain region*: Oklahoma Geological Survey Circular 44, 57 p., 3 pls.
- _____, 1958a, Haragan articulate brachiopods, *part 2 of Stratigraphy and paleontology of the Hunton group in the Arbuckle Mountain region*: Oklahoma Geological Survey Bulletin 78, p. 9–144, 14 pls.
- _____, 1958b, Bois d'Arc articulate brachiopods, *part 5 of Stratigraphy and paleontology of the Hunton group in the Arbuckle Mountain region*: Oklahoma Geological Survey Bulletin 82, 110 p., 5 pls.
- _____, 1960, Stratigraphy, *part 6 of Stratigraphy and paleontology of the Hunton group in the Arbuckle Mountain region*: Oklahoma Geological Survey Bulletin 84, 311 p., 17 pls.
- _____, 1961, Stratigraphy of the Frisco and Sallisaw Formations (Devonian) of Oklahoma: Oklahoma Geological Survey Bulletin 90, 121 p., 13 pls.
- _____, 1963a, Articulate brachiopods of the Sallisaw Formation (Devonian), *part 2 of Early Devonian brachiopods of Oklahoma*: Oklahoma Geological Survey Bulletin 94, p. 141–192, pls. 13–20.
- _____, 1963b, Silurian stratigraphic relations in the central part of the Arbuckle Mountains, Oklahoma: *Geological Society of America Bulletin*, v. 74, p. 631–636, 2 pls.
- _____, 1967, Chimneyhill limestone sequence (Silurian), Hunton Group, Oklahoma, revised: *American Association of Petroleum Geologists Bulletin*, v. 51 p. 942–945.
- _____, 1968, Articulate brachiopods of the St. Clair Limestone (Silurian), Arkansas, and the Clarita Formation (Silurian), Oklahoma: *Paleontological Society Memoir 1 (Journal of Paleontology*, v. 42, no. 3, supp.), 117 p., 20 pls.
- _____, 1969, A widespread zone of pentamerid brachiopods in subsurface Silurian strata of Oklahoma and Texas Panhandle: *Journal of Paleontology*, v. 43, p. 961–975, pls. 116–118.
- _____, 1971, *Triplexia alata* Ulrich and Cooper, in Dutro, J. T., Jr. (ed.), *Paleozoic perspectives: a paleontological tribute to G. Arthur Cooper*: Smithsonian Contributions to Paleobiology, no. 3, p. 143–154, 2 pls.
- _____, 1974, Late Ordovician and Early Silurian articulate brachiopods from Oklahoma, southwestern Illinois, and eastern Missouri: *Oklahoma Geological Survey Bulletin* 119, 154 p., 28 pls.
- _____, 1975, Hunton Group (Late Ordovician, Silurian, and Early Devonian) in the Anadarko basin of Oklahoma: *Oklahoma Geological Survey Bulletin* 121, 214 p., 15 pls.
- _____, 1980, Hunton Group (Late Ordovician, Silurian, and Early Devonian) in the Arkoma basin of Oklahoma: *Oklahoma Geological Survey Bulletin* 129, 136 p., 12 pls.
- _____, 1981, Biostratigraphic and paleoenvironmental relations: a Late Silurian example, in Broadhead, T. W. (ed.), *Lophophorates, notes for a short course organized by J. T. Dutro, Jr., and R. S. Boardman*: University of Tennessee, Department of Geological Sciences, *Studies in Geology* 5, p. 154–169.
- _____, 1989, Depositional and post-depositional history of middle Paleozoic (Late Ordovician through Early Devonian) strata in the ancestral Anadarko basin, in Johnson, K. S. (ed.), *Anadarko basin symposium, 1988*: Oklahoma Geological Survey Circular 90, p. 143–146.
- _____, 1993, Appendix; summary of wells in the Anadarko basin, in Amsden, T. W.; and Barrick, J. E., *Pre-Woodford subcrop map of the Anadarko basin, western Oklahoma and Texas Panhandle*: Oklahoma Geological Survey Geologic Map 34, 20 p., 2 pls.
- Amsden, T. W.; and Barrick, J. E., 1986, Late Ordovician–Early Silurian strata in the central United States and the Hirnantian Stage: *Oklahoma Geological Survey Bulletin* 139, 95 p., 7 pls.
- _____, 1988, Late Ordovician through Early Devonian annotated correlation chart and brachiopod range charts for the southern Midcontinent region, U.S.A., with a discussion of Silurian and Devonian conodont faunas: *Oklahoma Geological Survey Bulletin* 143, 66 p., 7 pls.
- Amsden, T. W.; and Klapper, Gilbert, 1972, Misener Sandstone (Middle–Upper Devonian), north-central Oklahoma: *American Association of Petroleum Geologists Bulletin*, v. 56, p. 2323–2334.
- Amsden, T. W.; and Rowland, T. L., 1965, Silurian stratigraphy of northeastern Oklahoma: *Oklahoma Geological Survey Bulletin* 105, 174 p., 20 pls.
- Amsden, T. W.; and Ventress, W. P. S., 1963, Articulate brachiopods of the Frisco Formation (Devonian), *part 1 of Early Devonian brachiopods of Oklahoma*: Oklahoma Geological Survey Bulletin 94, p. 9–140, pls. 1–12.
- Amsden, T. W.; Caplan, W. M.; Hilpman, P. L.; McGlasson, E. H.; Rowland, T. L.; and Wise, O. A., Jr., 1967, Devonian of the southern Midcontinent area, United States, in *v. 1 of International symposium on Devonian System*: Alberta Society of Petroleum Geologists, Calgary, p. 913–932.
- Anderson, R. F., 1939, A subsurface study of the Hunton formation in central Oklahoma: University of Oklahoma unpublished M.S. thesis, 30 p., 2 pls.
- Badiozamani, K., 1973, The dorag dolomitization model—application to the Middle Ordovician of Wisconsin: *Journal of Sedimentary Petrology*, v. 43, p. 965–984.
- Ballard, W. N., 1930, An isopachous map of the Hunton formation in the Seminole district: University of Oklahoma unpublished M.S. thesis, 33 p., 4 pls.
- Barrick, J. E., 1977, Multielement simple-cone conodonts from the Clarita Formation (Silurian), Arbuckle Mountains, Oklahoma: *Geologica et Palaeontologica*, v. 11, p. 47–68, 3 pls.
- Barrick, J. E.; and Klapper, Gilbert, 1976, Multielement, Silurian (late Llandoveryan–Wenlockian) conodonts of the

- Clarita Formation, Arbuckle Mountains, Oklahoma, and phylogeny of *Kochelella*: *Geologica et Palaeontologica*, v. 10, p. 59–108, 4 pls.
- Barrick, J. E.; Klapper, Gilbert; and Amsden, T. W., 1990, Late Ordovician–Early Devonian conodont succession in the Hunton Group, Arbuckle Mountains and Anadarko basin, Oklahoma, *in* Ritter, S. M. (ed.), Early to middle Paleozoic conodont biostratigraphy of the Arbuckle Mountains, southern Oklahoma: Oklahoma Geological Survey Guidebook 27, p. 55–62.
- Bathurst, R. G. C., 1975, Carbonate sediments and their diagenesis [2nd edition]: Elsevier, Amsterdam, 658 p.
- Beardall, G. B., 1983, Depositional environment, diagenesis and dolomitization of the Henryhouse Formation in the western Anadarko basin and northern shelf, Oklahoma: Oklahoma State University unpublished M.S. thesis.
- Beardall, G. B.; and Al-Shaieb, Zuhair, 1984, Dolomitization stages in a regressive sequence of the Hunton Group, Anadarko basin, Oklahoma: American Association of Petroleum Geologists Bulletin, v. 68, p. 452.
- Berg, O. R., 1974, North Custer City field, *in* Berg, O. R. (ed.), Oil and gas fields of Oklahoma reference report: Oklahoma City Geological Society, Supplement 1, p. 10.
- Berry, W. B. N.; and Boucot, A. J., 1970, Correlation of the North American Silurian rocks: Geological Society of America Special Paper 102, 289 p., 2 pls.
- Borak, B., 1978, Progressive and deep burial diagenesis in the Hunton (Late Ordovician to Early Devonian) and Simpson (Early to Middle Ordovician) Groups of the deep Anadarko basin in southwestern Oklahoma: Rensselaer Polytechnic Institute unpublished M.S. thesis.
- Bowles, J. P., 1959, Subsurface geology of Woods County, Oklahoma: Shale Shaker Digest, v. 3, p. 202.
- Briggs, Garrett, 1974, Carboniferous depositional environments in the Ouachita Mountains–Arkoma basin area of southeastern Oklahoma, *in* Briggs, Garrett (ed.), Carboniferous of the southeastern United States: Geological Society of America Special Paper 148, p. 225–239.
- Brown, H. A.; and Banta, A. D., 1993, Unusual occurrence of oil in the Viola limestone, Pratt anticline, Kansas, *in* Johnson, K. S.; and Campbell, J. A. (eds.), Petroleum-reservoir geology in the southern Midcontinent, 1991 symposium: Oklahoma Geological Survey Circular 95, p. 104–112.
- Bruce, L. G., 1989, Radial-drainage anomaly over Aledo gas field in the Anadarko basin: example of a poor man's remote-sensing technique: Oklahoma Geology Notes, v. 49, p. 125–130.
- Campbell, J. A., 1993, Lower Paleozoic fault blocks—Arkoma basin, Oklahoma and Arkansas, *in* Bebout, D. G.; White, W. A.; Hentz, T. F.; and Grasmick, M. K. (eds.), Atlas of major Midcontinent gas reservoirs: Gas Research Institute, Texas Bureau of Economic Geology, Austin, p. 77–79.
- Campbell, K. S. W., 1967, Trilobites of the Henryhouse Formation (Silurian) in Oklahoma: Oklahoma Geological Survey Bulletin 115, 68 p., 19 pls.
- , 1977, Trilobites of the Haragan, Bois d'Arc, and Frisco Formations (Early Devonian), Arbuckle Mountains region, Oklahoma: Oklahoma Geological Survey Bulletin 123, 227 p., 40 pls.
- Choquette, P. W.; and Pray, L. C., 1970, Geologic nomenclature and classification of porosity in sedimentary carbonates: American Association of Petroleum Geologists Bulletin, v. 54, p. 207–250.
- Choquette, P. W.; and Steinen, R. P., 1980, Mississippian nonsupratidal dolomite, Ste. Genevieve Limestone, Illinois basin: evidence for mixed-water dolomitization, *in* Concepts and models of dolomitization by ground water: Society for Sedimentary Geology (SEPM) Special Publication 28, p. 163–196.
- Christian, H. E., 1953, Geology of the Marble City area, Sequoyah County, Oklahoma: University of Oklahoma unpublished M.S. thesis, 160 p., 2 pls.
- Clark, N. J., 1969, Elements of petroleum reservoirs (revised edition): Society of Petroleum Engineers of American Institute of Mining and Metallurgical Engineers, Henry L. Doherty Series, 250 p.
- Clement, W. A., 1977, A case history of geoseismic modeling of basal Morrow–Springer sandstones, Watonga–Chickasha trend: Geary, Oklahoma—T13N, R10W, *in* Payton, C. E., Seismic stratigraphy—applications to hydrocarbon exploration: American Association of Petroleum Geologists Memoir 26, p. 451–476.
- Coleman, R. L., 1963, North Custer City, *in* Cramer, R. D.; Gatlin, L.; and Wessman, H. G. (eds.), Oil and gas fields of Oklahoma reference report: Oklahoma City Geological Society, v. 1, p. 37A–39A.
- Conkling, R. A., 1930, Pontotoc County, *in* Oil and gas in Oklahoma: Oklahoma Geological Survey Bulletin 40, v. 3, p. 109–131.
- Craig, F. F., Jr., 1971, The reservoir engineering aspects of waterflooding: Society of Petroleum Engineers of American Institute of Mining and Metallurgical Engineers Monograph, Henry L. Doherty Series, v. 3, 134 p.
- Davies, G. R., 1970, Carbonate bank sedimentation, eastern Shark Bay, Western Australia: American Association of Petroleum Geologists Memoir 13, p. 85–168.
- Decker, C. E., 1935, Graptolites from the Silurian of Oklahoma: Journal of Paleontology, v. 9, p. 434–446.
- Dott, R. H., Jr.; and Batten, R. L., 1971, Evolution of the Earth: McGraw-Hill, New York, 649 p.
- Dunham, R. J., 1962, Classification of carbonate rocks according to depositional texture, *in* Ham, W. E. (ed.), Classification of carbonate rocks—a symposium: American Association of Petroleum Geologists Memoir 1, p. 108–121.
- England, R. L., 1965, Subsurface study of the Hunton Group (Silurian–Devonian) in the Oklahoma portion of the Arkoma basin: Shale Shaker Digest 4, p. 19–35.
- Esteban, M.; and Klappa, C. F., 1983, Subaerial exposure environment, *in* Scholle, P. A.; Bebout, D. G.; and Moore, C. H. (eds.), Carbonate depositional environments: Springer-Verlag, New York, p. 2–72.
- Feazel, C. T.; and Schatzinger, R. A., 1985, Prevention of carbonate cementation in petroleum reservoirs, *in* Schneidermann, Nahum; and Harris, P. M. (eds.), Carbonate cements: Society for Sedimentary Geology (SEPM) Special Publication 36, p. 97–106.
- Feinstein, S., 1981, Subsidence and thermal history of southern Oklahoma aulacogen: implications for petroleum exploration: American Association of Petroleum Geologists Bulletin, v. 65, p. 2521–2533.
- Folk, R. L., 1962, Spectral subdivision of limestone types, *in* Ham, W. E. (ed.), Classification of carbonate rocks—a symposium: American Association of Petroleum Geologists Memoir 1, p. 62–84.
- Freeman, Tom; and Schumacher, Dietmar, 1969, Qualitative pre-Sylamore (Devonian–Mississippian) physiography delineated by onlapping conodont zones, northern Arkansas: Geological Society of America Bulletin, v. 80, p. 2327–2334, 1 pl.
- Fritz, R. D.; and Medlock, P. L., 1993, Sequence stratigraphy of the Hunton Group as defined by core, outcrop, and log data, *in* Johnson, K. S. (ed.), Hunton Group core workshop and field trip: Oklahoma Geological Survey Special Publication 93-4, p. 161–180.

- _____. 1995, Recognition of unconformities and sequences in Mid-Continent carbonates, in Hyne, N. J. (ed.), Sequence stratigraphy of the Mid-Continent: Tulsa Geological Society Special Publication 4, p. 49–80.
- Ham, W. E., 1969, Regional geology of the Arbuckle Mountains, Oklahoma: Oklahoma Geological Survey Guidebook 17, 52 p.
- Ham, W. E.; and Wilson, J. L., 1967, Paleozoic epeirogeny and orogeny in the central United States: *American Journal of Science*, v. 265, p. 332–407.
- Ham, W. E.; Denison, R. E.; and Merritt, C. A., 1964, Basement rocks and structural evolution of southern Oklahoma: Oklahoma Geological Survey Bulletin 95, 302 p., 16 pls.
- Hanshaw, B. B.; and Harris, P. M., 1979, A geochemical hypothesis for dolomitization by groundwater: *Economic Geology*, v. 66, p. 710–724.
- Harris, P. M., 1985, Carbonate cementation—a review, in Schneidermann, Nahum; and Harris, P. M. (eds.), Carbonate cements: Society for Sedimentary Geology (SEPM) Special Publication 36, p. 79–95.
- Harvey, R. L., 1969, West Campbell field—key to unlock Hunton: *Shale Shaker Digest* 6, p. 176–188.
- Hester, T. C.; and Schmoker, J. W., 1993, Regional geology of the Woodford Shale, Anadarko basin, Oklahoma—an overview of relevance to horizontal drilling, in Johnson, K. S.; and Campbell, J. A. (eds.), Petroleum-reservoir geology in the southern Midcontinent, 1991 symposium: Oklahoma Geological Survey Circular 95, p. 74–81.
- Hester, T. C.; Schmoker, J. W.; and Sahl, H. L., 1992, Tectonic controls on deposition and source-rock properties of the Woodford Shale, Anadarko basin, Oklahoma—loading, subsidence, and forebulge development, in Thorman, C. H. (ed.), Application of structural geology to mineral and energy resources of the central and western United States: U.S. Geological Survey Bulletin 2012-B, 11 p.
- Hollrah, T. L., 1977, Subsurface lithostratigraphy of the Hunton Group in parts of Payne, Lincoln, and Logan Counties, Oklahoma: *Shale Shaker Digest* 9, p. 76–91.
- Howery, S. D., 1993, A regional look at Hunton production in the Anadarko basin, in Johnson, K. S. (ed.), Hunton Group core workshop and field trip: Oklahoma Geological Survey Special Publication 93-4, p. 77–81.
- Isom, J. W., 1973, Subsurface stratigraphic analysis, Late Ordovician to Early Mississippian, Oakdale–Campbell trend, Woods, Major and Woodward Counties, Oklahoma: *Shale Shaker Digest* 8, p. 116–132.
- Jackson, J. A. (ed.), 1997, Glossary of geology (4th edition): American Geological Institute, Alexandria, Virginia, 769 p.
- Jaeger, H., 1967, Preliminary stratigraphic results from graptolite studies in the Upper Silurian and Lower Devonian of southeastern Australia: *Geological Society of Australia Journal*, v. 14, pt. 2, p. 281–285.
- Jenkins, W. A. M., 1970, Chitinozoa from the Ordovician Sylvan Shale of the Arbuckle Mountains, Oklahoma: *Palaeontology*, v. 13, p. 261–288, pls. 47–51.
- Jordan, Louise, 1959, Gas in Custer County, Oklahoma: Oklahoma Geology Notes, v. 19, p. 226–229.
- _____. 1964, Geology of Oklahoma—a summary: Oklahoma Geology Notes, v. 27, p. 215–228.
- Kennedy, C. L. (ed.), 1982, The deep Anadarko basin: Petroleum Information Corp., 359 p.
- Kerans, C., 1989, Karst-controlled reservoir heterogeneity and an example from the Ellenburger Group (Lower Ordovician) of West Texas: Texas Bureau of Economic Geology, Austin, 234 p.
- Kirk, M. S., 1974, Mustang field, in Berg, O. R. (ed.), Oil and gas fields of Oklahoma reference report: Oklahoma City Geological Society Supplement 1, p. 16.
- Kunsman, H. S., 1967, Hunton oil and gas fields, Arkansas, Oklahoma, and Panhandle of Texas, in Toomey, D. F. (ed.), Symposium—Silurian–Devonian rocks of Oklahoma and environs: Tulsa Geological Society Digest, v. 35, p. 165–197.
- Land, L. S., 1973, Holocene meteoric dolomitization of Pleistocene limestones, north Jamaica: *Sedimentology*, v. 20, p. 411–424.
- Leeder, M. R., 1983, Sedimentology, process and product: Allen and Unwin, London, 344 p.
- Logsdon, Truman; and Brown, A. R., 1967, “Hunton”—hot-test play in Oklahoma: *Shale Shaker*, v. 18, no. 4, p. 63–70.
- Lundin, R. F., 1965, Ostracodes of the Henryhouse Formation (Silurian) in Oklahoma: Oklahoma Geological Survey Bulletin 108, 104 p., 18 pls.
- _____. 1968, Ostracodes of the Haragan Formation (Devonian) in Oklahoma: Oklahoma Geological Survey Bulletin 116, 121 p., 22 pls.
- Lynch, M. T., 1990, Evidence of paleokarstification and burial diagenesis in the Arbuckle Group of Oklahoma: Oklahoma State University unpublished M.S. thesis, 163 p.
- Mann, Wallace, 1958, Subsurface geology of the Franks graben, Pontotoc and Coal Counties, Oklahoma: *Shale Shaker*, v. 8, no. 5, p. 11–28.
- Manni, F. M., 1985, Depositional environment, diagenesis, and unconformity identification of the Chimneyhill Subgroup in the western Anadarko basin and northern shelf, Oklahoma: Oklahoma State University unpublished M.S. thesis, 133 p.
- Matthews, F. D., 1992, Paleokarstic features and reservoir characteristics of the Hunton Group in the Anadarko basin, Oklahoma: Oklahoma State University unpublished M.S. thesis, 174 p.
- Matthews, F. D.; and Al-Shaieb, Zuhair, 1993, Paleokarstic features and reservoir characteristics of the Hunton Group in central and western Oklahoma, in Johnson, K. S.; and Campbell, J. A. (eds.), Petroleum-reservoir geology in the southern Midcontinent, 1991 symposium: Oklahoma Geological Survey Circular 95, p. 140–162.
- Maxwell, R. A., 1931, The stratigraphy and areal distribution of the “Hunton formation,” Oklahoma: Northwestern University unpublished Ph.D. dissertation, 120 p. [A summary of this dissertation was published in 1936 in Northwestern University Summaries of Ph.D. Dissertations, v. 4, p. 131–136.]
- Maxwell, R. W., 1959, Post-Hunton, pre-Woodford unconformity in southern Oklahoma: *Ardmore Geological Society*, v. 11, p. 101–125.
- McGee D. A.; and Jenkins, H. D., 1946, West Edmond oil field, central Oklahoma: *American Association of Petroleum Geologists Bulletin*, v. 30, p. 1797–1829.
- Medlock, P. L., 1984, Depositional environment and diagenetic history of the Frisco and Henryhouse Formations in central Oklahoma: Oklahoma State University unpublished M.S. thesis.
- Menke, K. P., 1986, Subsurface study of the Hunton Group in the Cheyenne Valley field, Major County, Oklahoma: Oklahoma State University unpublished M.S. thesis.
- Morgan, G. D., 1922, A Siluro–Devonian oil horizon in southern Oklahoma: Oklahoma Geological Survey Circular 10, 13 p.
- Morgan, W. A., 1985, Silurian reservoirs in upward-shoaling cycles of the Hunton Group, Mount Everette and Southwest Reeding fields, Kingfisher County, Oklahoma, in Roehl, P. O.; and Choquette, P. W. (eds.), Carbonate petroleum reservoirs: Springer-Verlag, New York, p. 109–120.
- Morrison, James, 1980, Richland–Yukon fields, Canadian

- County, Oklahoma, *in* Pipes, P. B. (ed.), Oil and gas fields of Oklahoma reference report: Oklahoma City Geological Society Supplement 2.
- Northcutt, R. A., 1985, Oil and gas development in Oklahoma, 1891–1984: *Shale Shaker*, v. 35, no. 6, p. 123–132.
- Northcutt, R. A.; and Campbell, J. A., 1996, Geologic provinces of Oklahoma, *in* Swindler, D. L.; and Williams, C. P. (compilers), Transactions of 1995 American Association of Petroleum Geologists, Mid-Continent Section meeting: Tulsa Geological Society, p. 128–134.
- Northcutt, R. A.; and Johnson, K. S., 1997, Major Simpson and Viola oil and gas reservoirs in Oklahoma, *in* Johnson, K. S. (ed.), Simpson and Viola Groups in the southern Midcontinent, 1994 symposium: Oklahoma Geological Survey Circular 99, p. 48–57.
- Oklahoma Geological Survey, 1972, Oklahoma gains deepest producer: Oklahoma Geology Notes, v. 32, p. 91.
- Oxley, M. L., 1958, A subsurface study of the Hunton in northwestern Oklahoma: University of Oklahoma unpublished M.S. thesis, 67 p.
- Posey, Ellen, 1932, The Hunton of Kansas: University of Oklahoma unpublished M.S. thesis, 25 p.
- Radke, B. M.; and Mathis, R. L., 1980, On the formation and occurrence of saddle dolomite: *Journal of Sedimentary Petrology*, v. 50, p. 1149–1168.
- Randazzo, A. F.; and Hickey, E. W., 1978, Dolomitization in the Floridan aquifer: *American Journal of Science*, v. 278, p. 1177–1184.
- Raza, S. H.; Treiber, L. E.; and Archer, D. L., 1968, Wettability of reservoir rocks and its evaluation: *Producers Monthly*, v. 32, p. 2–7.
- Reeds, C. A., 1911, The Hunton formation of Oklahoma: *American Journal of Science*, v. 182, p. 256–262.
- Rottmann, Kurt, 1993, Log-derived SP trends of the Hunton, with possible ramifications to Henryhouse–Chimneyhill depositional environments, Lincoln and Logan Counties, Oklahoma, *in* Johnson, K. S. (ed.), Hunton Group core workshop and field trip: Oklahoma Geological Survey Special Publication 93-4, p. 83–89.
- _____, 1999, Geological perspectives of reservoir engineering: a waterflood workshop: Oklahoma Geological Survey Special Publication 99-3, 101 p.
- _____, 2000, Defining the role of Woodford–Hunton depositional relationships in Hunton stratigraphic traps of western Oklahoma, *in* Johnson, K. S. (ed.), Platform carbonates in the southern Midcontinent, 1996 symposium: Oklahoma Geological Survey Circular 101, p. 139–146.
- Rottmann, Kurt; Crutchfield, D. R.; Tew, George; Wilson, Dan; Sutherland, Mark; and Nizami, Saleem, 1998, Geological considerations of waterflooding: a workshop: Oklahoma Geological Survey Special Publication 98-3, 171 p.
- Sarg, J. F., 1988, Carbonate sequence stratigraphy, *in* Sea level changes: an integrated approach: Society for Sedimentary Geology (SEPM) Special Publication 42, p. 155–182.
- Schramm, M. W., Jr., 1964, Paleogeologic and quantitative lithofacies analysis, Simpson Group, Oklahoma: American Association of Petroleum Geologists Bulletin, v. 48, p. 1164–1195.
- Selley, R. C., 1988, Applied sedimentology: Academic Press, San Diego, 446 p.
- Shannon, J. P., Jr., 1962, Hunton Group (Silurian–Devonian) and related strata in Oklahoma: American Association of Petroleum Geologists Bulletin, v. 46, p. 1–29.
- Sheriff, R. E., 1991, Encyclopedic dictionary of exploration geophysics [3rd edition]: Society of Exploration Geophysicists, Tulsa, 384 p.
- Solter, D. D., Jr., 1980, West Mayfield, T10N–R25W, Beckham County, Oklahoma, *in* Pipes, P. B. (ed.), Oil and gas fields of Oklahoma reference report: Oklahoma City Geological Society Supplement 2.
- Strimple, H. L., 1963, Crinoids of the Hunton Group (Devonian–Silurian) of Oklahoma: Oklahoma Geological Survey Bulletin 100, 169 p., 12 pls.
- Sutherland, P. K., 1965, Rugose corals of the Henryhouse Formation (Silurian) in Oklahoma: Oklahoma Geological Survey Bulletin 109, 92 p., 34 pls.
- Swesnick, R. M., 1948, Geology of the West Edmond oil field and related strata in Oklahoma, *in* Howell, J. V. (ed.), Structure of typical American oil fields: American Association of Petroleum Geologists, Tulsa, v. 3, p. 359–398.
- _____, 1950, Golden Trend of south-central Oklahoma: American Association of Petroleum Geologists Bulletin, v. 34, p. 386–422.
- Taff, J. A., 1902, Description of the Atoka quadrangle [Indian Territory]: U.S. Geological Survey Geologic Atlas, Folio 79, 8 p.
- Tarr, R. S., 1955, Paleogeologic map at base of Woodford and Hunton isopachous map of Oklahoma: American Association of Petroleum Geologists Bulletin, v. 39, p. 1851–1858.
- Throckmorton, H. C.; and Al-Shaieb, Zuhair, 1986, Core-calibrated log utilization in recognition of depositional facies and reservoir rock of the Henryhouse Formation (Silurian), Anadarko basin: Society of Professional Well Log Analysts, 27th Annual Logging Symposium, p. 1–18.
- Twenhofel, W. H., 1950, Principles of sedimentation: McGraw-Hill, New York, 673 p.
- Van Wagoner, J. C.; Mitchum, R. M.; Campion, K. M.; and Rahmanian, V. D., 1990, Siliciclastic sequence stratigraphy in well logs, cores, and outcrops: concepts for high-resolution correlation of time and facies: American Association of Petroleum Geologists Methods in Exploration Series, no. 7, 55 p.
- Walker, R. G.; and Mutti, Emiliano, 1973, Turbidite facies and facies associations, *in* Turbidites and deep water sedimentation: Society for Sedimentary Geology (SEPM) Short Course, Anaheim, p. 119–157.
- White, W. B., 1969, Conceptual models for carbonate aquifers: *Groundwater*, v. 7, p. 15–21.
- Wilson, J. L., 1975, Carbonate facies in geologic history: Springer-Verlag, New York, 471 p.
- Withrow, P. C., 1971, Hunton geology of the Star–Lacey field: *Shale Shaker Digest*, v. 19, p. 78–88.
- Wroblewski, E. F., 1967, Exploration problems in the “deep” Anadarko basin: *Shale Shaker*, v. 17, p. 131–136.

APPENDIXES



APPENDIX 1

Application of Submersible Pumps to Hunton Reservoirs

Pat BrownNew Dominion L.L.C.
Stillwater, Oklahoma

SUBMERSIBLE-PUMP HISTORY

In 1911, Armais Arutunoff, at the age of 18, organized the Russian Electrical Dynamo of Arutunoff Co. in Ekaterinoslav, Russia, and invented the first electric motor that would operate in water.

In 1919, Mr. Arutunoff changed the name of the firm to Reda. With development help from Phillips Petroleum Co., the first Reda pump was successfully installed in the United States in El Dorado field near Burns, Kansas, in 1927.

SUBMERSIBLE PUMPS IN THE CARNEY AREA

In the area of the Hunton play at Carney in Lincoln County, Oklahoma, the Hunton reservoir's high fluid-

TABLE A1. – Typical Submersible-Pump Application in the Hunton Reservoir at Carney, Lincoln County, Oklahoma

DESIGN CRITERIA

Casing	5½ in.
Tubing	2⅞ in.
Top performance	4,800 ft
Production rate	2,500 BPD
Intake pressure	550 psi
BOPD	80–100
MCFGPD	200–500

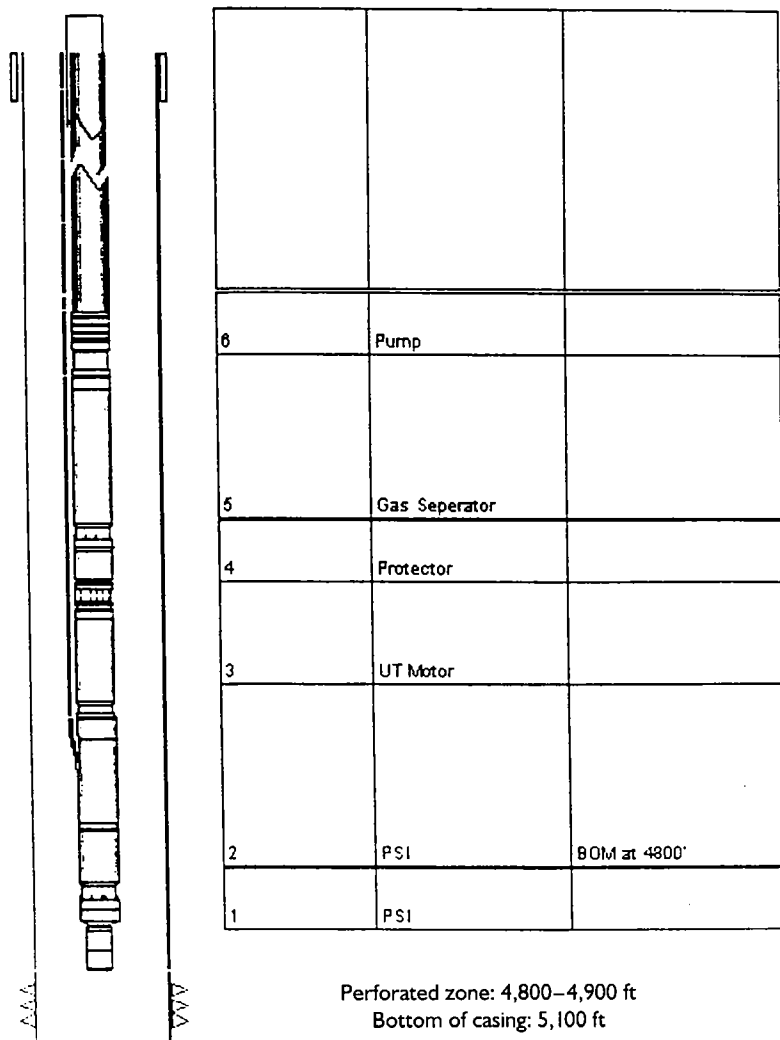


Figure A1. Diagram of a submersible pump of the type used at Carney, Lincoln County, Oklahoma.

volume output mandates the need for submersible pumps.

The first submersible pump was installed here in 1996. Currently, the Carney area has more than 100 operating submersible pumps. An average of one to two pumps per week are being installed in this area.

SUBMERSIBLE-PUMP COMPONENTS AND APPLICATION

The components of the submersible pumps used in the Carney area are shown in Figure A1 and are listed as follows:

1. Bottom-hole-pressure and temperature sensor. This item monitors the producing and static bottom-hole pressures.
2. Submersible motor, which supplies horsepower to the system.
3. Protector, which isolates the motor from wellbore fluids that may enter from the pump.
4. Gas separator, which aids in preventing the pump from gas-locking.
5. The pump itself, which discharges fluid to the surface.
6. Power cable, which supplies electricity from the surface to the motor.

Table A1 gives specifications for a typical submersible-pump application for the Hunton reservoir in the Carney area.

SUBMERSIBLE-PUMP RUN LIFE

Run times for the initial (early) Carney field installations exceeded 18 months per installation. Increased Hunton completions in the field have decreased the run times because of decreases in bottom-hole pressures. This has necessitated the need for redesigning the pump.

APPENDIX 2

Glossary of Terms

(as used in this volume)

Definitions modified from Jackson (1997), Van Wagoner and others (1990), and Sheriff (1991).

anticline—A fold, generally convex upward, whose core contains the stratigraphically older rocks.

aragonite—A white, yellowish, or gray orthorhombic mineral composed of calcium carbonate (CaCO_3). Not as stable as calcite.

arenaceous—Said of a sediment or sedimentary rock consisting wholly or in part of sand-size fragments, or having a sandy texture or the appearance of sand; pertaining to sand or arenite. Also said of the texture of such a sediment or rock. The term implies no special composition, and should not be used as a synonym of *siliceous*.

argillaceous—Pertaining to, largely composed of, or containing clay-size particles or clay minerals, such as an “argillaceous ore” in which the gangue is mainly clay; especially said of a sediment (such as marl) or a sedimentary rock (such as shale) containing an appreciable amount of clay.

arkosic—Said of a feldspar-rich sandstone, commonly pink or reddish, usually derived from the disintegration of granitic rocks.

aulacogen—A tectonic trough on a craton, bounded by convergent normal faults. Aulacogens have a radial orientation relative to cratons and are open outward.

biofacies—A subdivision of a stratigraphic unit, distinguished from adjacent subdivisions on the basis of its fossils, without respect to nonbiologic features; especially such a body of sediment or rock recognized by characters that do not affect lithology, such as the taxonomic identity or environmental implications of fossils.

biostratigraphy—Stratigraphy based on the paleontological aspects of rocks, or stratigraphy with paleontological methods; specifically the separation and differentiation of rock units on the basis of the description and study of the fossils they contain.

biozone—The basic unit in biostratigraphic classification and generally the smallest biostratigraphic unit on which intercontinental or worldwide correlations can be established.

boundstone—A term used by Dunham (1962) for a sedimentary carbonate rock whose original components were bound together during deposition and remained substantially in the position together during deposition and remained substantially in the position of growth (as shown by such features as intergrown skeletal matter and lamination contrary to gravity); e.g., most reef rocks and some biohermal and biostromal rocks.

brachiopod—Any solitary marine invertebrate belonging to the phylum Brachiopoda, characterized by a lophophore and two bilaterally symmetrical valves that may be calcareous or composed of chitinophosphate and that are commonly attached to a substratum but may also be free.

breccia—A coarse-grained clastic rock, composed of angular broken rock fragments held together by a mineral cement or in a fine-grained matrix; it differs from *conglomerate* in that the fragments have sharp edges and unworn corners.

bryozoan—Any invertebrate belonging to the phylum Bryozoa and characterized chiefly by colonial growth, a calcareous skeleton, or, less commonly, a chitinous membrane, and a U-shaped alimentary canal, with mouth and anus.

calcarenite—A limestone consisting predominantly (more than 50%) of detrital calcite particles of sand size; a consolidated calcareous sand.

calcite—A white, gray, or yellow common rock-forming hexagonal mineral composed of calcium carbonate (CaCO_3); more stable than aragonite.

carbonate—A sediment formed by the organic or inorganic precipitation from aqueous solution of carbonates of calcium, magnesium, or iron; e.g., limestone and dolomite.

cement—Mineral material, usually chemically precipitated, that occurs in the spaces among the individual grains of a consolidated sedimentary rock, thereby binding the grains together as a rigid, coherent mass; it may be derived from the sediment or its entrapped waters, or it may be brought in by solution from outside sources.

chert—A hard, extremely dense or compact, dull to semi-vitreous, microcrystalline or cryptocrystalline sedimentary rock, consisting dominantly of interlocking crystals of quartz less than about 30 μm in diameter. Chert occurs principally as nodular or concretionary segregations (chert nodules) in limestones and dolomites, and less commonly as areally extensive layered deposits (bedded chert); it may be an original organic or inorganic precipitate or a replacement product.

chitinozoan—A pseudochitinous marine microfossil of the extinct group Chitinozoa, having uncertain affinities but generally assumed to represent animal remains, shaped in general like a flask, occurring individually or in chains, and ranging primarily from uppermost Cambrian to Devonian.

clastic—Pertaining to a rock or sediment composed principally of broken fragments that are derived from preexisting rocks or minerals and that have been transported some distance from their place of origin.

chronostratigraphic unit—A body of rocks that are unified by having been formed during a specific interval of geologic time. It represents all the rocks formed during a certain time span of Earth history, and only the rocks formed during that time span. A chronostratigraphic unit is bounded by isochronous surfaces.

conodont—One of a large number of small, disjunct fossil elements assigned to the order Conodontophorida, phosphatic in composition and commonly toothlike in form but not in function; produced in bilaterally paired, serial arrangements by small vagile marine animals of uncertain affinity.

coral—A general name for any of a large group of bottom-dwelling, sessile, marine invertebrate organisms (polyps) that belong to the class Anthozoa (phylum Coelenterata), are common in warm intertropical modern seas and abundant in the fossil record in all periods later than the Cambrian, produce external skeletons of calcium carbonate, and exist as solitary individuals or grow in colonies.

craton—A part of the Earth's continental crust that has attained stability, and has been little deformed for a prolonged period.

crinoid—Any pelmatozoan echinoderm belonging to the class Crinoidea, characterized by quinquerradiate symmetry, by a disk-shaped or globular body enclosed by calcareous plates from which appendages, commonly branched, extend radially, and by the presence of a stem, or column, more common in fossil than in living forms.

depocenter—An area or site of maximum deposition; the thickest part of any specified stratigraphic unit in a depositional basin.

diachronous—Said of a rock unit that is of varying age in different areas or that cuts across time planes or biozones.

diagenesis—All the chemical, physical, and biological changes undergone by a sediment after its initial deposition, and during and after its lithification, exclusive of surficial alteration (weathering) and metamorphism.

disconformity—An *unconformity* in which the bedding planes above and below the break are essentially parallel.

dolomite—A common rock-forming mineral: calcium magnesium carbonate, $\text{CaMg}(\text{CO}_3)_2$; also a carbonate sedimentary rock of which more than half consists of the mineral dolomite.

dolomitization—The process by which limestone is wholly or partly converted to dolomitic rock or dolomitic limestone by the replacement of the original calcium carbonate (calcite) by magnesium carbonate (mineral dolomite), usually through the action of magnesium-bearing water (seawater or percolating meteoric water). It can oc-

cur penecontemporaneously or shortly after deposition of the limestone, or during lithification or at a later period.

doodlebug—A popular term for any of various kinds of geophysical prospecting equipment, often for a kind considered unscientific.

echinoderm—Any solitary marine benthic (rarely pelagic) invertebrate, belonging to the phylum Echinodermata, characterized by radial symmetry, an endoskeleton formed of plates or ossicles composed of crystalline calcite, and a water-vascular system.

fabric—The orientation (or lack of it) in space of the elements (discrete particles, crystals, cement) of which a sedimentary rock is composed.

facies—(a) A mappable, areally restricted part of a lithostratigraphic body, differing in lithology or fossil content from other beds deposited at the same time and in lithologic continuity. (b) A distinctive rock type, broadly corresponding to a certain environment or mode of origin.

fan—Usually a submarine fan, a terrigenous, cone- or fan-shaped deposit located seaward of large rivers and submarine canyons.

fauna—The entire animal population, living or fossil, of a given area, environment, formation, or time span.

flexure—See: *hinge*.

glauconite—A dull-green earth or granular mineral of the mica group: $(\text{K}, \text{Na})(\text{Al}, \text{Fe}^{3+}, \text{Mg})_2(\text{Al}, \text{Si})_4\text{O}_{10}(\text{OH})_2$. It has often been regarded as the iron-rich analogue of illite. Glauconite occurs abundantly in greensand, and seems to be forming in the marine environment at the present time; it is the most common sedimentary (diagenetic) iron silicate and is found in marine sedimentary rocks from the Cambrian to the present. Glauconite is an indicator of very slow sedimentation.

grainstone—A term used by Dunham (1962) for a mud-free (less than 1% of material with diameters less than 20 μm), grain-supported, carbonate sedimentary rock.

grain-supported—A term used by Dunham (1962) to describe a sedimentary carbonate rock with little or no muddy matrix, whose sand-size particles are so abundant that they are in three-dimensional contact and able to support one another.

grapestone—A term used to describe a cluster of small calcareous pellets or other grains, commonly of sand size, stuck together by incipient cementation shortly after deposition. The cluster has a lumpy outer surface that resembles a bunch of grapes.

graptolite—Any colonial marine organism belonging to the class Graptolithina, variously assigned to the phylum Coelenterata or to the Hemichordata, characterized by a cup- or tube-shaped, highly resistant exoskeleton of organic composition, arranged with other individuals along one or more branches to form a colony. Graptolites commonly occur in black shales.

graywacke—An old rock name that has been variously defined but is now generally applied to a dark-gray firmly indurated coarse-grained sandstone that consists of poorly sorted angular to subangular grains of quartz and feldspar, with a variety of dark rock and mineral fragments embedded in a compact clayey matrix having the general composition of slate and containing an abundance of very fine-grained illite, sericite, and chlorite minerals.

hiatus—A break or interruption in the continuity of the geologic record, such as the absence in a stratigraphic sequence of rocks that would normally be present but either were never deposited or were eroded before deposition of the overlying beds.

hinge—The locus of maximum curvature or bending in a folded surface, usually a line.

horst—An elongate, relatively uplifted crustal unit or block that is bounded by faults on its long sides.

hypersaline—Excessively saline; with a salinity substantially greater than that of normal seawater.

isopach—A line drawn on a map through points of equal true thickness of a designated stratigraphic unit or group of stratigraphic units; also the overall thickness and geometry of a unit or units portrayed by isopach mapping.

karst—A type of topography that is formed on limestone, gypsum, and other rocks by dissolution, and that is characterized by sinkholes, caves, and underground drainage.

limestone—A sedimentary rock consisting chiefly of calcium carbonate (CaCO_3), primarily in the form of the mineral calcite.

lithofacies—A lateral, mappable subdivision of a designated stratigraphic unit, distinguished from adjacent subdivisions on the basis of lithology, including all mineralogical and petrographic characters and those paleontological characters that influence the appearance, composition, or texture of the rock.

lithology—The description of rocks, especially in hand specimen and in outcrop, on the basis of such characteristics as color, mineralogical composition, and grain size.

lithostratigraphic unit—A body of rock that is unified by consisting dominantly of a certain lithologic type or combination of types, or by possessing other unifying lithologic features. It may consist of sedimentary, igneous, or metamorphic rocks, or of two or more of these. It may or may not be consolidated. The critical requirement is a substantial degree of overall lithologic homogeneity.

marlstone—An indurated rock of about the same composition as marl, more correctly called an earthy or impure argillaceous limestone. It has a blocky subconchoidal fracture, and is less fissile than shale.

matrix—The finer grained material enclosing, or filling the interstices between, the larger grains or particles of a sediment or sedimentary rock; the natural material in which a sedimentary particle is embedded.

meteoric—Pertaining to water of recent atmospheric origin.

moldic porosity—Porosity resulting from the removal, usually by solution, of an individual constituent of a rock, such as a shell.

mollusk—A solitary invertebrate belonging to the phylum Mollusca, characterized by a nonsegmented body that is bilaterally symmetrical and by a radially or biradially symmetrical mantle and shell. Among the classes included in the mollusks are the gastropods, pelecypods, and cephalopods.

mudstone—An indurated mud having the texture and composition of shale, but lacking its fine lamination or fissility; a blocky or massive, fine-grained sedimentary rock in which the proportions of clay and silt are approximately equal; a nonfissile mud shale.

oolite—A sedimentary rock, usually a limestone, made up chiefly of ooliths cemented together.

oolith—One of the small round or ovate accretionary bodies in a sedimentary rock, resembling the roe of fish, and having diameters of 0.25 to 2 mm (commonly 0.5 to 1 mm). It is usually formed of calcium carbonate, but may be of dolomite, silica, or other minerals, in successive concentric layers, commonly around a nucleus such as a shell fragment, an algal pellet, or a quartz-sand grain, in shallow, wave-agitated water; some ooliths show an internal radiating fibrous structure indicating outward growth or enlargement at the site of deposition. Ooliths are frequently formed by inorganic precipitation, although many noncalcareous ooliths are produced by replacement, in which case they are less regular and spherical, and the concentric or radial internal structure is less well developed, than in accretionary ooliths.

ostracode—Any aquatic crustacean belonging to the subclass Ostracoda, characterized by a bivalve, generally calcified carapace with a hinge along the dorsal margin. Most are of microscopic size (0.4–1.5 mm long) although freshwater forms up to 5 mm long and marine forms up to 30 mm long are known.

packstone—A term used by Dunham (1962) for a sedimentary carbonate rock whose granular material is arranged in a self-supporting framework, yet also contains some matrix of calcareous mud.

parasequence—In sequence stratigraphy, a relatively conformable succession of genetically related beds or bedsets bounded by flooding surfaces or their correlative surfaces.

pelamatozoan—Any echinoderm, with or without a stem, that lives attached to a substrate.

peloid—An allochem composed of micrite, irrespective of size or origin. Includes both pellets and intraclasts; useful term where exact origin is unknown.

peneplain—A low, nearly featureless, gently undulating land surface of considerable area, which presumably has been produced by the processes of long-continued sub-aerial erosion.

permeability—The capacity of a porous rock, sediment, or soil for transmitting a fluid; it is a measure of the relative ease of fluid flow under unequal pressure. The customary unit of measure is the millidarcy.

platform—A flat or gently sloping underwater erosional surface extending seaward or lakeward from the shore; specifically, a wave-cut platform or an abrasion platform.

porosity—The ratio of the aggregate volume of interstices in a rock or soil to its total volume; it is usually stated as a percentage.

seismic—Having to do with elastic waves. Energy may be transmitted through the body of an elastic solid by body waves of two kinds: *P*-waves (compressional waves) or *S*-waves (shear waves).

sequence stratigraphy—The study of rock relationships within a time-stratigraphic framework of repetitive, genetically related strata bounded by surfaces of erosion or nondeposition, or their correlative conformities.

shelf—A stable cratonic area that was periodically flooded by shallow-marine waters and received a relatively thin, well-winnowed cover of sediments.

sparite—A descriptive term for the crystalline transparent or translucent interstitial component of limestone, consisting of clean, relatively coarse-grained calcite or aragonite that either accumulated during deposition or was introduced later as a cement. It is more coarsely crystalline than micrite.

stoichiometric—With reference to a compound or a phase, pertaining to the exact proportions of its constituents specified by its chemical formula.

subaerial—Said of conditions and processes, such as erosion, that exist or operate in the open air on or directly adjacent to the land surface; or of features and materials, such as eolian deposits, that are formed or situated on the land surface.

substrate—The substance, base, or nutrient on which, or the medium in which, an organism lives and grows, or the surface to which a fixed organism is attached.

suprafan—An upbulging zone at the downslope end of a fan valley, confined to fans composed of relatively coarse sediment.

terrigenous—Derived from the land or continent.

time-stratigraphic unit—See: *chronostratigraphic unit*.

trilobite—Any marine arthropod belonging to the class Trilobita, characterized by a three-lobed, ovoid to sub-elliptical exoskeleton divisible longitudinally into axial and side regions and transversely into cephalon (anterior), thorax (middle), pygidium (posterior).

unconformity—A substantial break or gap in the geologic record where a rock unit is overlain by another that is not next in stratigraphic succession, such as an interruption in the continuity of a depositional sequence of sedimentary rocks.

vuggy—Pertaining to a vug or having numerous vugs (small cavities in a vein or a rock).

wackestone—A term used by Dunham (1962) for a mud-supported carbonate sedimentary rock containing more than 10% grains (particles with diameters greater than 20 μm).

APPENDIX 3

Abbreviations and Symbols Used in This Volume

API	American Petroleum Institute	MCFGPD	thousand cubic feet of gas per day
BC	barrels of condensate	MMBO	million barrels of oil
BBL	barrel	MMCFG	million cubic feet of gas
BCFG	billion cubic feet of gas	MMCFGPD	million cubic feet of gas per day
BHP	bottom-hole pressure	NC	no control
BLW	barrels of load water	NDE	not deep enough
BO	barrels of oil	NEU ϕ	neutron porosity
BOPD	barrels of oil per day	NRIS	Natural Resources Information System (University of Oklahoma)
BOPM	barrels of oil per month	P_{BP}	bubble-point pressure
BSW	barrels of salt water	perf.	perforations
BSWPH	barrels of salt water per hour	P_i	initial pressure
BW	barrels of water	pk.	packer
BWPD	barrels of water per day	psi, PSI	pounds per square inch
CAL	caliper	psia	pounds per square inch, absolute
cp	centipoise (a measure of viscosity)	RB	reservoir barrels
D&A	dry and abandoned	rec.	recovered
DEN	density	RES	resistivity
DEN COMP	density compensated	ROC	“retrograde oil cut”
DEN ϕ	density porosity	R_{si}	initial gas/oil ratio
DNP	did not penetrate	R_t	resistivity of uninvaded zone, or true resistivity
DST	drillstem test	R_{xo}	resistivity of flushed zone
F	flowing	SCF	standard cubic feet
FFP	final flowing pressure	SGCM	slightly gas-cut mud
FSIP	final shut-in pressure	SGCW	slightly gas-cut water
FVF	formation volume factor	SIP	shut-in pressure
gal.	gallon	SITP	shut-in tubing pressure
GCM	gas-cut mud	SP	spontaneous potential
GFR	gas/fluid ratio	sqzd.	squeezed
GOR	gas/oil ratio	STB	stock-tank barrel(s)
GR	gamma ray	STBO	stock-tank barrels of oil
HGCW	highly gas-cut water	S_w	water saturation
HHB	Henryhouse and Haragan/Bois d’Arc Formations	swbd.	swabbed
HOGCM	highly oil- and gas-cut mud	TD	total depth
IFP	initial flowing potential	W, wtr.	water
IPP	initial pumping potential	WOR	water/oil ratio
LW	load water	ϕ	porosity
MCFG	thousand cubic feet of gas		